January 2008

Petrology and Provenance of the Triassic Sugarloaf Arkose, Deerfield Basin, Massachusetts

Matthew P. Walsh
University of Massachusetts - Amherst, mwalsh@geo.umass.edu

PETROLOGY AND PROVENANCE OF THE TRIASSIC SUGARLOAF ARKOSE, DEERFIELD BASIN, MASSACHUSETTS

A Thesis Presented

by

Matthew Patrick Walsh

Submitted to the Graduate School of the
University of Massachusetts Amherst in partial fulfillment
of the requirements for the degree of

MASTER OF SCIENCE

September 2008

Department of Geosciences

PETROLOGY AND PROVENANCE OF THE TRIASSIC SUGARLOAF ARKOSE, DEERFIELD BASIN, MASSACHUSETTS

A Thesis Presented

by

Matthew Patrick Walsh

Approved as to style and content by:

_____
John F. Hubert, Chair

_____
Donald U. Wise, Member

_____
Richard Yuretich, Member

_____
Michael Williams, Department Head
Department of Geosciences

ACKNOWLEDGMENTS

I first want to thank my advisor, John Hubert. I benefited not only from John's academic knowledge, but also from his patience and wisdom. The coffee break conversations will always be appreciated. Don Wise and Richard Yuretich each critically reviewed this text and made many useful observations.

The author benefited greatly from field accompaniment of Jim Dutcher, as well as discussions with Chris Koteas and Terri Poruznick – both worthy sources for all things granitic. My capable field assistant, Arlynn Henderson, was always happy to feign interest, provide company and otherwise be a stand-up guy.

This study was in part funded by the 2006 Gloria Radke Memorial Award from the Department of Geosciences.

Most of all, I thank my family for the love and support they provided through my time here. Having a personal cheering squad is a very nice thing – maybe the nicest thing one can ask for. I could not have done without Mom, Dad, Jenny, and Jenn. Thanks for everything, Boo.

ABSTRACT

PETROLOGY AND PROVENANCE OF THE TRIASSIC SUGARLOAF ARKOSE, DEERFIELD BASIN, MASSACHUSETTS

SEPTEMBER 2008

MATTHEW PATRICK WALSH, B.A., UNIVERSITY OF MASSACHUSETTS AMHERST

M.A., UNIVERSITY OF MASSACHUSETTS AMHERST

Directed by: Dr. John F. Hubert

The ~2 km-thick Late Triassic Sugarloaf Arkose is the basal unit of the half-graben Deerfield basin, Massachusetts. Valley-river, piedmont-river, and alluvial-fan depositional facies within the arkose are defined by paleocurrent data and style of sedimentation. The valley rivers flowed from northeast to southwest, and the facies is present from the bottom to the top of the formation. Piedmont rivers built a megafan eastward into the basin, beginning about in the middle of the arkose. The local alluvial-fan built from east to west in the upper third of the formation.

The petrology of the medium sand and conglomerate was used to delineate the source areas for each facies. The medium sand in the valley rivers is mostly granite and granite gneiss fragments, coarsely-polycrystalline quartz grains, and twinned plagioclase. This assemblage is a mixture of granite from continental basement uplift, granite gneiss

from a dissected magmatic arc, and phyllites and schist from a recycled collision orogen. The medium sand in the piedmont-river facies lacks granite fragments, and untwinned plagioclase is more abundant than twinned: the provenance is continental basement uplift and recycled collision orogen. The alluvial-fan provenance is similar to the valley rivers, combining recycled collision orogen and dissected magmatic arc. Unlike the valley rivers, granite gneiss and untwinned plagioclase in the alluvial fan are dominant over granite and twinned plagioclase. Quartz provenance in the three facies was granite, trending to granite gneiss in the piedmont-river and alluvial-fan facies.

In all facies, plagioclase feldspar is more common than K-feldspar in the medium sand. The conglomerate pebbles, however, are dominated by K-feldspar, most likely due to erosion of pegmatites in the source terrane. Gray quartzite, white and translucent varieties of quartz, and pink granitoid pebbles are also common.

The post-depositional diagenesis of the Sugarloaf Arkose affects provenance determination. Diagenetic events include: hematite grain coats, mechanical compaction, albitization of feldspars, albite and quartz overgrowths, authigenic hematite cement, carbonate cement, and illite replacement of feldspars.

Within the dry-dominated monsoonal paleoclimate, each facies formed in response to tectonism. The initial appearance of each facies is used to determine the timing of tectonic events. The valley rivers flowed from the northeast in an early NNE-SSW-trending ‘sag’ basin, associated with minor normal faulting. The initial appearance of the east-flowing piedmont rivers about half way up the section implies an early, down to the west, basin-bounding normal fault, which formed perpendicular to N70E-S70E extension. This fault propagated, and, on reaching the northeast corner of the basin, the

alluvial fan built to the west off the fault scarp. The Amherst block is a relay ramp between basin-bounding faults in the Deerfield and Hartford basins. Linkage of the two basin-bounding faults through the Amherst block created an integrated basin linking the Triassic strata in the early Hartford and Deerfield basins, and may have caused the unconformity present at the top of the arkose.

CONTENTS

Page

LIST OF TABLES

LIST OF FIGURES

CHAPTER 1

INTRODUCTION

1.1 Objective

This thesis determines the petrology of sandstones and lithology of conglomerates in each of the three depositional facies of the Sugarloaf Arkose. To help determine potential source terranes of the arkose the data are integrated with regional tectonism and lithology, extensional sedimentary basin and river processes, and weathering and diagenetic effects on petrology.

1.2 Newark Supergroup

The early Mesozoic rift basins of the Newark supergroup along the Central Atlantic Margin (CAM) formed during the breakup of Pangea (Figure 1) (Froelich and Olsen, 1984; Luttrell, 1989). Buried and exposed basins are located from off-shore Newfoundland to Florida (Olsen, 1997). The basins filled with terrestrial strata and basalts as North America drifted northward at about 21^{o}N paleolatitude during the Late Triassic to Early Jurassic (Olsen, 1997). The exposed basins are typically half-grabens (Hibbard et al., 2006), although some are grabens (Hutchinson and Klitgord, 1988).

Rifting thinned the lithosphere sufficiently for extrusion of flood basalts of the Central Atlantic Magmatic Province (CAMP) (Marzoli et al., 2004). The basalt flows in the basins north of the Culpeper basin of Virginia date at about 201 Ma and were extruded in approximately 600,000 years (Olsen, 1997). The lavas covered an area of

Figure 1. Rift basins in eastern North America of the Newark supergroup, and related basins in North Africa. CAM Basins modified from Olsen et al. (2000). Diagonal lines indicate early Mesozoic latitude. Crosses indicate modern latitude and longitude (unlabeled); north arrow in legend indicates present magnetic north for Deerfield basin.

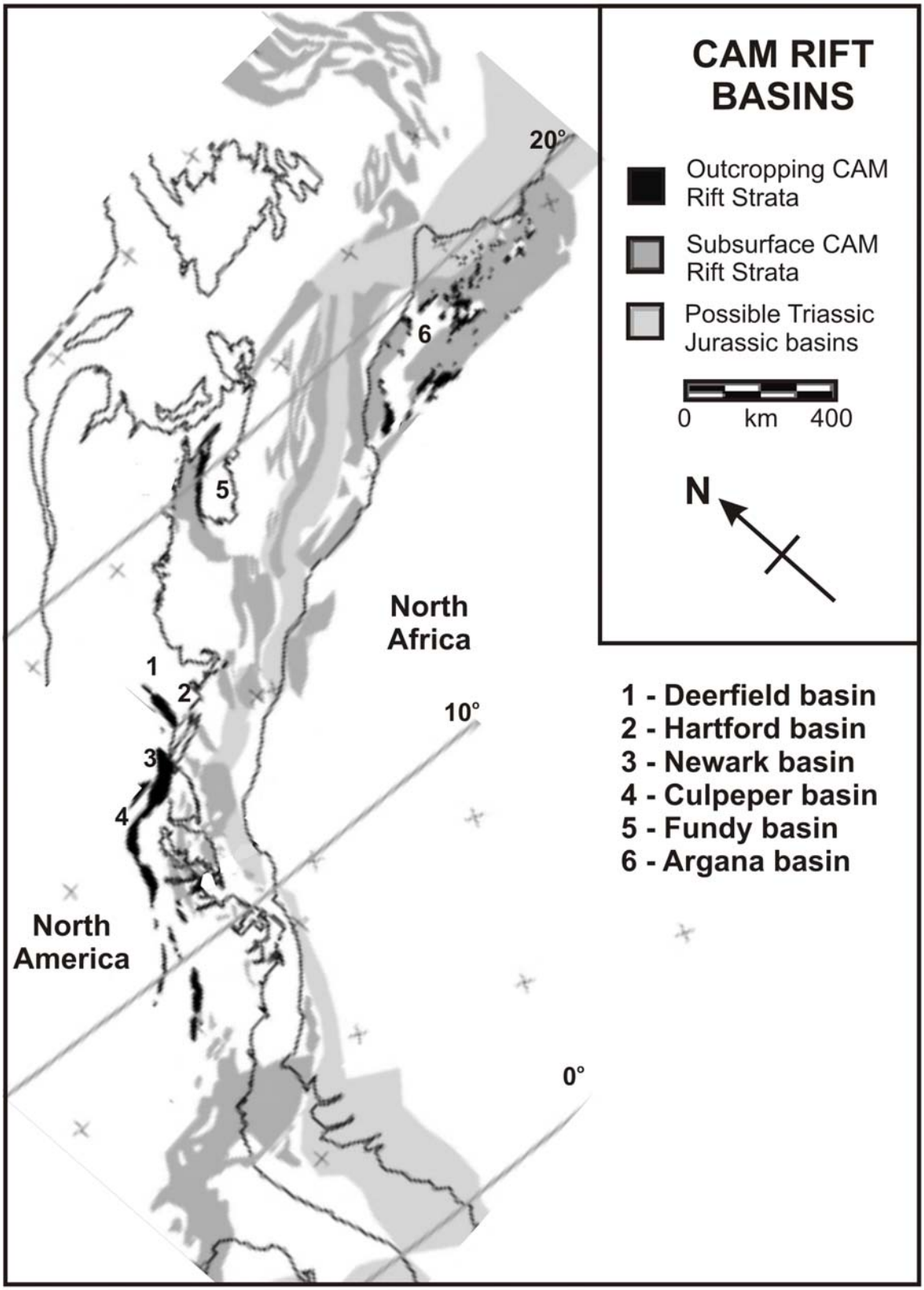
CAM RIFT BASINS
Outcropping CAM Rift Strata
Subsurface CAM Rift Strata
Possible Triassic Jurassic basins
0 km 400
N
1 - Deerfield basin
2 - Hartford basin
3 - Newark basin
4 - Culpeper basin
5 - Fundy basin
6 - Argana basin
North Africa
North America
20°
10°
0°
1
2
3
4
5
6

$10\text{-}11 \times 10^6$ km^2 across the CAM (Rampino and Stothers, 1988; Marzoli et al., 1999; McHone, 2000; Schlische et al., 2002). Traditionally, the CAMP event was thought to have preceded the mass extinctions at the Triassic-Jurassic boundary by as little as a few hundred thousand years (Courtillot, 1996; Pálfy et al., 2000). Dunning and Hodych (1990) redefined the Triassic-Jurassic boundary using CAMP basalts; they also observed that the last terrestrial fossils of Triassic age are commonly found a few meters, perhaps as little as a few thousand years, below the oldest basalt in each basin (Olsen et al., 1990; Olsen, 1997). However, recent correlation between marine and non-marine stratigraphic markers challenges the placement of the Triassic-Jurassic boundary before the oldest basalt units, and instead places the boundary after the first CAMP eruptions (Lucas and Tanner, 2007).

The proximity of the last Triassic-aged fossils to the CAMP event led to the suggestion that volcanic degassing was the primary cause of the extinction event (Courtillot, 1996; Cohen and Coe, 2002). However, Tanner et al. (2001) found that CO_2 increase during the CAMP event was insufficient to cause the mass extinction. In addition, marine and non-marine extinctions were not simultaneous, but began just before 201 Ma (pre-CAMP) and continuing into the CAMP event (Lucas and Tanner, 2007). Olsen (1997) and Olsen et al. (2003) have also suggested that a bolide impact may have caused the climatic and biotic crisis.

The Deerfield basin of western Massachusetts formed in the Late Triassic, and filled with terrestrial sediments and flood basalt to at least the Early Jurassic (Figure 2) (Olsen, 1997). Approximately 6-7 km of terrestrial strata and basalt flows are inferred to have filled the basin, though only 4 km are preserved (Pratt et al., 1988; Hubert and

Figure 2. A. Geologic map after Zen (1983), showing Deerfield basin stratigraphic units, normal faults, and structural blocks buried by Mesozoic strata. Cross section X-X' is Figure 3. B. Locations of areas depicted in Figures 1A, 4, and 6. S is Springfield, W is Worcester, G is Greenfield, and A is Amherst. C. Distribution of continents during early Pangean break-up at ~200 Ma, with location of Deerfield basin.

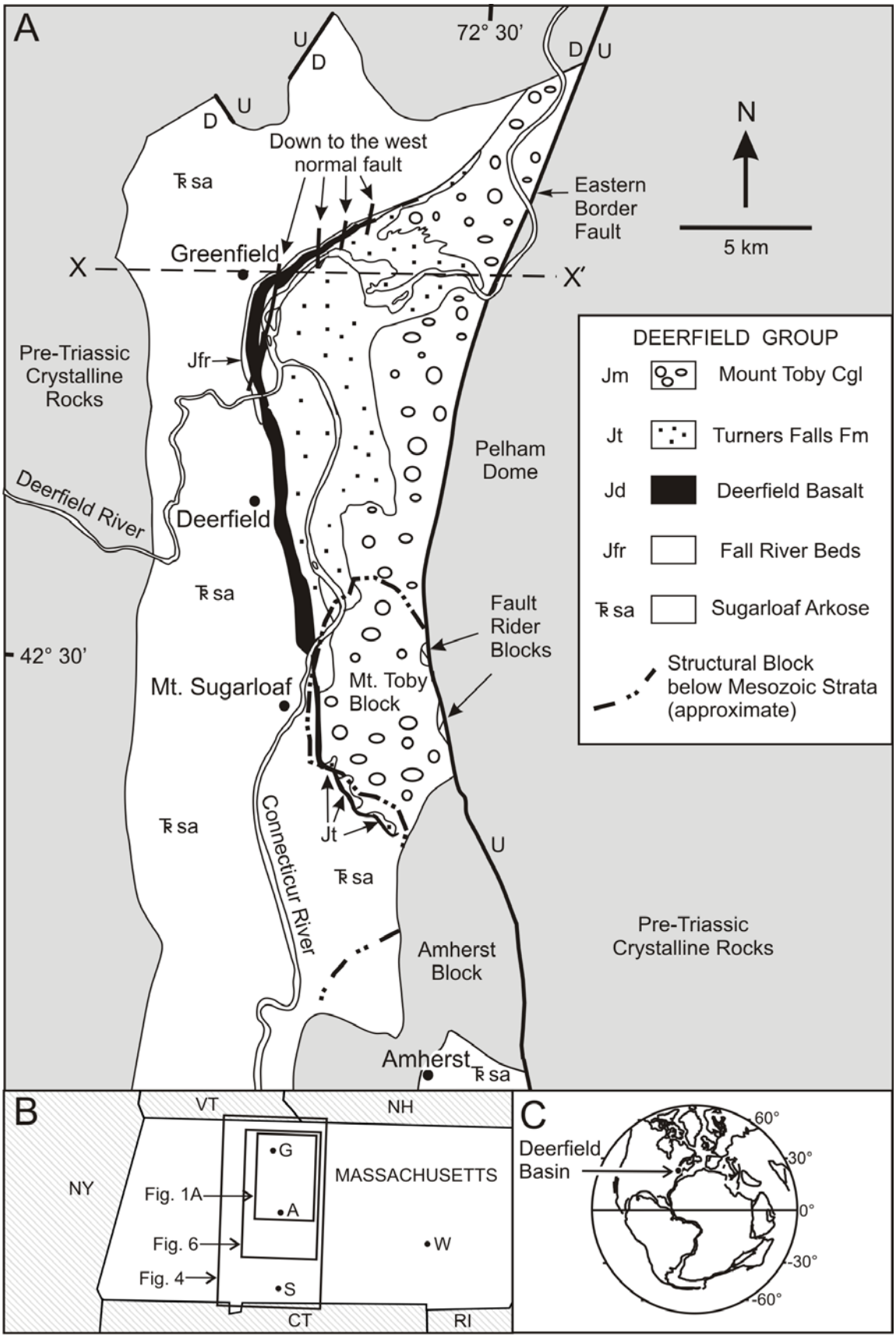
A
72° 30'
42° 30'
U
D
Down to the west
normal fault
Eastern
Border
Fault
N
5 km
X
X'
Greenfield
Deerfield
Deerfield River
Pre-Triassic
Crystalline
Rocks
Jfr
Pelham
Dome
Fault
Rider
Blocks
Mt. Sugarloaf
Mt. Toby
Block
Jt
Connecticut River
Amherst
Block
Amherst
Pre-Triassic
Crystalline Rocks
DEERFIELD GROUP
Jm
Mount Toby Cgl
Jt
Turners Falls Fm
Jd
Deerfield Basalt
Jfr
Fall River Beds
Sugarloaf Arkose
Structural Block
below Mesozoic Strata
(approximate)
B
VT
NH
NY
MASSACHUSETTS
Fig. 1A
Fig. 6
Fig. 4
G
A
W
S
CT
RI
C
Deerfield
Basin
60°
30°
0°
-30°
-60°

Dutcher, 1999). The basin is a half-graben bounded by the west-dipping, listric Eastern Border Fault (EBF) (Figure 3).

The Deerfield and Hartford basins are separated by the Amherst block, an inlier of Paleozoic basement down-faulted by the EBF (Willard, 1951; Balk, 1956). The Sugarloaf Arkose thins across the block through Hatfield and Northampton, and thickens south of the Amherst block in Holyoke as the New Haven arkose (Chandler, 1978). The Hartford basin is also a half-graben bound by the EBF, though locally a western border fault creates a graben (Zen, 1983). The Deerfield and Hartford basins together comprise the Connecticut Valley basin.

Stratigraphically, the basins are similar: 1) Triassic fluvial arkose, 2) basalt flows near the Triassic-Jurassic boundary, and 3) early Jurassic lacustrine and playa strata and border-fault fanglomerates (Figure 4) (Wessel, 1969; Handy, 1977; Luttrell, 1989; Hubert and Reed, 1978; Olsen, 1997). Notably absent in the Deerfield basin are the Hampden and Talcott basalts below and above the Holyoke basalt. The Talcott thins northward in the Hartford basin, ending by erosion or non-deposition.

The Northfield basin is ~1.3 km north of the Deerfield basin, and is also bounded on the east by the EBF. The basin comprises ~1000 m of Mt. Toby Conglomerate, thinning to the southwest by erosion to 0 m (Wessel, 1969; Zen, 1983). The basin is truncated on the north by a WNW-ESE-striking, down to the SW normal fault that splays from the EBF (Figure 5). A once continuous Northfield/Deerfield basin is implied by proximity and similar basin fills.

Figure 3. E-W transverse cross section of the Deerfield basin through Greenfield, after Zen, 1983. Stratigraphic units are the same as Figure 1. Dashed lines in pre-Triassic crystalline rocks are basement nappes and faults.

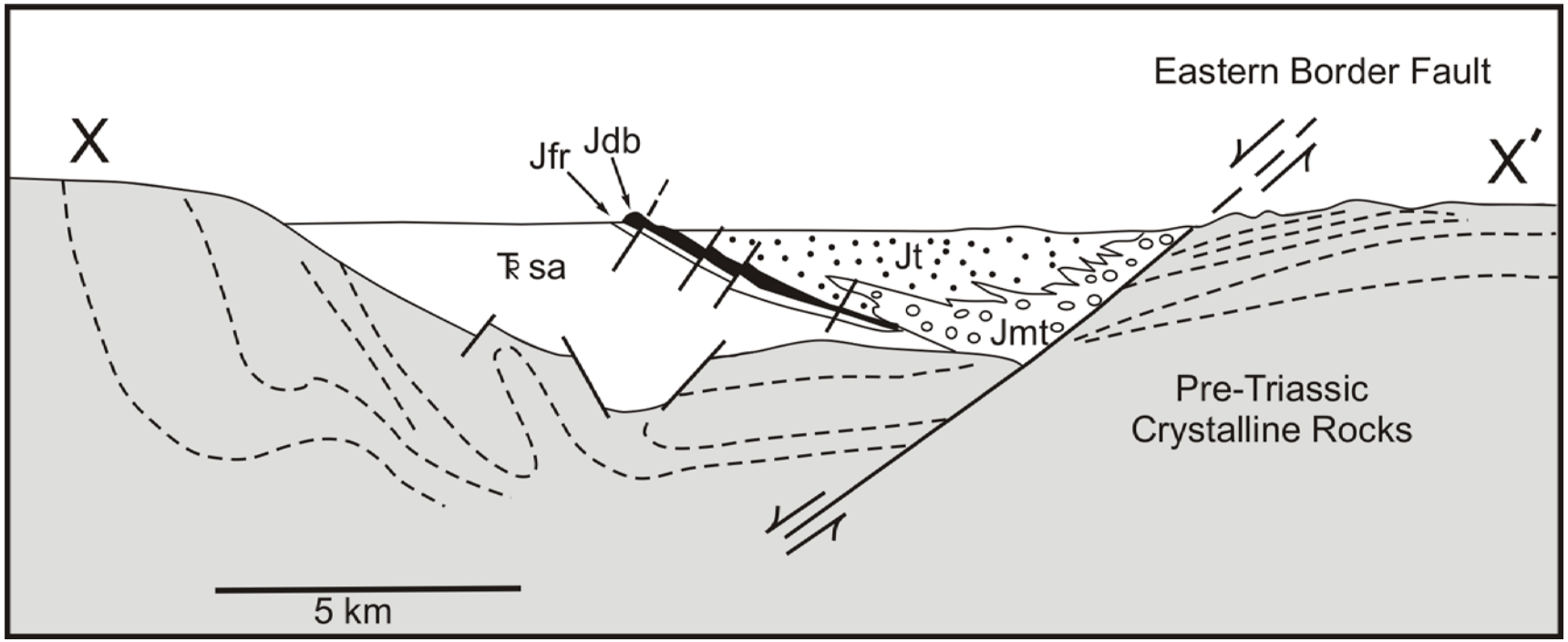
Eastern Border Fault
X
X'
Jfr
Jdb
Jt
Jmt
Pre-Triassic
Crystalline Rocks
5 km

Figure 4. Stratigraphic columns of the Deerfield, Hartford, and Pomperaug basins compiled from Hubert et al. (1992), LeTourneau and Huber (2005), Olsen et al. (1992), Rogers et al. (1985), and Zen (1983). The Granby tuff of the Hartford is 'Jtb' to avoid confusion with the Turners Falls Formation of the Deerfield basin.

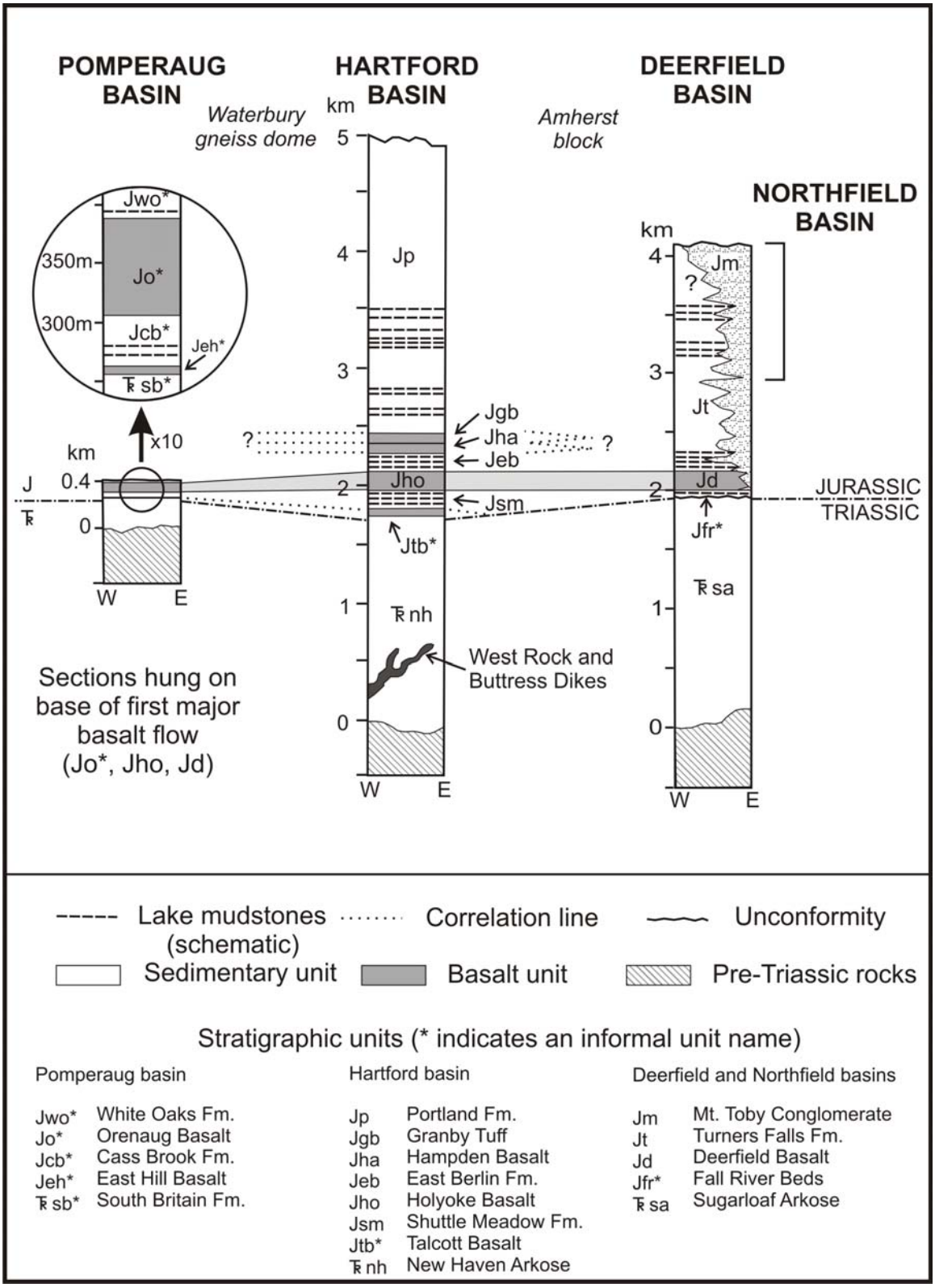
POMPERAUG BASIN
HARTFORD BASIN
DEERFIELD BASIN
NORTHFIELD BASIN
Waterbury gneiss dome
Amherst block
km
Jwo*
Jo*
Jcb*
Jeh*
Trsb*
350m
300m
x10
Jp
Jgb
Jha
Jeb
Jho
Jsm
Jtb*
Trnh
West Rock and Buttress Dikes
Jm
Jt
Jd
Jfr*
Trsa
JURASSIC
TRIASSIC
W
E
Sections hung on base of first major basalt flow (Jo*, Jho, Jd)
Lake mudstones (schematic)
Correlation line
Unconformity
Sedimentary unit
Basalt unit
Pre-Triassic rocks
Stratigraphic units (* indicates an informal unit name)
Pomperaug basin
Jwo* White Oaks Fm.
Jo* Orenaug Basalt
Jcb* Cass Brook Fm.
Jeh* East Hill Basalt
Trsb* South Britain Fm.
Hartford basin
Jp Portland Fm.
Jgb Granby Tuff
Jha Hampden Basalt
Jeb East Berlin Fm.
Jho Holyoke Basalt
Jsm Shuttle Meadow Fm.
Jtb* Talcott Basalt
Trnh New Haven Arkose
Deerfield and Northfield basins
Jm Mt. Toby Conglomerate
Jt Turners Falls Fm.
Jd Deerfield Basalt
Jfr* Fall River Beds
Trsa Sugarloaf Arkose

Figure 5. Basement and structural features proximal to the Deerfield basin. Regional extension during the Late Triassic to Early Jurassic was orthogonal to N20^{o}E (Wise, 1992). Tectonic features deviate from this general trend at the Pelham Dome and the Belchertown Igneous Complex, pre-existing structures which created basement strength anisotropies.

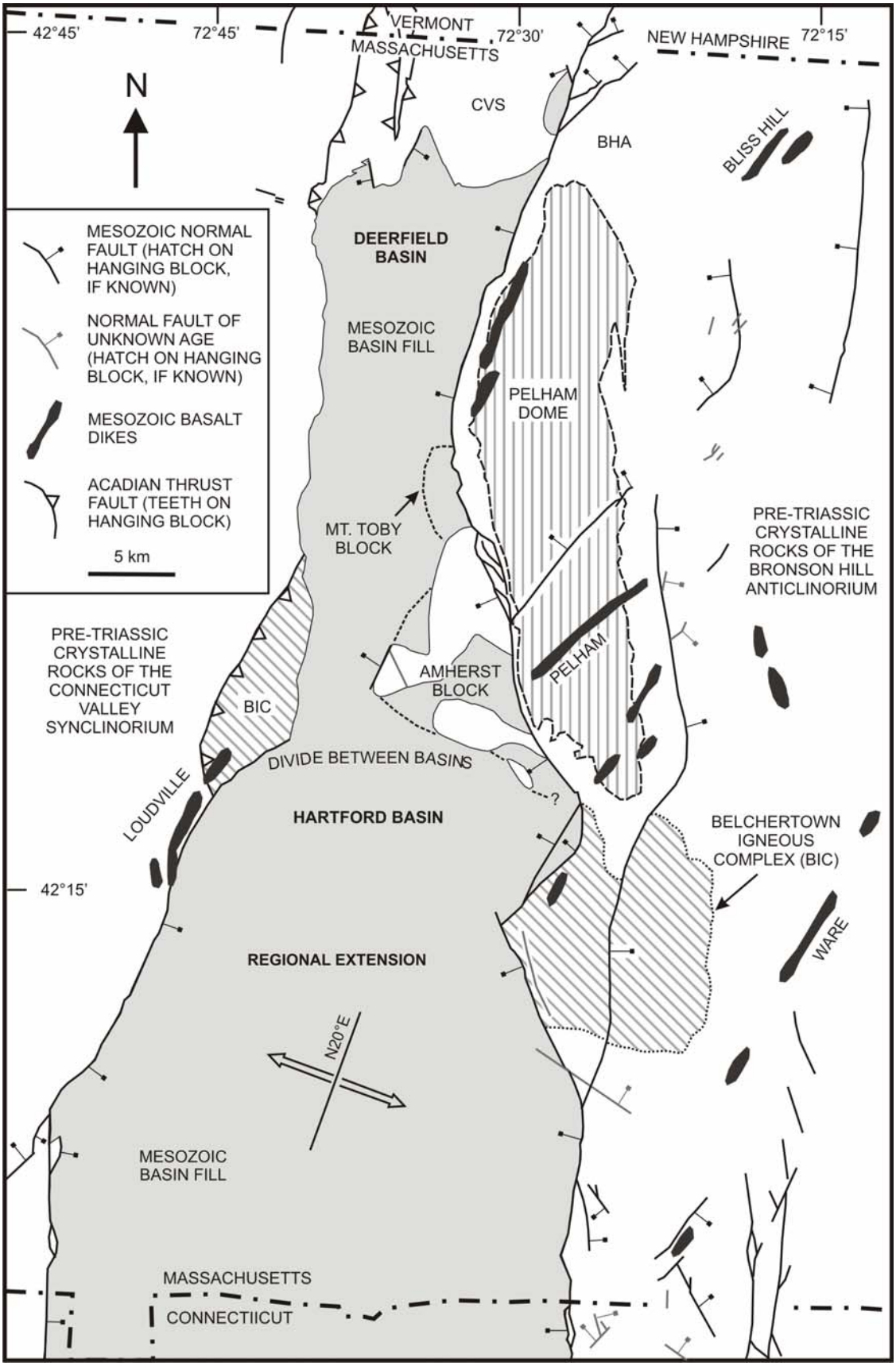
42°45'
72°45'
VERMONT
MASSACHUSETTS
72°30'
NEW HAMPSHIRE
72°15'
N
CVS
BHA
BLISS HILL
MESOZOIC NORMAL FAULT (HATCH ON HANGING BLOCK, IF KNOWN)
NORMAL FAULT OF UNKNOWN AGE (HATCH ON HANGING BLOCK, IF KNOWN)
MESOZOIC BASALT DIKES
ACADIAN THRUST FAULT (TEETH ON HANGING BLOCK)
5 km
DEERFIELD BASIN
MESOZOIC BASIN FILL
PELHAM DOME
MT. TOBY BLOCK
PRE-TRIASSIC CRYSTALLINE ROCKS OF THE BRONSON HILL ANTICLINORIUM
PRE-TRIASSIC CRYSTALLINE ROCKS OF THE CONNECTICUT VALLEY SYNCLINORIUM
AMHERST BLOCK
PELHAM
BIC
DIVIDE BETWEEN BASINS
LOUDVILLE
HARTFORD BASIN
BELCHERTOWN IGNEOUS COMPLEX (BIC)
42°15'
WARE
REGIONAL EXTENSION
N20°E
MESOZOIC BASIN FILL
MASSACHUSETTS
CONNECTIICUT

The Pomperaug basin of western Connecticut is about 20 km west of the Hartford Basin; it filled with sediment and basalts similar to the Hartford basin (Rodgers, 1985). However, fluvial paleocurrents and sandstone petrology with eastern and western sources indicate they were isolated basins (Hubert et al., 1992; LeTourneau and Huber, 2007). The Deerfield, Hartford, Northfield, and Pomperaug basins share a common overall stratigraphic sequence, style and age (Figure 4).

Re-evaluation of fluvial paleocurrents in the Deerfield basin by Hubert et al. (2008) demonstrates that the Sugarloaf Arkose rivers not only flowed northeast to southwest, but also west to east. The west-to-east pattern is present in the southern two-thirds of the basin, at the same stratigraphic levels as the northeast-southwest flowing rivers in the northern third of the basin.

Apatite and zircon fission-track data date major normal motion on the EBF to Late Jurassic-Early Cretaceous time (Roden-Tice and Wintsch, 2002; 2007; Wintsch et al., 2003; Roden-Tice et al., 2008). Similar late post-depositional tilting and half-graben formation was called upon by Faill (2003) in the southern Newark basins.

This thesis presents a tectono-sedimentary model that integrates sedimentary facies, paleocurrents, and sandstone petrology. The paleocurrents and petrology determined the source areas for the arkose. The timing of the early faulting is based on spatial and temporal changes in paleocurrents and sedimentary facies.

1.3 Allogenic Controls and Geologic Setting

Before describing the Deerfield basin in detail, the tectonic and paleoclimatic allogenic controls on sedimentation must be addressed (Miall, 1996). A third allogenic control is base-level, determined by the interplay of eustasy and tectonism; in a non-

marine basin, however, eustasy is not a factor, and tectonic subsidence controls accommodation space (Miall, 1996; Boggs, 2006). In addition to syn-depositional tectonism, the Paleozoic orogenies are discussed because orogenic events led to deposition and emplacement of the basement rocks, which are potential source terranes around the basin. Also, Paleozoic deformations created basement anisotropies, the major controls on Mesozoic tectonism (Swanson, 1986; Wise, 1992; Wintsch et al., 2003). Pleistocene and Holocene cover are also described.

1.3.1 Pre-Mesozoic Basement

The basement rocks are Proterozoic and Paleozoic metamorphic and igneous rocks of the Connecticut Valley belt and Bronson Hill zone (Figure 5) (Zen, 1983). East of the basin is the Bronson Hill anticlinorum (BHA) made of Upper Proterozoic to Ordovician rocks (Dry Hill Gneiss to Collinsville Formation) and Pennsylvanian intrusives (Pauchaug Gneiss; Robinson, 2003). These rocks are unconformably overlain by Middle Ordovician volcanic rocks (Ammonoosuc volcanics) and black shales (Partridge Formation; Zen, 1983). The BHA package is interpreted as a volcanic island arc (Bronson Hill arc), the eastern-most member of "medial New England" (Robinson et al., 1998). This arc-terrane docked on the Laurentian margin in the Late Ordovician, generating the structural and metamorphic features of the Taconian orogeny (Robinson and Hall, 1979; Robinson, 2003).

West of the basin is the Connecticut Valley synclinorum (CVS), comprising rocks of Silurian (Clough Quartzite to Russel Mountain Formation) to Lower Devonian age (Littleton Formation to Putney Volcanics). These metamorphic rocks were shallow-water sediments and minor volcanics deposited in a back-arc basin in the Middle

Devonian, as the Avalon plate docked onto the margin of the amalgamated Laurentia and medial New England. Although the rocks in the CVS were deposited east of the BHA, they now lie to the west. The CVS rocks were evidently structurally emplaced over the BHA by nappe folding and thrust faulting to the west and subsequently eroded to expose the BHA (Thompson et al., 1968; Robinson et al., 1991; and Robinson, 2003).

Both the BHA and CVS were affected by the Acadian (410-385 Ma), Quaboagian (formerly Neo-Acadian; 370-350 Ma), and Northfieldian orogenies (305-285 Ma; Robinson and Hall, 1979; Robinson, 2003). The Acadian orogeny involved an early nappe stage, where fold nappes transported CVS rocks undergoing regional metamorphism tens of kilometers westward (Robinson et al., 1991). Later thrust nappes cut the earlier fold nappes, again moving rocks westward (Thompson, 1985; Robinson, 2003).

During the Quaboagian and Northfieldian orogenies, backfolding and cataclasis occurred as the BHA was overturned to the east (Robinson and Hall, 1979; Robinson, 2003). This was followed by dome formation through density-driven upward movement of BHA gneisses through overlying rocks. Mantled domes from these orogenic stages are responsible for the Pelham dome and Ordovician gneiss domes of the BHA, as well as the 'Vermont Line' of domes along the suture of the Laurentian/medial New England margin and the BHA (Figure 5) (Robinson and Hall, 1979; Robinson, 2003).

Tectonic to post-tectonic gabbroic to granitic plutons were intruded beginning during the Acadian orogeny. Among the earliest was the Ashuelot pluton of the Kinsman quartz monzodiorite of southern New Hampshire (Clark and Lyons, 1986; Lyons, 1997). The Belchertown igneous complex is a zoned, two-pyroxene quartz monzodiorite that

intruded BHA rocks southwest of the Pelham dome some time between the Acadian and Quaboagian orogenies (Zen, 1983; Robinson, 2003). The last intrusive events occurred during the Northfieldian orogeny, when granitic pegmatites of the Warwick dome and Kempfield anticline intruded the BHA (Robinson, 2003). All plutons were affected by regional metamorphism, and now typically display gneissic foliation.

The Late Permian Alleghanian orogeny (270-260 Ma) resulted from collision of Gondwana and the amalgamated Laurentian margin (Robinson et al., 1998; Robinson, 2003). In southern New England, Acadian to Quaboagian metamorphism west of the EBF was overprinted by Alleghanian metamorphism, whereas Northfieldian metamorphism east of the EBF was not overprinted.

1.3.2 Mesozoic Tectonism

Continental extension across the CAM began in the Middle Triassic, with increasing rates of extension in Late Triassic time (Olsen, 1997; Roden-Tice and Wintsch, 2002; Wintsch et al., 2003; Wise and Hubert, 2003). Seismic studies in southern and central New England, New York, and New Jersey show crustal thinning is closely linked to and most likely accommodated by Newark basin faults and other Mesozoic normal faults (Wenk, 1989; Schlische, 2003). Early extension in the brittle upper crust was accommodated by listric, normal faulting and corresponding formation of half-grabens: a process reproduced in sand box tectonic experiments and observed in deep imaging of active rift zones (Wernicke and Burchfield, 1982; Rosendahl, 1987; McClay et al., 2002; Morley, 2002). Listric normal faults in eastern North America likely soled into master, southeast-dipping detachments at mid-crustal depths. These

detachments are hypothesized to be Paleozoic thrust faults reactivated with low-angle, normal motion (Ando et al., 1984; Crespi, 1988; Marple and Talwani, 2006).

In both crystalline basement and Mesozoic basin fills, numerous Middle Triassic to Middle Jurassic faults and joints have an average strike of N20^{o}E, as do basalt dikes across northeastern North America and northern Africa (de Boer and Clifton, 1988; McHone, 1988; de Boer, 1992; McHone, 2000; Wise and Hubert, 2003). Although faults may be deflected by pre-existing anisotropies in the crust, as discussed below, dikes form perpendicular to σ_3 and are therefore good indicators of paleo-stress vectors (McHone, 1988; de Boer, 1992; Schlische, 2003). Similar NNE-SSW strikes are observed in Middle to Late Triassic quartz veins throughout western Massachusetts and Connecticut (Eberly, 1985). The common strike amongst basalt dikes, quartz veins, and brittle features indicates extension normal to N20E (110^{o} to 290^{o}) from Middle Triassic to Middle Jurassic (Wise, 1992; Withjack et al., 1998; Schlische, 2003).

Extension and crustal thinning in the Triassic led to adiabatic rise of the asthenosphere and generation of basalt magma, a common feature in ancient and modern rift systems (Wilson, 1989). Basalt magma was intruded and erupted during the CAMP event near the Triassic-Jurassic boundary (Dunning and Hodych, 1990; Courtillot, 1996; Pálfy et al., 2000; Lucas and Tanner, 2007). CAMP basalts are present in the northern Newark basins, as well as across northeastern South America, western Africa, and Iberia. The basalt bodies include basalt feeder dikes and sea-ward dipping reflectors (SDRs) along the Atlantic margins, and extensive flood basalts (McHone, 2000).

Extension continued into the Early Jurassic, when new faults formed, pre-existing faults propagated, and rider blocks were created as motion was abandoned along one fault

and taken up by another (Rosendahl, 1987; McClay et al., 2002; Schlische, 2003). The greatest displacement and throw are near the centers of fault segments because faults nucleate, then propagate at each end (Schlische and Anders, 1996; Contreras et al., 1997).

Fault-bounded basins 1) deepen at the center; 2) widen perpendicular to fault strike due to hanging wall on-lap; and 3) lengthen parallel to fault strike as the fault tips propagate (Withjack et al., 1990; Barnett et al., 1987; Cowie, 1998; Gawthorpe and Leeder, 2000). In some cases, fault linkage across relay ramps leads to a composite basin, formed of two former basins that down drop as an integrated hanging wall basin (Schlische, 2003). Differential subsidence along, and linkage between, normal faults leads to syn- and post-depositional transverse folding. The hanging wall basement and basin-fill synclines are at the center of fault segments, whereas anticlines are at fault tips (Schlische, 1995; 2003).

In the Newark basins, regional extension changed to transpression at about 180 Ma, reactivating many normal faults with reverse and strike-slip motions, and creating small-scale thrust faults and folds. The most likely reason for regional transpression and basin inversion was formation of the mid-Atlantic ridge, and transition from continental rift to drift (Withjack et al., 1995; Wintsch et al., 2003; Wise and Hubert, 2003). Farther afield, Mesozoic sedimentary rocks in the Abda and Essaouira basins of Morocco were also affected by post-early Jurassic compression events (Le Roy et al., 1997; Echarfaoui et al., 2002).

Transpression across the central Atlantic margin reverted to extension in the Late Jurassic to Early Cretaceous, although the cause is unknown. Fission-track thermometers show major Middle Jurassic-Cretaceous motion along the EBF in New Hampshire,

Massachusetts, and Connecticut; similar studies of the border faults of the Newark basins also show the tilting of strata was post-Middle Jurassic (Harrison et al., 1989; Steckler et al., 1993; Roden-Tice and Wintsch, 2002). Regional Cretaceous normal motion also occurred south of Long Island, in the eastern Adirondacks, and in coastal and offshore Maine (Hutchinson and Grow, 1985; Hutchinson et al., 1988; Roden-Tice et al., 2000; West and Roden-Tice, 2003).

The Deerfield basin and surrounding basement rocks record all stages of Mesozoic tectonism (Figure 5). Early normal faults provided the accommodation space for Late Triassic fluvial redbeds; the faults possibly soled into Paleozoic thrust sheets similar to the Acadian thrust exposed just west of the basin. Basement faults, including the EBF north of the Mt. Toby block, and basalt dikes strike N20^{o}E. The dikes and basalts are typical CAMP intrusive and extrusive bodies. Post-CAMP extension in the Early Jurassic allowed continued sedimentation, and locally deformed the basin fill, including normal faults and transverse synclinal folds near Greenfield (Figure 2). The transpression at 180 Ma is recorded by reverse and strike-slip reactivation of normal faults in the basin (Wise and Hubert, 2003). Late Jurassic-Cretaceous extension tilted the basin fill to the east along the EBF (Roden-Tice and Wintsch, 2002; Wintsch et al., 2003).

1.3.3 Paleoclimate

The basin was drifting north at about 12^{o}N paleolatitude when deposition of the Sugarloaf Arkose began (~218 Ma), and at about 23^{o}N by the time of the Deerfield Basalt flows at 201 Ma (Kent and Tauxe, 2005). Paleoclimate modeling cited by these workers shows northward-drift brought the basin into a subtropical arid belt between equatorial

and temperate humid belts. This aridity is reflected in the ventifacts widely found in the Sugarloaf Arkose. Poorly-formed ventifacts with incipient facets are also common. Both types may have desert varnish (Hubert et al., 2008).

The latitude-induced aridity was modulated by seasonal monsoon rains, part of the Late Triassic megamonsoon that affected much of Laurentia in the Late Triassic-Early Jurassic (Dubiel et al., 1991; Kent and Muttoni, 2003; Loope et al., 2004). The megamonsoon was caused by the large area of Pangea centered on the equator with the Tethys Sea the source of moisture-laden air moving inland on tropical easterlies (Chandler et al., 1992). The abundant ventifacts in the Sugarloaf Arkose indicate the dry season greatly dominated over the wet (Hubert et al., 2008). Other indicators that the paleoclimate was strongly dry-dominated are: 1) calcrete paleosols in fluvial sandstones and thin eolian sandstones of the New Haven arkose (Sugarloaf Arkose equivalent, Hartford basin); and 2) early Jurassic eolian sandstones in the Cass Brook and Portland formations of the Pomperaug and Hartford basins, respectively (Smoot, 1991; LeTourneau and Huber, 2006; Rasbury et al., 2006).

Milankovitch climate-forcing cycles modified the length and intensity of monsoonal wet and dry seasons (Olsen, 1986; Smoot and Olsen, 1994; Olsen and Kent, 1996). Relatively thick gray to black mudstones in the Early Jurassic Turners Falls Formation record wet cycles due to long (400 ka) eccentricity cycles (Olsen et al., 1992). Lower-order cyclicity of about 23 ka is referred to as the Van Houten cycle, and is seen in couplets about 8-10-m thick of lacustrine gray and black mudstone and playa redbeds (Olsen, 1986; Smoot and Olsen, 1994; Olsen and Kent, 1996; Olsen et al., 2005; Drzewiecki and Zuidema, 2007).

1.4 The Deerfield Basin

Before erosion, the Deerfield basin extended at least over the Belchertown igneous complex west of the Amherst block (Figure 5). In Whately, this Devonian pluton locally contains abundant joints filled with pink, poorly consolidated siltstone (Wise and Hubert, 2003). Mesozoic silt filled the void spaces of the joints, which apparently formed on the hinge zone of the hanging wall, possibly created during the Late Jurassic-Cretaceous motion of the EBF. Post-depositional normal movements of the EBF significantly tilted the basin fill eastward toward the EBF, resulting in erosion that preserves only the 'keel' of the basin along the EBF.

1.4.1 Stratigraphy

There are about 4 km of terrestrial strata and basalt flows in the deepest part of the basin near Greenfield (Figures 2, 3). Hydrocarbon maturation data suggest that 2-3 km of strata were removed by erosion, mostly in the mid-Jurassic to Cretaceous (Pratt et al., 1988; Hubert and Dutcher, 1999).

The Sugarloaf Arkose is the basal unit in the basin, deposited by braided rivers and alluvial fans over ~16.5 Ma, from the Late Triassic Carnian-Norian boundary at ~218 Ma to the earliest Jurassic (Olsen, 1997). The arkose is thickest (2300 m) at Greenfield, thinning to the northeast by erosion to 0 m at the edge of the basin, and southward to ~800 m at the type section at Mount Sugarloaf in South Deerfield (Figure 6). The basement between Greenfield and South Deerfield is faulted, causing variations in thickness from <1 km to almost 2 km.

Figure 6. N-S longitudinal cross section of the Sugarloaf Arkose, Fall River beds, and Deerfield Basalt. A. No vertical exaggeration. Cross section is about parallel to strike of beds. Faults that cut the basalt are not shown. B. 5x vertical exaggeration. Numbers indicate the stratigraphic positions of outcrops. C. Map of cross section. EBF is the Eastern Border Fault.

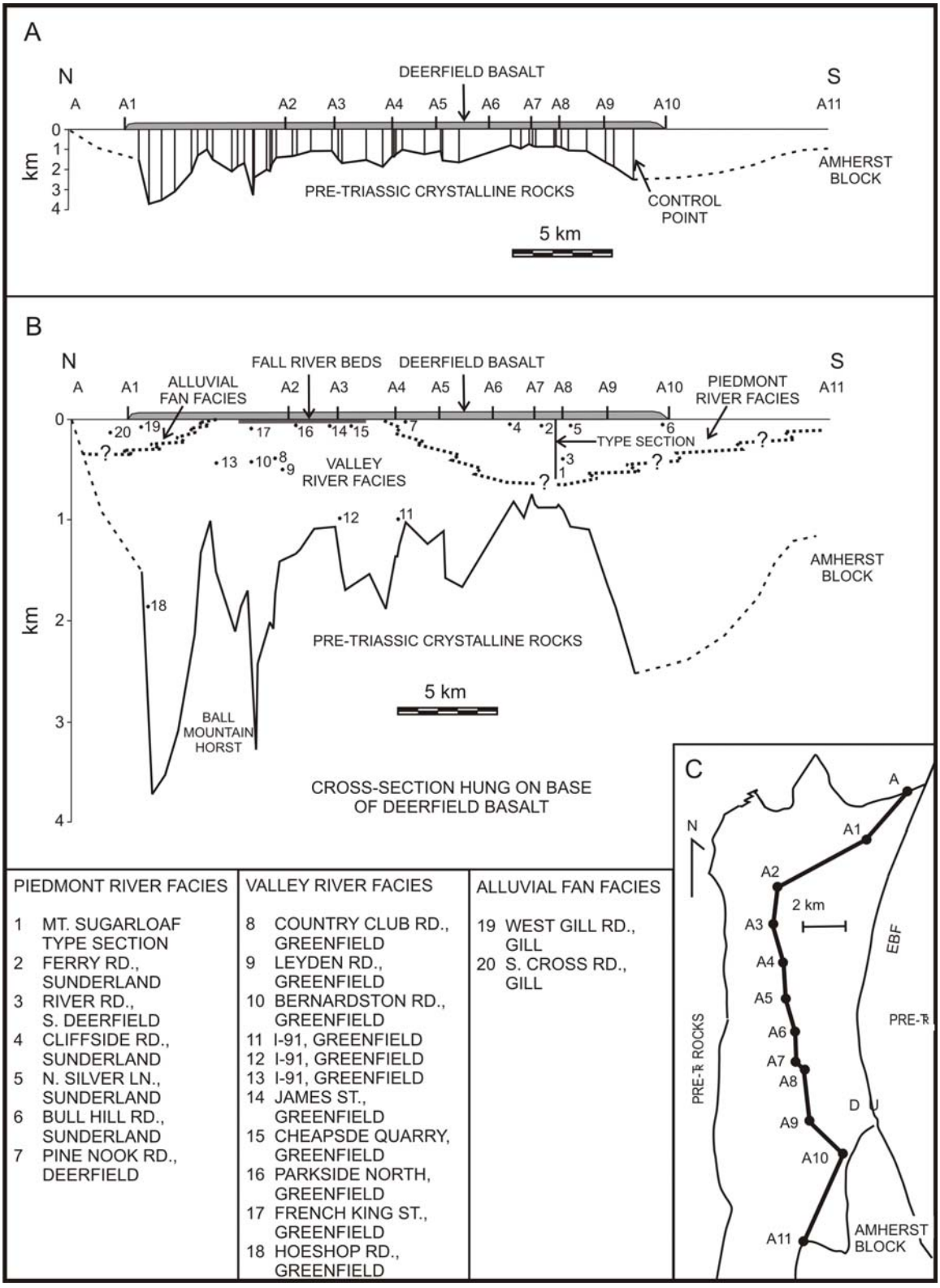
A
N
S
DEERFIELD BASALT
A
A1
A2
A3
A4
A5
A6
A7
A8
A9
A10
A11
km
0
1
2
3
4
PRE-TRIASSIC CRYSTALLINE ROCKS
AMHERST BLOCK
CONTROL POINT
5 km
B
N
S
FALL RIVER BEDS
DEERFIELD BASALT
ALLUVIAL FAN FACIES
PIEDMONT RIVER FACIES
TYPE SECTION
VALLEY RIVER FACIES
PRE-TRIASSIC CRYSTALLINE ROCKS
AMHERST BLOCK
BALL MOUNTAIN HORST
5 km
CROSS-SECTION HUNG ON BASE OF DEERFIELD BASALT
C
N
A
A1
A2
A3
A4
A5
A6
A7
A8
A9
A10
A11
2 km
EBF
PRE-TR ROCKS
AMHERST BLOCK
PIEDMONT RIVER FACIES
1 MT. SUGARLOAF TYPE SECTION
2 FERRY RD., SUNDERLAND
3 RIVER RD., S. DEERFIELD
4 CLIFFSIDE RD., SUNDERLAND
5 N. SILVER LN., SUNDERLAND
6 BULL HILL RD., SUNDERLAND
7 PINE NOOK RD., DEERFIELD
VALLEY RIVER FACIES
8 COUNTRY CLUB RD., GREENFIELD
9 LEYDEN RD., GREENFIELD
10 BERNARDSTON RD., GREENFIELD
11 I-91, GREENFIELD
12 I-91, GREENFIELD
13 I-91, GREENFIELD
14 JAMES ST., GREENFIELD
15 CHEAPSDE QUARRY, GREENFIELD
16 PARKSIDE NORTH, GREENFIELD
17 FRENCH KING ST., GREENFIELD
18 HOESHOP RD., GREENFIELD
ALLUVIAL FAN FACIES
19 WEST GILL RD., GILL
20 S. CROSS RD., GILL

An angular (~3°) unconformity separates the arkose from the lacustrine and paludal strata of the Fall River beds (Olsen, 1992; Hubert and Dutcher, 1999). Although the angular difference is slight, the unconformity represents a major transition from fluvial strata deposited in a hydraulically-open basin to deposition in a closed-basin of mostly lacustrine and playa strata, with some alluvial fan and fluvial strata, and basalt lavas (Tectono-sedimentary stages III and IV of Olsen, 1997; Hubert et al., 2008).

Cornet (1977) used spores and pollen to date the 0-9-m-thick Fall River beds as Early Jurassic, leading Zen (1983) to arbitrarily place the Triassic-Jurassic boundary 100 m below the top of the Sugarloaf Arkose on the geologic map of Massachusetts. More recent work suggests the Triassic-Jurassic boundary was removed by the erosional unconformity (Hubert and Dutcher, 1999; Lucas and Tanner, 2007). The Fall River beds have been mapped between Gill and Greenfield (Figure 2) (Olsen et al., 1992).

The 0-133-m-thick Deerfield Basalt comprises two flows (Wise and Hubert, 2003). Pillows, pipe vesicles, and wet-sediment folds indicate the lower flow traveled downslope eastward into a shallow lake at the top of the Fall River beds (Hubert and Dutcher, 1999). The high-iron, quartz-normative basalt correlates with the Holyoke and Orenaug basalts of the Hartford and Pomperaug basins, respectively (Philpotts et al., 1996; Philpotts, 1998), and is similar to basalt flows in the Newark basin (Olsen, 1997). The Deerfield and Holyoke basalts are a once-continuous lava-flow unit now separated by erosion (Philpotts, 1998). The Deerfield Basalt has an intermediate composition between a tholeiitic basalt and spillite, enriched in Na and depleted in Ca and Sr; the basalt was evidently diagenetically altered in the hot intraformational brines (O'Toole, 1981; Hubert and Dutcher, 1999). The age of the basalt

is ~200 Ma by correlation with the isotopically-dated Palisades sill in New Jersey (McHone and Philpotts, 1995; Schlische et al., 2002).

The Deerfield Basalt pinches out on Mt. Toby Conglomerate east of Mount Sugarloaf (Figure 3). The 300-2000-m thick conglomerate was deposited by four west-building alluvial fans with apices at the EBF (Wessel, 1969). The fanglomerate interfingers to the west with the Turners Falls Formation, which consists of ~2 km of interbedded playa redbeds, gray to black lacustrine strata, and minor fluvial redbeds (Handy, 1977; Hubert et al., 2008).

1.4.2 Basin Cross Sections

It is likely that in the Early Jurassic the basin was a half-graben created by a normal fault. The evidence is: 1) west-building alluvial fans in the Sugarloaf Arkose and Mt. Toby Conglomerate (Figure 3) (Wessel, 1969; Hubert et al., 2008); 2) lack of syn-depositional antithetic faults on the western edge of the basin or further to the west (Wise, 1992; Zen et al, 1983); and 3) eastward flow down the hanging block of piedmont rivers in the Sugarloaf Arkose, Deerfield Basalt flows, and some rivers in the Turners Falls Formation (Hubert and Dutcher, 1999; Hubert et al., 2008).

Figure 6 shows the N-S longitudinal cross section of the basin from the basement to the Deerfield Basalt. The basin has two ‘deeps’ near Greenfield and Deerfield. Depth to basement decreases between these ‘deeps’ in steps, apparently due to faulting. The horst near Ball Mountain in the northwest corner of the basin modifies the Greenfield ‘deep’ by the basement shallowing over the horst and deepening on the flanks. This horst cuts Triassic redbeds, indicating it formed after Sugarloaf Arkose deposition (Wise, 1992).

1.5 Depositional Facies in the Sugarloaf Arkose

This section summarizes the three depositional facies of the Sugarloaf Arkose (Hubert et al., 2008). Each facies is defined by paleocurrent vector means and sedimentary style (Figure 7). This thesis uses petrologic attributes to further define each facies (Chapter 2).

1.5.1 Valley-River Facies

Seventeen outcrops in the valley-river facies have average paleocurrent flow to the southwest, with individual outcrop vector means ranging from southwest to southeast.

The strata are predominantly pale red channel sandstones. Trough cross-bed sets and horizontally-laminated sandstones are common; less common are planar cross-beds of gravel and pebbly sandstone and ripple cross-laminated fine-grained sandstones. Mud drapes on cross-bed sets occur locally, in places contributing rip-up clasts in subsequent channel-fills. Grayish-red overbank mudstones make-up 10-20% of outcrop strata. The mudstones are poorly-sorted with significant sand and coarse silt, and are pervasively bioturbated. Traces to abundant ventifacts are found in pebbly sandstone strata, many from 10 to 40 cm in size. *Camborygma* isp. (crayfish) burrows, log casts, plant debris, and root casts are locally present.

The facies crops out in the northern third of the basin, from the bottom to the top of the arkose. The channel sandstones and overbank mudstones were deposited by a channel-overbank river system with a gravel and sand bedload. The river was mostly braided, as shown by numerous graded channel fills within individual channel bodies,

Figure 7. Paleocurrent and facies map of the Sugarloaf Arkose (Hubert et al., 2008). The solid arrows show paleoflow vector means for the fluvial redbeds. Open arrows are flow directions for the Deerfield Basalt. Numbers correspond to locations in Figure 6.

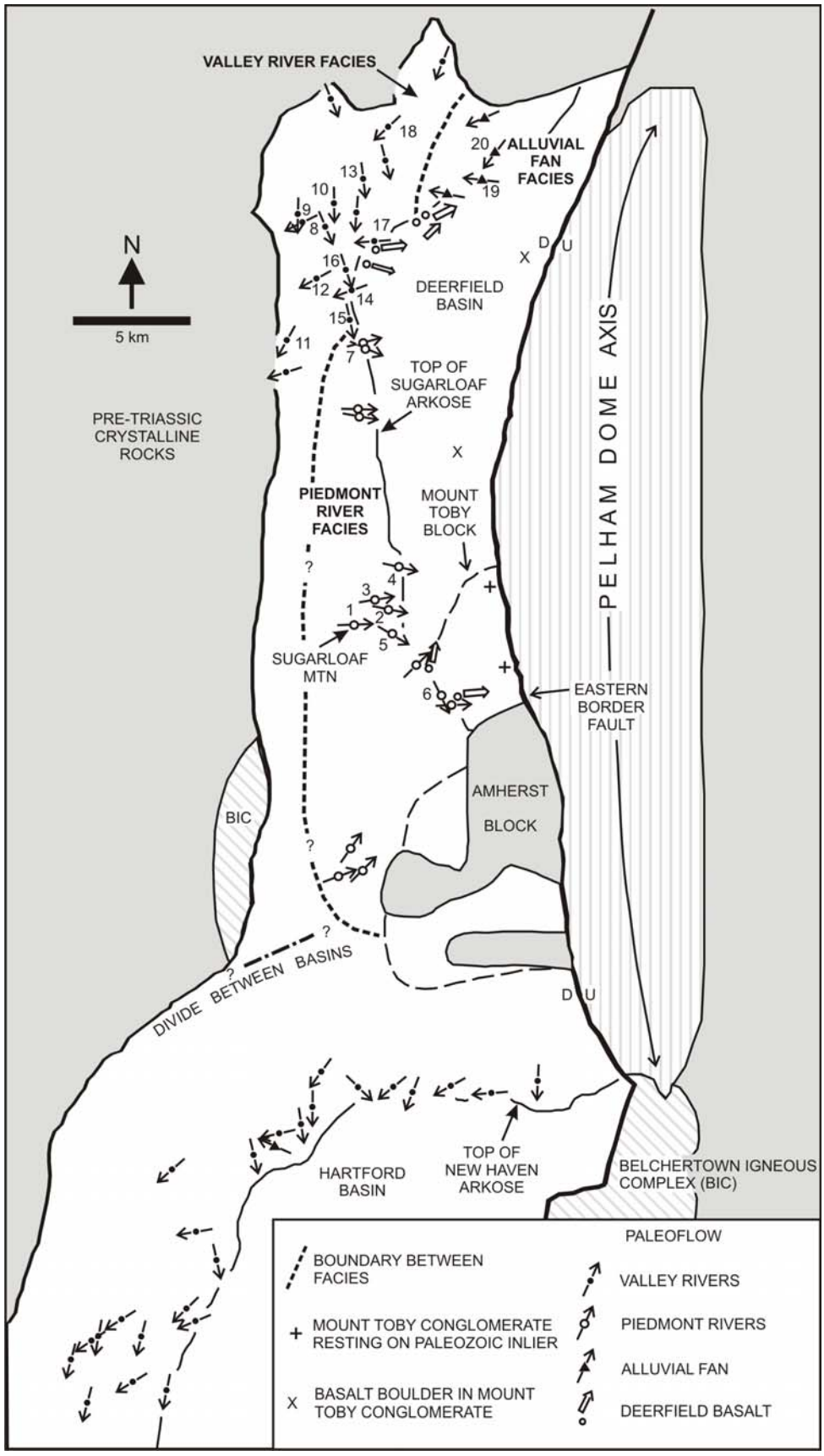
VALLEY RIVER FACIES
ALLUVIAL FAN FACIES
N
5 km
DEERFIELD BASIN
TOP OF SUGARLOAF ARKOSE
PRE-TRIASSIC CRYSTALLINE ROCKS
PIEDMONT RIVER FACIES
MOUNT TOBY BLOCK
PELHAM DOME AXIS
SUGARLOAF MTN
EASTERN BORDER FAULT
AMHERST BLOCK
BIC
DIVIDE BETWEEN BASINS
D U
HARTFORD BASIN
TOP OF NEW HAVEN ARKOSE
BELCHERTOWN IGNEOUS COMPLEX (BIC)
PALEOFLOW
BOUNDARY BETWEEN FACIES
VALLEY RIVERS
MOUNT TOBY CONGLOMERATE RESTING ON PALEOZOIC INLIER
PIEDMONT RIVERS
ALLUVIAL FAN
BASALT BOULDER IN MOUNT TOBY CONGLOMERATE
DEERFIELD BASALT

combined with the absence of lateral accretion surfaces and crevasse splay deposits. Similar braided river channels are present in the Massachusetts section of the Hartford basin (Figure 7) (Franz, 1978; Hubert et al., 1992).

1.5.2 Piedmont-River Facies

Paleocurrents are predominantly west to east, with flow vectors at 15 outcrops ranging from northeast to southeast.

The stacked channel fills of pebbly sandstone are mostly single stories made of fining-upward trough-cross-bed sets and minor horizontally-laminated sandstones. Planar cross-bed sets of gravel or pebbly sandstone are common near channel banks, or are present isolated within trough cross-bed cosets. Gleying and 'rainbow stone' occur locally. *Scoyenia* isp. burrows are pervasive, locally obliterating sedimentary structures. Pebble means of the 10 largest clasts range from 20-30 cm, with large boulders >50 cm. Overbank mudstones are rare, and do not make up a significant proportion of outcrop strata. Ventifacts are widespread.

The facies is present in the southern two-thirds of the basin, including the entire type section at Mount Sugarloaf. The lowest known occurrence of the facies is about in the middle of the arkose. The pebbly sandstones were deposited by braided rivers that drained highlands west of the basin. Individual river 'fans' coalesced on the east-dipping slope of the hanging wall, creating a megafan, which, compared to modern megafans, is relatively small, apparently limited by the size of the basin (Gawthorpe and Leeder, 2000; Leier et al., 2005).

1.5.3 Alluvial-Fan Facies

Two of the four outcrops have east to west paleocurrents, and two are to the southwest. At the best-exposed outcrop on West Gill Road, the beds grade upward from cobble-boulder conglomerate to pebbly sandstone. The beds have erosional bases, standing wave/antidune bedforms, minor pebbly sandstone plane beds, and subangular to rounded boulders. The mean of the 10 largest clasts is 25 cm. Ventifacts are present.

The facies crops out in the northeastern corner of the basin, about two-thirds up from the base of the arkose. Turbulent, shallow flash floods flowed westward from eastern highlands to build the alluvial fan. The floods spread, decelerated, and thinned on the fan surface, depositing the graded beds. The strata of this alluvial fan continue into the Mt. Toby Conglomerate, where it is named the Pisgah Mountain fan (Wessel, 1969).

Alluvial fan strata are also located along I-91 near the power plant just south of the Amherst block in the Massachusetts section of the New Haven arkose (Franz, 1979).

1.6 Pleistocene and Holocene Cover

The Connecticut River valley is located between the central Massachusetts uplands to the east and the Berkshire Mountains to the west. Pleistocene tills, glacial outwash, and varved lake-bottom clays and delta sands of glacial-lake Hitchcock are present in and around the valley, and cover Mesozoic strata of the Deerfield and Hartford basins (Brigham-Grette and Rittenour, 2003). Holocene alluvium of the Connecticut River blankets both glacial sediments and bedrock in the valley (Skehan, 2001). Pre-Mesozoic and Mesozoic rocks crop out predominantly along road cuts and river banks.

CHAPTER 2

PETROLOGY OF THE SUGARLOAF ARKOSE

2.1 Methods of Study

Except where noted, all data presented in this thesis was collected by the author using the methods described below.

2.1.1 Field Methods

Sandstones were collected from 17 outcrops distributed throughout the Sugarloaf Arkose. A hand lens and visual comparator were used to select samples made mostly of medium sand (0.25-0.5 mm). Three sandstones from each outcrop were selected for petrographic study. The locations of sampled outcrops in the valley-river facies are listed in Appendix A1, piedmont-river facies in A2, and alluvial-fan facies in A3.

Field work included 16 counts of pebble lithology (100 pebbles each) from 12 outcrops. Pebbles were randomly selected, and their long axis measured prior to determining lithology on a fresh surface. To reduce the effects of clast size on composition, only pebbles with long axes between 2.5 and 7.5 cm were tabulated; the lithology of larger clasts was also noted. Pebble data was combined with unpublished data from Stevens (1977). Pebble data generated from outcrops also sampled for medium sand are listed in Appendices A1, A2, and A3. Outcrops with only pebble counts are in Appendix A4.

Paleocurrent data from Hubert et al. (2008) were combined with additional paleocurrent azimuths. Cross-beds, parting lineations, flute and groove casts, and

channel axes were measured using a Brunton® compass. All paleocurrent measurements from strata dipping >10° were rotated to horizontal prior to plotting.

2.1.2 Laboratory Methods

Petrographic thin sections were made from 34 sandstones collected in the field. These thin sections were combined with existing thin sections from Taylor (1991) to yield 51 thin sections: 21 from the valley-river facies, 24 from the piedmont-river facies, and six from the alluvial-fan facies. Each thin section was impregnated with blue epoxy to minimize grain plucking during preparation. The thin sections were etched with HF acid prior to staining with sodium cobaltinitrate to distinguish K-feldspar from untwinned plagioclase, and with potassium ferrycyanide and Alizarin red-S to identify carbonates (Friedman, 1971).

Each thin section was examined using a Leitz model Laborlux 11 POL petrographic microscope and a point-count stage. Modal analyses were performed based on 400 counts per slide in four random traverses, using a modified Gazzi-Dickinson (G-D) point-counting method (Gazzi, 1966; Dickinson, 1970; Dickinson, 1985; Ingersoll et al., 1984).

The G-D method minimizes the effect of grain size on petrographic composition by separately tabulating the individual minerals within all rock fragments larger than the matrix (>0.0625 mm) as if they were detrital grains not in rock fragments. Dickinson (1985) cautioned that the G-D method does not correct for inherent or genetic variations in composition with grain size. For example, all plagioclase crystals in a source rock may be smaller than 0.25 mm, and can not be in a modal analysis of medium sand.

Grain size is a fundamental control on mineralogy. The G-D method of modal analysis used in this thesis is based on medium-sized sand (0.25-0.5 mm) and reduces the inherent correlation of composition with grain size. Evidence for this effect is seen in the work on mineralogy in modern sediments by Whitmore et al. (2004). They used 27 sample suites to demonstrate the range of variation of 34 modal and geochemical variables. Their results include variation: 1) from analytical error; 2) between different years in the same locality; 3) between multiple localities downstream; and 4) across grain sizes. Using variation expressed as a % departure from the average abundance of each mineral, the variation across grain sizes is generally greater than 50%, and variations due to analytical error (~10%), time (15-25%), and transport (~<50%) contributed less to overall compositional variation. Medium-sand samples generally displayed average values for most variables, with coarser and finer grain sizes plotting as outliers on ternary and "caterpillar" plots.

The first 100 points counted in each thin section determined the volume proportions of the whole-rock components, namely framework grains of all sizes, authigenic cements, accessory minerals, matrix, and pore space. The next 300 points were medium sand only, ignoring larger and smaller framework grains, cements, matrix, and pore space. Petrographic operational definitions are in Appendix B. Results of sandstone modal analyses using the G-D point-counting methodology for the valley-river, piedmont-river, and alluvial-fan facies are in Appendices C1, C2, and C3, respectively.

The degree of undulosity and number of subunits for 100 medium-sized quartz grains were noted during point-counting for use in provenance determination (Basu et al., 1975; Basu, 1985; Tortosa et al., 1991). To estimate roundness and sphericity of quartz,

grains were compared with visual standards (Pettijohn et al., 1987). Degree of sorting was estimated using visual comparators from Longiaru (1987). Results of sandstone modal analyses using the Basu-Tortosa method and textural estimations for the valley-river, piedmont-river, and alluvial-fan facies are in Appendices C4, C5, and C6, respectively.

Micrographs of representative grains were taken using a 10-bit Olympus® Q-Color 5 down-scope digital camera.

2.2 Sandstone Petrology

Table 1 summarizes the definitions of each ternary-plot pole and its components; Table 2 summarizes the mean values and 95% confidence limit for all ternary plots. Values may not add up to 100% due to rounding errors. WR is whole-rock and MS is medium-sand compositions.

2.2.1 Valley-river Facies

Detrital quartz grains are on average subangular and moderately-poorly sorted (Appendix C4). Quartz grains with high sphericity (52%) are more common than low (48%) (Pettijohn et al., 1987).

Figure 8. The major framework grain in whole rock and medium sand is unit quartz, comprising 26% and 28%, respectively. Granitoid grains and unit plagioclase are also major framework components. Interstitial detrital matrix (<30 μm; Appendix B) is ubiquitous. The proportions of cements and Fe-oxide-stained matrix are excluded from the medium-sand composition. Detrital micas are typically larger than medium-sand sized, reducing their contribution to the medium-sand. Medium-sand framework grains have more quartzite and monocrystalline vein quartz than the whole-rock.

Table 1: Definitions and components of plot poles

Pole	Definition	Components (Appendices B, C)
Qm	Total monocrystalline quartz	Unit quartz + monocrystalline vein quartz + quartz in granite, gneiss, schistose quartz, and schist
Qp	Total polycrystalline quartz	Annealed polycrystalline quartz + polycrystalline vein quartz + quartzite
Qt or Q	Total quartz	Qm+Qp
Tp	Twinned plagioclase (all laws)	Twinned single grain + twinned in granite and gneiss
Up	Untwinned plagioclase	Untwinned single grain + untwinned in granite and gneiss
P	Total plagioclase	Tp + Up + albitized single grain
Uk	Untwinned K-feldspar	Untwinned single grain + perthite single grain + untwinned in granite and gneiss + perthite in granite and gneiss
M	Microcline	Microcline single grain + microcline in granite and gneiss
K	Total K-feldspar	Uk + M
F	Total feldspar	P+K
Gr	Granite rock fragments	Quartz in granite, twinned and untwinned plagioclase in granite, untwinned K-feldspar and microcline in granite, illite replacement in granite, muscovite and biotite in granite
Gn	Granite-gneiss rock fragments	Quartz in gneiss, twinned and untwinned plagioclase in gneiss, untwinned K-feldspar and microcline in gneiss, illite replacement in gneiss, muscovite and biotite in gneiss
Qtzte	Quartzite rock fragments	Quartz in quartzite, groundmass in quartzite, muscovite and biotite in quartzite
L or R	Lithic fragments	Groundmass in schistose quartz, schist, and quartzite
Lt	Total lithic fragments	L/R + Qp
Qu	Undulose monocrystalline quartz	Qu
Qnu	Non-undulose monocrystalline quartz	Qnu
Qp (2-3)	Polycrystalline quartz with 2-3 subunits	Qp (2-3)
Qp (≥4)	Polycrystalline quartz with ≥4 subunits	Qp (≥4)

Table 2: Summary of Sandstone Composition

	Valley-river Facies		Piedmont-river Facies		Alluvial-fan Facies	
	WR Mean	MS Mean	WR Mean	MS Mean	WR Mean	MS Mean
Q	56.3±4.5	64.6±2.1	59.7±2.5	70.9±1.9	63.6±7.4	66.5±3.7
F	33.4±3.0	29.1±2.4	29.0±2.2	23.4±1.7	26.3±5.8	25.3±3.0
L or R	10.3±3.6	6.2±1.5	11.3±1.3	5.7±1.0	10.1±3.2	8.2±3.5
Qm	40.6±5.3	43.1±2.8	42.0±2.1	49.4±2.1	39.9±5.4	42.4±1.0
F	33.4±3.0	29.1±2.4	29.0±2.2	23.4±1.7	26.3±5.8	25.3±3.0
Lt	26.1±4.9	27.8±3.5	29.0±1.8	27.2±2.2	33.8±6.1	32.3±2.5
Qm	53.9±4.9	59.7±2.4	59.2±2.8	68.0±2.2	60.4±7.0	62.7±2.9
P	32.4±5.9	28.3±3.5	24.8±1.5	20.0±2.6	22.2±5.9	25.2±3.2
K	13.7±4.0	12.1±2.7	16.0±2.3	12.0±1.5	17.4±10.0	12.1±4.6
Qtzte	30.5±5.9	38.0±6.0	31.5±5.2	35.4±3.9	30.4±9.6	39.7±4.4
Gr	**40.9±5.8**	**34.0±4.5**	12.2±3.0	2.8±1.8	13.1±13.1	7.2±12.9
Gn	28.6±5.6	27.9±4.7	**56.3±4.3**	**61.8±4.6**	**54.5±12.4**	**53.1±13.6**
K	35.2±9.2	33.2±7.5	43.9±4.4	40.0±5.3	43.9±19.2	31.9±11.1
Tp	**23.4±4.9**	**41.4±4.6**	35.0±3.3	22.3±3.2	44.4±17.0	16.9±9.1
Up	41.4±6.4	25.5±4.0	21.1±2.5	37.7±4.1	11.6±8.5	51.2±8.7
P	69.5±7.4	69.8±6.6	61.5±3.5	61.6±4.7	59.2±17.7	68.1±10.4
Uk	17.8±6.7	24.0±5.2	28.4±3.8	32.5±4.6	20.0±20.0	22.7±9.6
M	12.7±6.7	6.2±2.3	10.1±3.6	5.9±1.5	20.7±10.1	9.1±4.3
Qnu	-	21.7±3.7	-	20.7±2.7	-	**9.7±1.7**
Qu	-	56.1±4.1	-	59.3±3.0	-	**72.2±4.9**
Qp(2-3)	-	18.5±1.6	-	13.1±1.4	-	10.0±2.6
Qp(≥4)	-	3.6±0.8	-	7.0±1.0	-	8.2±2.1

Figure 8. Pie diagrams of whole rock (A) and medium-sand (B) petrographic compositions of the valley-river facies. Micas are muscovite, biotite, and chlorite. Kspar is K-feldspar; Poly. is polycrystalline quartz; RF is rock fragment. For 7A, vein quartz includes monocrystalline and polycrystalline.

A

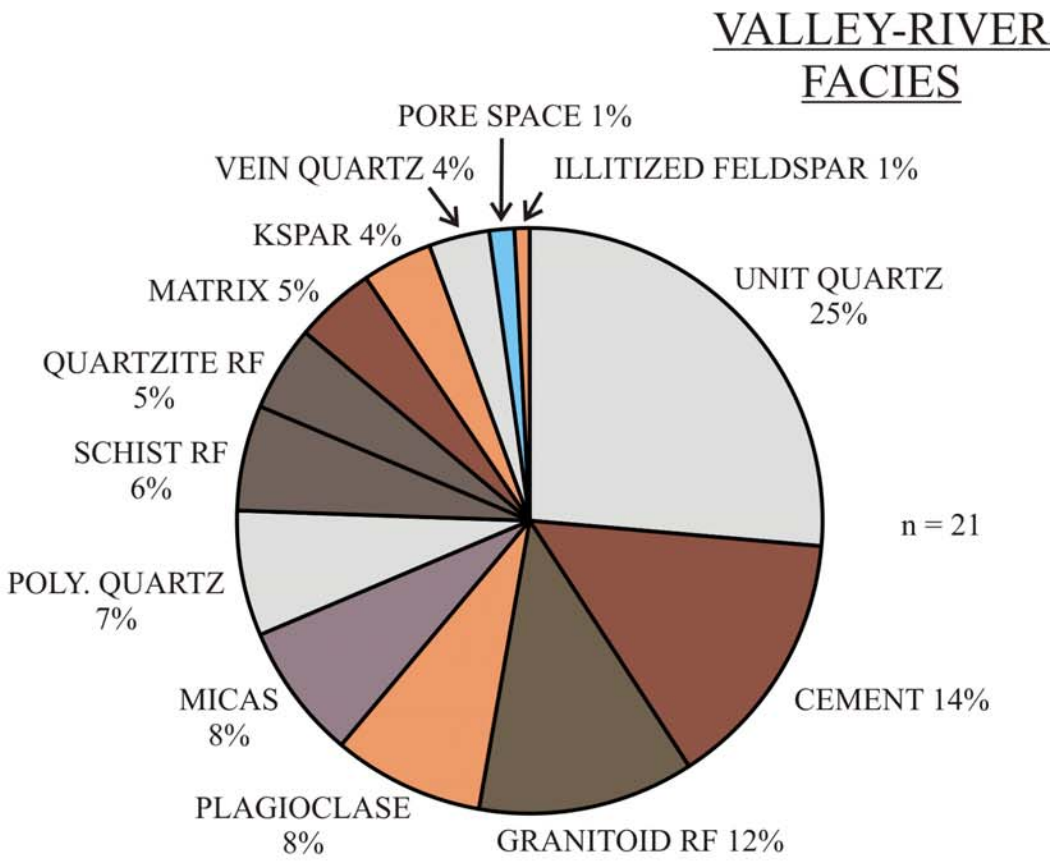
VALLEY-RIVER FACIES
PORE SPACE 1%
VEIN QUARTZ 4%
ILLITIZED FELDSPAR 1%
KSPAR 4%
MATRIX 5%
QUARTZITE RF 5%
SCHIST RF 6%
POLY. QUARTZ 7%
MICAS 8%
PLAGIOCLASE 8%
GRANITOID RF 12%
CEMENT 14%
UNIT QUARTZ 25%
n = 21

B

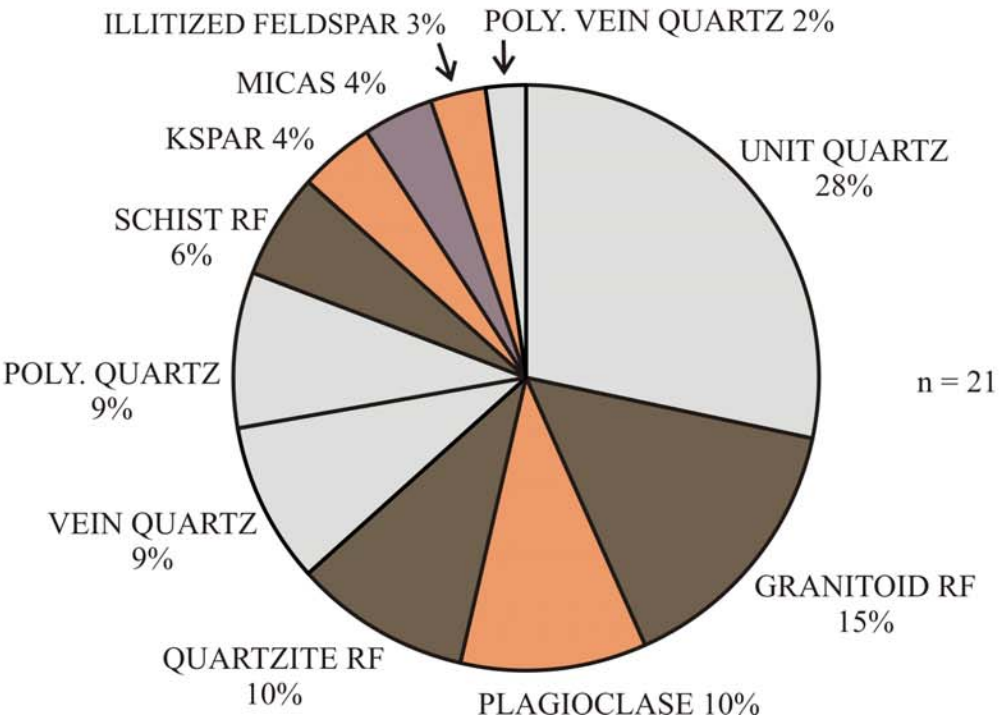
ILLITIZED FELDSPAR 3%
POLY. VEIN QUARTZ 2%
MICAS 4%
KSPAR 4%
SCHIST RF 6%
POLY. QUARTZ 9%
VEIN QUARTZ 9%
QUARTZITE RF 10%
PLAGIOCLASE 10%
GRANITOID RF 15%
UNIT QUARTZ 28%
n = 21

The means of the whole-rock and medium-sand samples are minerlogically-immature arkose on the Q-F-R classification diagram. (Pettijohn, 1975) (Figure 9). Whole-rock sample 13 is a lithic arenite and 14 and 15 are lithic arkoses. For medium sand, the samples shift away from the R pole and towards the Q pole. The quartz enrichment in the medium sand is due to abrasion of micaceous rock fragments and increase in monocrystalline vein quartz and quartzite (Figure 8B). The tighter cluster of points in the medium sand compared to the whole rock reflects the interaction between grain size and mineralogy (Section 2.1.2).

Figure 9. Whole-rock and medium-sand samples 1-6 are more mineralogically-mature sublitharenites and quartz arenites. These samples are from I-91 location 1 and Lower Rd., Greenfield. Detrital feldspars and albite cement in these samples were replaced by illite during a hydrothermal event about 184 Ma (Taylor, 1991; Hubert et al., 2001). Although relict grain boundaries of feldspar can occasionally be discerned, the data remain non-representative of original rock petrology, and so were not used to calculate means (Helmold, 1985).

Figure 10A. On the Qt-F-L plot, eight samples plot in the transitional field of the continental block provenance, and seven in the recycled orogen provenance (Dickinson, 1985). There are no trends of maturity or stability among the data. The mean is on the transition between continental block and recycled orogen provenance.

Figure 10B. Combining polycrystalline quartz with lithic fragments on the Qm-F-Lt plot shifts the samples towards the Lt pole (Figure 10B). Only one sample remains in the continental block provenance; six now plot in the dissected arc field of the magmatic arc provenance, and the remaining points and the mean plot within the ‘mixed’

Figure 9. Q-F-R plots of whole rock (A) and medium-sand (B) in the valley-river facies (Pettijohn, 1975). A circled point is the mean, and a dashed hexagon shows the 95% confidence interval around the mean. A shaded field indicates samples from the illite diagenetic pattern (Taylor, 1991; Hubert et al, 2001). The poles are defined in Table 1; Q is quartz, F is feldspar, and R is rock fragments. Numbers correspond to sample numbers in Appendix C.

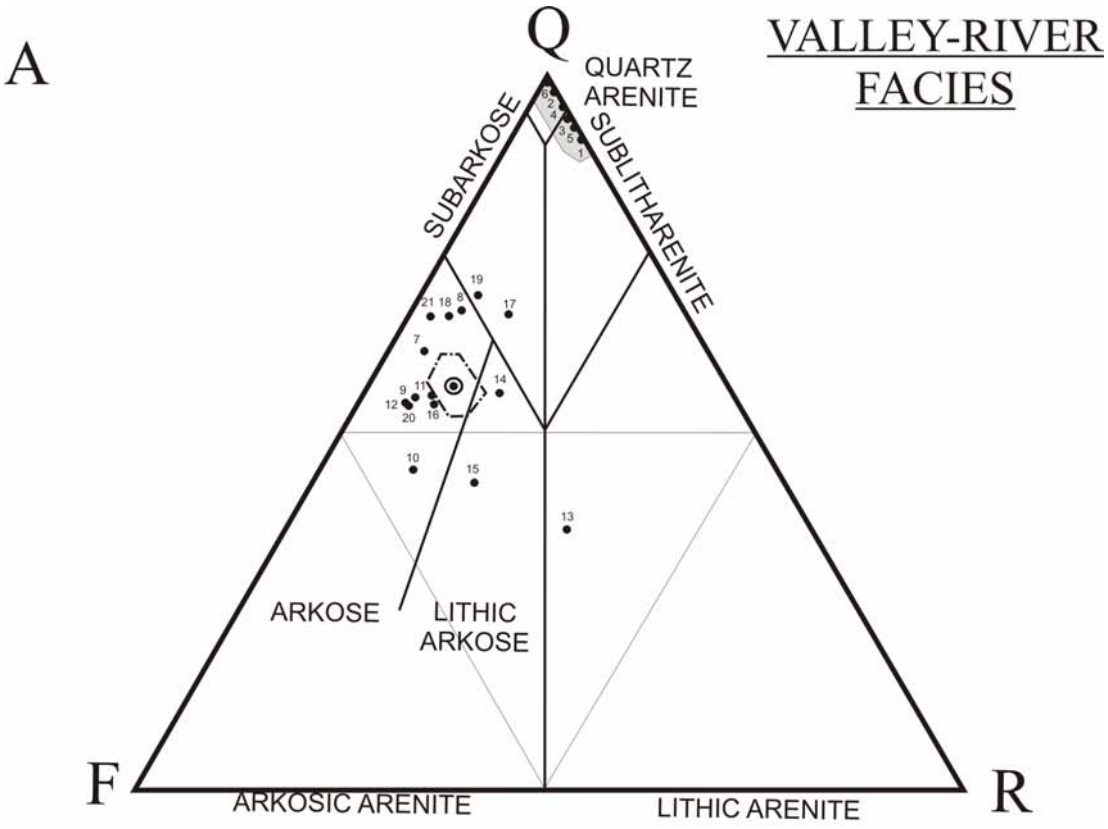
A
VALLEY-RIVER FACIES
Q
QUARTZ ARENITE
SUBARKOSE
SUBLITHARENITE
ARKOSE
LITHIC ARKOSE
F
R
ARKOSIC ARENITE
LITHIC ARENITE

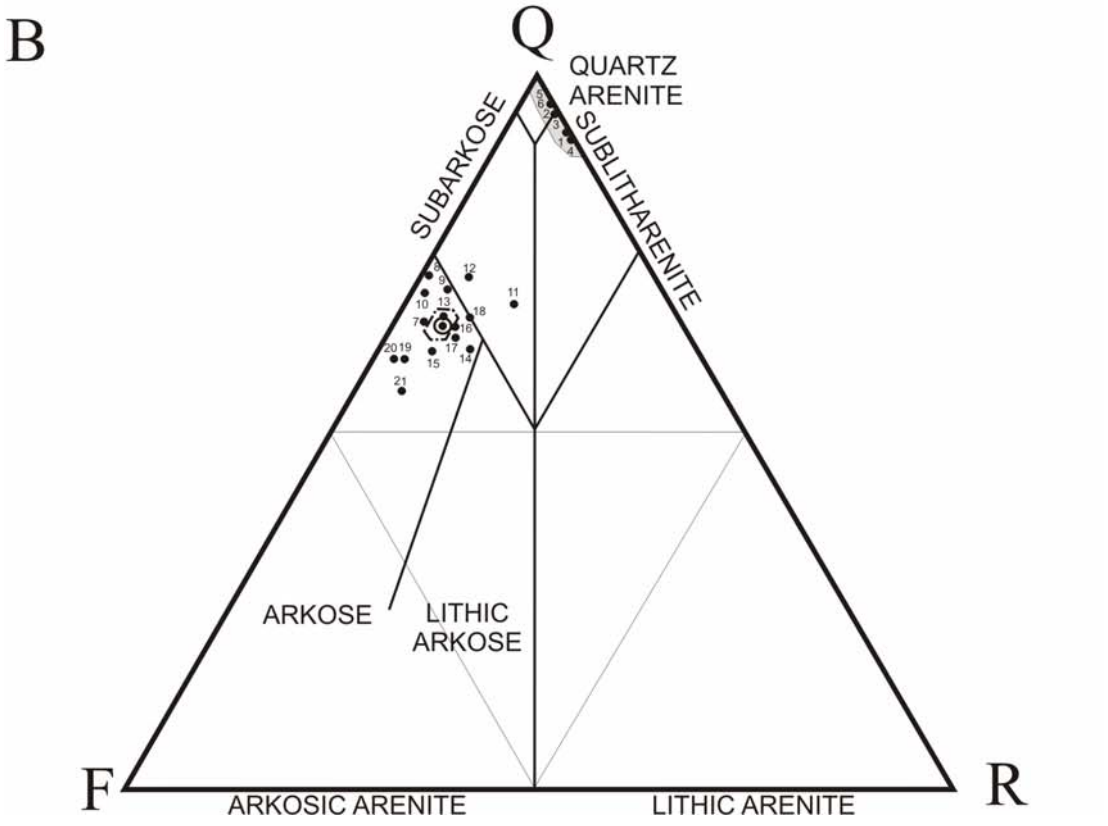
B
Q
QUARTZ ARENITE
SUBARKOSE
SUBLITHARENITE
ARKOSE
LITHIC ARKOSE
F
R
ARKOSIC ARENITE
LITHIC ARENITE

Figure 10. Qt-F-L (A) and Qm-F-Lt (B) plots of medium sand in the valley-river facies (Dickinson, 1985). For 10B, the center field is mixed provenance. A circled point is the mean, and a dashed hexagon shows the 95% confidence interval around the mean. The poles are defined in Table 1; Qt is total quartz, F is feldspar, L is lithic fragments, Qm is monocrystalline quartz, and Lt is total lithic fragments. Numbers correspond to sample numbers in Appendix C.

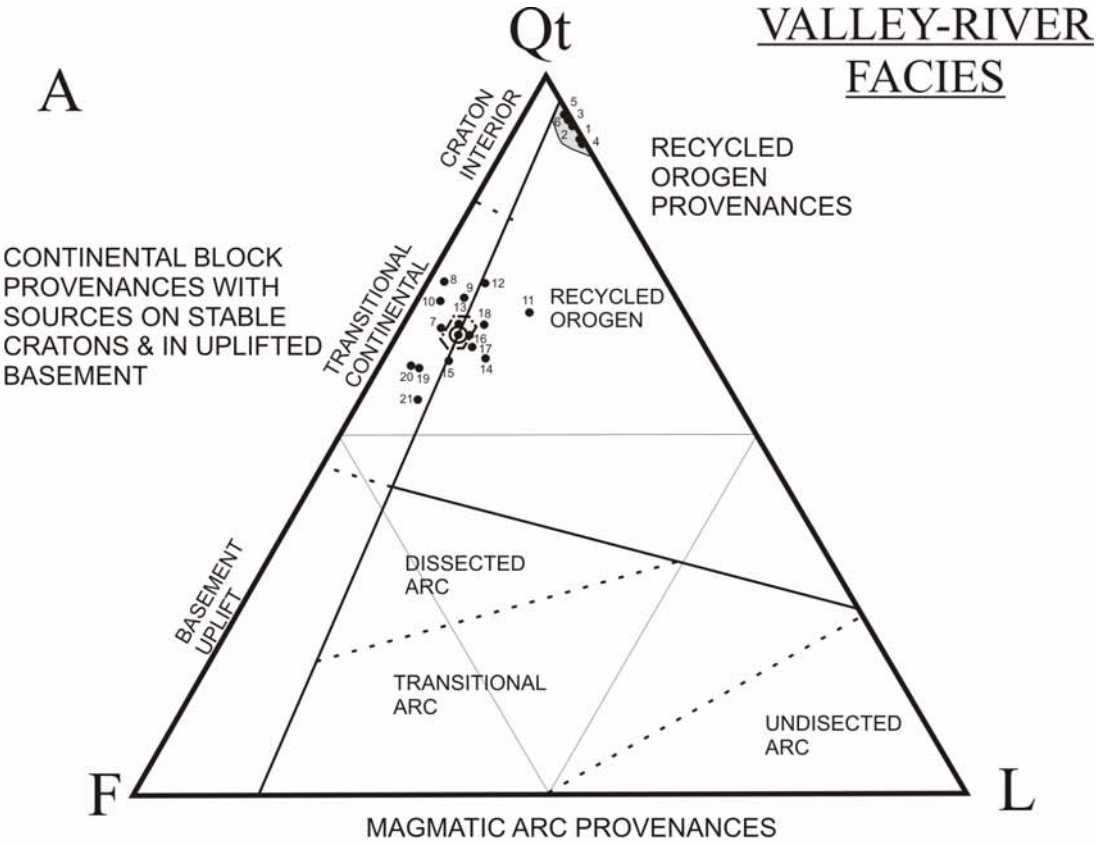
A
Qt
VALLEY-RIVER FACIES
CRATON INTERIOR
RECYCLED OROGEN PROVENANCES
CONTINENTAL BLOCK PROVENANCES WITH SOURCES ON STABLE CRATONS & IN UPLIFTED BASEMENT
TRANSITIONAL CONTINENTAL
RECYCLED OROGEN
BASEMENT UPLIFT
DISSECTED ARC
TRANSITIONAL ARC
UNDISECTED ARC
F
L
MAGMATIC ARC PROVENANCES

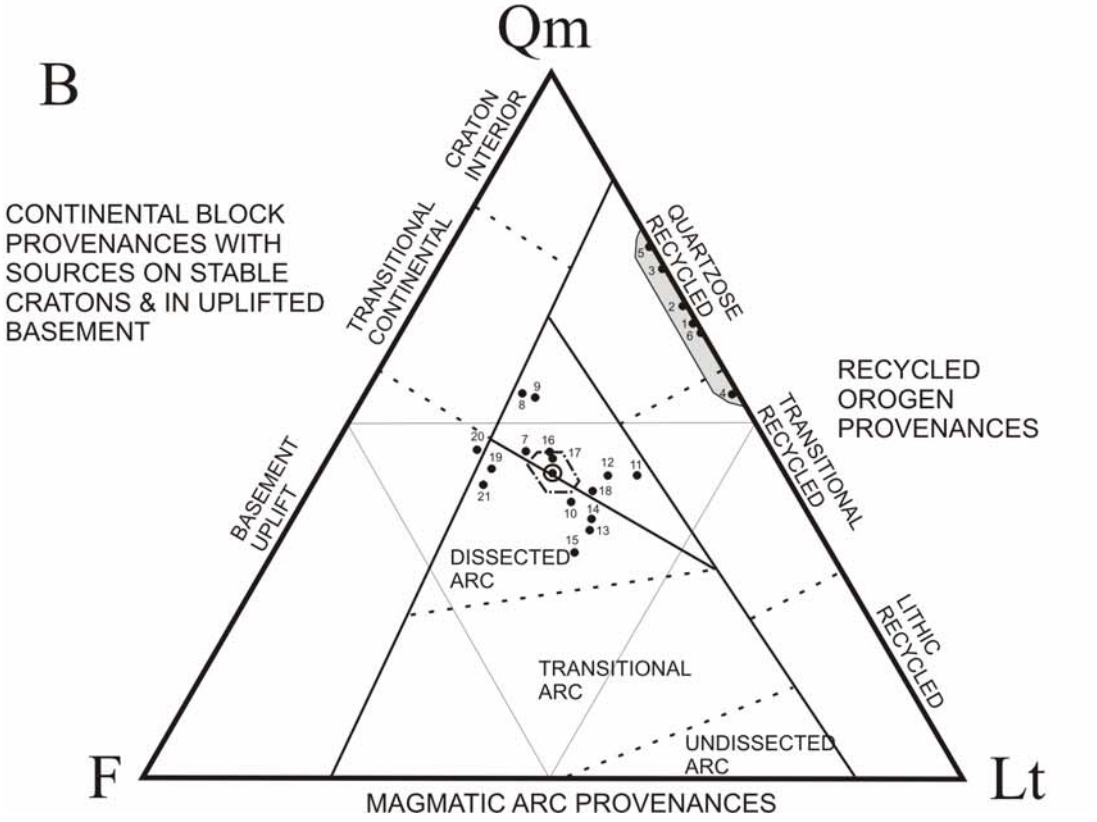
B
Qm
CRATON INTERIOR
CONTINENTAL BLOCK PROVENANCES WITH SOURCES ON STABLE CRATONS & IN UPLIFTED BASEMENT
TRANSITIONAL CONTINENTAL
QUARTZOSE RECYCLED
RECYCLED OROGEN PROVENANCES
TRANSITIONAL RECYCLED
BASEMENT UPLIFT
DISSECTED ARC
LITHIC RECYCLED
TRANSITIONAL ARC
UNDISSECTED ARC
F
Lt
MAGMATIC ARC PROVENANCES

field at the center of the diagram.

Figure 11A. Monocrystalline framework grains are plotted on the Qm-P-K diagram (Dickinson, 1985). Samples 1-6 are omitted because of illitization of feldspars. The valley-river facies is enriched with monocrystalline quartz, with only one sample plotting at <50% Qm. Plagioclase is more abundant than K-feldspar by a ratio of ~4:1 (Table 2). Samples 13, 14, and 15 are furthest towards the P pole, a position described by Dickinson and Suczek (1979) as an immature or unstable continental block provenance. Positions closer to the Qm pole indicate increasing maturity or stability.

Figure 11B. Here granite is defined as felsic, phaneritic grains with non-sutured quartz, twinned plagioclase, and microcline and/or untwinned K-feldspar (Figure 12 A; Appendix B). Granite gneiss has the same minerals, but metamorphism tended to produce untwinned plagioclase with or without sericitization, and quartz with sutured and/or crenulated boundaries (Figure 12B). Granite grains are slightly more common than granite gneiss in the valley-river facies, but none of the samples plots closer than 48% towards either pole. The mean is close to the center of Figure 11B, indicating that the three rock fragments plotted are subequal.

Figure 13A. Twinning of feldspars in rock fragments is a key part of the operational definitions of granites and granite gneisses used in this thesis. No valley-river samples have more than 50% untwinned plagioclase, and the mean is 41.4% twinned plagioclase. Diagenetic albitization of detrital plagioclase occasionally obscures twinning, so only grains with minor albite replacement or albite overgrowths were plotted (Figure 14A).

Figure 11. Qm-P-K (A; Dickinson, 1985) and Qtzte-Gr-Gn (B) plots of medium sand in the valley-river facies. Samples 1 through 6 are omitted from 11A due to diagenetic illitization of feldspars. A circled point is the mean, and a dashed hexagon is the 95% confidence interval around the mean. The poles are defined in Table 1; Qm is monocrystalline quartz, P is plagioclase, K is K-feldspar, Qtzte is quartzite, Gr is granite, and Gn is gneiss. Numbers correspond to sample numbers in Appendix C.

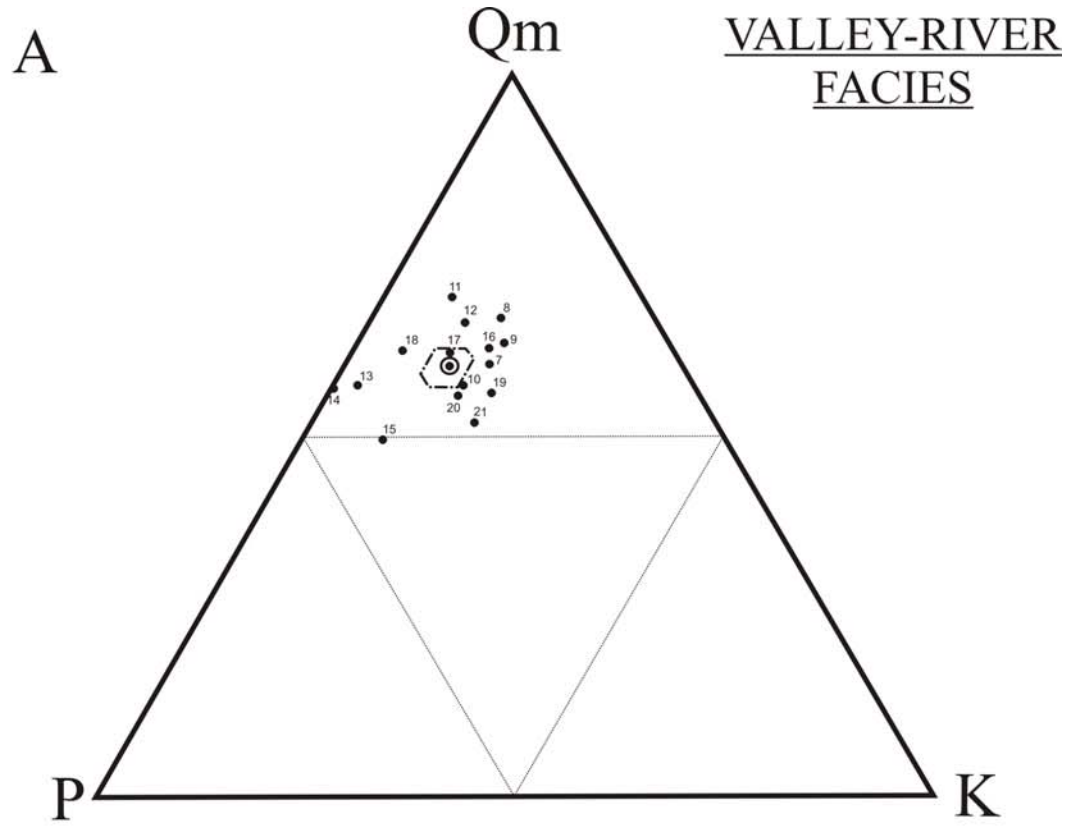
A
Qm
VALLEY-RIVER
FACIES
P
K
11
12
8
18
17
16
9
7
13
14
10
19
20
21
15

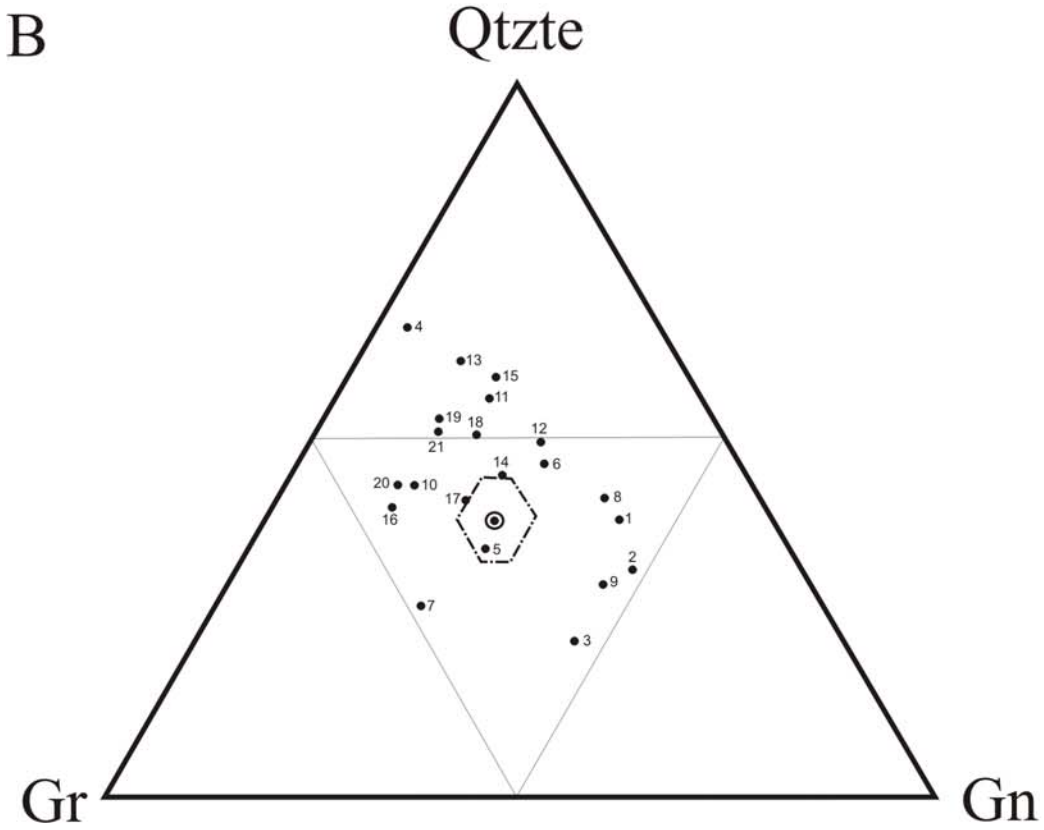
B
Qtzte
Gr
Gn
4
13
15
11
19
18
12
21
14
6
20
10
17
8
16
1
5
2
9
7
3

Figure 12. Micrographs of granite (A) and granite gneiss (B). P is plagioclase (twinned in A; untwinned in B); K is K-feldspar; Q is quartz; SQ is stretched quartz with crenulated grain boundaries (white arrow); M is muscovite; and A is albite overgrowth in optical continuity with albite replacement of plagioclase (black arrow). Crossed nicols; scale bars are 0.5 mm.

A

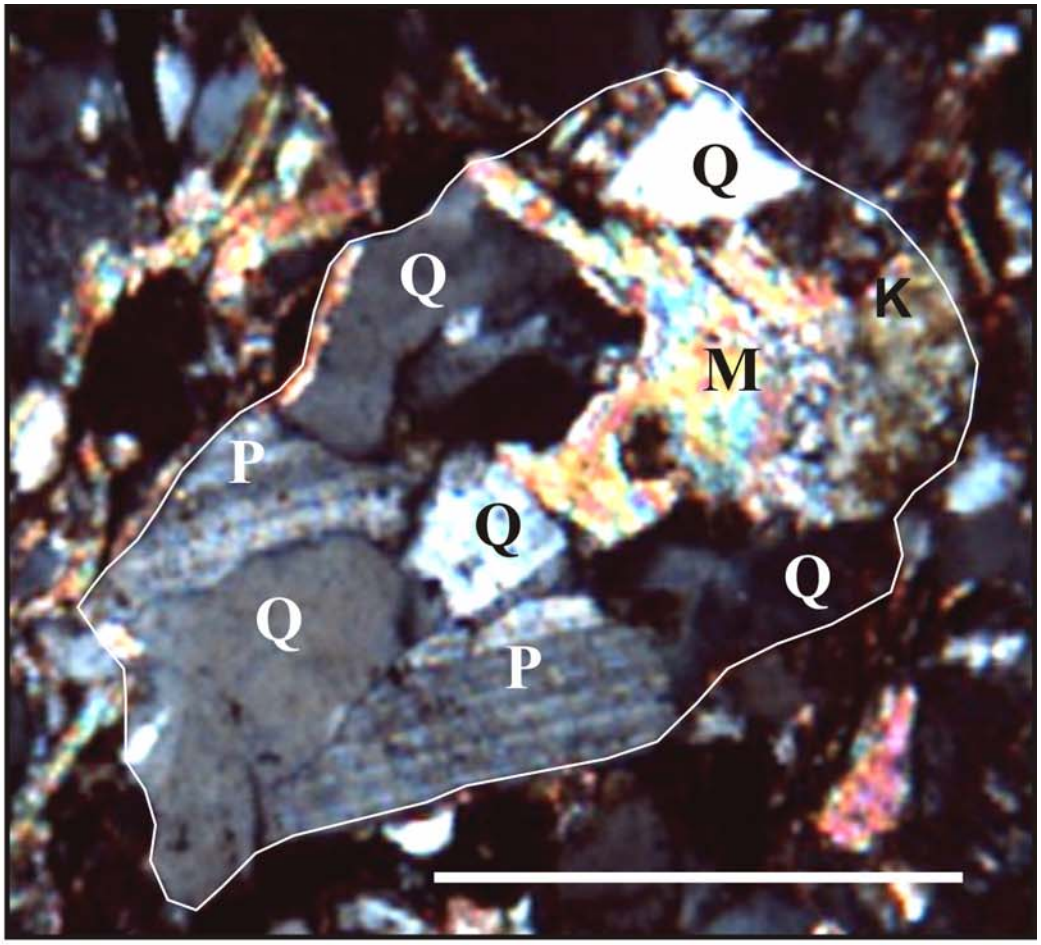

B

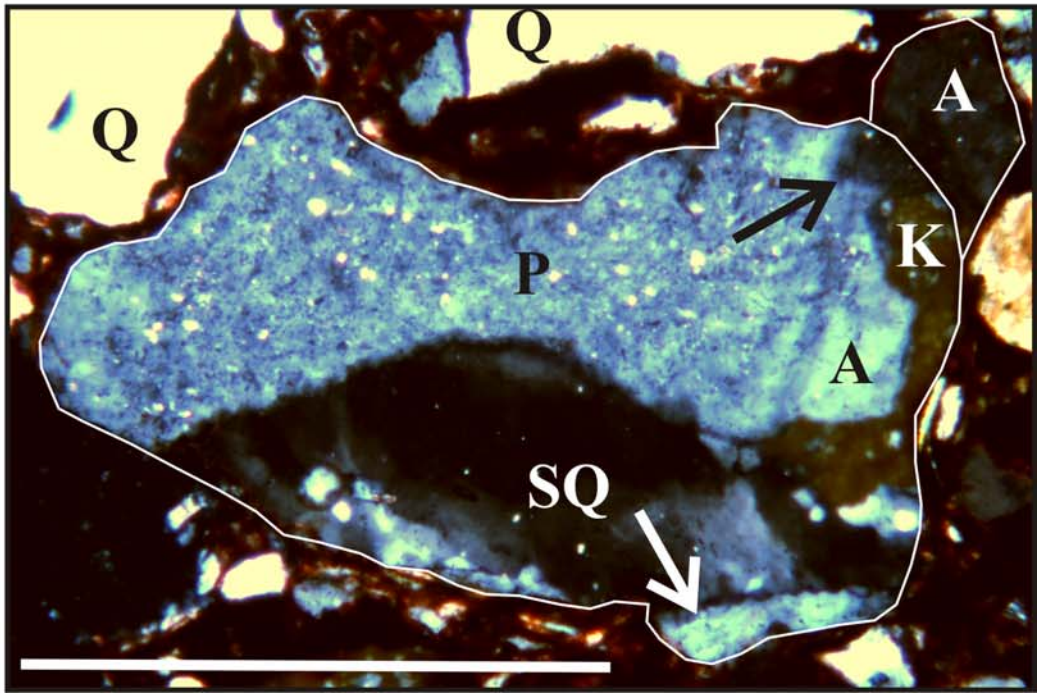

Figure 13B. The ratio of untwinned K-feldspar, including orthoclase and perthite, to microcline in the valley-river samples is ~4:1. Most samples have less than 10% microcline; samples 7-9 were collected from I-91 location 3, Greenfield, and contain the most microcline, with an outcrop mean of 13%. Again, only grains with minor albite replacement are plotted (Figure 14B).

Figure 15A. The undulosity and polycrystallinity of quartz grains are plotted on modified provenance diagrams (Basu et al., 1975; Basu, 1985). These workers constructed a polygonal plot from two ternary plots that share a common baseline that links monocrystalline non-undulose quartz (Qnu) and undulose quartz (Qu) (Appendix B). In the upper triangle, the Qp pole is polycrystalline quartz with ≥75% polycrystalline quartz composed of two or three subunits. In the lower, inverted triangle, the Qp pole has >25% polycrystalline quartz composed of four or more subunits.

All valley-river samples plot in the upper triangle, indicating coarsely-polycrystalline quartz is more common than finely-polycrystalline quartz. Of the 21 samples, 18 plot in the low-rank (<500^{o}C) metamorphic field (Figure 15A). Samples 19, 20, and 21, collected just below the Deerfield Basalt at Poet's Seat in Greenfield, contain considerably more non-undulose monocrystalline quartz than the other samples and are in the middle- and upper-rank metamorphic field, (500-700^{o}C).

Figure 15B. Here the provenance fields are added to the polygonal diagram (Tortosa et al., 1991). These authors generated the fields by examination of Holocene sands in first-order streams that drain terrains of granitic, gneissic, and low-rank metamorphic rocks. The boundary between low- and high-rank gneisses is the 500^{o}C line in Figure 15A.

Figure 13. K-Tp-Up (A) and P-Uk-M (B) plots of medium sand in the valley-river facies. A circled point is the mean, and a dashed hexagon is the 95% confidence interval around the mean. The poles are defined in Table 1; K is K-feldspar, Tp is twinned plagioclase, Up is untwinned plagioclase, P is plagioclase, Uk is untwinned K-feldspar, and M is microcline. Numbers correspond to sample numbers in Appendix C. Samples 1 through 6 are omitted due to diagenetic illitization of feldspars.

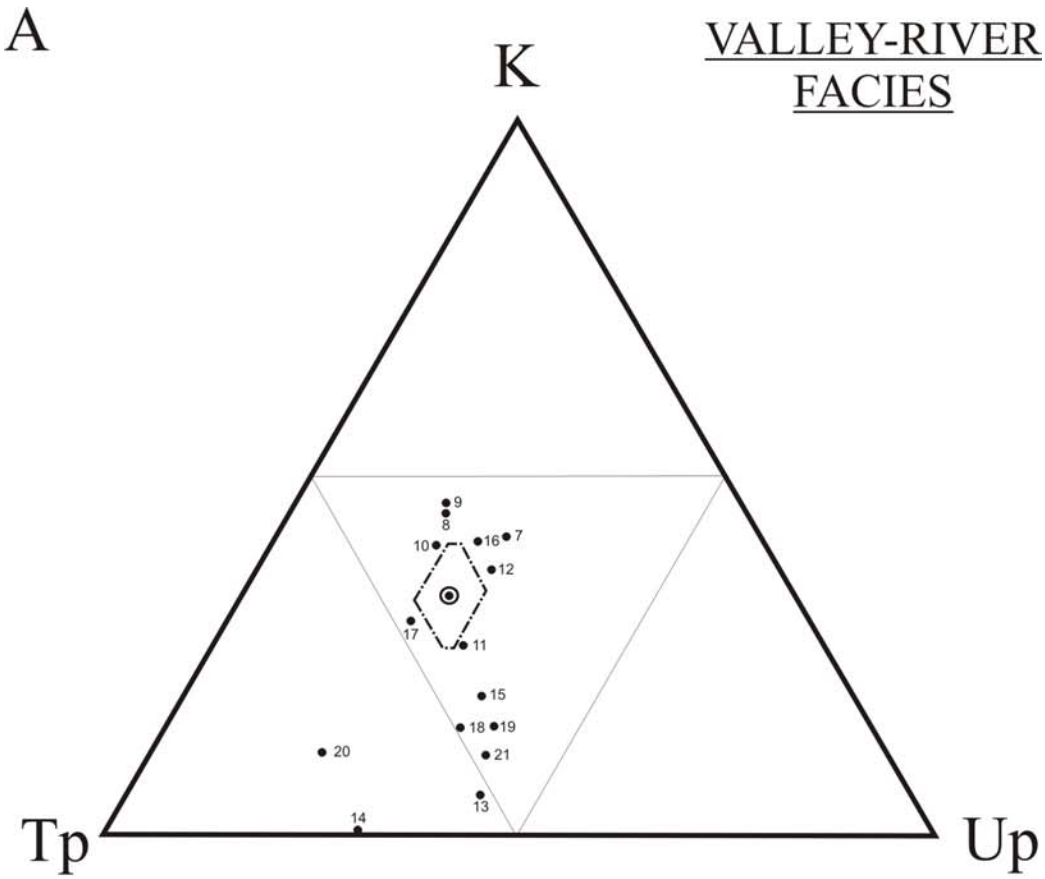
A
VALLEY-RIVER FACIES
K
Tp
Up
9
8
10
16
7
12
17
11
15
18
19
20
21
13
14

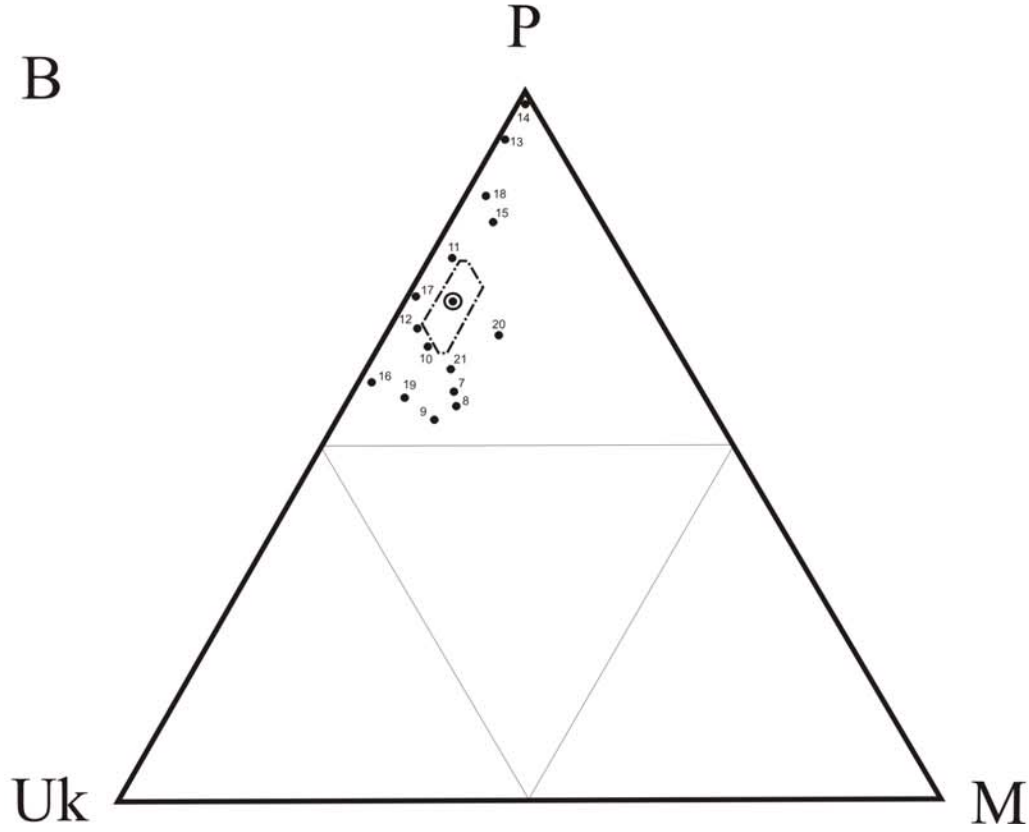
B
P
Uk
M
14
13
18
15
11
17
12
20
10
21
16
19
7
8
9

Figure 14. Micrographs of grains of twinned plagioclase (A) and untwinned K-feldspar (B; at extinction). H1 is early hematite rim formed by dehydration of yellow-brown surface stain; H2 is late hematite cement (Taylor, 1991; Hubert et al., 2001); Q is quartz; P is plagioclase; A is albite replacement along mineral fractures; and C is Fe-dolomite with minor Fe-calcite cements. White arrows point to albite overgrowths. Crossed nicols; scale bars are 0.25 mm.

A

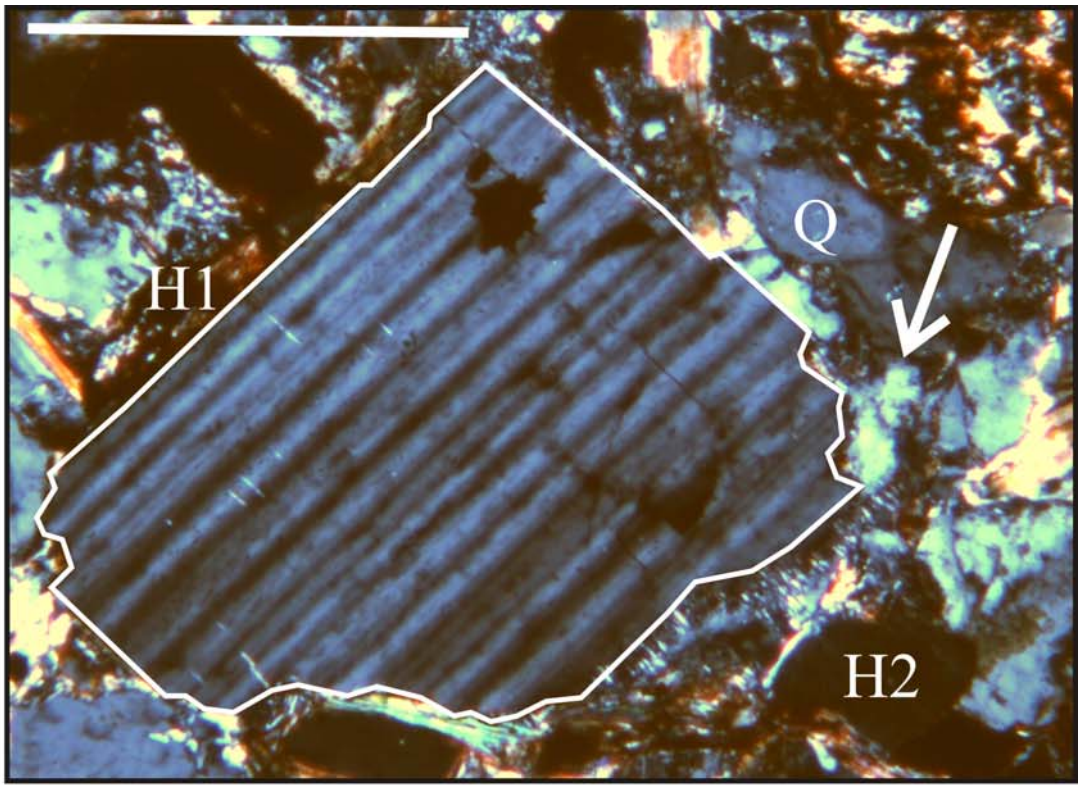

B

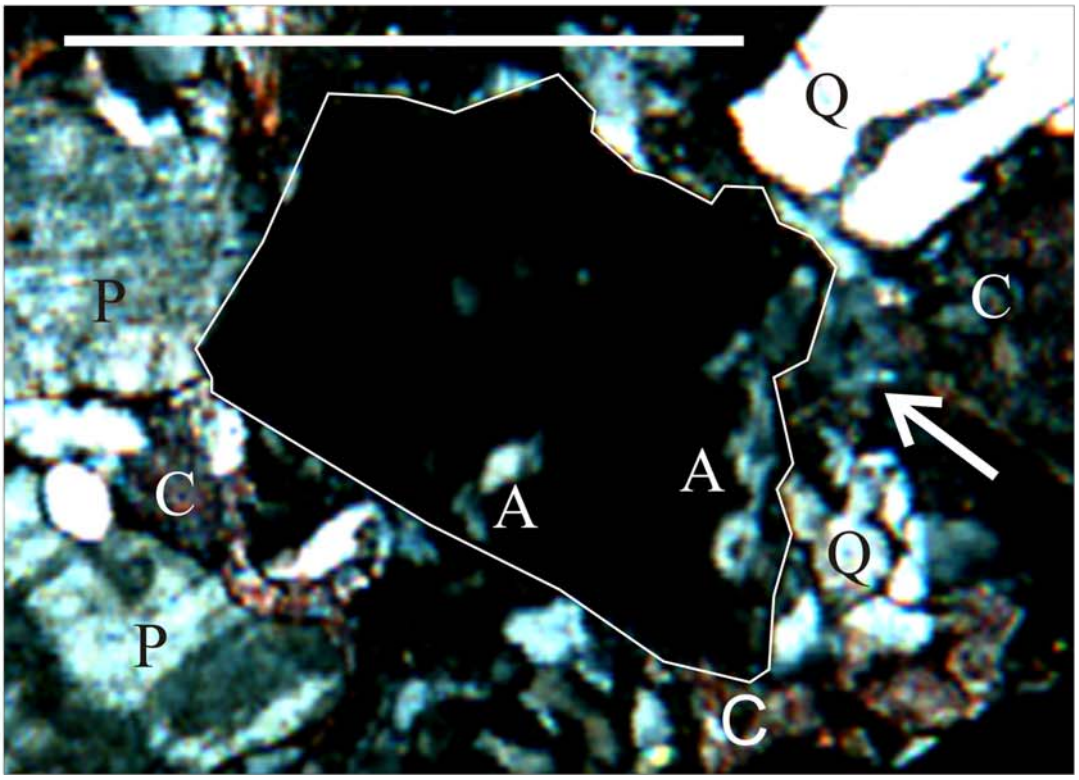

Figure 15. A. Qp-Qnu-Qu modified plot of provenance of medium-sand quartz in the valley-river samples (Basu, 1985). B. Qp-Qnu-Qu modified plot of Tortosa et al. (1991). The plots are truncated at 50% Qp. A circled point is the mean, and a dashed hexagon is the 95% confidence interval around the mean. The poles are defined in Table 1; Qp 2-3 is polycrystalline quartz with two or three subunits, Qp ≥4 is polycrystalline quartz with four or more subunits, Qnu is non-undulose monocrystalline quartz, and Qu is undulose monocrystalline quartz. Numbers correspond to sample numbers in Appendix C.

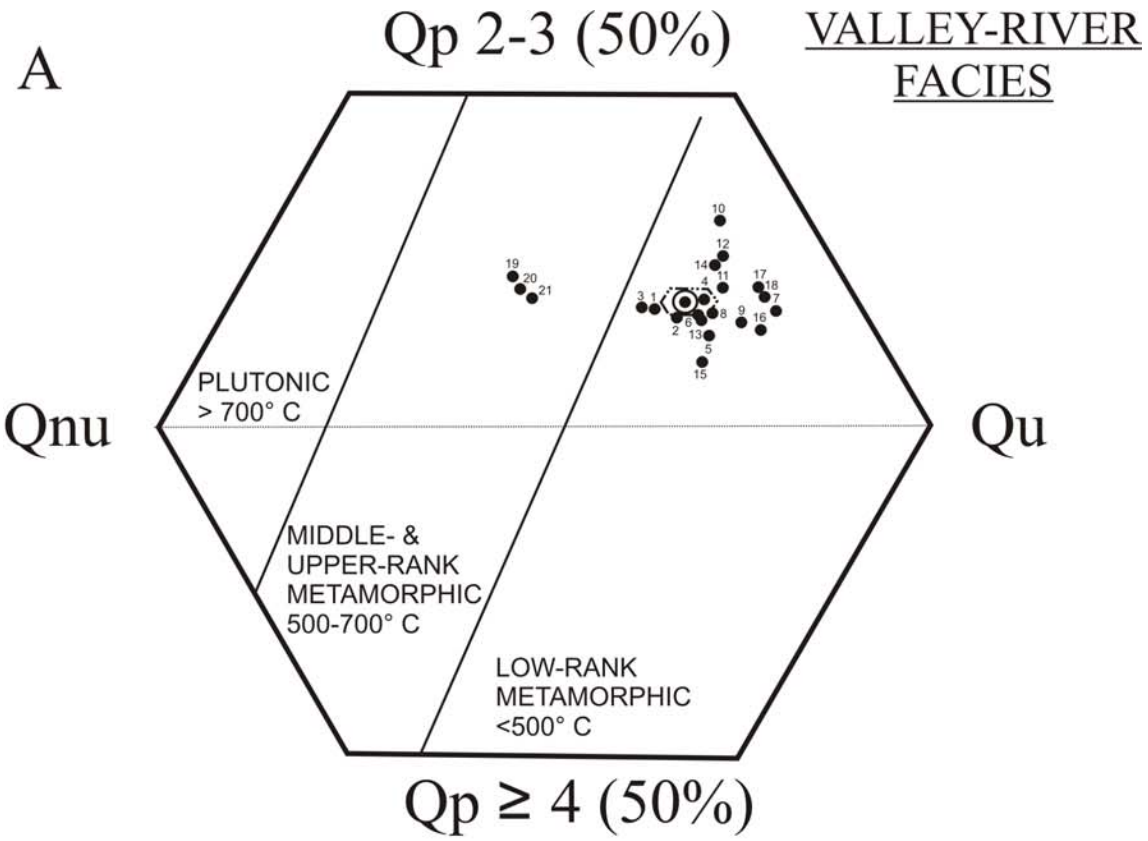
A
Qp 2-3 (50%)
VALLEY-RIVER FACIES
PLUTONIC
> 700° C
MIDDLE- &
UPPER-RANK
METAMORPHIC
500-700° C
LOW-RANK
METAMORPHIC
<500° C
Qnu
Qu
Qp ≥ 4 (50%)

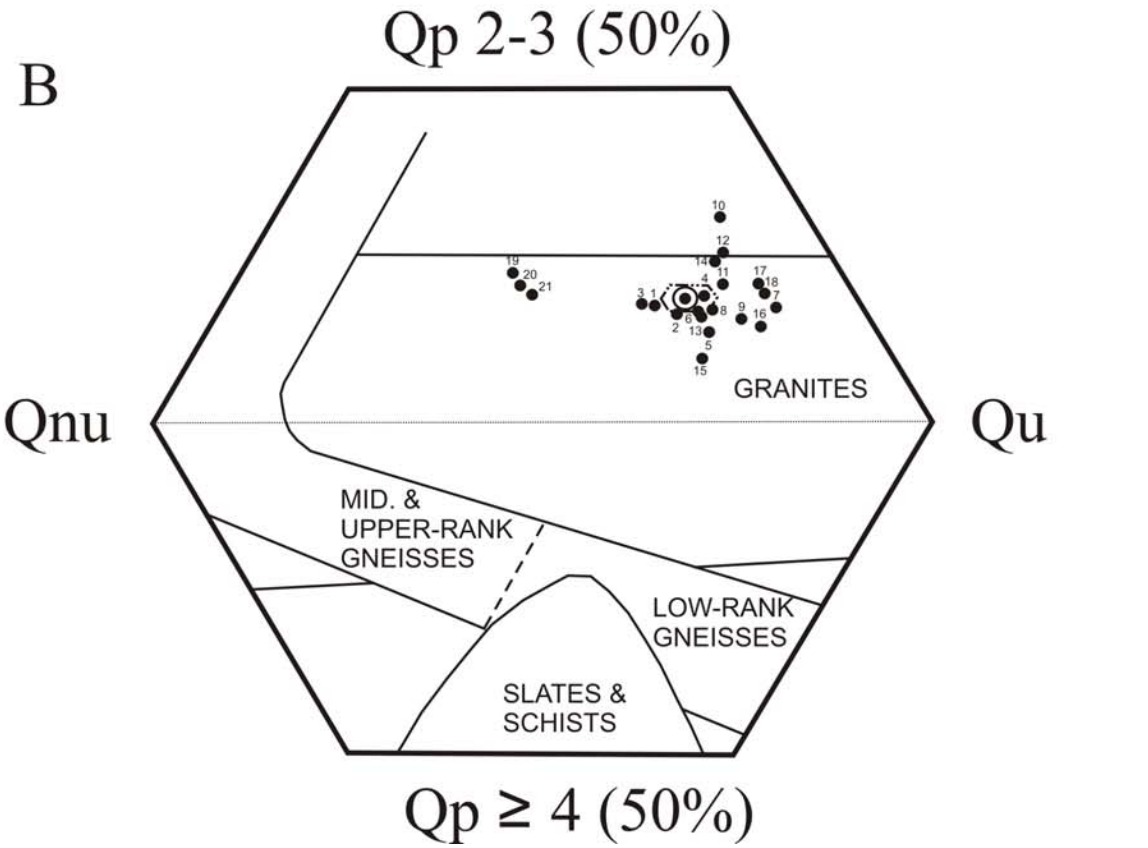
B
Qp 2-3 (50%)
GRANITES
MID. &
UPPER-RANK
GNEISSES
LOW-RANK
GNEISSES
SLATES &
SCHISTS
Qnu
Qu
Qp ≥ 4 (50%)

The samples plot in the same positions as Figure 15A, with 19 samples in the granite field. Samples 19, 20, and 21 are closer to upper-rank gneiss. Samples 10 and 12 plot just above the granite field, because the provenance fields are gradational.

Summary. Whole-rock and medium-sand framework grains in the valley-river samples are dominated by unit quartz, granite, granite gneiss rock fragments, and plagioclase (Figures 8 and 9). The medium sands contain fewer rock fragments and more quartz than whole-rock samples, indicating a mixed continental block and recycled orogen provenance (Figure 10A). Combining polycrystalline quartz with rock fragments shifts the samples away from a continental block provenance towards a mixed provenance including dissected arc (Figure 10B). Monocrystalline framework grains are mostly quartz with plagioclase, and minor K-feldspar (Figure 11A); polycrystalline framework grains contain slightly more quartzite and granite than granite gneiss (Figure 11B). Twinned is more abundant than untwinned plagioclase (Figure 13A), and microcline is rare compared to untwinned K-feldspar (Figure 13B). Medium-sized quartz grains are mostly monocrystalline and undulose. Polycrystalline quartz with two or three subunits is more common than aggregates of four or more subunits (Figure 15).

2.2.2 Piedmont-river Facies

The piedmont-river pebbly sandstones are immature, first cycle sediments. The quartz grains typically have low sphericity, are mostly subangular, and moderately to poorly sorted. Feldspar grains are more angular and less spherical than quartz, and, during diagenesis, grain boundaries were etched and replaced by hematite, illite, and carbonates.

Figure 16. Pie-diagrams of whole-rock (A) and medium-sand (B) compositions of the piedmont-river facies. Micas are muscovite, biotite, and chlorite. Kspar is K-feldspar; Poly. is polycrystalline quartz; RF is rock fragment. Vein quartz includes monocrystalline and polycrystalline varieties.

A

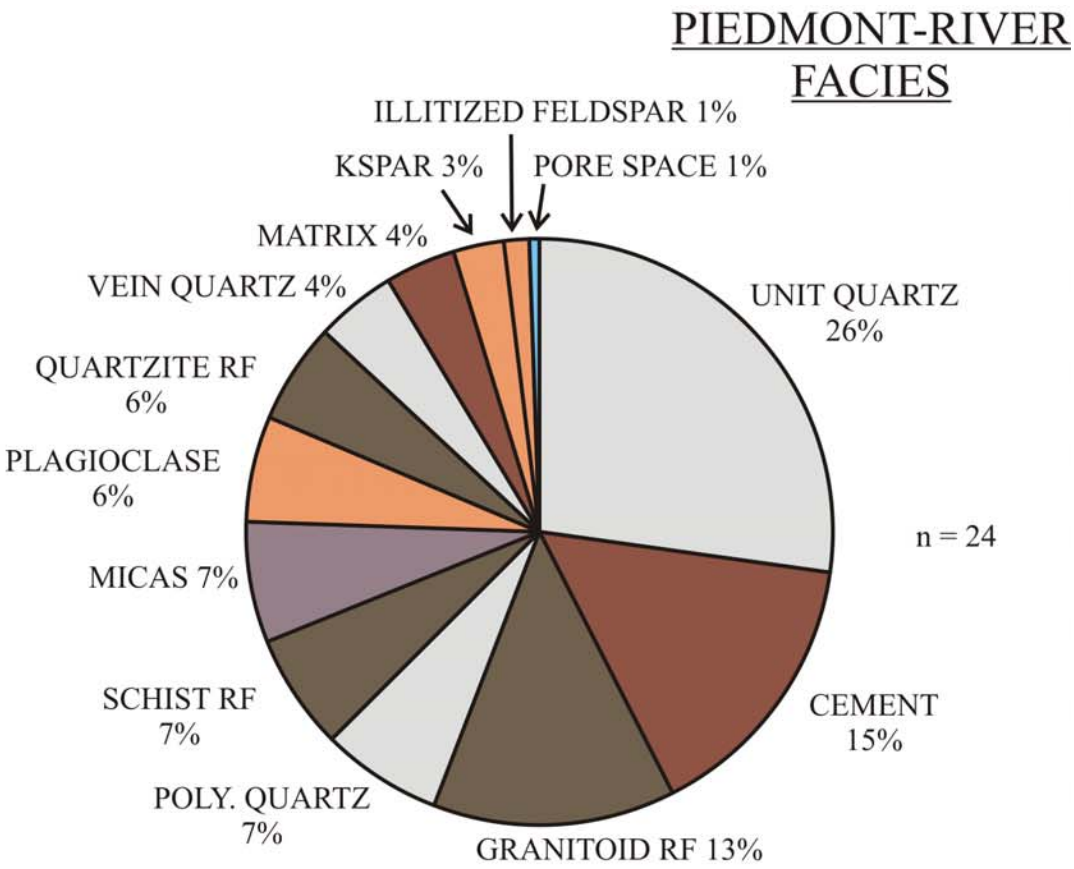
PIEDMONT-RIVER FACIES
ILLITIZED FELDSPAR 1%
KSPAR 3%
PORE SPACE 1%
MATRIX 4%
VEIN QUARTZ 4%
UNIT QUARTZ 26%
QUARTZITE RF 6%
PLAGIOCLASE 6%
n = 24
MICAS 7%
SCHIST RF 7%
CEMENT 15%
POLY. QUARTZ 7%
GRANITOID RF 13%

B

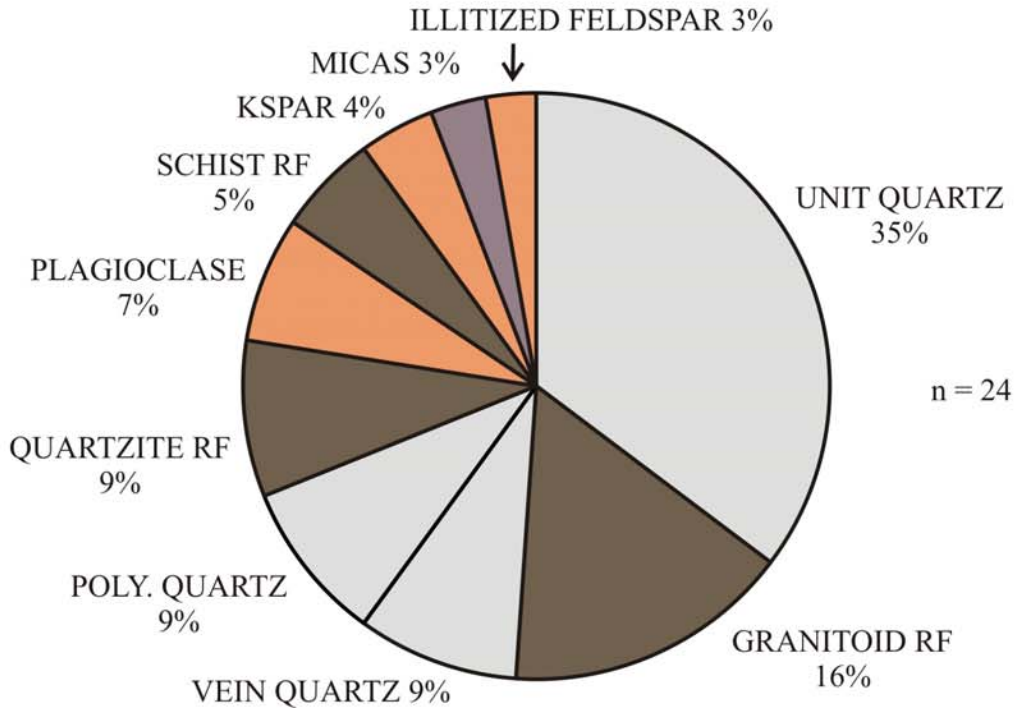
ILLITIZED FELDSPAR 3%
MICAS 3%
KSPAR 4%
SCHIST RF 5%
UNIT QUARTZ 35%
PLAGIOCLASE 7%
n = 24
QUARTZITE RF 9%
POLY. QUARTZ 9%
GRANITOID RF 16%
VEIN QUARTZ 9%

Figure 17. Q-F-R plots of whole rock (A) and medium sand (B) of the piedmont-river facies (Pettijohn, 1975). A circled point is the mean, and a dashed hexagon shows the 95% confidence interval around the mean. For 9B, the 95% confidence interval is smaller than the symbol for the mean. A shaded field indicates samples from the illite diagenetic pattern (Taylor, 1991). The poles are defined in Table 1; Q is quartz, F is feldspar, and R is rock fragments. Numbers correspond to sample numbers in Appendix C.

A

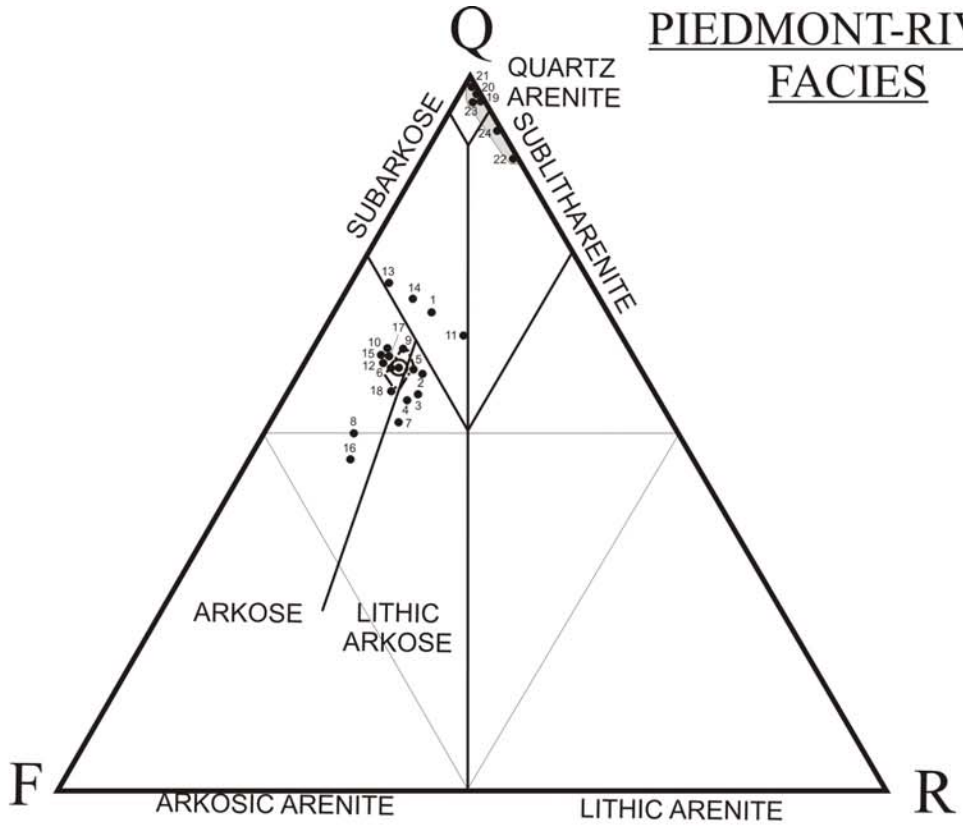
PIEDMONT-RIVER FACIES
Q
QUARTZ ARENITE
SUBARKOSE
SUBLITHARENITE
ARKOSE
LITHIC ARKOSE
F
R
ARKOSIC ARENITE
LITHIC ARENITE

B

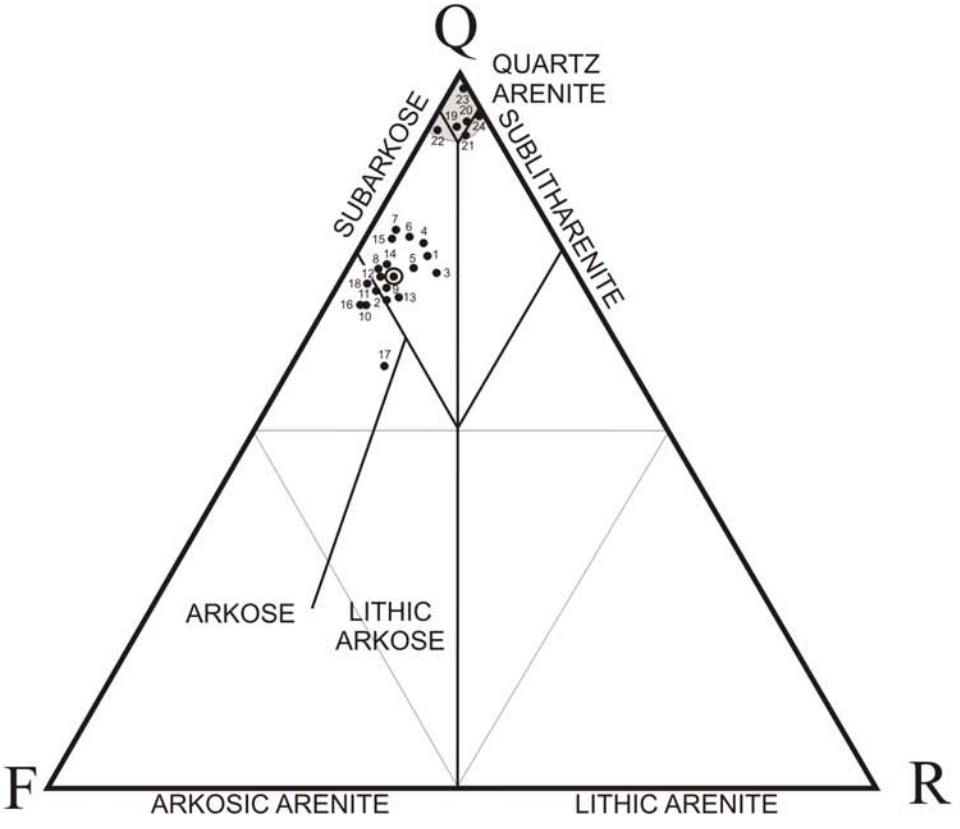
Q
QUARTZ ARENITE
SUBARKOSE
SUBLITHARENITE
ARKOSE
LITHIC ARKOSE
F
R
ARKOSIC ARENITE
LITHIC ARENITE

Figure 16A. The whole-rock composition of the piedmont-river facies shows that unit quartz (27%) and granitoids (13%) are the most abundant framework grains, similar to the valley-river facies. Plagioclase is less abundant than polycrystalline quartz, schistose rock fragments, and micas.

Figure 16B. More than 50% of the medium sand is unit quartz and granitoids; vein quartz, polycrystalline quartz, and quartzite are more abundant than plagioclase. Fe-oxide-stained matrix comprises 4% of whole-rock volume.

Figure 17A. The Q-F-R classification shows the whole-rock mean is arkose, with samples plotting as arkose, lithic arkose, and subarkose. Samples 19 through 24 are excluded because feldspars are replaced by illite.

Figure 17B. Medium sands are in the subarkose and arkose fields, and the mean is subarkose. Again, narrowing counted grains to medium sand enriches the proportions of quartz at the expense of rock fragments.

Figure 18A. On the Qt-F-L whole-rock samples are a mix of transitional continental block and recycled orogen provenance. The mean is slightly more quartzofeldspathic than the boundary between the two provenance fields.

Figure 18B. On the Qm-F-Lt plot, all samples except those affected by illite-replacement plot in the 'mixed' provenance field, similar to the valley-river samples. A difference is that on the Qm-F-Lt plot none of the piedmont-river samples is in the magmatic arc provenance.

Figure 19A. In the plot of monocrystalline framework grains, K-feldspar is slightly more common in the piedmont-river samples than in the valley river, but the piedmont-river samples have slightly less plagioclase. Quartz is more abundant in the

Figure 18. Qt-F-L (A) and Qm-F-Lt (B) plots of medium sand of the piedmont-river facies (Dickinson, 1985). For 10B, the center field is mixed provenance. A circled point is the mean, and a dashed hexagon shows the 95% confidence interval around the mean. For 10A, the 95% confidence interval around the mean is smaller than the symbol for the mean. The poles are defined in Table 1; Qt is total quartz, F is feldspar, L is lithic fragments, Qm is monocrystalline quartz, Lt is total lithic fragments. Numbers correspond to sample numbers in Appendix C.

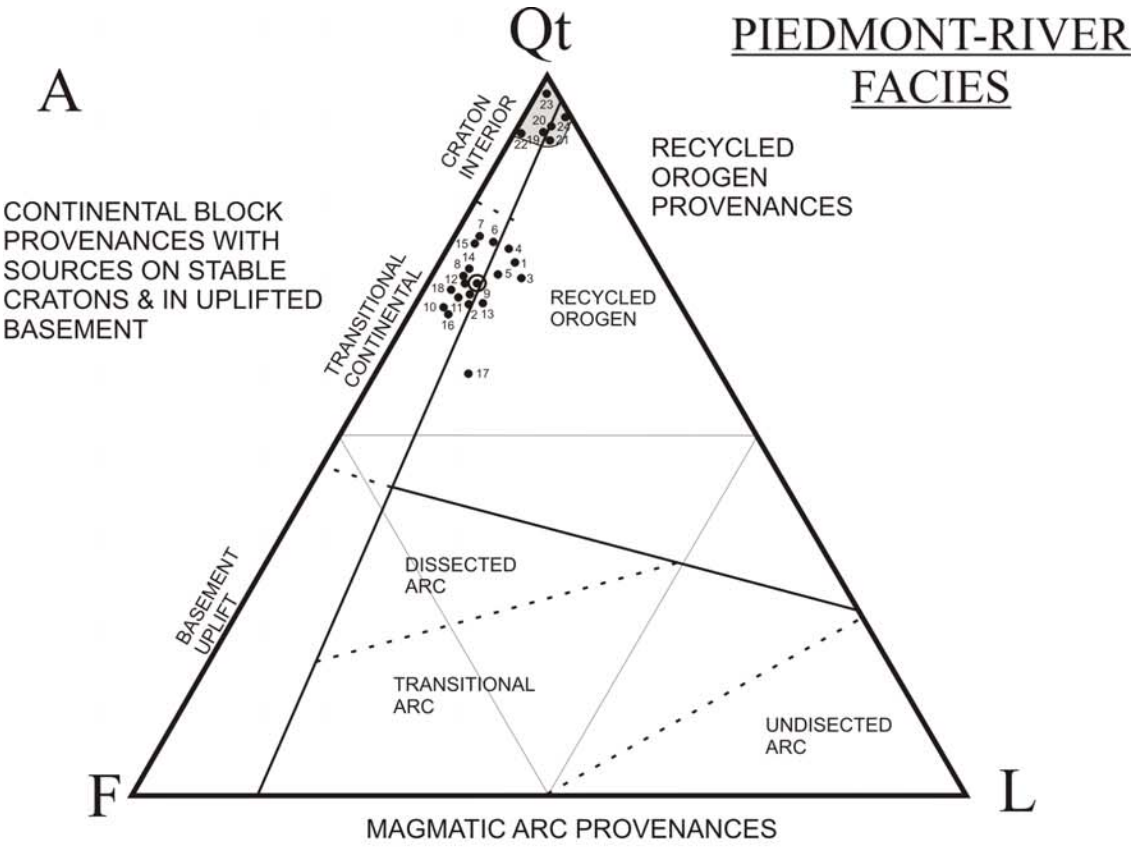
Qt
PIEDMONT-RIVER FACIES
A
CONTINENTAL BLOCK PROVENANCES WITH SOURCES ON STABLE CRATONS & IN UPLIFTED BASEMENT
CRATON INTERIOR
TRANSITIONAL CONTINENTAL
BASEMENT UPLIFT
RECYCLED OROGEN PROVENANCES
RECYCLED OROGEN
DISSECTED ARC
TRANSITIONAL ARC
UNDISECTED ARC
F
L
MAGMATIC ARC PROVENANCES

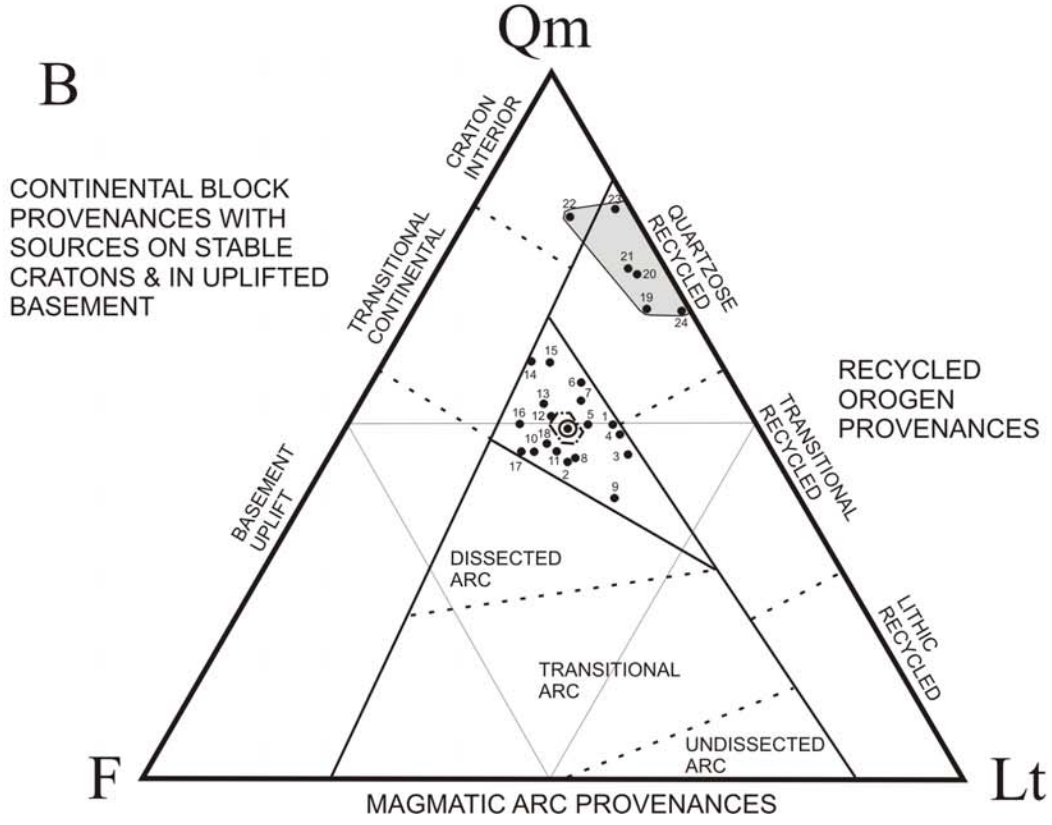
Qm
B
CONTINENTAL BLOCK PROVENANCES WITH SOURCES ON STABLE CRATONS & IN UPLIFTED BASEMENT
CRATON INTERIOR
TRANSITIONAL CONTINENTAL
BASEMENT UPLIFT
QUARTZOSE RECYCLED
TRANSITIONAL RECYCLED
LITHIC RECYCLED
RECYCLED OROGEN PROVENANCES
DISSECTED ARC
TRANSITIONAL ARC
UNDISSECTED ARC
F
Lt
MAGMATIC ARC PROVENANCES

Figure 19. Qm-P-K (A; Dickinson, 1985) and Qtzte-Gr-Gn (B) plots of medium-sand in the piedmont-river facies. Samples 19 through 24 are omitted from 19A due to illitization of feldspars. A circled point is the mean, and a dashed hexagon is the 95% confidence interval around the mean. The poles are defined in Table 1; Qm is monocrystalline quartz, P is plagioclase, K is K-feldspar, Qtzte is quartzite, Gr is granite, and Gn is gneiss. Numbers correspond to sample numbers in Appendix C.

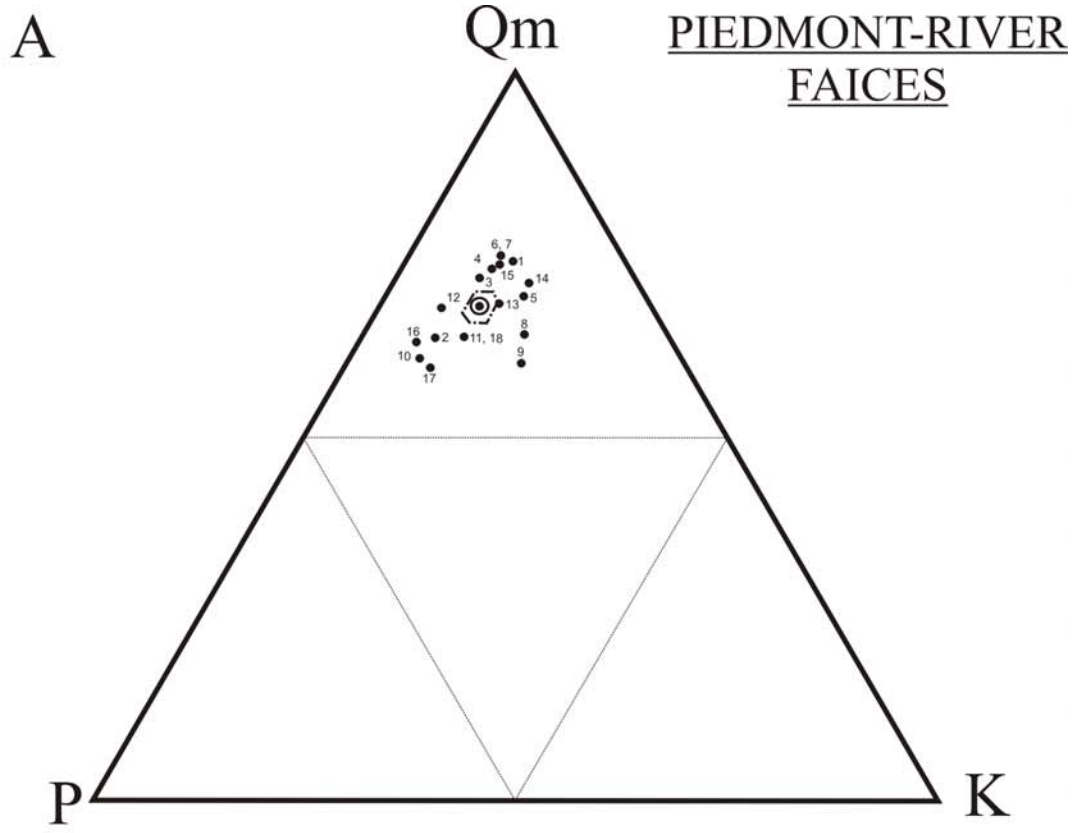
A
Qm
PIEDMONT-RIVER
FAICES
P
K

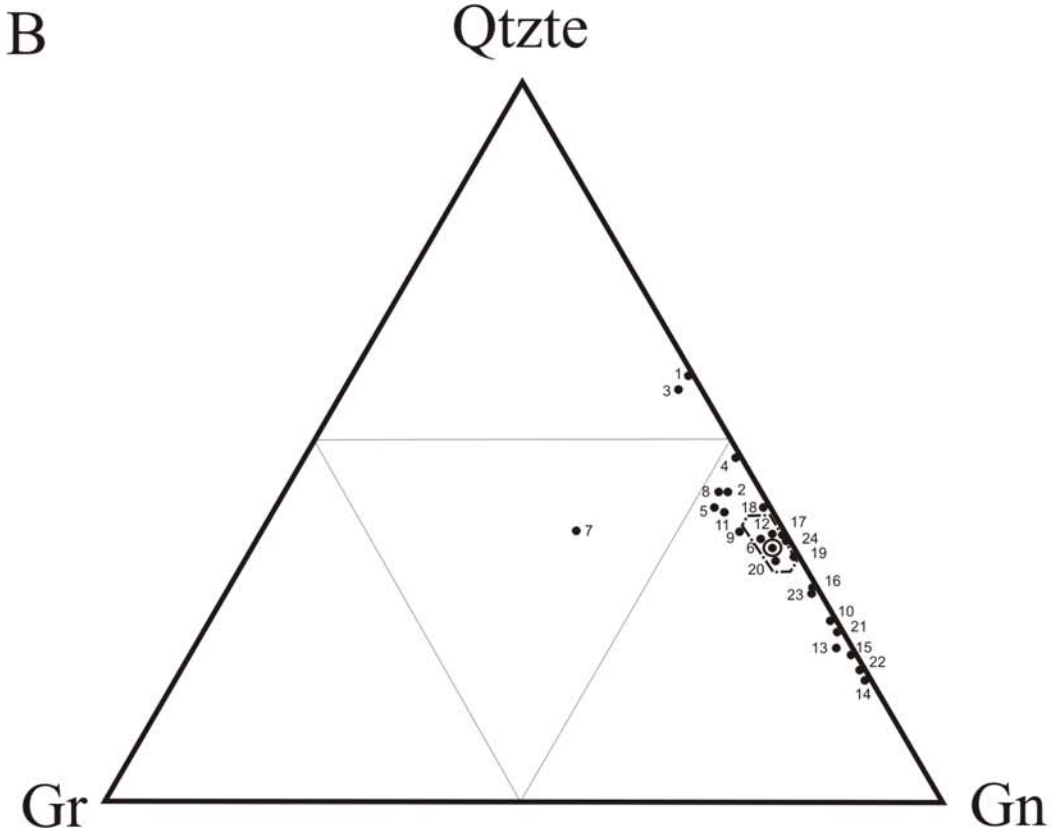
B
Qtzte
Gr
Gn

Piedmont-river facies than in the other two facies.

Figure 19B. Of the 24 samples, 11 entirely lack granite, and only one has more than 10% granite. Granite grains comprise only 3% of the mean, and the confidence interval shows that the mean has a 95% chance of being <5% (Table 2). The ratio of quartzite to the polycrystalline rock fragments is slightly lower than in the valley-river samples.

Figure 20A. In the piedmont-river samples, untwinned plagioclase is more abundant than twinned by almost 4:1, unlike the twinned-plagioclase-rich composition of the valley-river facies. No piedmont-river samples contain more than 40% twinned plagioclase. Samples 5, 8, 9, and 14 have K-feldspar as the dominant feldspar.

Figure 20B. Samples 5, 8, 9, and 14 have the largest amount of untwinned K-feldspar among all piedmont-river samples. Microcline comprises ~6% of all feldspars, as in the valley-river samples.

Figure 21. In all piedmont-river samples, more than 25% of the polycrystalline quartz grains had four or more subunits, and plot on the inverted lower triangle. Undulose monocrystalline quartz is more abundant than non-undulose. The mean is in the low-rank metamorphic field in Figure 21A, but in the granite field in Figure 21B.

Summary. Framework grains in the piedmont-river samples are predominantly unit quartz and granitoids (Figure 16). The medium sand is quartz-rich compared to the whole rock. The sandstones vary from arkose and lithic arkose to subarkose; subarkose is more common in the medium-sand samples (Figure 17).

The provenance is a mixture of transitional continental block and recycled orogen, with no clear contribution from a magmatic arc (Figure 18). Unit quartz is the dominant

Figure 20. K-Tp-Up (A) and P-Uk-M (B) plots of medium sand in the piedmont-river facies. A circled point is the mean, and a dashed hexagon is the 95% confidence interval around the mean. The poles are defined in Table 1; K is K-feldspar, Tp is twinned plagioclase, Up is untwinned plagioclase, P is plagioclase, Uk is untwinned K-feldspar, and M is microcline. Numbers correspond to sample numbers in Appendix C. Samples 19 through 24 are omitted due to diagenetic illitization of feldspars (Taylor, 1991; Hubert et al, 2001).

A

PIEDMONT-RIVER FACIES

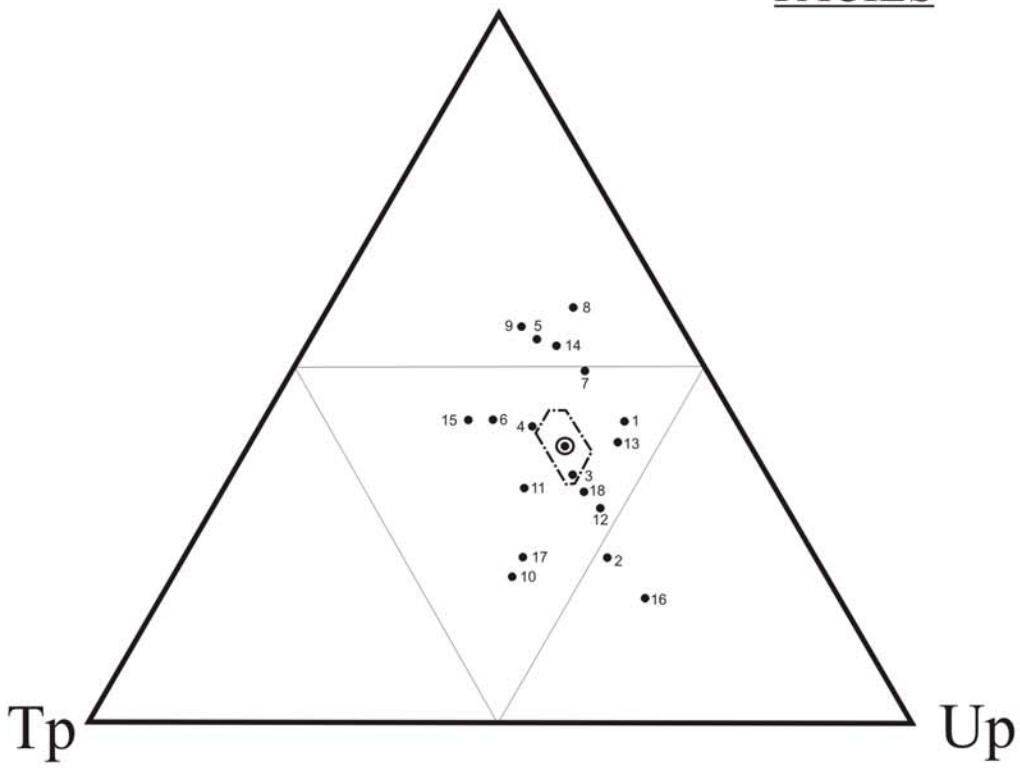

B

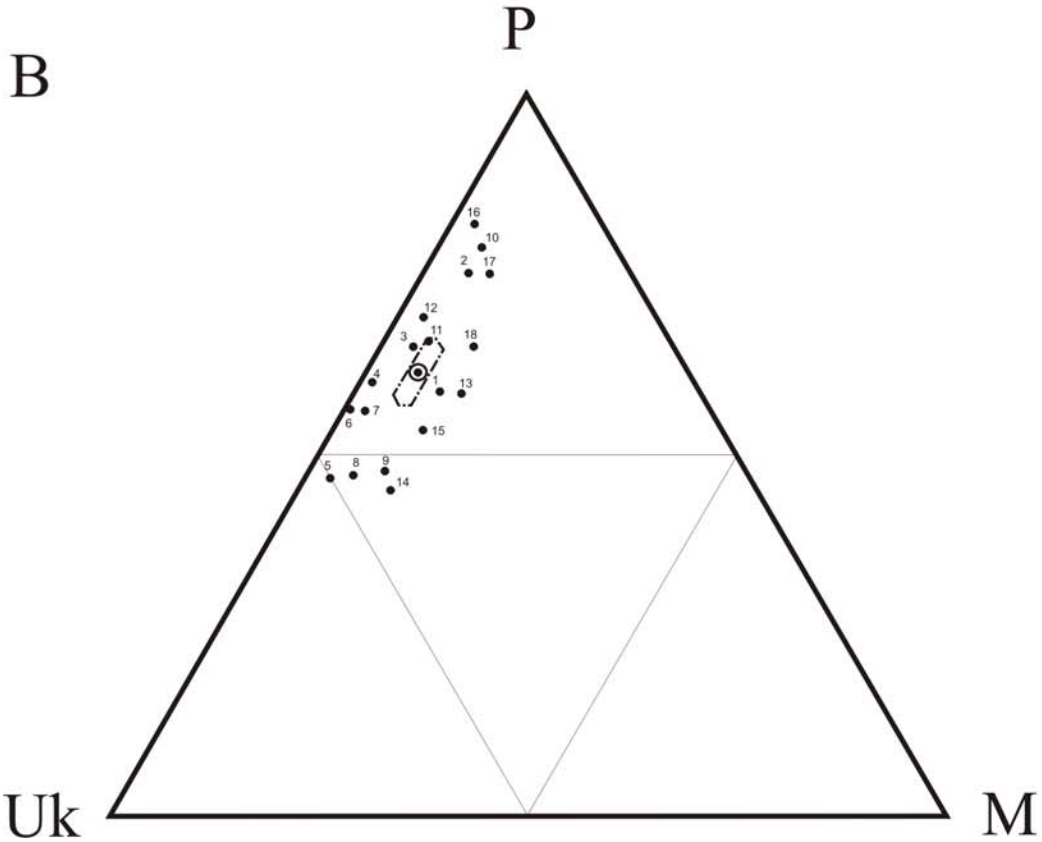

Figure 21. A. Qp-Qnu-Qu modified plot of provenance of medium-sand quartz in the piedmont-river facies (Basu, 1985). B. Qp-Qnu-Qu modified plot of Tortosa et al. (1991). The plots are truncated at 50% Qp. A circled point is the mean, and a dashed hexagon is the 95% confidence interval around the mean. The poles are defined in Table 1; Qp 2-3 is polycrystalline quartz with two or three subunits, Qp ≥4 is polycrystalline quartz with four or more subunits, Qnu is non-undulose monocrystalline quartz, and Qu is undulose monocrystalline quartz. Numbers correspond to sample numbers in Appendix C.

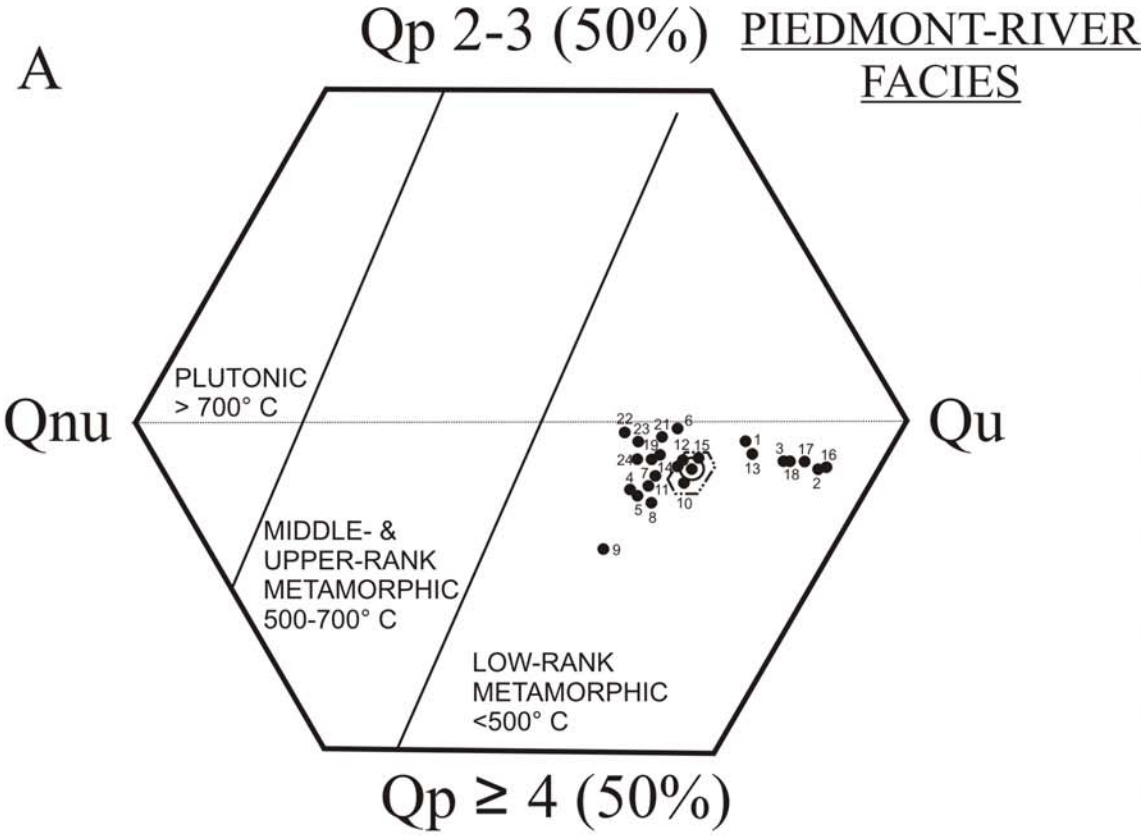
A
Qp 2-3 (50%)
PIEDMONT-RIVER FACIES
Qnu
Qu
PLUTONIC
> 700° C
MIDDLE- &
UPPER-RANK
METAMORPHIC
500-700° C
LOW-RANK
METAMORPHIC
<500° C
Qp ≥ 4 (50%)

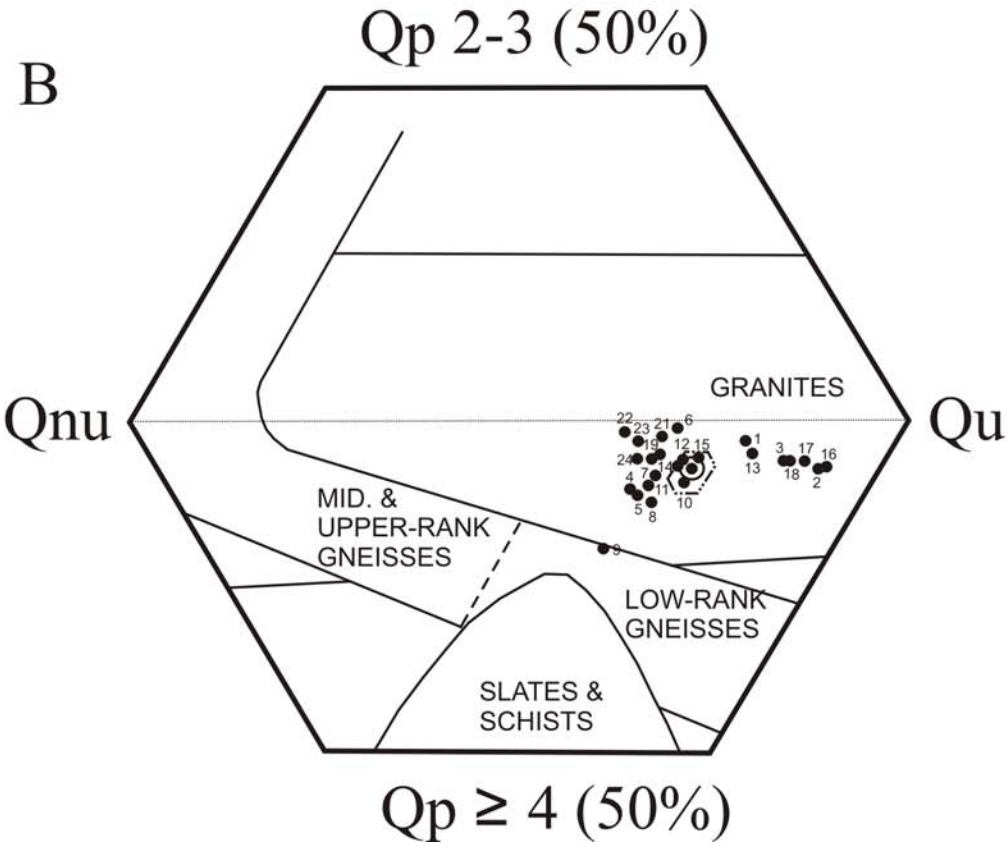
B
Qp 2-3 (50%)
Qnu
Qu
GRANITES
MID. &
UPPER-RANK
GNEISSES
LOW-RANK
GNEISSES
SLATES &
SCHISTS
Qp ≥ 4 (50%)

monocrystalline grain, with plagioclase less abundant, and K-feldspar more abundant than in the valley-river samples. Granite gneiss is the major polycrystalline fragment; granite is virtually absent. Plagioclase and K-feldspar are mostly untwinned (Figures 19 and 20). In all samples, more than 25% of the polycrystalline quartz has four or more subunits, and undulose monocrystalline quartz is more abundant than non-undulose (Figure 21).

2.2.3 Alluvial-fan Facies

Quartz grains are subangular, with low sphericity and poor sorting.

Figure 22. The major framework grains in the whole rock are unit quartz (22%) granitoids (14%) and polycrystalline quartz (11%). Medium sand is almost 75% unit quartz (25%) and rock fragments (45%). None of the outcrops was affected by illitization of feldspars.

Figure 23. All samples in whole rock and medium sand are arkose and subarkose on the Q-F-R diagram. The means of whole rock and medium sand are arkose and subarkose, respectively. The 95% confidence interval around both means spans the fields of arkose, subarkose and lithic arkose.

Figure 24. The alluvial-fan mean plots in the recycled orogen provenance of the Qt-F-L diagram. Individual samples plot in recycled orogen and transitional continental block. In Figure 24B, the mean and four of the six samples are the ‘mixed’ provenance field, and two are dissected magmatic arc. On both plots, the alluvial-fan samples plot in similar positions to the valley-river and piedmont-river samples. Some valley-river samples also plot in the dissected magmatic arc.

Figure 22. Pie diagrams of whole rock (A) and medium-sand (B) petrographic compositions of the alluvial-fan facies. Accessories are micas and garnet; Micas are muscovite, biotite, and chlorite; Kspar is K-feldspar; Poly. is polycrystalline quartz; RF is rock fragment. Vein quartz includes monocrystalline and polycrystalline.

A

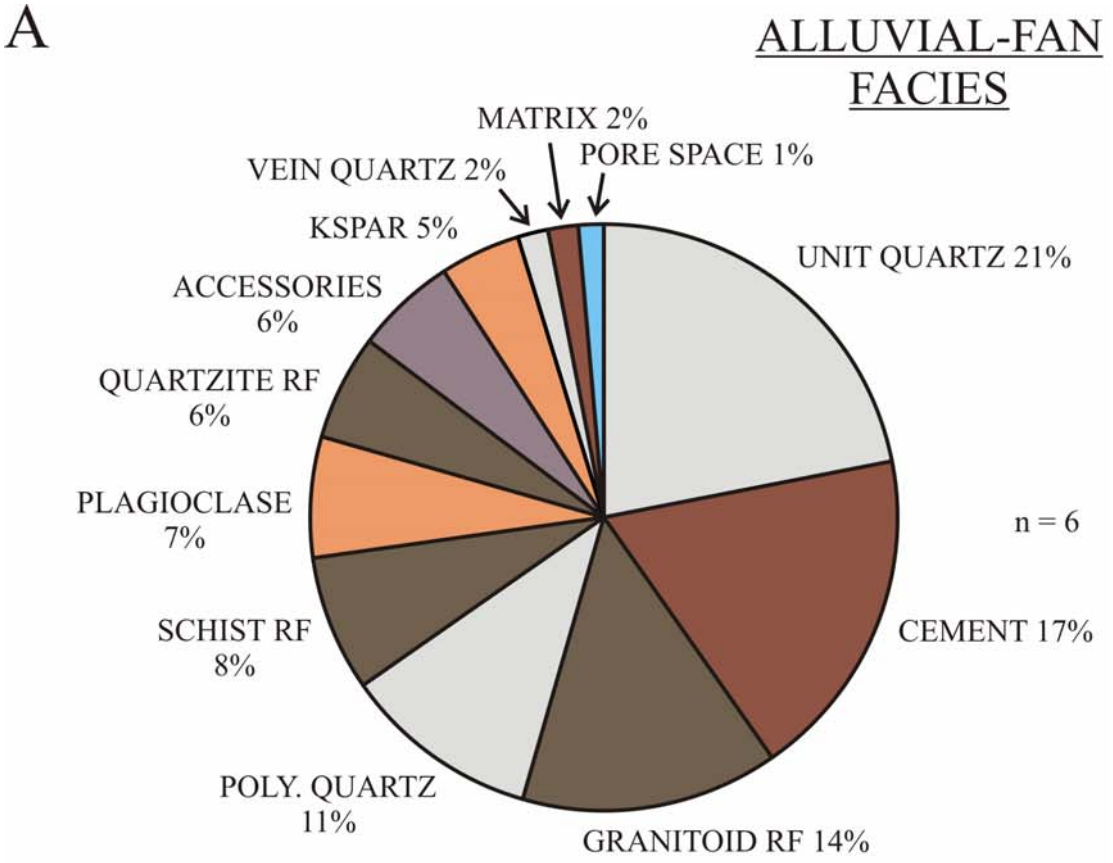
ALLUVIAL-FAN FACIES
MATRIX 2%
PORE SPACE 1%
VEIN QUARTZ 2%
KSPAR 5%
UNIT QUARTZ 21%
ACCESSORIES 6%
QUARTZITE RF 6%
PLAGIOCLASE 7%
n = 6
SCHIST RF 8%
CEMENT 17%
POLY. QUARTZ 11%
GRANITOID RF 14%

B

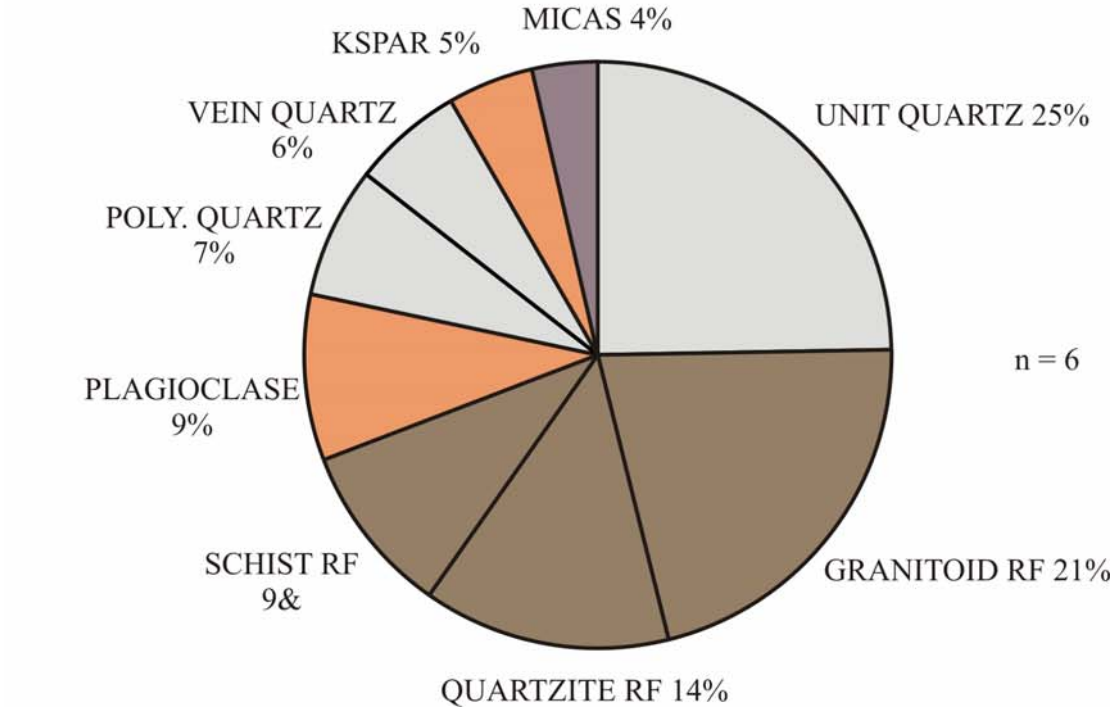
MICAS 4%
KSPAR 5%
VEIN QUARTZ 6%
UNIT QUARTZ 25%
POLY. QUARTZ 7%
n = 6
PLAGIOCLASE 9%
SCHIST RF 9&
GRANITOID RF 21%
QUARTZITE RF 14%

Figure 23. Q-F-R plots of whole rock (A) and medium sand (B) compositions in the alluvial-fan facies (Pettijohn, 1975). A circled point is the mean, and a dashed hexagon shows the 95% confidence interval around the mean. The poles are defined in Table 1; Q is quartz, F is feldspar, and R is rock fragments. Numbers correspond to sample numbers in Appendix C.

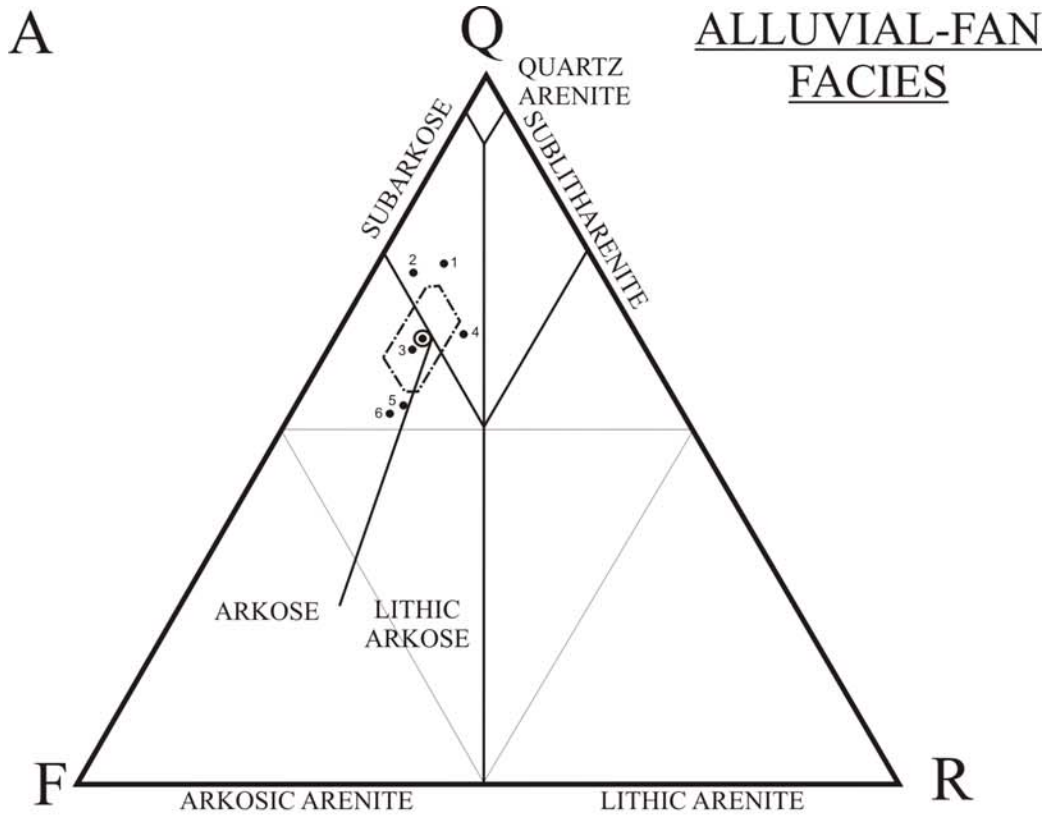
A
Q
ALLUVIAL-FAN FACIES
QUARTZ ARENITE
SUBARKOSE
SUBLITHARENITE
1
2
3
4
5
6
ARKOSE
LITHIC ARKOSE
F
R
ARKOSIC ARENITE
LITHIC ARENITE

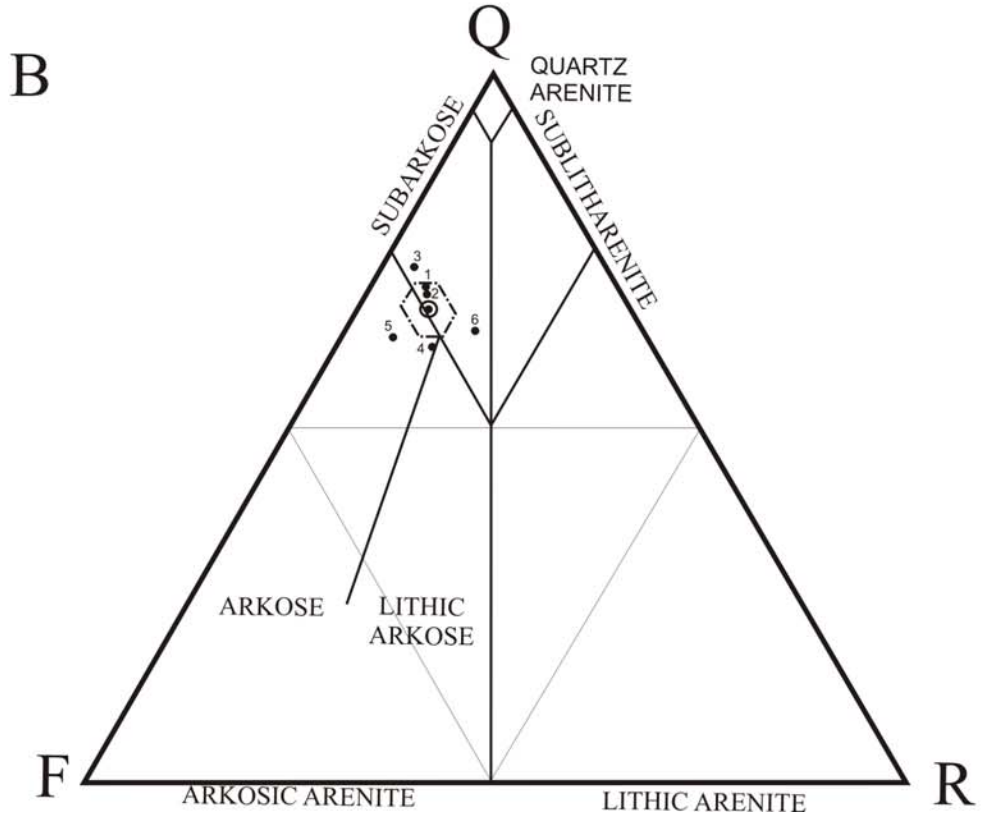
B
Q
QUARTZ ARENITE
SUBARKOSE
SUBLITHARENITE
1
2
3
4
5
6
ARKOSE
LITHIC ARKOSE
F
R
ARKOSIC ARENITE
LITHIC ARENITE

Figure 24. Qt-F-L (A) and Qm-F-Lt (B) plots of medium sand in the alluvial-fan facies (Dickinson, 1985). For 24B, the center field is mixed provenance. A circled point is the mean, and a dashed hexagon shows the 95% confidence interval around the mean. The poles are defined in Table 1; Qt is total quartz, F is feldspar, L is lithic fragments, Qm is monocrystalline quartz, and Lt is total lithic fragments. Numbers correspond to sample numbers in Appendix C.

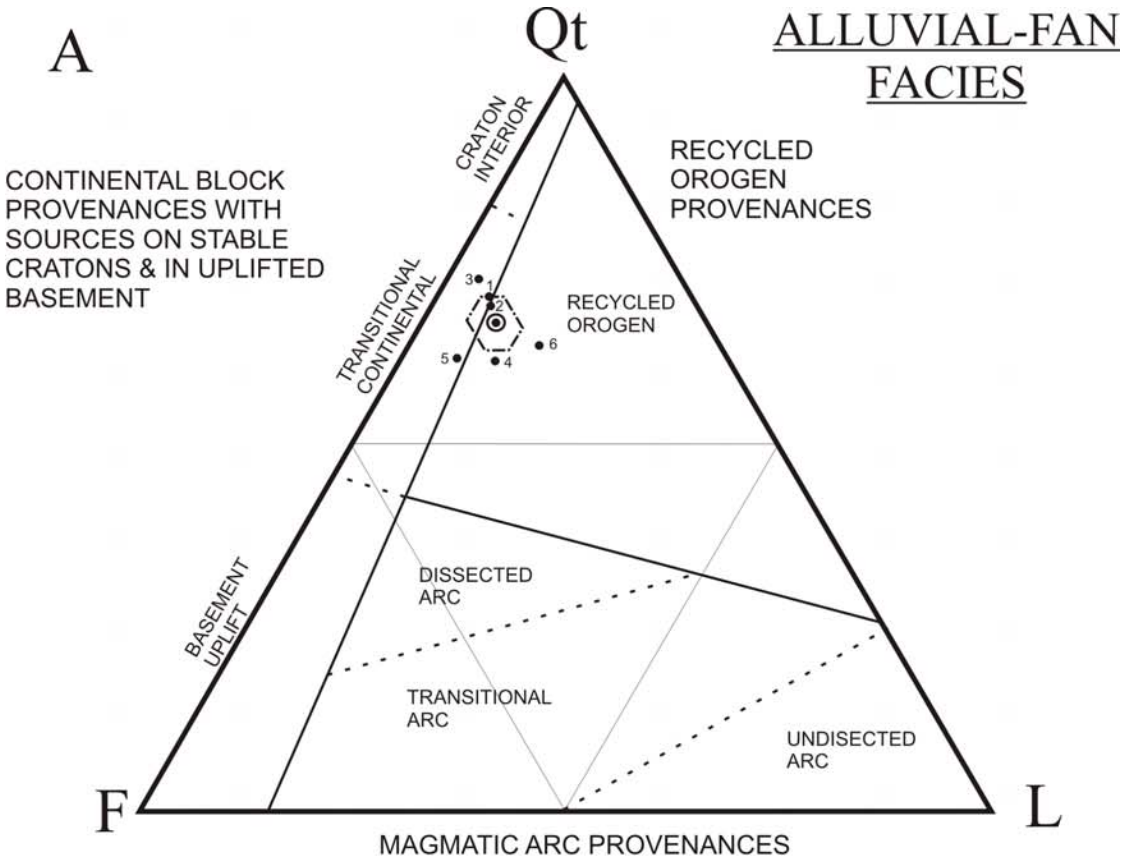
A
Qt
ALLUVIAL-FAN FACIES
CONTINENTAL BLOCK PROVENANCES WITH SOURCES ON STABLE CRATONS & IN UPLIFTED BASEMENT
CRATON INTERIOR
RECYCLED OROGEN PROVENANCES
TRANSITIONAL CONTINENTAL
RECYCLED OROGEN
BASEMENT UPLIFT
DISSECTED ARC
TRANSITIONAL ARC
UNDISECTED ARC
F
L
MAGMATIC ARC PROVENANCES

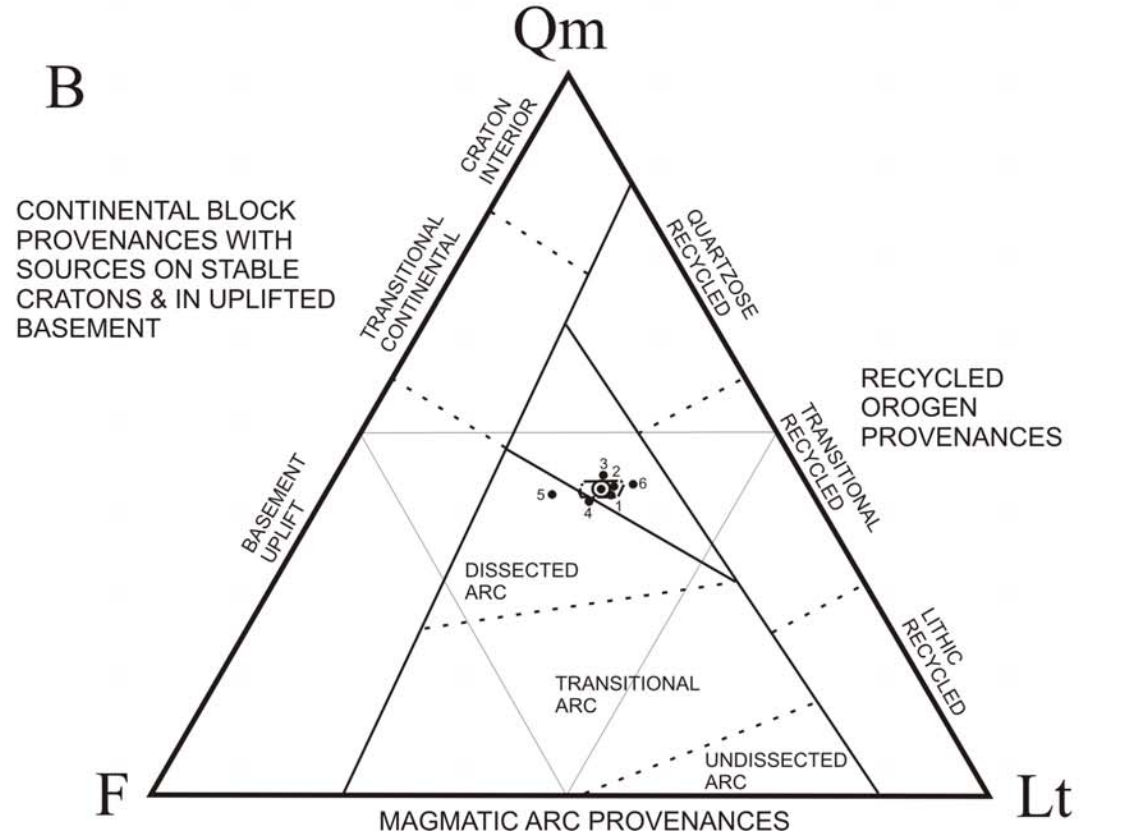
B
Qm
CONTINENTAL BLOCK PROVENANCES WITH SOURCES ON STABLE CRATONS & IN UPLIFTED BASEMENT
CRATON INTERIOR
TRANSITIONAL CONTINENTAL
QUARTZOSE RECYCLED
RECYCLED OROGEN PROVENANCES
TRANSITIONAL RECYCLED
BASEMENT UPLIFT
DISSECTED ARC
TRANSITIONAL ARC
LITHIC RECYCLED
UNDISSECTED ARC
F
Lt
MAGMATIC ARC PROVENANCES

Figure 25. The alluvial-fan samples have an average ratio of plagioclase to K-feldspar of 2:1. Unit quartz is the dominant monocrystalline grain in all three facies. Granite gneiss is the most abundant rock fragment in the alluvial-fan facies. Like the piedmont-river facies, granite is a minor component. The variability of granite and granite gneiss among the samples is large, with 95% confidence intervals of ±13% and ±14%, respectively.

Figure 26. The majority of plagioclase grains are untwinned, and commonly contain vacuoles and sericite (Figure 27A). K-feldspar is mostly untwinned, but microcline is more abundant than in the valley-river and piedmont-river facies (Figure 27B).

Figure 28. The alluvial-fan samples are similar to the piedmont-river, plotting in the low-rank metamorphic or granite provenance of the lower, inverted triangle. Fine-grained polycrystalline quartz makes up more than 25% of all polycrystalline quartz, and most monocrystalline quartz grains are undulose.

Summary. Medium-sand samples are subarkose and are almost 75% unit quartz and rock fragments; whole-rock samples include more polycrystalline quartz and are classified as arkose (Figures 22 and 23). Provenance of medium-sand samples is a mix of recycled orogen and magmatic arc (Figure 24). Plagioclase is more abundant than K-feldspar, and granite gneiss is much more abundant than granite (Figure 25). Most of the plagioclase is untwinned, and microcline is more abundant in alluvial-fan samples than valley-river and piedmont-river samples (Figure 26). Most monocrystalline quartz is undulose, and more than 25% of polycrystalline quartz has four or more subunits. Quartz provenance is low-grade metamorphic or granite (Figure 28).

Figure 25. Qm-P-K (A) and Qtzte-Gr-Gn (B) plots of medium sand in the alluvial-fan facies. A circled point is the mean, and a dashed hexagon is the 95% confidence interval around the mean. The poles are defined in Table 1; Qm is monocrystalline quartz, P is plagioclase, K is K-feldspar, Qtzte is quartzite, Gr is granite, and Gn is gneiss. Numbers correspond to ample numbers in Appendix C.

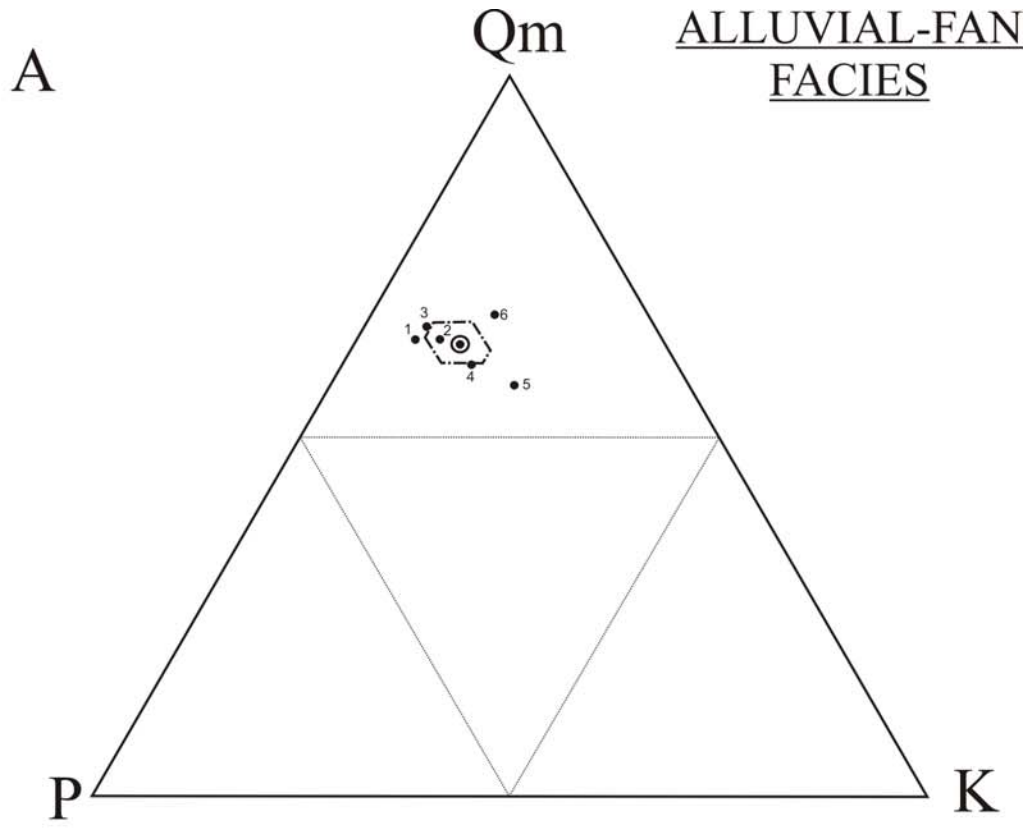
A
Qm
ALLUVIAL-FAN
FACIES
P
K
1
2
3
4
5
6

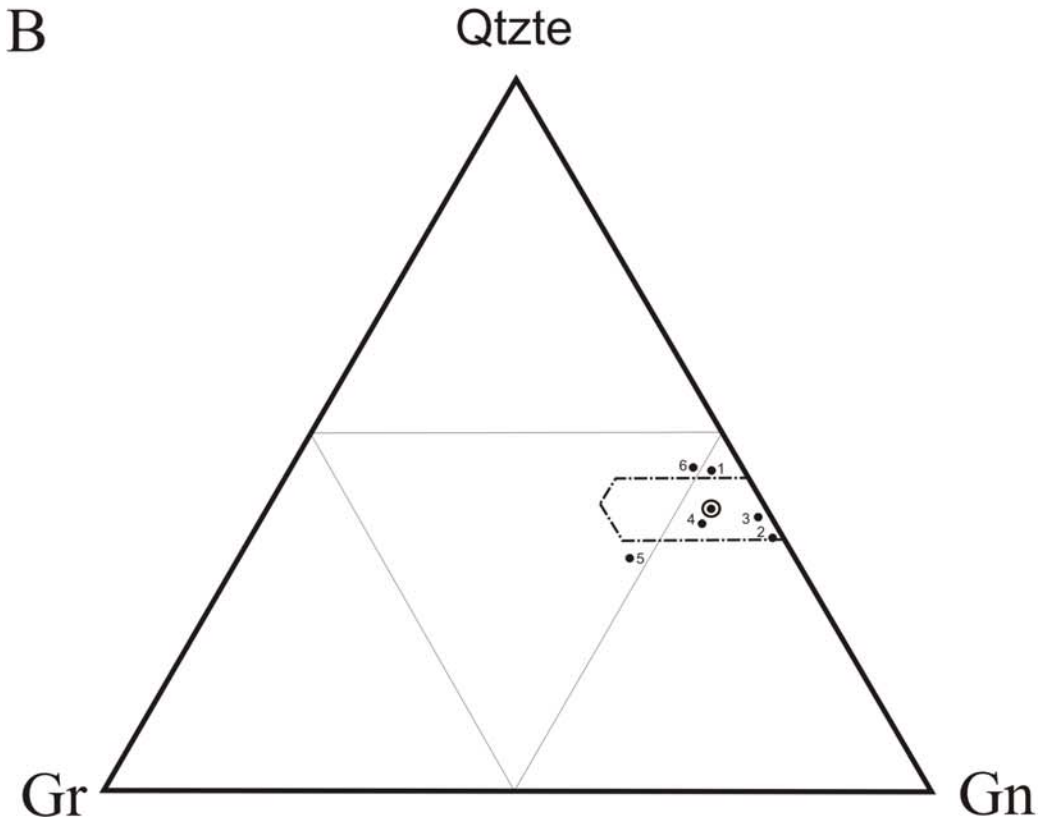
B
Qtzte
Gr
Gn
1
2
3
4
5
6

Figure 26. K-Tp-Up (A) and P-Uk-M (B) plots of medium sand in the alluvial-fan facies. A circled point is the mean, and a dashed hexagon is the 95% confidence interval around the mean. The poles are defined in Table 1; K is K-feldspar, Tp is twinned plagioclase, Up is untwinned plagioclase, P is plagioclase, Uk is untwinned K-feldspar, and M is microcline. Numbers correspond to sample numbers in Appendix C.

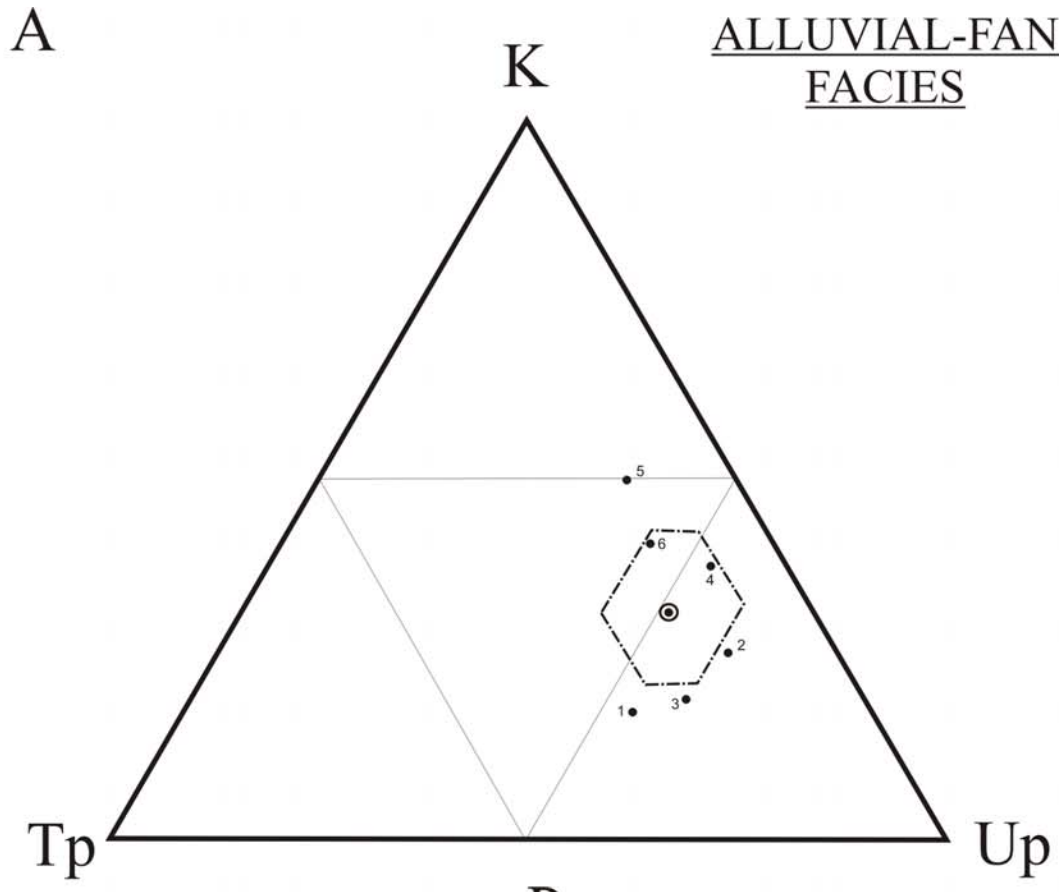
A
ALLUVIAL-FAN FACIES
K
Tp
Up
1
2
3
4
5
6

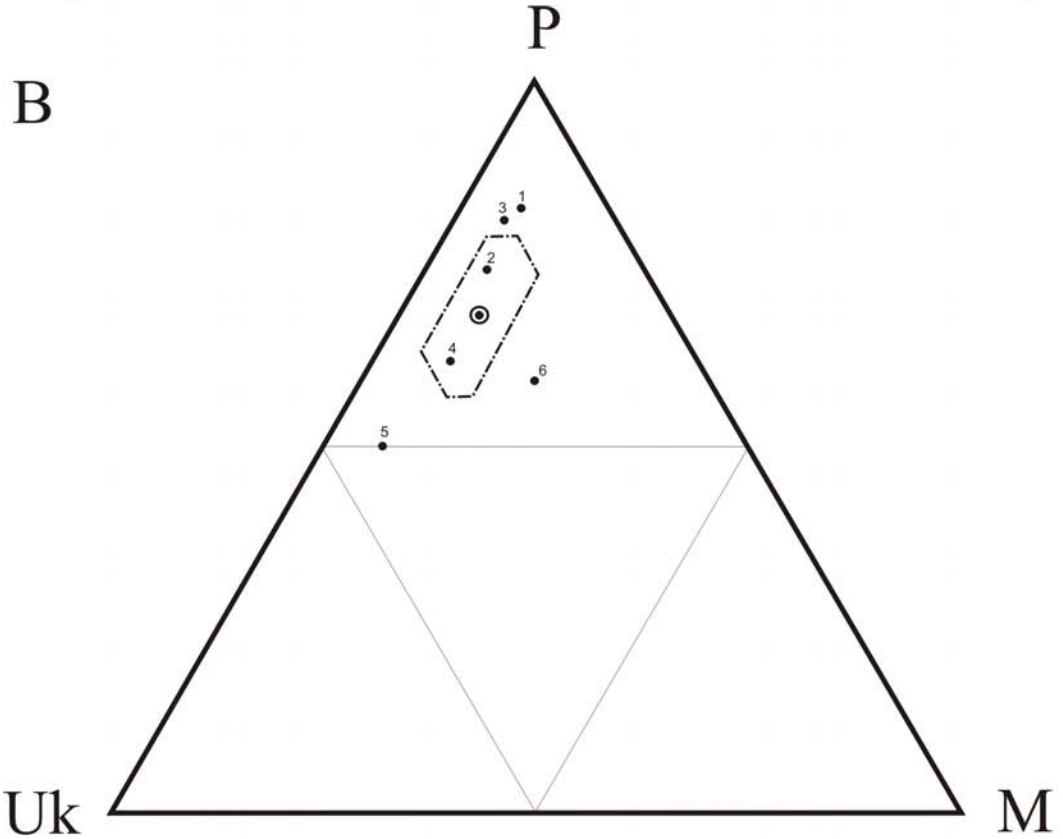
B
P
Uk
M
1
2
3
4
5
6

Figure 27. Micrographs of untwinned plagioclase in a gneiss grain (A) and microcline in a granite grain (B). M is muscovite; Q is quartz; H is hematite fracture fill and cement; P is plagioclase; A is albite replacement along mineral fractures; and C is Fe-dolomite with minor Fe-calcite cements. White arrows point to albite overgrowths, and black arrow points to quartz overgrowth. Crossed nicols; scale bar in A is 0.5 mm; in B, 0.25 mm.

A

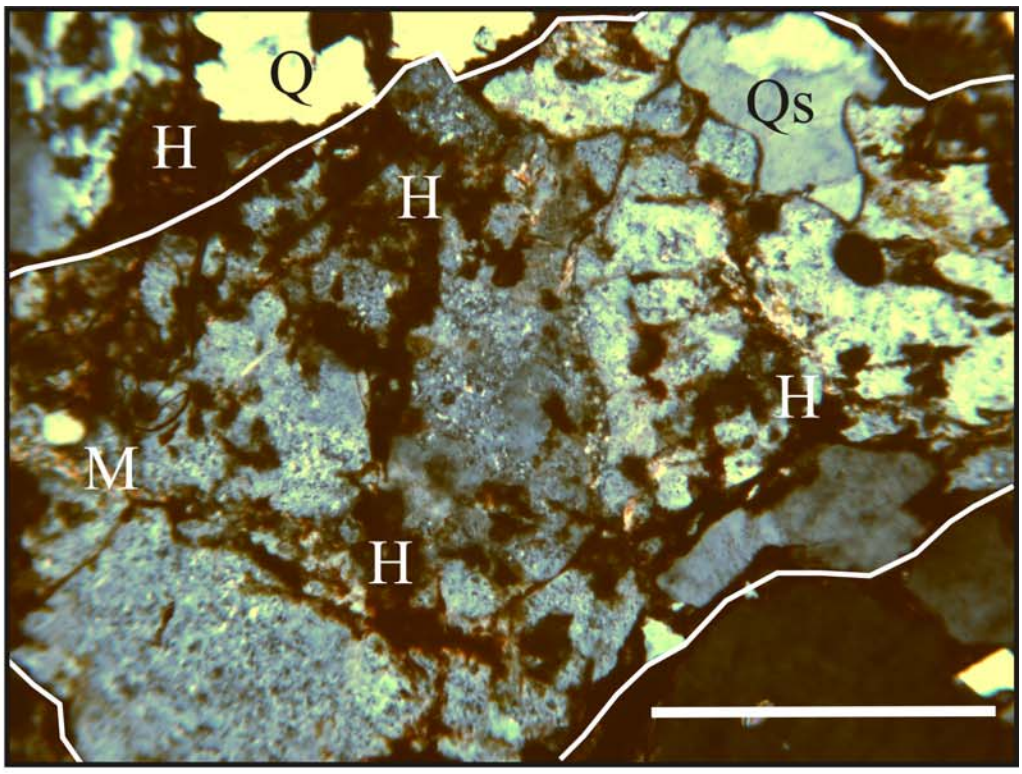

B

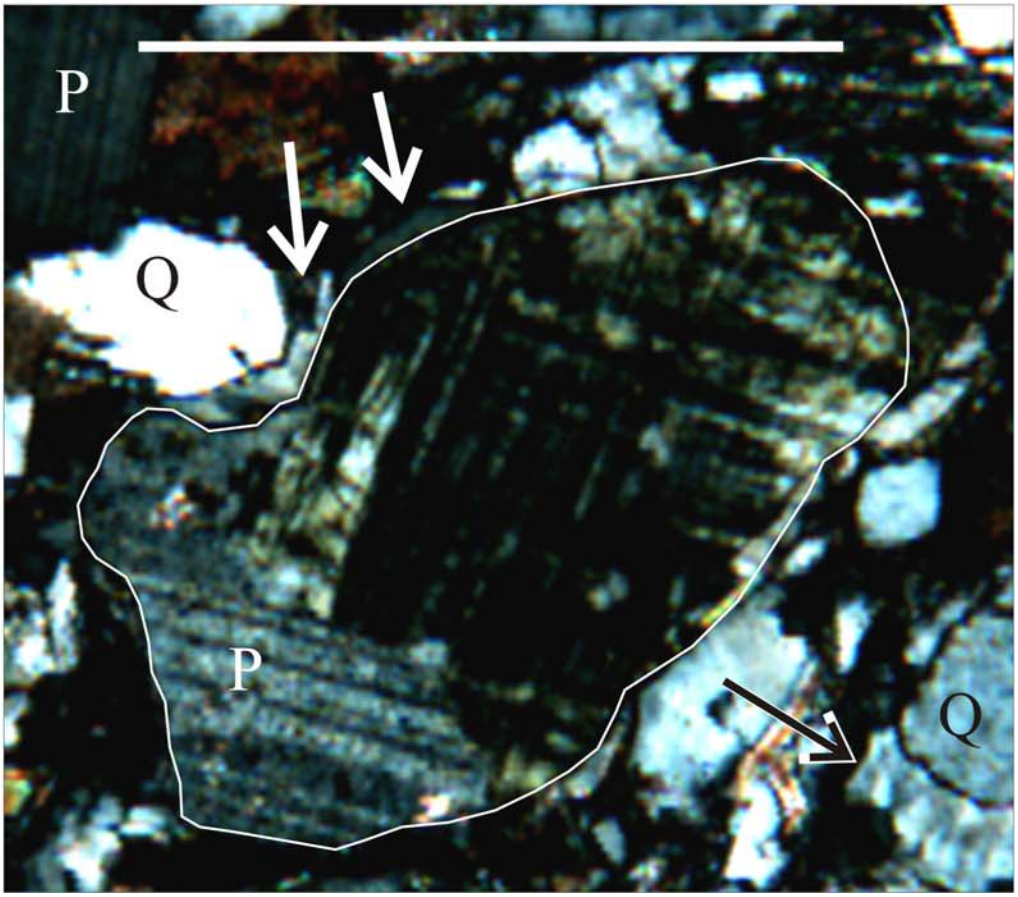

Figure 28. A. Qp-Qnu-Qu modified plot of provenance of medium-sand quartz in the alluvial-fan facies (Basu, 1985). B. Qp-Qnu-Qu modified plot of Tortosa et al. (1991). The plots are truncated at 50% Qp. A circled point is the mean, and a dashed hexagon is the 95% confidence interval around the mean. The poles are defined in Table 1; Qp 2-3 is polycrystalline quartz with two or three subunits, Qp ≥4 is polycrystalline quartz with four or more subunits, Qnu is non-undulose monocrystalline quartz, and Qu is undulose monocrystalline quartz. Numbers correspond to sample numbers in Appendix C.

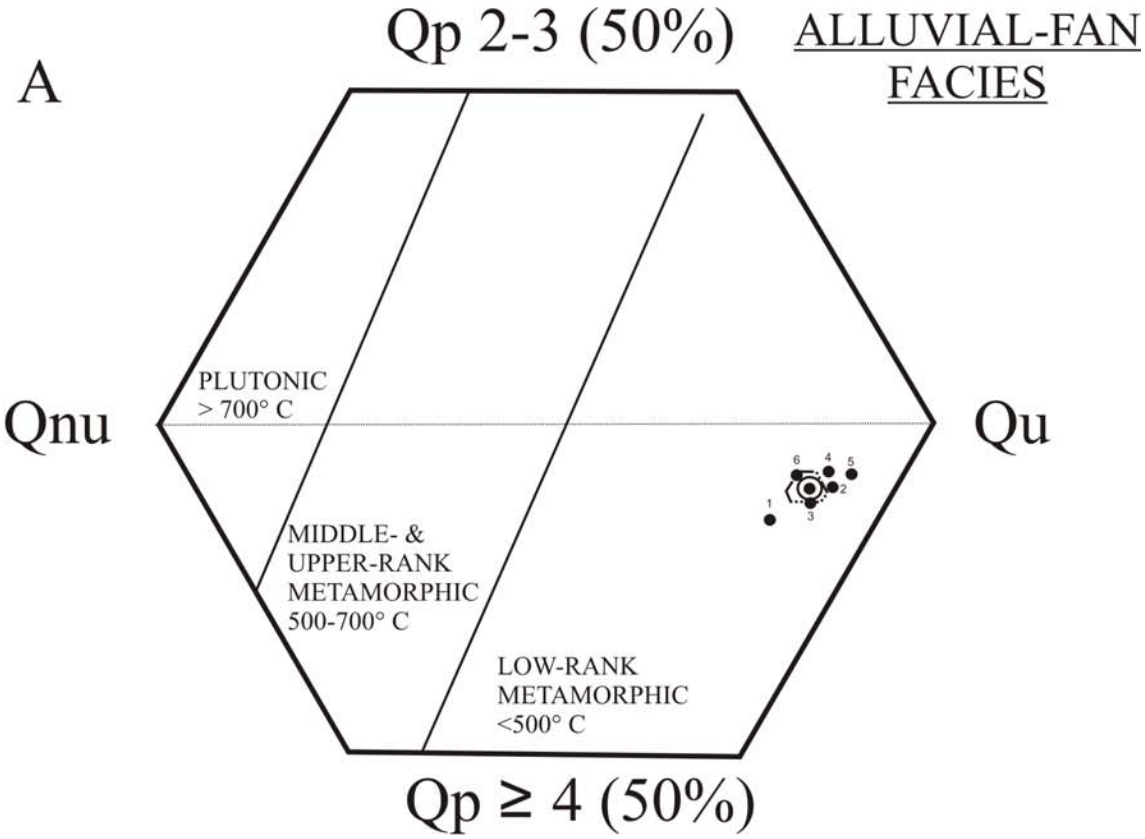
A
Qp 2-3 (50%)
ALLUVIAL-FAN FACIES
Qnu
Qu
PLUTONIC
> 700° C
MIDDLE- &
UPPER-RANK
METAMORPHIC
500-700° C
LOW-RANK
METAMORPHIC
<500° C
Qp ≥ 4 (50%)

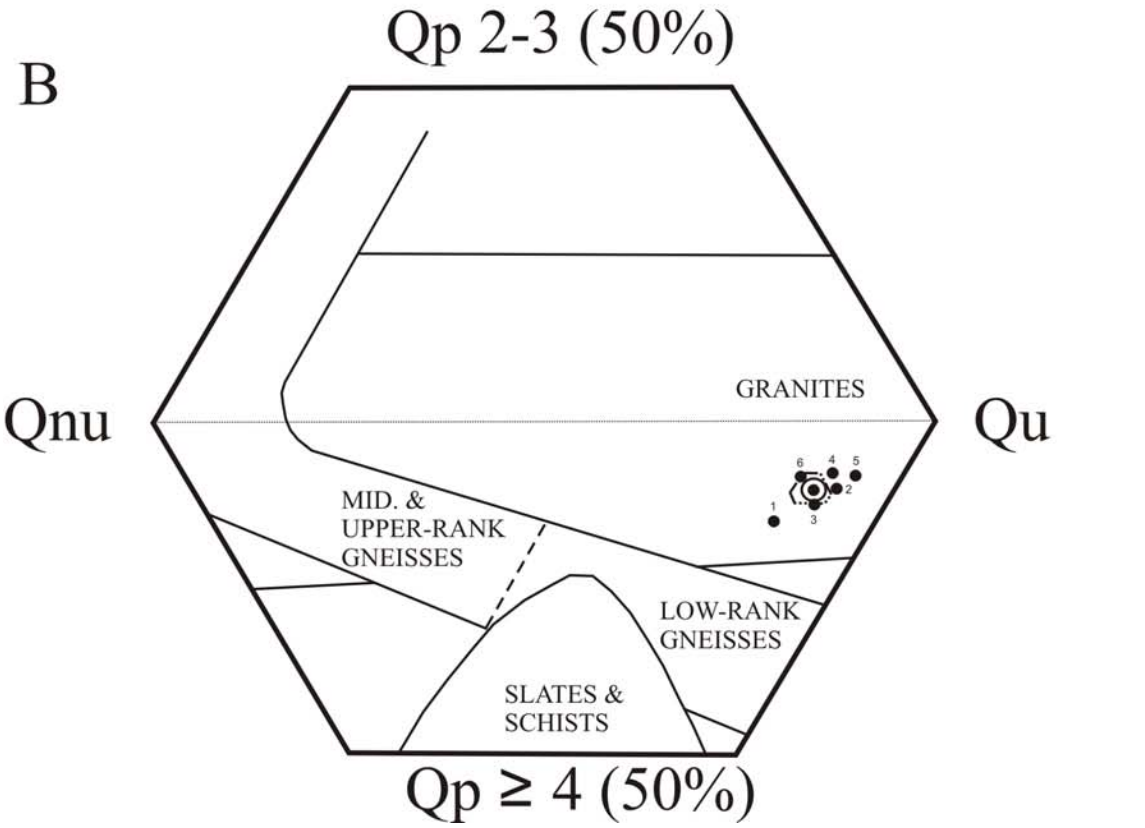
B
Qp 2-3 (50%)
Qnu
Qu
GRANITES
MID. &
UPPER-RANK
GNEISSES
LOW-RANK
GNEISSES
SLATES &
SCHISTS
Qp ≥ 4 (50%)

2.3 Diagenesis

The diagenetic history of the Deerfield basin is described in Taylor (1991) and Hubert et al. (2001). Diagenetic modification of framework grains, especially feldspars, must be recognized during provenance analysis (Dickinson, 1970; Helmold, 1985).

Post-depositional fluids altered the detrital mineralogy of the Sugarloaf Arkose through 1) intrastratal dissolution of Fe-rich heavy minerals and feldspars; 2) albite replacement of feldspar; and 3) clay-mineral replacement of feldspar (Carozzi, 1993; Helmold, 1985; Taylor, 1991; Hubert et al., 2001).

2.3.1 Early Mesogenesis

Early mesogenesis starts after effective burial to a few tens of meters at near surface temperature, and continues to depths of 2-3 km and 70-100^{o}C (Morad et al., 2000; Boggs, 2006). Early diagenetic events include hematite grain coats, mechanical compaction, albitization of feldspars, and precipitation of albite and quartz cements (Figure 29). The relative timing of diagenetic effects is based on thin-section observations. The percentages of all cements in the valley-river, piedmont-river, and alluvial-fan samples are shown in Figures 30 and 31A.

Hematite grain coats are common in all three facies because they are derived from soil stains of yellow-brown limonite iron-hydroxides (Hubert and Reed, 1978; Hubert et al., 2001) (Figure 14, 27B, 30, 31A, 32B, 33). Dehydration of the limonite in oxidizing, alkaline water produces hematite in about 300 to 3.000 ka (Walker, 1976). The hematite coats inhibit overgrowths of other cements, and are negatively correlated with the volumes of albite and quartz overgrowths.

Figure 29. Summary of sandstone diagenesis, in part modified from Hubert et al. (2001).

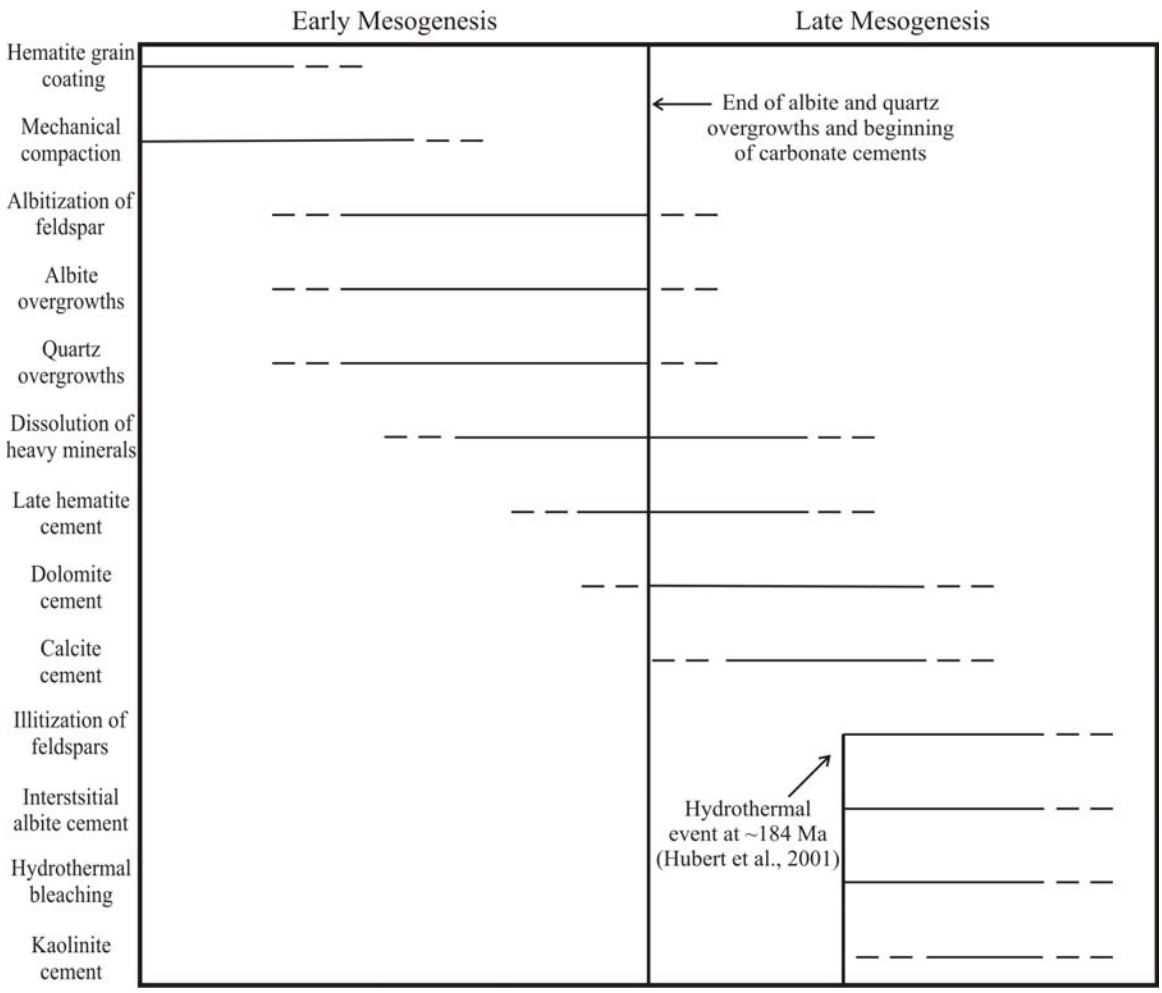
Early Mesogenesis
Late Mesogenesis
Hematite grain coating
Mechanical compaction
Albitization of feldspar
Albite overgrowths
Quartz overgrowths
Dissolution of heavy minerals
Late hematite cement
Dolomite cement
Calcite cement
Illitization of feldspars
Interstsitial albite cement
Hydrothermal bleaching
Kaolinite cement
End of albite and quartz overgrowths and beginning of carbonate cements
Hydrothermal event at ~184 Ma (Hubert et al., 2001)

Figure 30. Pie diagrams of cements in the valley-river (A) and piedmont-river (B) samples recalculated to 100%.

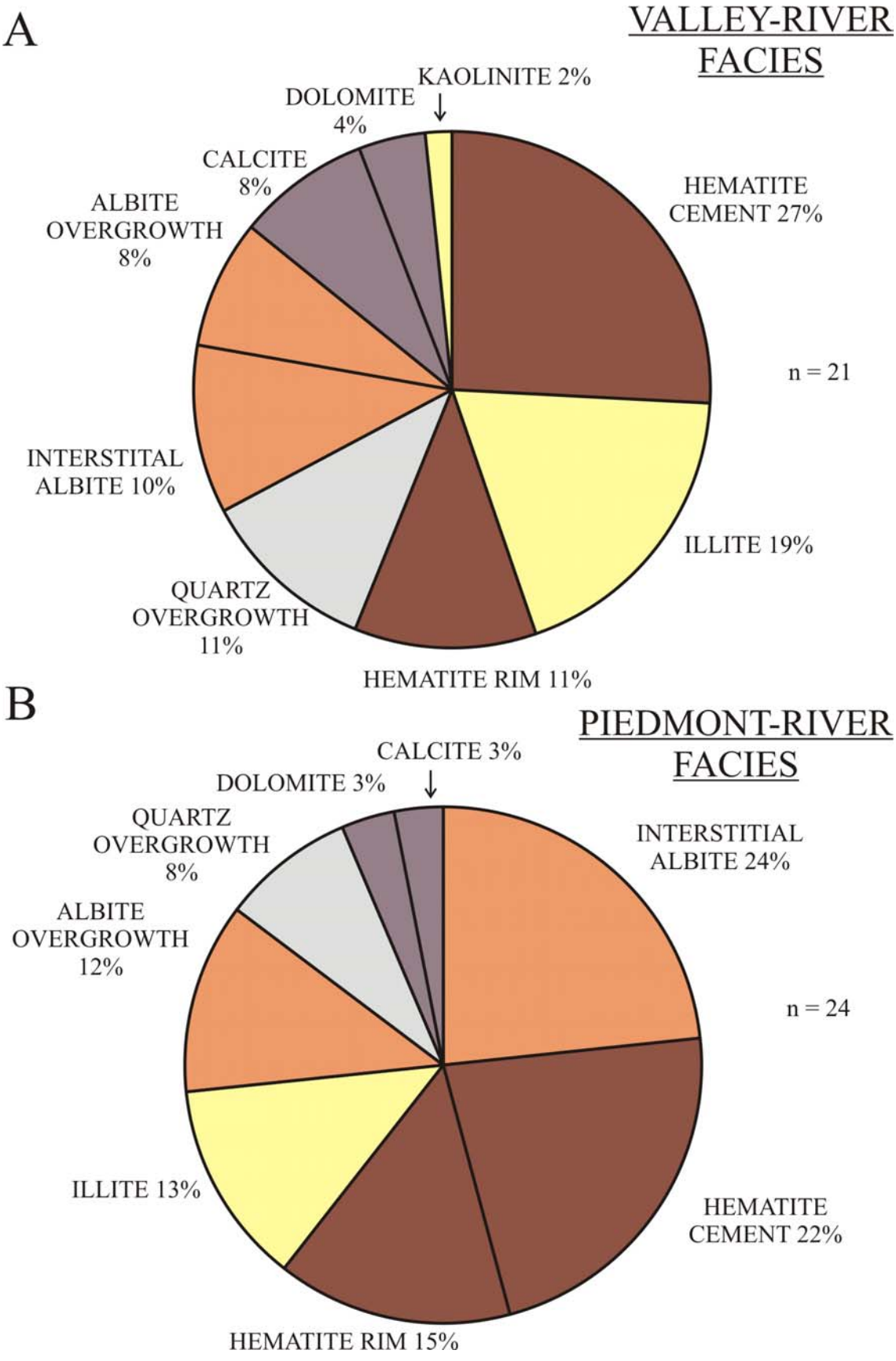
A
VALLEY-RIVER FACIES
KAOLINITE 2%
DOLOMITE 4%
CALCITE 8%
ALBITE OVERGROWTH 8%
HEMATITE CEMENT 27%
n = 21
INTERSTITAL ALBITE 10%
ILLITE 19%
QUARTZ OVERGROWTH 11%
HEMATITE RIM 11%
B
PIEDMONT-RIVER FACIES
CALCITE 3%
DOLOMITE 3%
QUARTZ OVERGROWTH 8%
INTERSTITIAL ALBITE 24%
ALBITE OVERGROWTH 12%
n = 24
ILLITE 13%
HEMATITE CEMENT 22%
HEMATITE RIM 15%

The relative importance of mechanical compaction versus cementation in reducing porosity is assessed by comparing the intergranular volume (porosity plus cements) to cement volume (Loucks et al., 1984; Houseknecht, 1987) (Figure 31B). Figure 31B assumes initial surface porosity of 40%, and shows that porosity lost to compaction in the valley-river, piedmont-river, and alluvial-fan facies is 66%, 58%, and 54%. Ten samples in both the valley-river and piedmont-river facies lost ≥75% of initial porosity to mechanical compaction. Two valley-river, four piedmont-river, and two alluvial-fan samples contain >20% cement, indicating compaction of the sand is younger than major cementation. Three samples have ~5% remaining porosity, the remainder have <3%. Remaining porosity is likely a combination of original porosity and secondary porosity from grain dissolution. Reduction of porosity from 40% to 15-20% in an arkose is consistent with burial to 2-3.5 km (Tucker, 2001).

In addition to porosity loss, detrital micas are greatly distorted by compaction, and are often bent around relatively rigid framework grains (Figure 32A). Compaction locally modified framework grain contact boundaries (Figure 32B). Pressure-dissolution is uncommon, indicating matrix and/or early cements spread overburden load (Tucker, 2001).

Albitization is a well-documented process in sedimentary basins, and affected both the Deerfield and Hartford basins (Boles, 1982; Morad et al., 1990, Hubert et al., 1992, 2001). Many grains of plagioclase and K-feldspar have overgrowths of nearly-pure albite ($Ab_{99.69}An_{0.08}Or_{0.23}$; Meriney, 1988) (Figures 12A, 14A, 14B, 27B, 32B). Overgrowths are in optical continuity with albite-rich host plagioclase grains and twins occasionally continue onto the overgrowths.

Figure 31. Pie diagram of alluvial-fan cements recalculated to 100% (A) and chart depicting porosity loss to compaction versus cementation assuming an initial porosity of 40% (Houseknecht, 1987) Approximately equal volumes of porosity were lost to compaction and cement in the piedmont-river and alluvial-fan facies; compaction was more important than cementation in the valley-river facies. Lightly-shaded points are facies means. Samples affected by illite replacement are plotted as X, because illite pseudomorphs are difficult to distinguish from pore-filling cement, and late mesogenetic pressure-solution strongly biases towards compaction over cementation. Primary and secondary cements were not differentiated during modal analysis. Porosity increases away from diagonal line, and is the amount of remaining original porosity and secondary porosity.

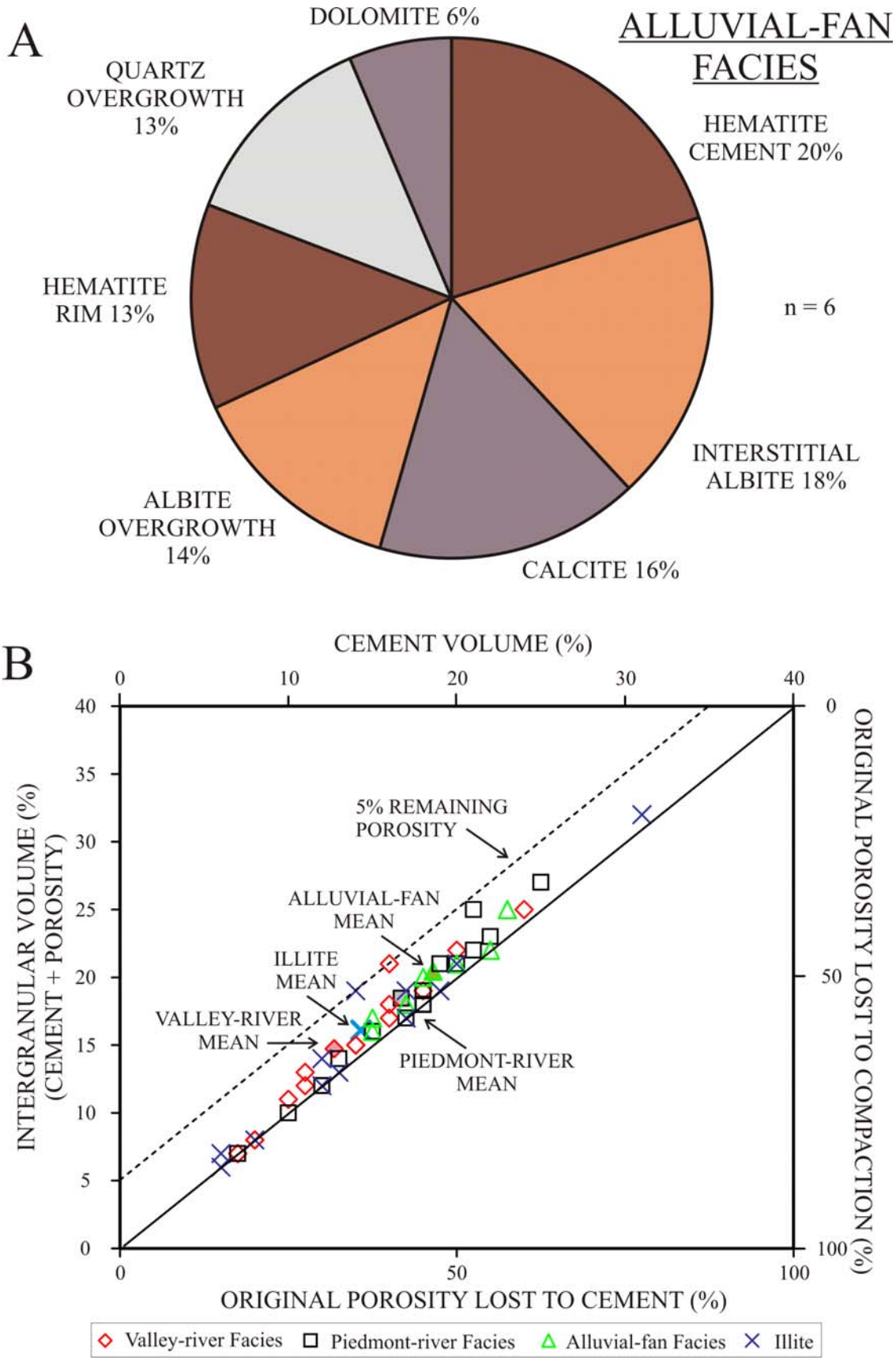
A
ALLUVIAL-FAN FACIES
DOLOMITE 6%
QUARTZ OVERGROWTH 13%
HEMATITE CEMENT 20%
HEMATITE RIM 13%
n = 6
INTERSTITIAL ALBITE 18%
ALBITE OVERGROWTH 14%
CALCITE 16%
B
CEMENT VOLUME (%)
0
10
20
30
40
INTERGRANULAR VOLUME (%) (CEMENT + POROSITY)
35
25
15
5
5% REMAINING POROSITY
ALLUVIAL-FAN MEAN
ILLITE MEAN
VALLEY-RIVER MEAN
PIEDMONT-RIVER MEAN
ORIGINAL POROSITY LOST TO COMPACTION (%)
50
100
ORIGINAL POROSITY LOST TO CEMENT (%)
Valley-river Facies
Piedmont-river Facies
Alluvial-fan Facies
Illite

Figure 32. Micrographs of compaction, cement, and grain replacement. Mx is hematite-stained matrix; Q is quartz; H is hematite cement; B is biotite bent due to compaction in 32A and altered by hematite in 32B; P is plagioclase with albite replacement; QTZTE is quartzite grain with sutured and crenulated boundaries; IR is illite replacement of plagioclase; IC is illite cement; C is ferroan dolomite and calcite cements. White arrow points to albite overgrowth, and black arrow points to compaction-altered grain boundary. Crossed nicols; scale bar is 0.5 mm.

A

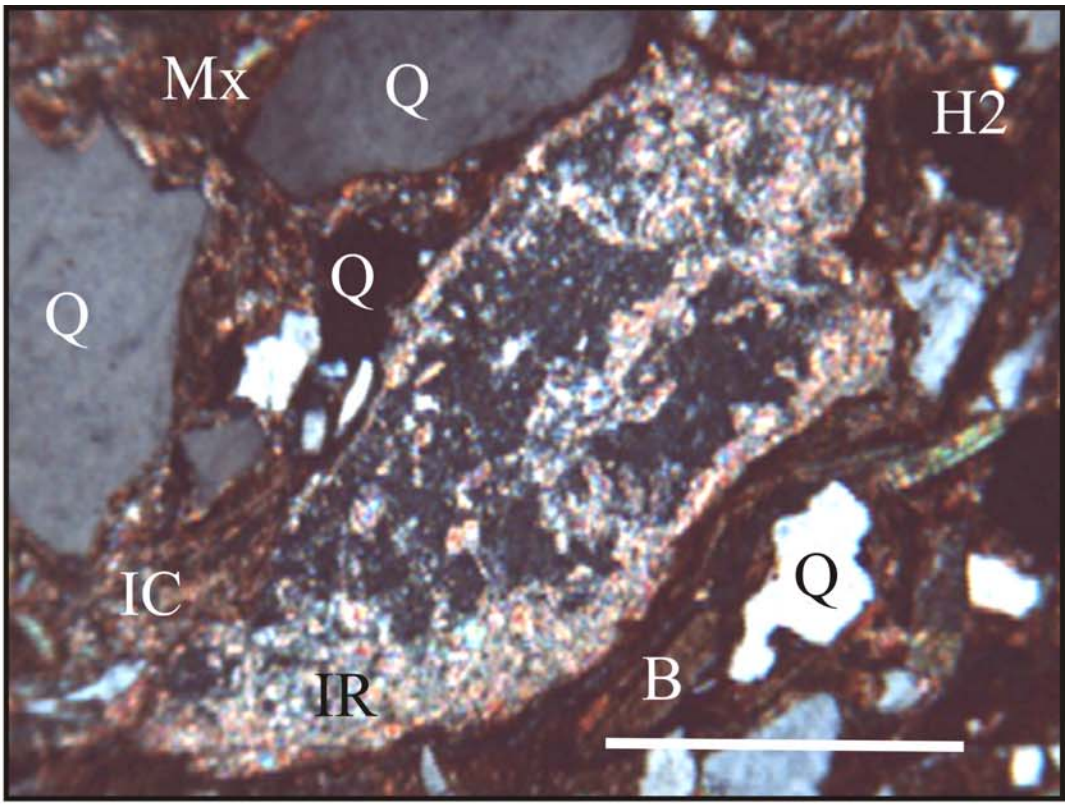

B

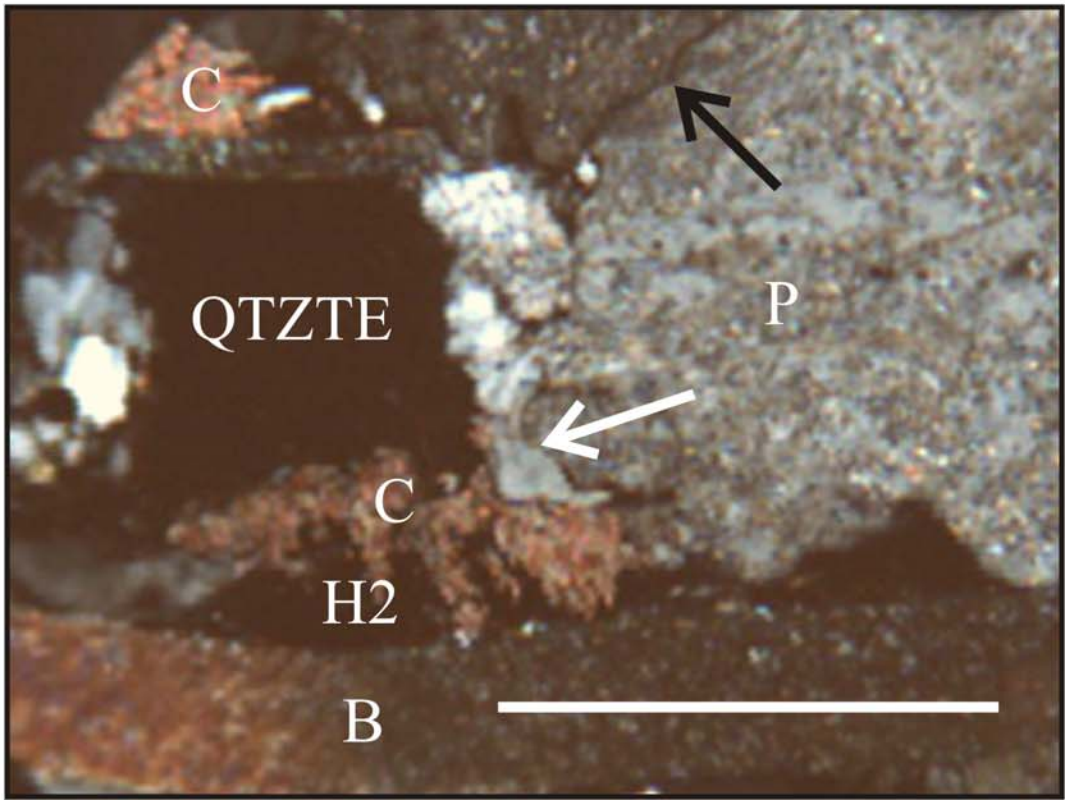

Precipitation of albite overgrowths was accompanied by replacement of plagioclase grains by albite along grain boundaries, cleavage planes, and grain fractures; replacement proceeded inward into the grains. Most albitized grains also host albite overgrowths, and the replacement domains and overgrowths are commonly in optical continuity (Figures 12A and 14B). Albite pseudomorphs are recognized by lack of vacuoles and sericite, and by optical continuity with overgrowths.

The timing of alteration events is very difficult to establish. The vacuoles and sericite common in plagioclase and K-feldspar may be inherited from the source rock, added during weathering and transport, or developed during diagenesis (Helmold, 1985). Vacuoles and sericite are lost during albite replacement, but many albite overgrowths have vacuoles as well, which indicates vacuolization and sericite formed prior to and after albitization.

Interpenetration of quartz and albite overgrowths suggests coeval precipitation (Figures 27B and 33A). Quartz overgrowths are generally in optical continuity with host grains, and are discerned by thin hematite rims on grain surfaces. Quartz and albite overgrowths are more common in sandstones with minor hematite rims because the rims prevent nucleation of overgrowths.

Albitization, including overgrowths, and quartz overgrowths require pore water saturated with Na^{2+} and Si^{4+}, respectively. Both intra-basinal and extra-basinal sources may contribute to the formation waters. Descending groundwater may have percolated down through the unconsolidated sediment and enriched interstitial water with Na^{2+} and Si^{4+} (Hubert et al., 2001). Authigenic-quartz fluid inclusions in North Sea sandstones

indicate groundwater-derived overgrowths precipitate at temperatures from 75° to 150°C, consistent with burial depths of 2-5 km (Morad et al., 2000).

2.3.2 Late Mesogenesis

Late mesogenesis takes place at depths greater than 3 km and temperatures above 100°C (Morad et al., 2000). Following precipitation of albite and quartz cements, late hematite cement filled much of the remaining pore space (Figures 14A, 27A, and 32). Dissolution of Fe-bearing heavy minerals, including biotite, hornblende, and augite, released iron for authigenic hematite (Handy, 1977; Hubert and Reed, 1978). Biotite grains grade from unaltered biotite to complete replacement by hematite.

Carbonate cements are present in sandstones from all facies, and comprise 25% of the cements in the alluvial-fan facies (Figures 14B, 31A, 32B). Dolomite and ferroan dolomite are younger than pore-filling hematite (Figure 32B), and the dissolution of heavy minerals that supplied iron for authigenic hematite may also have supplied magnesium. Calcite and ferroan calcite partially to completely replace older dolomite cement. Carbonate cements younger than quartz overgrowths is a global phenomena, evidently related to retrogressive solubility of carbonates and progressive solubility of quartz with increasing burial temperature (Morad et al, 2000).

Diagenetic reactions plus high-heat flow peaking at about 185 Ma generated hot brine deep in the basin. The brine strongly affected strata in the lower 1400 m of the Sugarloaf Arkose, replacing almost all detrital plagioclase and albite overgrowths with illite. Argon spectra for detrital microcline indicate cooling through ~150°C at about 170-150 Ma, well above the threshold of illite replacement at 130°C (Ehrenberg and Nadeau, 1989; Hubert et al., 1991).

Figure 33. Micrographs of overgrowths and pseudomorphs. Albite and quartz overgrowths in original pore space now filled with blue epoxy (A), and illite and kaolinite pseudomorph of plagioclase grain (B). Q is quartz; H is hematite grain coat; and I is intraclast. White arrow points to relict hematite grain coat that separates pseudomorph from illite cement. Kaolinite 'books' are first-order gray in 33B. Plane light in 33A, crossed nicols in 33B; scale bar is 0.5 mm.

A

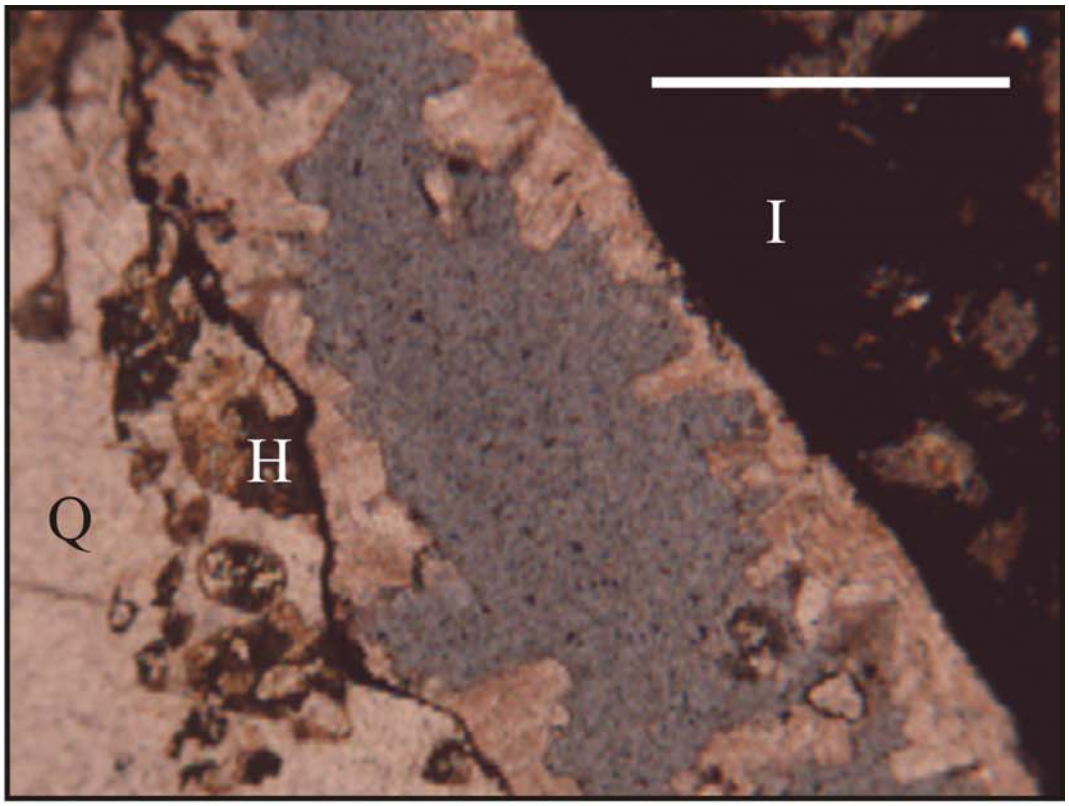

B

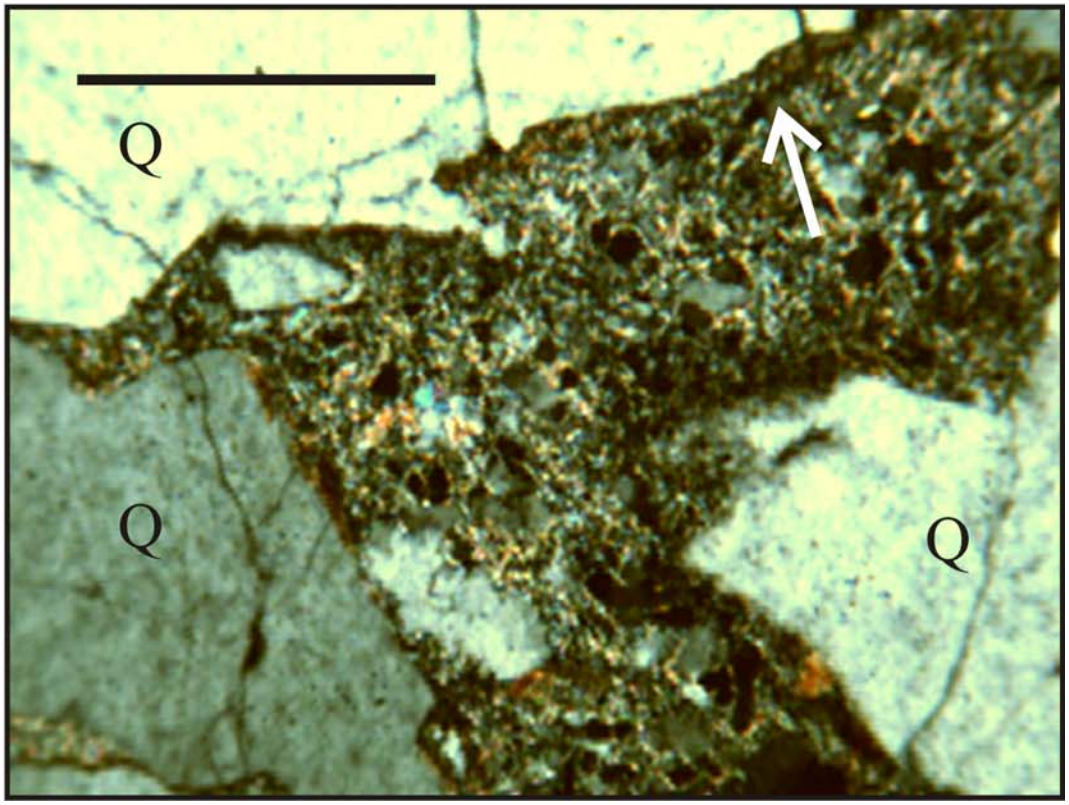

The small amount of remaining plagioclase is heavily illitized along grain boundaries and fractures (Figure 32A). Illite pseudomorphs of plagioclase are identifiable by relict hematite rims; where hematite rims are rare, illite pseudomorphs commonly cannot be distinguished from pore-filling illite (Figure 33B). The remaining feldspar is almost entirely K-feldspar in granite and gneiss, though illite replacement heavily affects K-feldspar as well. Pressure-solution contacts between quartz grains are more common in rocks that have been illitized, perhaps because removal of plagioclase increased lithostatic load on the remaining framework (Hubert et al., 2001). 'Books' of hydrothermal kaolinite are commonly found intergrown with or replacing illite (Figure 33B).

Interstitial mosaic albite precipitation occurred in the upper ~600 m of the Sugarloaf Arkose during the hydrothermal event, and is characterized by randomly oriented tabular to prismatic crystals not in optical continuity with detrital plagioclase or albite overgrowths (Hubert et al., 2001). Mosaic albite pore-fills are often twinned, and most are cloudy and turbid due to vacuolization. The sandstones just below the Deerfield Basalt are extensively bleached by removal of hematite rims and cements (Hubert et al., 2001).

2.4 Conglomerate Lithology

Most of the Sugarloaf Arkose is pebbly sandstone, locally a conglomerate, especially adjacent to channel banks (Section 1.5). Granitoids are common in conglomerates in all three facies, and comprise >25% of the valley-river and piedmont-river conglomerates (Figures 34 and 35A). Granitoids are: coarse-grained, phaneritic, acidic rocks of granite, granodiorite, and tonalite; foliated gneiss; granite pegmatites; and

graphic granite of quartz and microcline intergrowths (Streickeisen, 1979; Winter, 2001) (Figure 35B). Quartz and K-feldspar phenocrysts and megacrysts >3 cm are common in non-foliated, phaneritic pebbles. Degrees of foliation vary among granitoids: many 'granites' have weak-moderate gneissic foliation, and many 'granite gneisses' become less foliated across the observed face.

Almost all granites and granite gneisses are rich in K-feldspar with a pink or salmon color. White-hued, medium-grained, muscovite-rich granodiorite to tonalite is found rarely among valley-river and piedmont-river conglomerates. Biotite is the common mafic mineral in the phaneritic rocks, amphibole less so. Pyroxenes and amphibole are more common in the granite gneisses. Pegmatites commonly do not have mafic minerals, and graphic granite pebbles always lack mafic minerals. Muscovite is common, especially in pegmatites and gneisses. Many granitoids are heavily altered by hematite infiltration along fractures and feldspar dissolution and replacement, especially in the illite diagenetic zone.

Conglomeratic beds in the valley- and piedmont-river facies commonly have 'floods' of granitoids and K-feldspar, quartz, and K-feldspar-quartz megacrysts (Figure 36). Again, K-feldspar is colored pink or salmon due to microscopic inclusions of hematite in the crystal lattice (Dyar et al., 2008). Hematite inclusions form during re-equilibration of plutonic rocks and late fluids, and may continue as the rocks are uplifted and weathered (Kerr, 1994; Putnis et al., 2007). Pervasive authigenic hematite also stains pebbles in the arkose, perhaps further saturating K-feldspar pores with hematite inclusions. Color saturation decreases inward and away from fractures and cleavage

Figure 34. Pie diagrams of conglomerate lithology in the valley-river (A) and piedmont-river (B) facies.

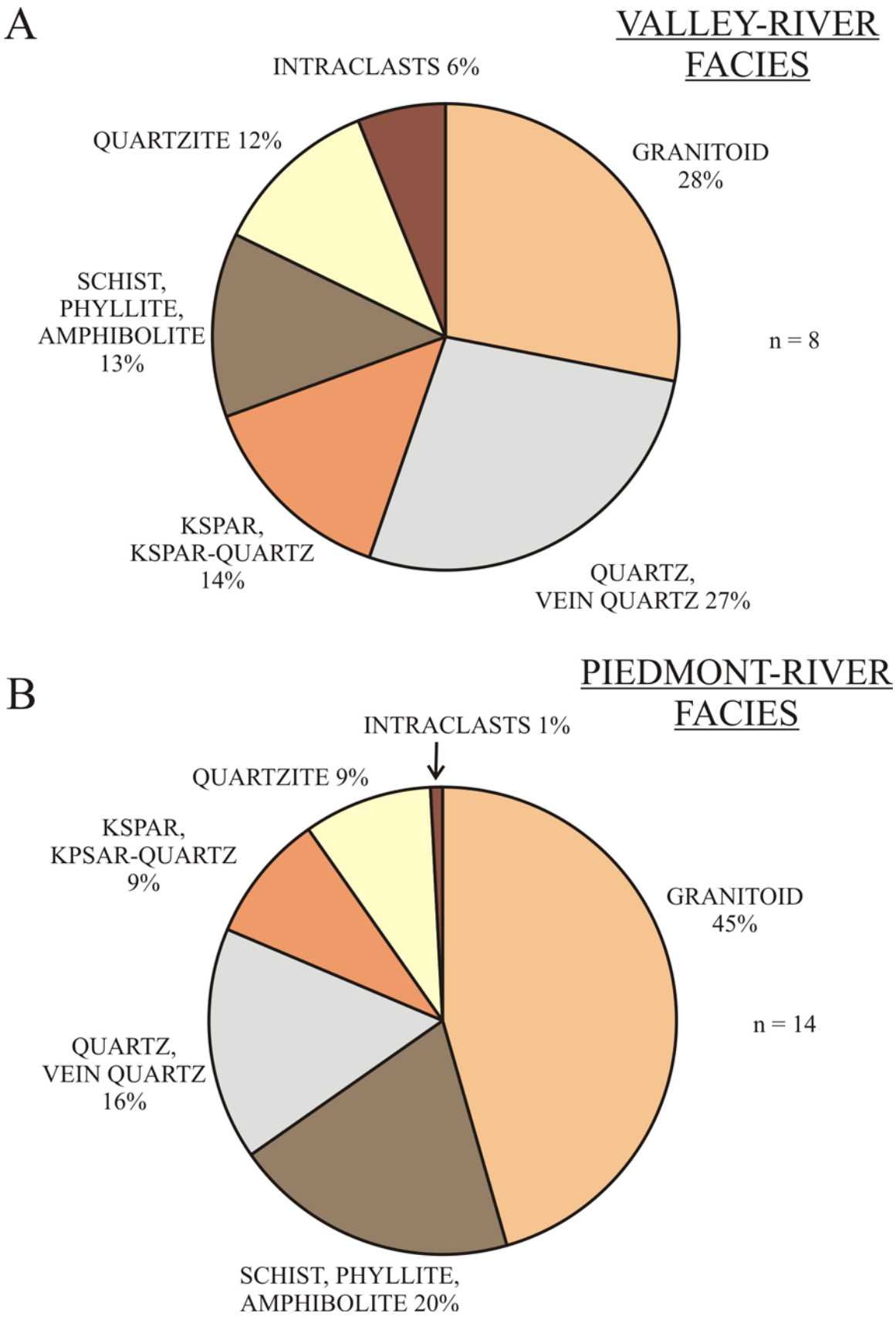
A
VALLEY-RIVER FACIES
INTRACLASTS 6%
QUARTZITE 12%
GRANITOID 28%
SCHIST, PHYLLITE, AMPHIBOLITE 13%
n = 8
KSPAR, KSPAR-QUARTZ 14%
QUARTZ, VEIN QUARTZ 27%
B
PIEDMONT-RIVER FACIES
INTRACLASTS 1%
QUARTZITE 9%
KSPAR, KPSAR-QUARTZ 9%
GRANITOID 45%
n = 14
QUARTZ, VEIN QUARTZ 16%
SCHIST, PHYLLITE, AMPHIBOLITE 20%

Figure 35. Pie diagram of conglomerate lithology in the alluvial-fan facies (A) and photograph of graphic granite pebbles (B). Heavy lines indicate orientation of quartz intergrowths in pink K-feldspar, presumably microcline. Pencil is 15 cm; sample on right is propped up with gray rock.

A

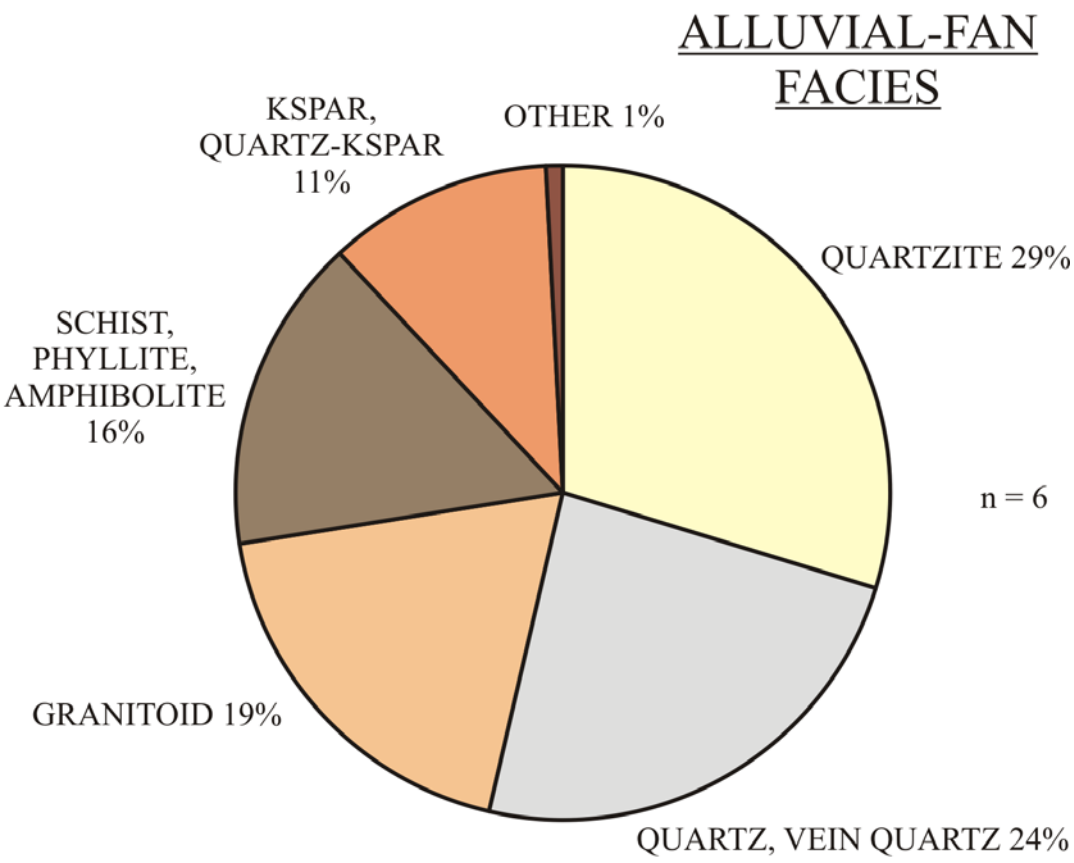
ALLUVIAL-FAN FACIES
KSPAR, QUARTZ-KSPAR 11%
OTHER 1%
QUARTZITE 29%
SCHIST, PHYLLITE, AMPHIBOLITE 16%
n = 6
GRANITOID 19%
QUARTZ, VEIN QUARTZ 24%

B

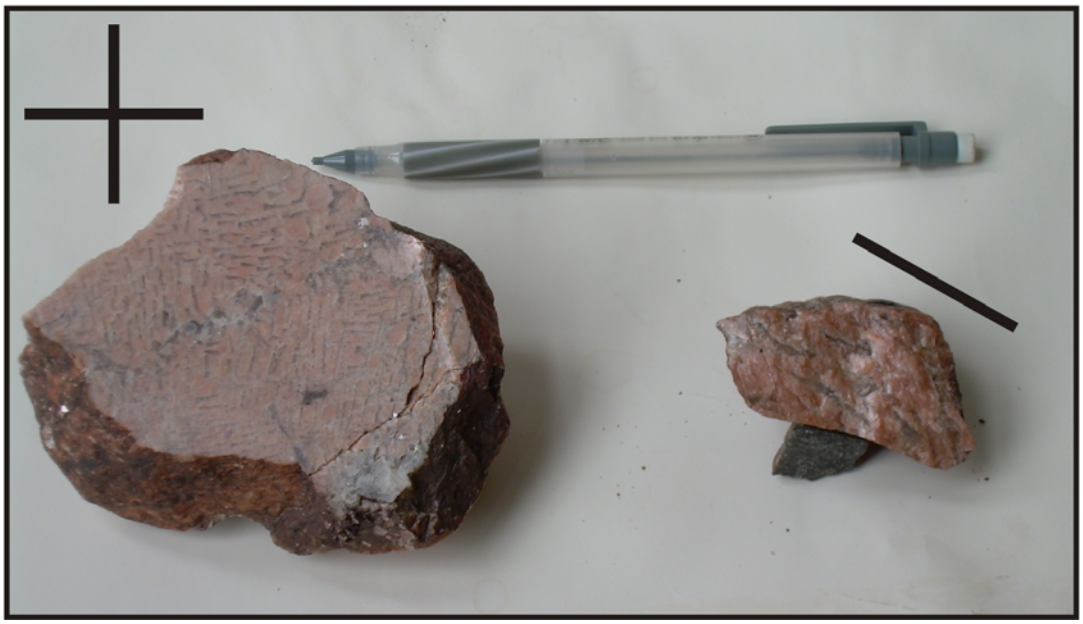

planes (Figure 36A). Red-brown hematite coats stain rinds and open fractures of pebbles (Figure 36B).

Milky-white vein quartz is less common than clear quartz (Figure 36B). The hue is due to fluid and gas inclusions, open vacuoles, and 'comb-like' interpenetrating sub-units (Folk, 1980). The two types of quartz are combined because no rigorous operational definitions exist.

Quartzite is the dominant pebble in the alluvial-fan facies (31%), and is present in the other facies. In all facies, gray quartzite with up to 15% muscovite is most common (Figure 37A). Pink to red quartzite with 'blips' of white quartz is rare in the piedmont-river conglomerates; only the gray quartzites appear in the valley-river and alluvial-fan facies. Both types of quartzite are fine-grained and contain relict bedding 1-2-cm thick.

Other metamorphic pebbles include phyllites, schist, and amphibolite. Rarely are schists garnetiferous. The combined lithologies comprise 20% of pebbles in the piedmont river, and 17% in alluvial fan.

Mud rip-up intraclasts are present throughout the valley-river facies and in the upper ~350 m of the piedmont-river facies (Hubert et al., 2008). The mudstones are sandy, micaceous, and occasionally contain calcite caliche nodules, casts of rootlets and *Scoyenia* burrows.

The mean sphericity of 16 samples of 100 pebbles each is plotted on a modified Zingg classification where shape is based on the ratio of the short, intermediate, and long axes (Zingg, 1935; Boggs, 2006) (Figure 37B). On the plot, sphericity increases on both axes to spherical (1.0). Lithology influences sphericity: granitoid, quartz, and K-feldspar are commonly equant, and metamorphic pebbles are oblate. In theory, sphericity

Figure 36. Photographs of K-feldspar pebbles (A) and quartz and K-feldspar-quartz pebbles (B). In A, K-feldspars have broken along cleavage planes. Arrows point to areas where pink color is absent. Sample on right is propped up with a gray rock. In B, pebble A is mostly K-feldspar with clear quartz (white arrow) and propped up with a gray rock; pebble B is milky-white vein quartz with hematite-stained fractures (black arrow). Pebble C is uncharacteristic dark-gray, slightly translucent quartz. Pencil is 15 cm.

A

B

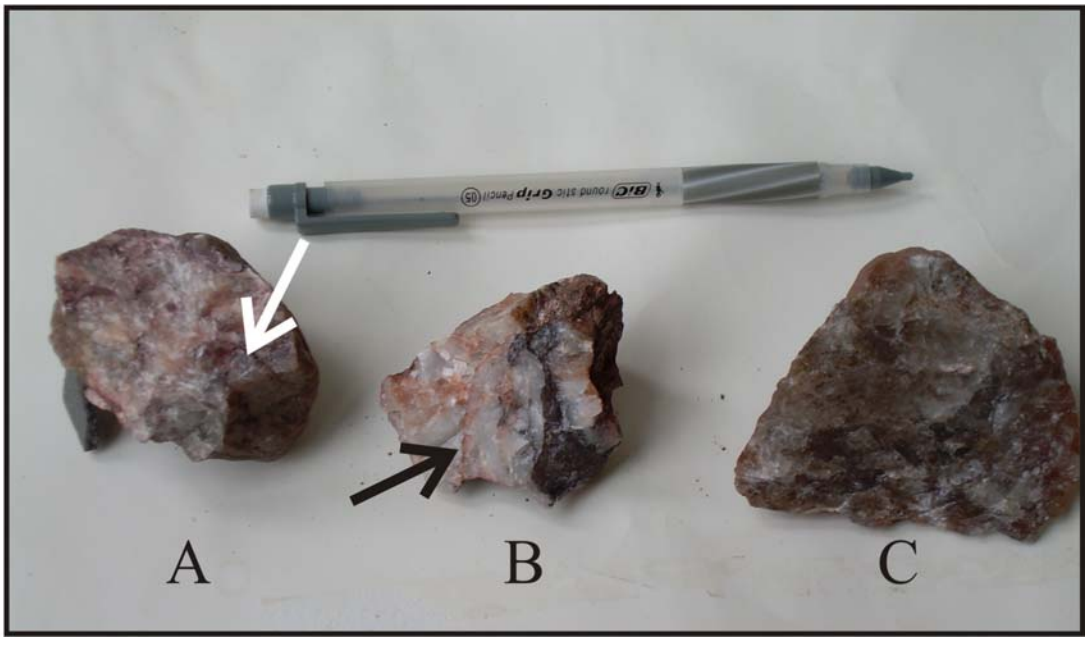

Figure 37. Photograph of quartzite pebble (A) and modified Zingg (1935) diagram of pebble sphericity (B). In A, thin-bedded, gray quartzite is propped up by gray rock chip; pencil is 15 cm. In B, means of 16 samples (100 pebbles each) are plotted for average sphericity. Facies means (not shown) plot in the equant field for valley river; oblate field for piedmont river; and triaxial field for alluvial fan.

A

B

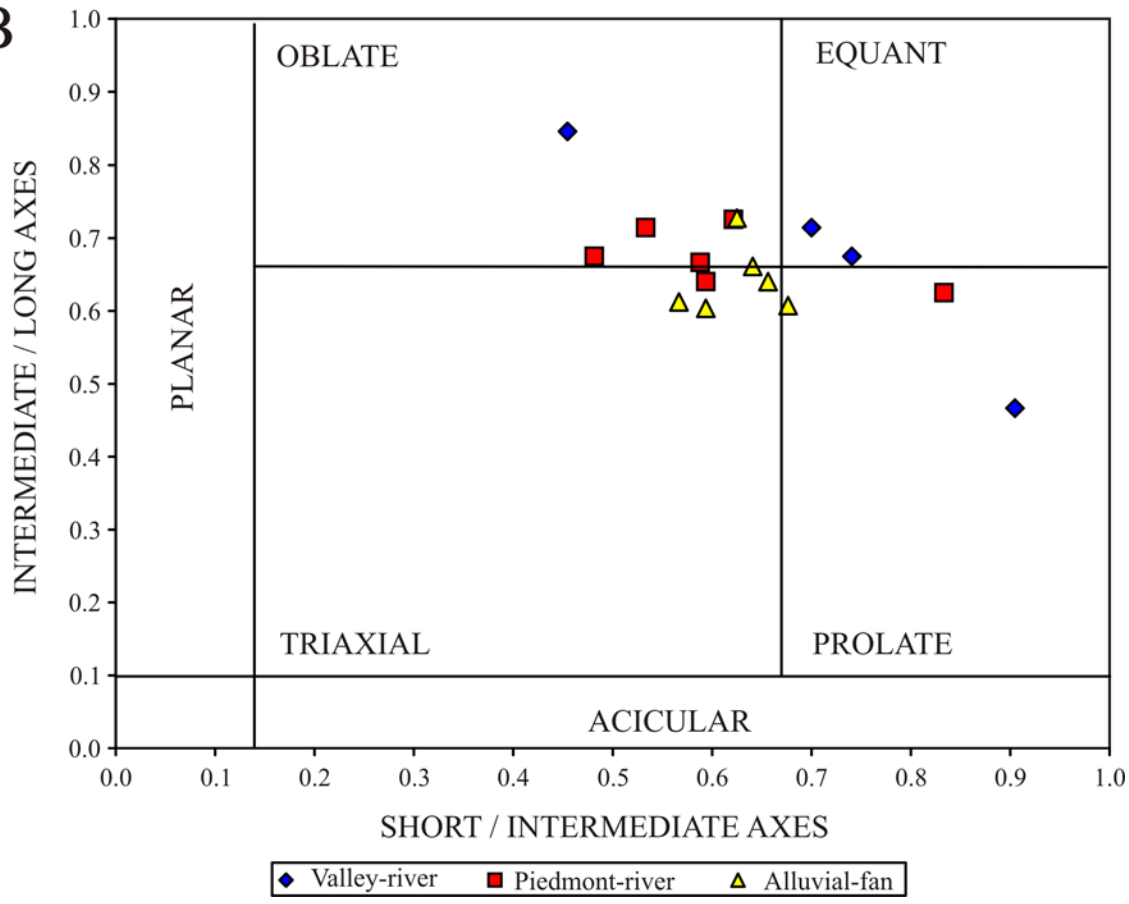
OBLATE
EQUANT
PLANAR
TRIAXIAL
PROLATE
ACICULAR
INTERMEDIATE / LONG AXES
SHORT / INTERMEDIATE AXES
0.0
0.1
0.2
0.3
0.4
0.5
0.6
0.7
0.8
0.9
1.0
Valley-river
Piedmont-river
Alluvial-fan

increases with distance of transport due to abrasion; however the sphericities are similar in each facies. The valley-river pebbles are slightly more rounded than the other facies, as might be expected, but the large scatter and small number of samples does not provide much support for this conclusion. Pebbles in each facies are dominantly sub-rounded, with sub-angular pebbles nearly as common as sub-rounded in the alluvial-fan conglomerates.

When using pebble lithologies to infer source terranes, they must be compared to medium-sand compositions because grain-size is strongly related to composition. Schist and phyllites pebbles are easily reduced to sand during weathering and transport, whereas quartzite resists abrasion. Granites weather to particles from finely-phaneritic sand to pegmatitic boulders. Table 3 compares pebble and medium-sand composition. G+K is granitoids plus K-feldspar. For conglomerates, K includes K-feldspar and K-feldspar-quartz pebbles. In medium sands, G+K includes quartz, plagioclase, K-feldspar, and micas in granite and granite gneiss, plus unit K-feldspar. Qtzte is quartzite, and Mtx is phyllite, schist, and amphibolite. For medium sand, Mtx includes quartz and micas in schist and schistose quartz (Appendix C).

Figure 38. Conglomerate in the valley-river facies is G+K-rich (64%), with granitoids more common than K-feldspar by 2:1 (Appendix D). Qtzte and Mtx are about equal, with mean values <20%. In medium sand, the percentage of Qtzte doubles at the expense of G+K; Mtx is the same in conglomerate and medium sand.

Figure 39. The piedmont-river conglomerates have the same G+K as in the valley river, but the ratio of G:K is >4:1. Qtzte is less common and Mtx more common in piedmont-river conglomerates than in the other two facies. Similar to the valley rivers,

Table 3: Summary of sandstone and pebble composition			
	Valley-river Facies	Piedmont-river Facies	Alluvial-fan Facies
PEBBLES			
Gran + Kspar	64.1±5.2	63.9±6.8	39.4±2.2
Qtzte	17.1±5.5	10.8±4.0	**39.3±6.4**
Mtx	18.9±4.8	25.2±6.4	21.3±6.7
MEDIUM-SAND			
Gran + Kspar	50.4±4.7	53.3±4.1	47.6±5.9
Qtzte	31.0±3.6	28.9±2.9	31.2±3.8
Mtx	18.6±2.7	17.8±3.1	21.2±7.0
Ventifacts	4.3%	11.8%	6.8%
Incipient Ventifacts	15.3%	24.0%	9.8%
Desert Varnish	0.8%	3.0%	4.5%

Figure 38. G+K-Qtzte-Mtx plots of conglomerate (A) and medium sand (B) in the valley-river facies. A circled point is the mean, and a dashed hexagon shows the 95% confidence interval around the mean. The poles are defined in the text. Numbers correspond to sample numbers in Appendix C.

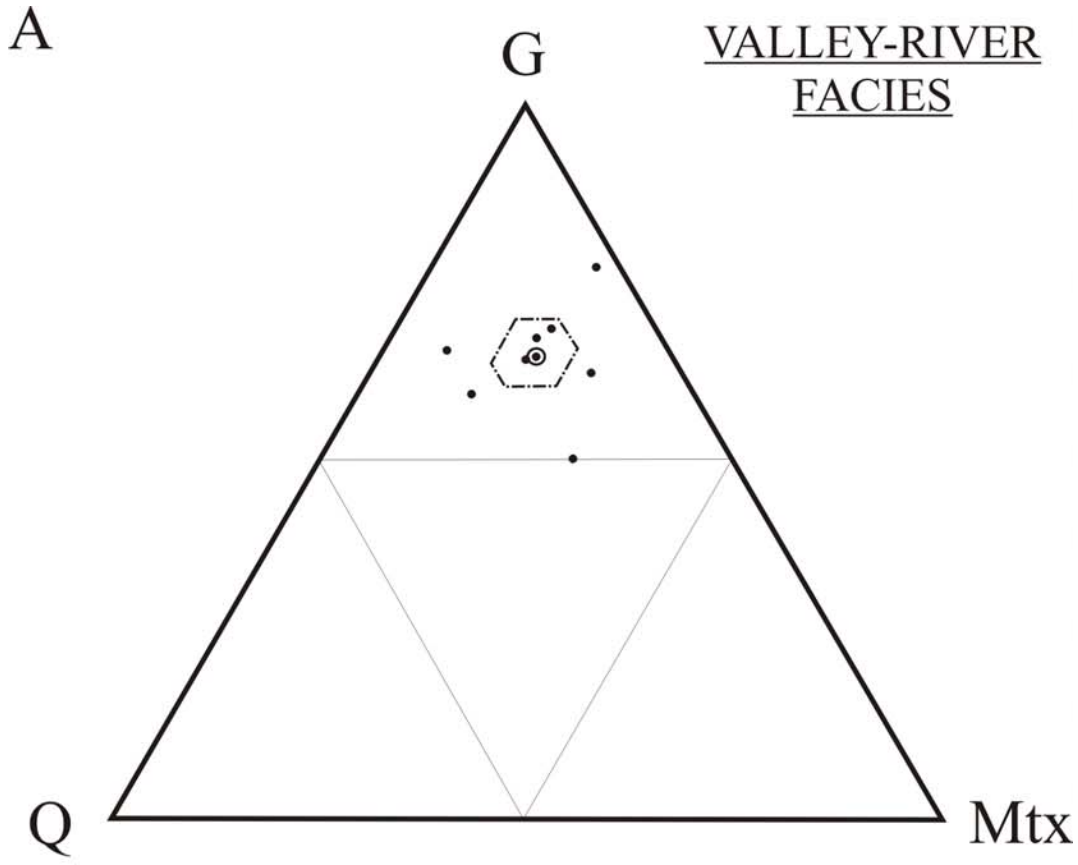
A
G
VALLEY-RIVER
FACIES
Q
Mtx

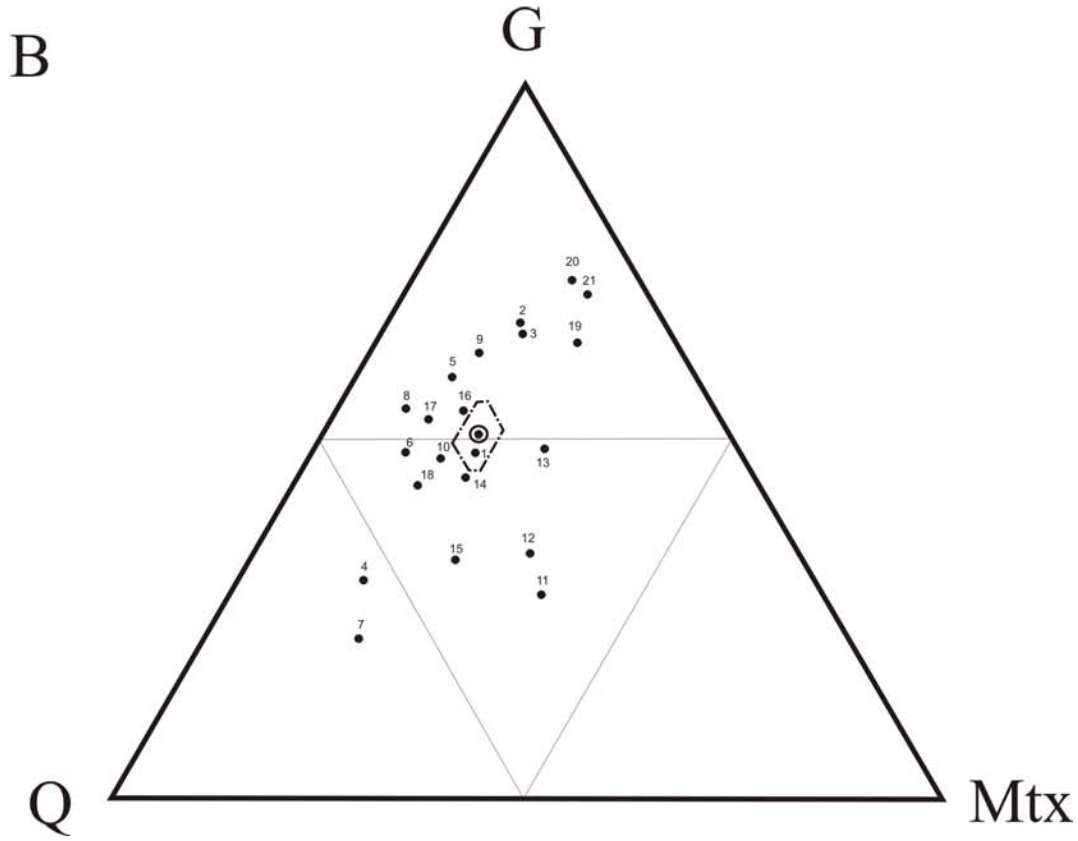
B
G
20
21
2
3
19
9
5
8
17
16
6
10
1
13
18
14
15
12
4
11
7
Q
Mtx

Figure 39. G+K-Qtzte-Mtx plots of conglomerate (A) and medium sand (B) in the piedmont-river facies. A circled point is the mean, and a dashed hexagon shows the 95% confidence interval around the mean. The poles are defined in the text. Numbers correspond to sample numbers in Appendix C.

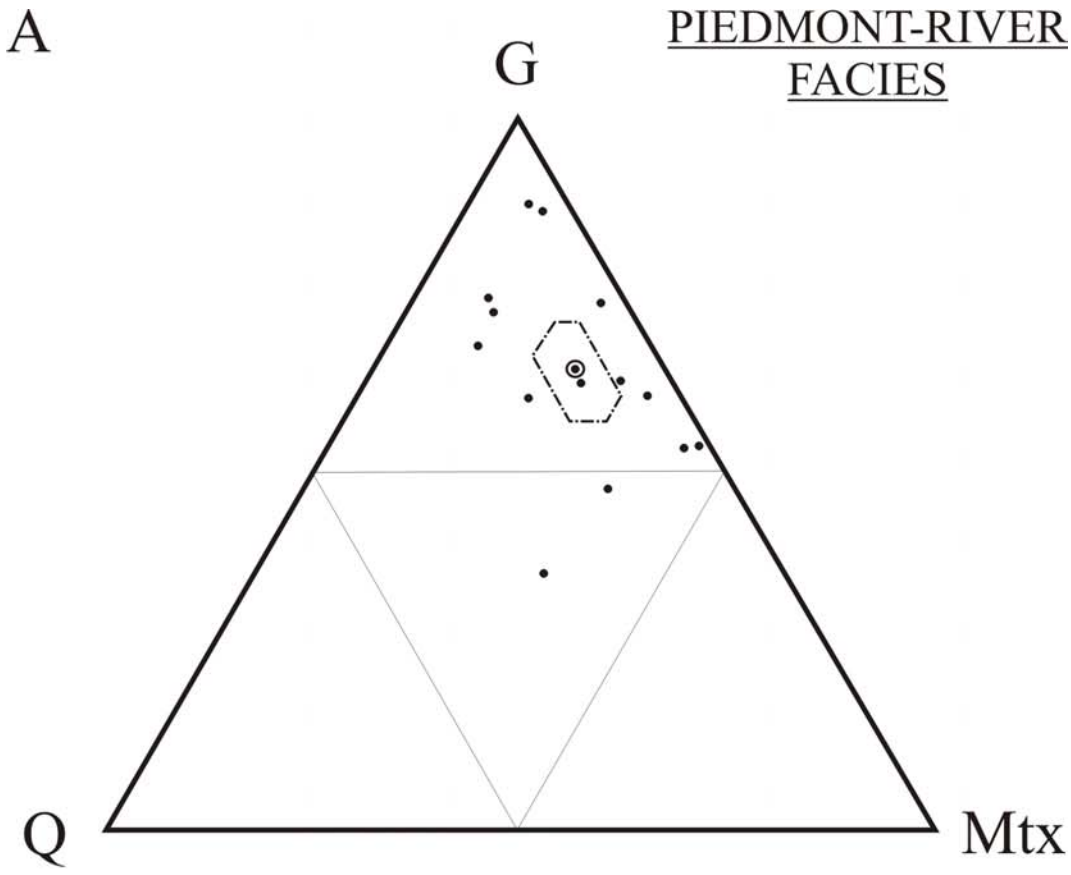
A
PIEDMONT-RIVER
FACIES
G
Q
Mtx

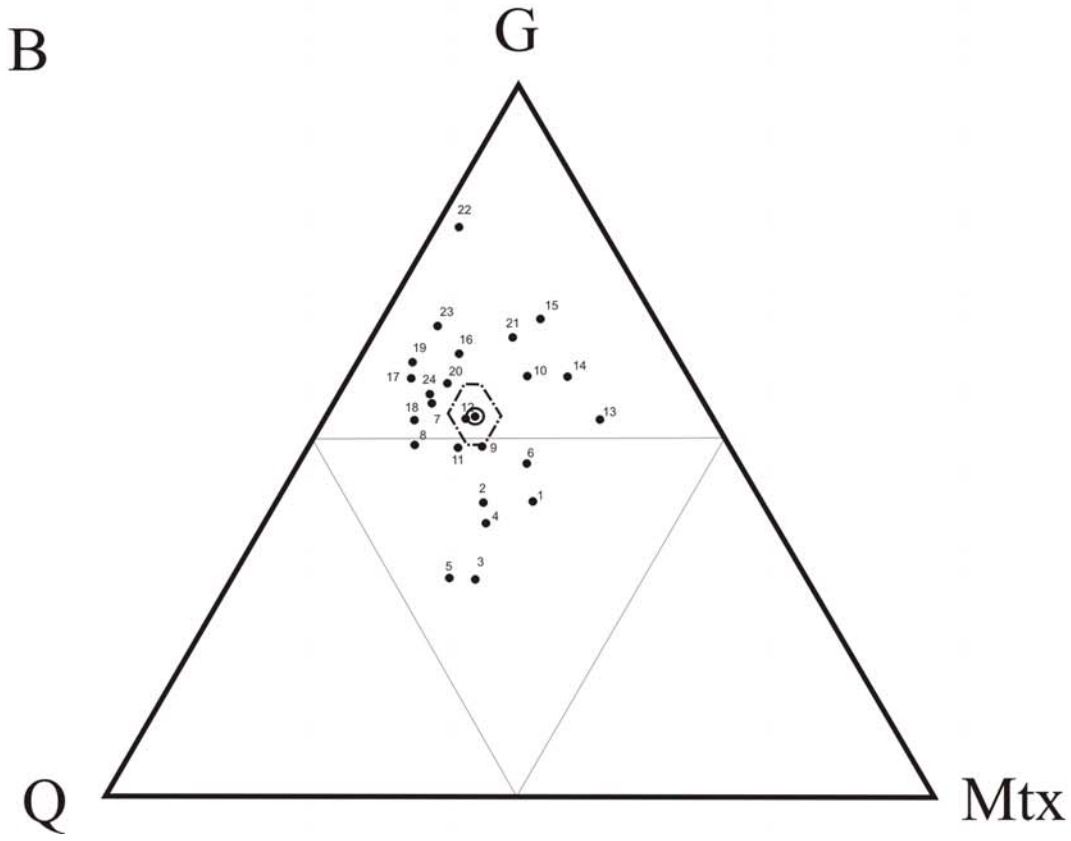
B
G
22
23
15
21
16
19
17
24
20
10
14
18
7
12
13
8
11
9
6
2
1
4
5
3
Q
Mtx

Qtzte abundance increases in medium sand. Unlike the valley rivers, Mtx and G+K abundances decrease in response to quartzite-enrichment.

Figure 40. Alluvial-fan conglomerates have equal amounts of Qtzte and G+K. The ratio of G:K is about 2:1. Mtx are more common than in valley-river conglomerates, but less than in piedmont rivers. Alluvial-fan medium sand has more G+K than Qtzte, but is still Qtzte-rich compared to medium sand in the other facies.

Summary. G+K dominates composition of valley-river and piedmont-river conglomerates, making up almost two-thirds of all pebbles in each facies. However, the valley-river conglomerates contain twice as much K-feldspar as piedmont-river conglomerates. Qtzte is slightly more abundant in the valley rivers; the same is true of Mtx in piedmont rivers. Medium-sand compositions are more Qtzte-rich than the conglomerates in both facies; Mtx is less common in piedmont-river medium sands than in conglomerate. The alluvial-fan conglomerates contain equal amounts of Qtzte and G+K, and more Mtx than the valley-river facies. Unlike the other facies, the medium sand contains less Qtzte, and more G+K.

Figure 40. G+K-Qtzte-Mtx plots of conglomerate (A) and medium sand (B) in the alluvial-fan facies. A circled point is the mean, and a dashed hexagon shows the 95% confidence interval around the mean. The poles are defined in the text. Numbers correspond to sample numbers in Appendix C.

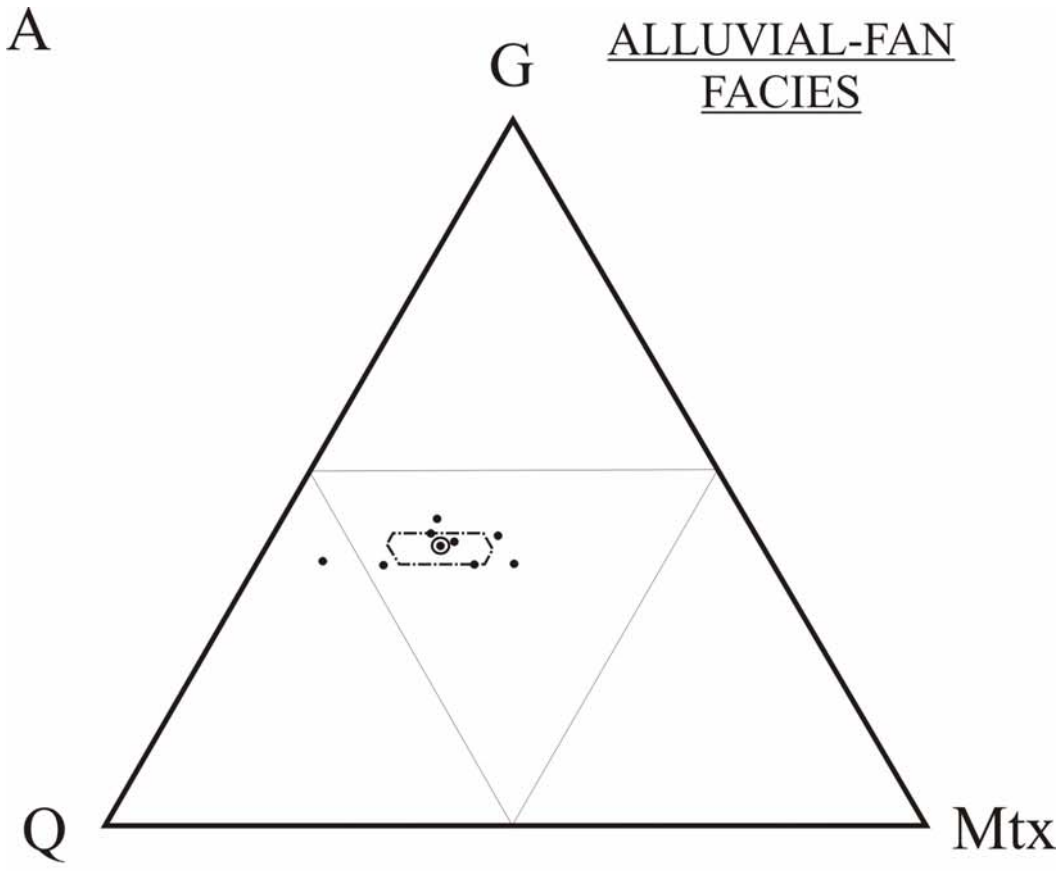
A
G
ALLUVIAL-FAN
FACIES
Q
Mtx

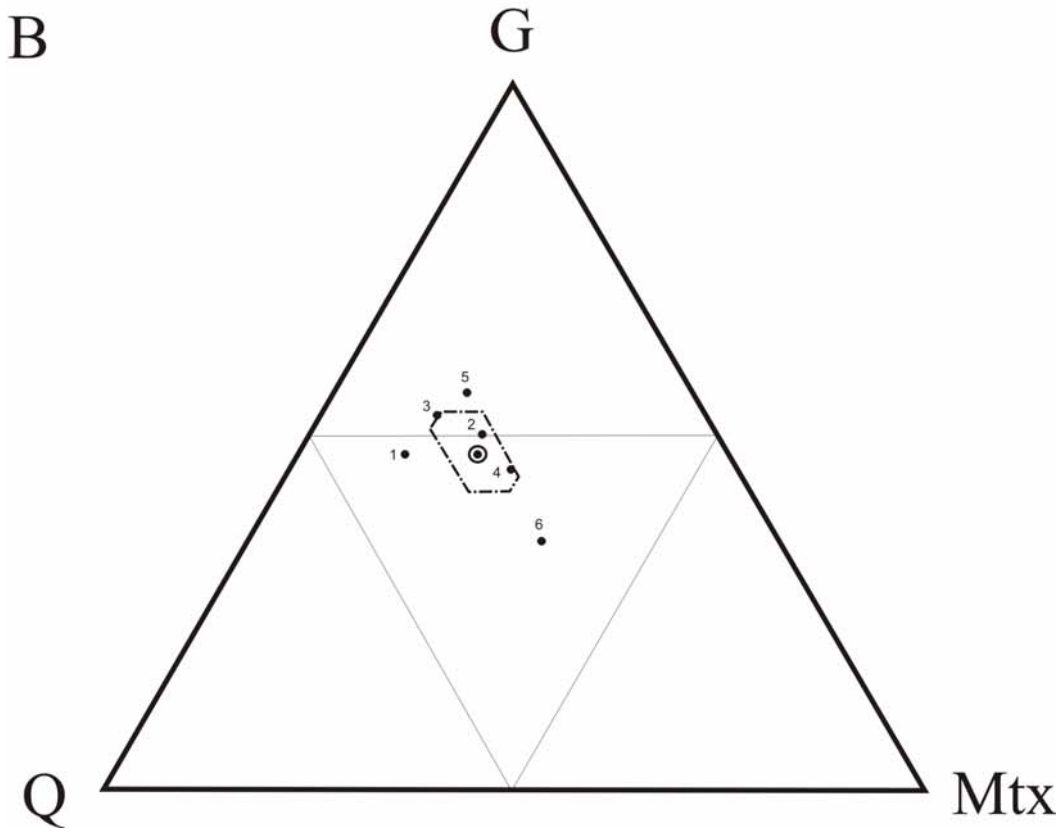
B
G
1
2
3
4
5
6
Q
Mtx

CHAPTER 3

PROVENANCE AND TECTONO-SEDIMENTARY HISTORY

3.1 Provenance of the Sugarloaf Arkose

Each of the depositional facies has aspects of two or three of the provenance fields (Figures 10, 18, and 24). This is in part because of the complicated regional geology created by multiple orogenies. Mixed provenance signals may also be related to limits and shortfalls of the Qt-F-L and Qm-F-Lt provenance diagrams (Dickinson, 1985). The empirically-derived models have been criticized because not all sandstones plot in the proper tectonic setting; however, other workers have shown the method is valid when average values are used (Boggs, 2006).

3.1.1 Valley-river Facies

The valley-river facies has a mixed provenance of continental block, magmatic arc, and recycled orogen (Table 4; Figures 41 and 10). The high ratio of quartz to feldspar indicates a mixture of feldspathic basement uplift and quartzose craton interior (Figures 41 and 10). Uplift sources are traditionally associated with rift-basin sands shed from basement granites and gneiss, whereas cratonic sources imply mature quartzose sand recycled from a continental shield or deposited in deep-water (Dickinson and Suczek, 1979). The valley-river sands have a 4:1 ratio of plagioclase to K-feldspar, which favors immature basement-derived sand over mature, plagioclase-poor cratonic sand (Figures 41 and 11A).

Table 4: Summary of Provenance

	Valley-river Facies	Piedmont-river Facies	Alluvial-fan Facies
Framework Grains			
Monocrystalline quartz	Undulose	Undulose	Undulose
Polycrystalline quartz	**2-3 subunits**	4+ subunits	4+ subunits
Plagioclase:K-feldspar	**4:1**	2:1	2:1
Plagioclase	**Twinned > untwinned**	Untwinned > twinned	Untwinned > twinned
Lithic Fragments	Quartzite = granite = gneiss	**Gneiss > quartzite >>> granite**	**Gneiss > quartzite >> granite**
Conglomerate			
Granitoids+K-feldspar:quartzite	G+K > Q	G+K > Q	**G+K = Q**
Granitoids:K-feldspar	2:1	**4:1**	2:1
Quartz Provenance			
Basu (1985)	Low- to mid-rank metamorphic	Low-rank metamorphic	Low-rank metamorphic
Tortosa et al. (1991)	Granite	Granite to low-rank gneiss	Granite to low-rank gneiss
Qt-F-L Provenance			
Qt-F-L	65-29-6	71-23-6	67-25-8
Dickinson (1985)	Mixed transitional continental and recycled collision orogen	Mixed transitional continental and recycled collision orogen	Mixed transitional continental and recycled collision orogen
Qm-F-Lt Provenance			
Qm-F-Lt	43-29-28	49-23-27	42-25-32
Dickinson (1985)	Mixed basement uplift and dissected arc ± recycled collision orogen	Mixed continental block and recycled collision orogen	Dissected arc± recycled collision orogen ± continental block

Figure 41. Summary of petrologic plots. The means and 95% confidence intervals of the valley-river (blue), piedmont-river (red), and alluvial-fan (yellow) facies are shown. Pole abbreviations are as follows: Qt is total quartz; F is feldspar; L is lithic fragments; Qm is monocrystalline quartz; Lt is lithic fragments and polycrystalline quartz; P is plagioclase; K is K-feldspar; Qtzte is quartzite rock fragments; Gr is granitic rock fragments; Gn is gneissic rock fragments; Tp is twinned plagioclase; Up is untwinned plagioclase; Uk is untwinned K-feldspar; M is microcline; Qp2-3 is polycrystalline quartz with two or three subunits; Qp>3 is polycrystalline quartz with more than three subunits; Qnu is non-undulose monocrystalline quartz; and Qu is undulose monocrystalline quartz. Field abbreviations are as follows: RO is recycled orogen; CI is continental interior; TC is transitional continental; BU is basement uplift; DA is dissected arc; TA is transitional arc; UA is undissected arc; QR is quartzose recycled; TR is transitional recycled; LR is lithic recycled; PLU is plutonic; M&U-R Mtx is medium- and upper-rank metamorphic; L-R Mtx is lower-rank metamorphic; M&U-R Gn is medium- and upper-rank gneiss; L-R Gn is lower-rank gneiss; and S&S is slate and schist.

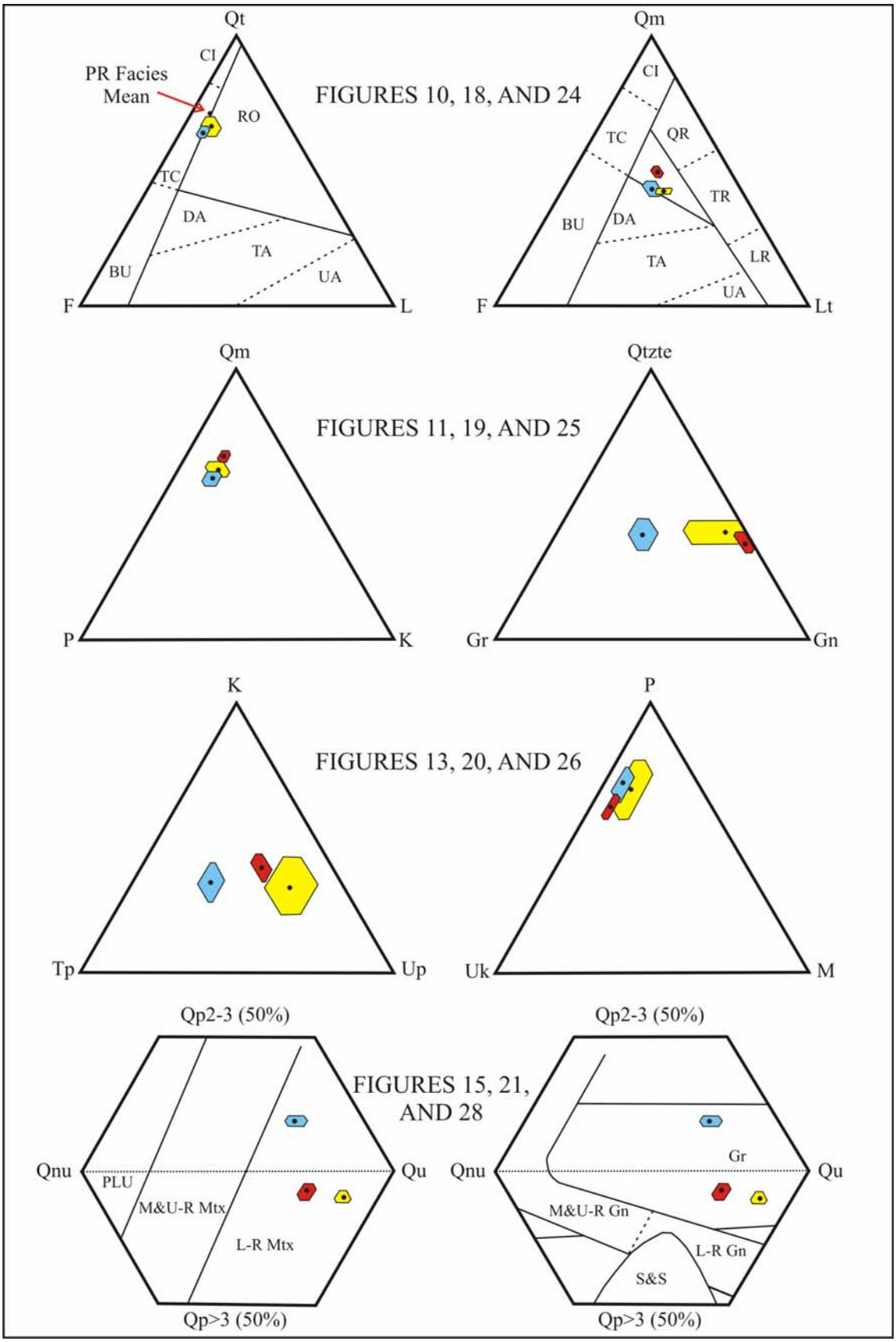
Qt
CI
PR Facies
Mean
RO
TC
DA
TA
BU
UA
F
L
FIGURES 10, 18, AND 24
Qm
CI
TC
QR
TR
BU
DA
TA
LR
UA
F
Lt
Qm
P
K
FIGURES 11, 19, AND 25
Qtzte
Gr
Gn
K
Tp
Up
FIGURES 13, 20, AND 26
P
Uk
M
Qp2-3 (50%)
Qnu
Qu
PLU
M&U-R Mtx
L-R Mtx
Qp>3 (50%)
FIGURES 15, 21,
AND 28
Qp2-3 (50%)
Qnu
Gr
Qu
M&U-R Gn
L-R Gn
S&S
Qp>3 (50%)

The criteria to differentiate continental and magmatic-arc plutons are gradational, shifting toward magmatic arc with increasing lithic fragments (Dickinson, 1985). When polycrystalline quartz is removed from the Q pole, the valley river mean becomes more feldspathic, with all but two sands having <50% monocrystalline quartz, and the sands shift strongly towards the Lt pole (Figures 41 and 10B). This shift indicates that the arkose in the valley rivers reflects continental and magmatic-arc plutons. Regardless of the tectonic heritage, the plutonic source rocks were granite and granite gneiss (Figures 41 and 11B), although the quartz grains indicate granite was more important than gneiss (Figures 41 and 15).

The valley-river sands lack chert and volcanic grains, and are enriched with schist and schistose quartz, quartzite, polycrystalline quartz, and feldspar, which is typical of a recycled collision orogen (Dickinson and Suczek, 1979; Dickinson, 1985) (Appendix C). During crustal collisions, continental and/or arc plutons are draped with metasedimentary rocks transported by nappes or thrust sheets. Subsequent erosion produces sands not only typical of a continental block or magmatic arc, but also with substantial amounts of slate, phyllite, schist, and quartzite (Dickinson and Suczek, 1979).

The valley-river sands most likely came from the mantled gneiss domes of the Oliverian plutonic suite and their nappe-emplaced metasedimentary cover, and the Kinsman granodiorite of the New Hampshire plutonic suite (Figure 42; Zen, 1983; Lyons, 1997). These rocks lie upstream of the paleocurrents in the area northeast of the Deerfield basin, where the BHA extends into southwestern New Hampshire (Figure 7).

The Late Ordovician Oliverian suite are variably metamorphosed mantled gneiss domes of the BHA, with granite, granodiorite, and tonalite (Lyons, 1997). These rocks

Figure 42. Summary cartoon of provenance. 'Bubbles' summarize the three source terranes for the Sugarloaf Arkose. Blue arrows indicate approximate sediment dispersal paths into the Deerfield basin. B.I.C. is Belchertown igneous complex.

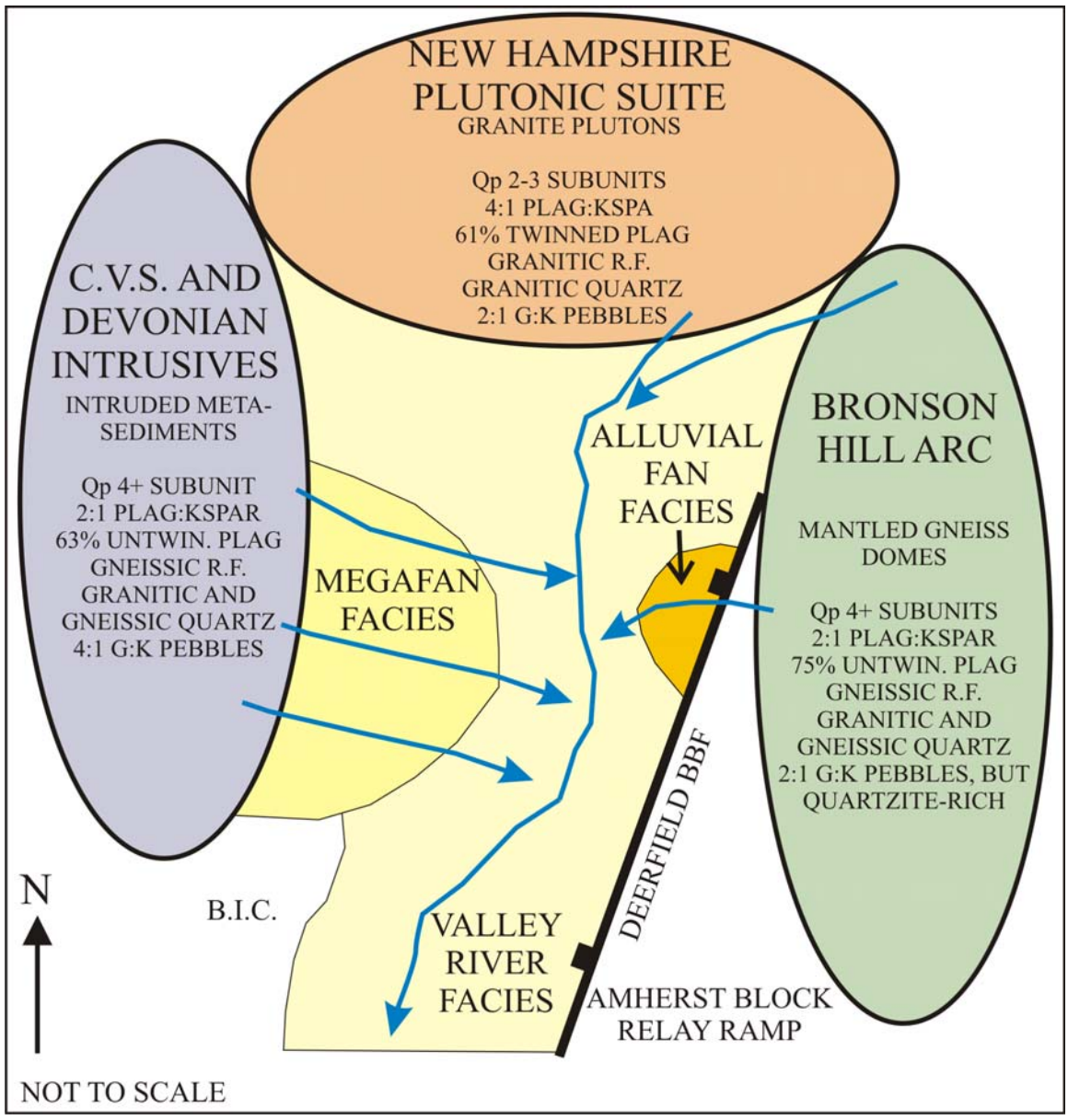
NEW HAMPSHIRE
PLUTONIC SUITE
GRANITE PLUTONS
Qp 2-3 SUBUNITS
4:1 PLAG:KSPA
61% TWINNED PLAG
GRANITIC R.F.
GRANITIC QUARTZ
2:1 G:K PEBBLES
C.V.S. AND
DEVONIAN
INTRUSIVES
INTRUDED META-
SEDIMENTS
Qp 4+ SUBUNIT
2:1 PLAG:KSPAR
63% UNTWIN. PLAG
GNEISSIC R.F.
GRANITIC AND
GNEISSIC QUARTZ
4:1 G:K PEBBLES
ALLUVIAL
FAN
FACIES
MEGAFAN
FACIES
BRONSON
HILL ARC
MANTLED GNEISS
DOMES
Qp 4+ SUBUNITS
2:1 PLAG:KSPAR
75% UNTWIN. PLAG
GNEISSIC R.F.
GRANITIC AND
GNEISSIC QUARTZ
2:1 G:K PEBBLES, BUT
QUARTZITE-RICH
DEERFIELD BBF
N
B.I.C.
VALLEY
RIVER
FACIES
AMHERST BLOCK
RELAY RAMP
NOT TO SCALE

are the core of the Bronson Hill island arc, modified to gneiss during their emplacement in the Taconian orogeny (Robinson, 2003). The Warwick dome of Massachusetts and New Hampshire is notable among them because the gneiss is pegmatitic; this dome may be the source of some of the quartz and K-feldspar megacrysts in the valley-river conglomerates (Zen, 1983).

The metamorphosed shallow-water sediments of the CVS were emplaced over the BHA by nappe folding during the Acadian, and include Ordovician schists of the Partridge Formation, Silurian Cough quartzite, and Devonian mica schists and phyllites of the Littleton Formation (Zen, 1983; Robinson, 2003). The underlying gneiss rose as domes after nappe folding, creating the Ordovician mantled gneiss domes of the BHA. Probably medium sand from the mantled domes provides the signal of the dissected arc and collision orogen, plus schist, quartzite and granite gneiss. The valley-river conglomerates contain similar proportions of schist, phyllite, and quartzite derived from the same source (Table 3, Appendix D).

The Devonian Kinsman is a medium- to coarse-grained granodiorite emplaced during and after the Acadian orogeny (Dorais, 2003). This compound pluton would yield quartzo-feldspathic sand characteristic of an uplifted continental basement: namely monocrystalline non-undulose quartz, unit plagioclase and K-feldspar, and granite. The granodiorite locally includes white to light pink K-feldspar megacrysts up to 15-cm long, which may be another source of the K-feldspar-rich conglomerates (Lyons, 1997; Dorais, 2003).

3.1.2 Piedmont-river Facies

The piedmont-river samples have a mixed continental block and recycled orogen provenance (Figures 41 and 18). Monocrystalline quartz is more abundant than polycrystalline (Figures 41 and 21), implying there is no magmatic arc component to the sandstone provenance (Figures 41 and 18B). The piedmont-river sands are rich in plagioclase and lack volcanic grains, indicating basement uplift and collision orogen sources similar to the valley-river sands. Quartz provenance is also somewhat similar: both facies are dominated by undulose monocrystalline quartz and so belong to granite-derived fields. Piedmont-river polycrystalline quartz is fine-grained, implying the granite was commonly slightly metamorphosed (Figures 41 and 21).

A major delineation between valley- and piedmont-river sands is the difference between granitic and gneissic rock fragments and the feldspar component of those rock fragments (Figures 41, 18 and 21). The valley rivers contain approximately equal amounts of granite and granite gneiss, and twinned and untwinned plagioclase. Granite is all but absent from the piedmont rivers, and twinned plagioclase is uncommon (Table 4). Granite gneiss is the most common quartzo-feldspathic rock fragment, and untwinned plagioclase the most common feldspar (Figures 41, 19B and 20A). In addition, K-feldspar grains are about twice as abundant as in the valley-river facies (Table 4).

The piedmont rivers also transported granitoid pebbles of unfoliated granite that grades into strongly foliated granite gneiss. K-feldspar is much less common among piedmont-river conglomerate than in the other facies; however, K-feldspar is still more common than granitoid pebbles by 2:1. Reduced abundance of K-feldspar indicates pegmatite is less common in the source rock west of the basin.

The delineation of granite gneiss from granite in thin section is based in-part on lack of twinning in plagioclase. This operational definition is based on the observation that surface defects, like twin boundaries, tend to 'heal' as temperature rises during metamorphism (Yardley, 1989). Dislocation climb and cross-slip in experimentally-deformed plagioclase occurs at pressures and temperatures of 10-15 kbar and 600-900^{o}C. In naturally-deformed samples, plagioclase recovers at temperatures >550^{o}C (Yardley, 1989). Hydrolitic weakening can lower the temperature required to induce slip by 200^{o}C per ~0.1 wt % water (Tullis, 1983). In the piedmont-river sands, individual untwinned grains are more common than twinned, further supporting the inferred gneissic source (Figures 41 and 20A).

Paleocurrents in the piedmont-river facies indicate eastward flow into the Deerfield basin from the west, and potential source rocks include Devonian strata of the CVS (Figure 42). The Littleton, Erving, Goshen, Waits River, and Gile Mountain Formations are composed of schists and phyllites locally interbedded with amphibolite and granofels. The Goshen and Gile Mountain Formations have extensive gray quartzite members west of the Deerfield basin (Zen, 1983). The formations are interpreted to be shallow-water sediments emplaced during the nappe stage of the Acadian orogeny, and locally warped by the 'Vermont Line' of gneiss domes (Robinson, 2003). Sands derived from these metamorphic rocks have the characteristics of collision recycled orogeny, rich in schist, schistose quartz, and quartzite grains. Schist, phyllites, and quartzite pebbles are produced by weathering of these rocks.

The piedmont rivers drained a terrane of intruded metasediments. Devonian granodiorite gneiss, foliated granite and pegmatite of the Williamsburg and Middlefield

intrusions are common surface rocks west of the Deerfield basin (Zen, 1983). Dikes and larger plutonic bodies of these intrusives are present in all of the metasediment units cited above, especially west of the southern part of the basin. The Belchertown igneous complex now exposed in Whately may have contributed quartz monzodiorite, perhaps including the local boulder-sized clasts. The rivers transported grains of gneiss, untwinned plagioclase, and finely-polycrystalline quartz grains characteristic of uplifted continental basement and a recycled collision orogen.

3.1.3 Alluvial-fan Facies

The medium sand has a mixed provenance, with basement uplift and collision recycled orogen like the other two facies, but also a dissected magmatic arc, similar to the valley rivers (Figures 41 and 24). Also similar to the valley-river facies is the abundance of K-feldspar pebbles (Table 4).

The similarity of the alluvial-fan and piedmont-river is striking because the sources are on opposite sides of the basin. Medium sand in the alluvial fan is rich in gneiss, untwinned plagioclase, finely-polycrystalline quartz, and K-feldspar grains, but poor in granite and twinned plagioclase (Figures 41, 25, 26, and 28).

Gray quartzite pebbles are as abundant as granitoid and K-feldspar. Other metamorphic pebbles are about as common as in the valley-river facies (Table 3). Thus the source area of the alluvial fan had mantled plutons as did the valley river, but with the addition of significant amounts of quartzite.

A proximal source is implied by the boulders up to 0.5-m long and the alluvial fan itself. Alluvial-fan paleocurrents were from the northeast, off the northern flank of the Pelham Dome (Figures 42 and 7). Another source could be the Warwick dome on the

Massachusetts-New Hampshire line mantled by CVS metasedimentary Erving and Littleton Formations, and Ordovician Ammonoosuc metavolcanic rock (Zen, 1983).

In general, weathering of a mantled gneiss dome provides gneiss, untwinned plagioclase, schist, and schistose quartz. The accompanying pebbles are pegmatite, granitoid, and schist and phyllite. These types of grains and pebbles are present in the alluvial-fan and valley-river facies.

The abundant quartzite pebbles are not adequately explained by either the Pelham or Warwick dome. The Silurian Clough quartzite crops out northeast of the alluvial fan, but the Clough is a metaconglomerate that does not resemble the quartzite pebbles. A more likely scenario is that the quartzite-rich member of the Gile Mountain Formation was present, but removed by erosion. This possibility is supported by cross-sections in Zen (1983) (sheet 2, section A-A').

3.2 Tectono-sedimentary History of the Sugarloaf Arkose

The three sedimentary facies appear in the basin due to changes in one or more of the sedimentary controls. Paleoclimate was monsoonal and arid-dominated throughout deposition (Section 1.3.3), and therefore not responsible for changes in depositional facies. Thus tectonism was the major determinate of paleocurrent flow, sedimentary style, and source terrane.

In this section, tectonic events in the pre-CAMP Deerfield basin are reconstructed (Figure 43). Each facies constrains the time of formation, location, and motion of basin-defining normal faults, herein referred to as basin-bounding faults (BBF). The Eastern Border Fault (EBF) is a separate faulting event that is younger than and incorporates parts

Figure 43. Schematic tectono-sedimentary evolution of the Sugarloaf Arkose in the Deerfield basin. In A-D, only active fault scarps, channels, and fans are shown; abandoned and buried features are not. Channels are darker where paleocurrents are available. The scale in A applies to all panels. A. Valley rivers flowed SSW down an early 'sag' basin. One or more valley rivers probably were present in areas to the south now covered or eroded. B. Formation of the Deerfield BBF redirects the valley rivers and causes east-flowing piedmont rivers to begin building a megafan. C. Propagation of the Deerfield BBF to the NNE and SSW increases the size of hanging wall accommodation space and thus the megafan. Alluvial fans build from the fault scarp. The Central graben BBF (Wise, 1992) propagates NNE as well, and the two faults overlap at the Amherst block, forming a relay ramp. D. The Deerfield BBF and Central graben BBF connect across the Amherst block, forming an integrated BBF. Channels are lighter where paleocurrent data are unknown.

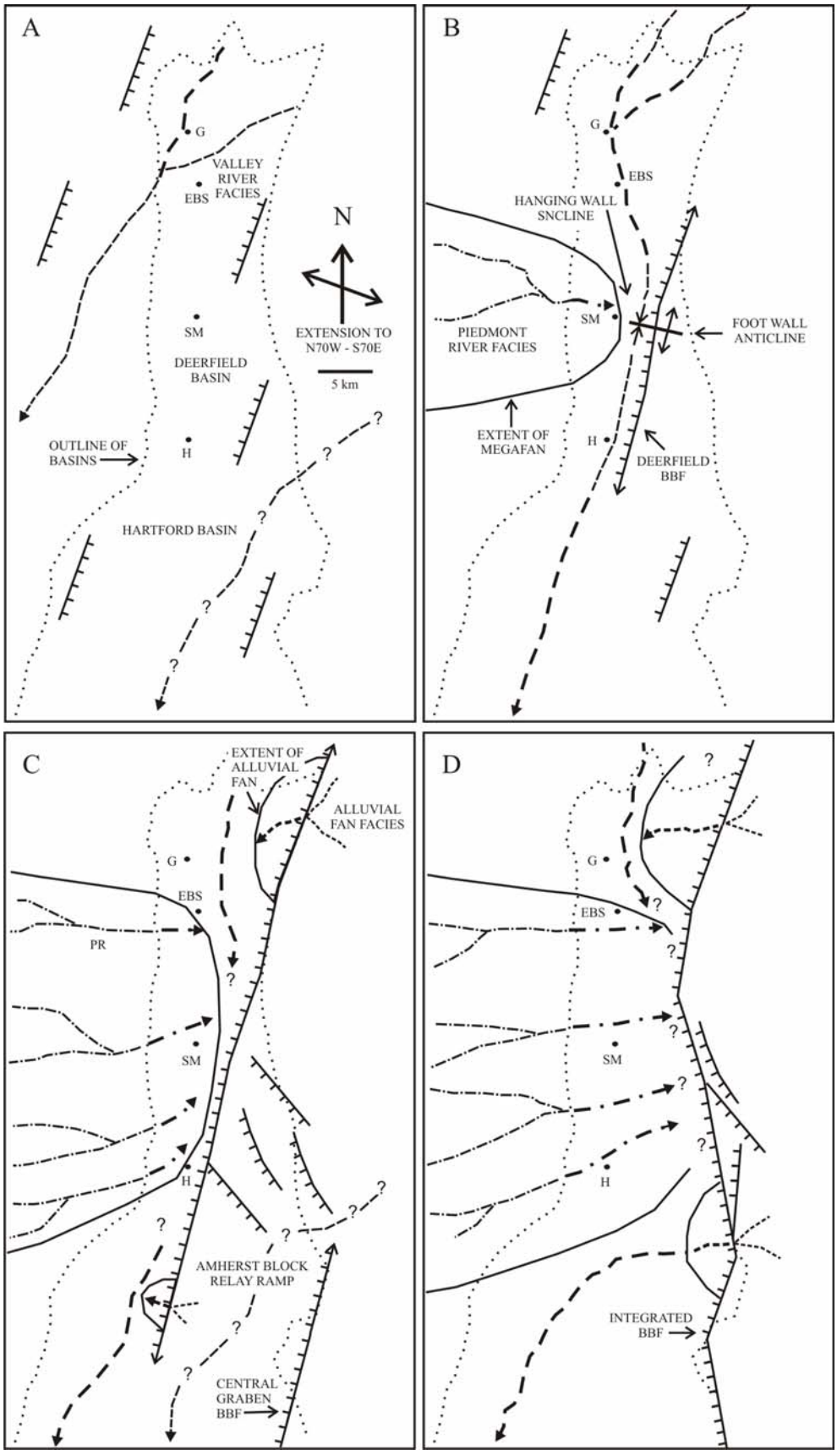
A
G
VALLEY
RIVER
FACIES
EBS
N
SM
EXTENSION TO
N70W - S70E
5 km
DEERFIELD
BASIN
OUTLINE OF
BASINS
H
HARTFORD BASIN
B
G
EBS
HANGING WALL
SNCLINE
SM
FOOT WALL
ANTICLINE
PIEDMONT
RIVER FACIES
EXTENT OF
MEGAFAN
H
DEERFIELD
BBF
C
EXTENT OF
ALLUVIAL
FAN
ALLUVIAL
FAN FACIES
G
EBS
PR
SM
H
AMHERST BLOCK
RELAY RAMP
CENTRAL
GRABEN
BBF
D
G
EBS
SM
H
INTEGRATED
BBF

of Triassic BBFs in the Deerfield and Hartford basins. The three facies record the formation of a hydraulically-open 'sag' basin, widening and deepening of the basin, and the change to a hydraulically-closed basin.

3.2.1 Sag Basin and Valley Rivers

Initial faulting parallel to N20E was widespread across much of the northern CAM area, including Massachusetts (Section 1.3.2, Figure 5). The relatively small throw on the numerous nascent faults led to a Deerfield 'sag' basin, similar to those observed in early East African rifts (Wise, 1992; Morley, 2002). Minor horst and graben topography within the synformal sag probably led to shallow valleys trending NNE-SSW; the uneven topography at the base of the Deerfield basin may partly be valleys created at this time (Figure 6, A2 to A8).

Re-direction of the previous, probably east-to-west, drainage pattern into the horst valleys led to deposition of the valley-river facies in numerous isolated depocenters (Wintsch et al., 2003) (Figure 43A). Antecedent drainage may also have incised into relatively easily eroded areas of basement, especially low-rank metasediments in the CVS. The fluvial redbeds indicate the sag basin was hydraulically-open and the rate of sedimentation exceeded subsidence. The braided rivers filled horst valleys and avulsed over growth folds into newly created or unoccupied valleys, thereby connecting isolated mini-basins (Gawthorpe and Leeder, 2000). The high rate of avulsions reduced the amount of time detritus spent exposed on interfluves, and so few ventifacts formed (Table 3). Not shown on Figure 43A are tributaries to the valley rivers that drained areas underlain by Ordovician mantled gneiss domes and Devonian plutons (Section 3.1.1).

Valley rivers are the earliest depositional facies in the Deerfield basin (Figure 7). Deposition began at about 218 Ma (Olsen, 1997), so the onset of rifting and basin formation was no older than late Carnian (Figure 44). The valley-river facies continues through the arkose to the unconformity at the top of the formation (Figure 4, Section 1.4.1)

3.2.2 Basin-bounding Fault and Piedmont-River Megafan

The lowest known outcrop of the piedmont rivers is at the base of the type section along Route 116 at Mount Sugarloaf in South Deerfield, about 600 m below the Deerfield Basalt (Figure 6). Assuming uniform depositional rates, the piedmont-river facies appears in the middle Norian, ~210 Ma (Figure 44). Whether valley-river redbeds underlie the piedmont-river megafan is unknown because there are no outcrops between the western margin and the outcrop along Route 116. However, SSW-flowing valley rivers are preserved in the Hartford basin from about this time on, suggesting that through-going valley rivers existed in both basins (Figure 7).

The formation of the Deerfield BBF led to initiation of the piedmont-river facies and increased variability in valley-river paleocurrents (Figure 43B). Several piedmont river fans coalesced into the prominent, low-angle megafan that built eastward into the basin (Gawthorpe and Leeder, 2000) (Figure 43B). Ventifacts are abundant in the piedmont-river facies, indicating substantial storage time on megafan interfluves. Coeval with the megafan was increased variation in valley-river paleocurrent vectors (Figure 7).

The Deerfield BBF perhaps formed from two or more of the minor normal faults that linked into a larger fault (Section 1.3.2). The initial location of the BBF is based on: 1) a location east of the lowest occurrence of the megafan; 2) the western edge of the

Figure 44. Summary of Deerfield basin history. Sedimentation in the early fluvial basin (TS III of Olsen, 1997) begins at ~218 Ma, and is modified through time by formation and interaction of basin-bounding faults (BBF). Above the unconformity, the basin is topographically closed, with playas, lakes, BBF fanglomerates, and minor fluvial strata. Hydrothermal diagenesis of the sands peaked at 185 Ma. Opening of the spreading center at the Mid-Atlantic Ridge started basin inversion at 180 Ma. The EBF formed after deposition, diagenesis, and inversion of basin strata (Roden-Tice and Wintsch, 2002).

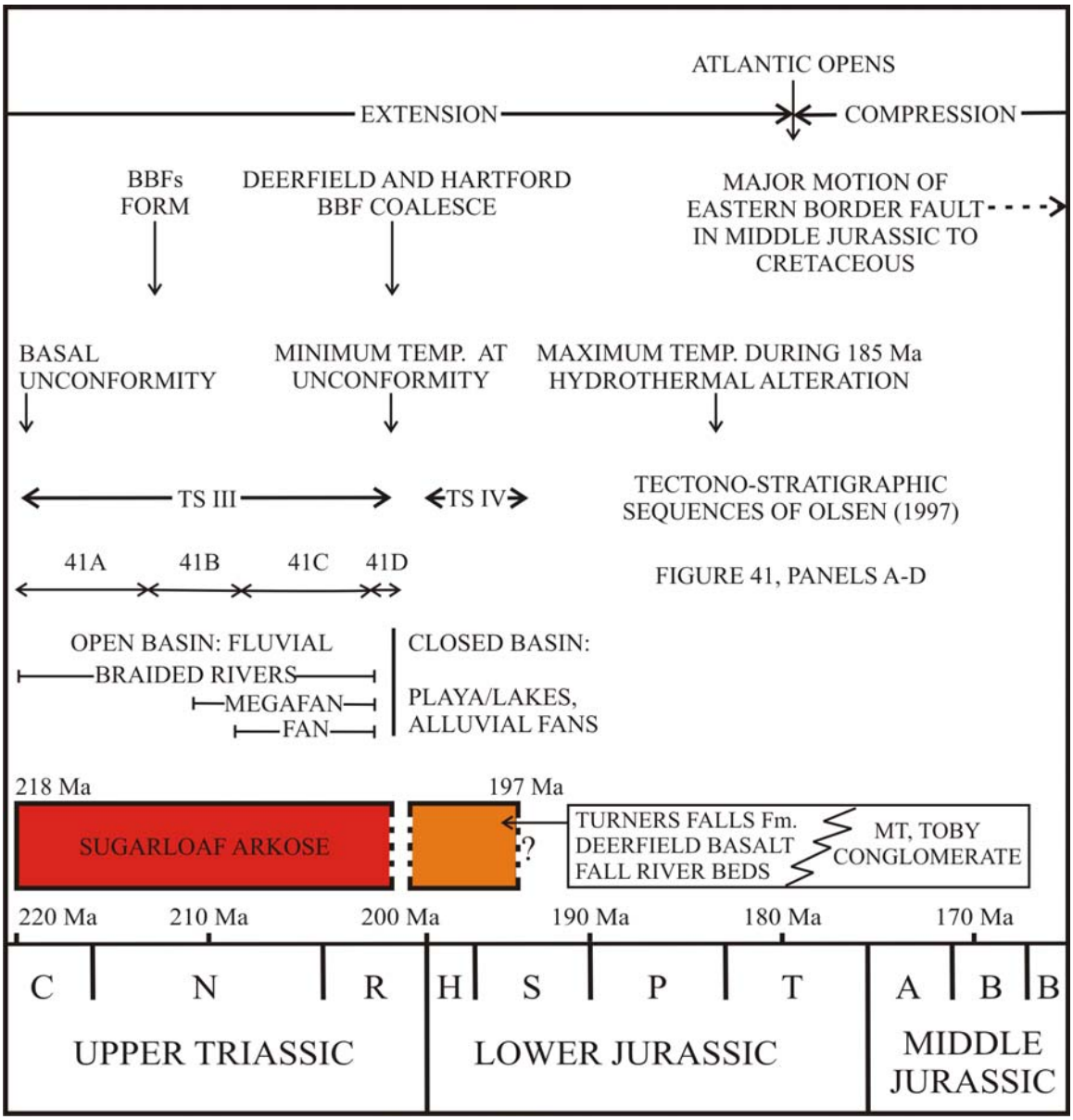
ATLANTIC OPENS
EXTENSION
COMPRESSION
BBFs FORM
DEERFIELD AND HARTFORD BBF COALESCE
MAJOR MOTION OF EASTERN BORDER FAULT IN MIDDLE JURASSIC TO CRETACEOUS
BASAL UNCONFORMITY
MINIMUM TEMP. AT UNCONFORMITY
MAXIMUM TEMP. DURING 185 Ma HYDROTHERMAL ALTERATION
TS III
TS IV
TECTONO-STRATIGRAPHIC SEQUENCES OF OLSEN (1997)
41A
41B
41C
41D
FIGURE 41, PANELS A-D
OPEN BASIN: FLUVIAL
BRAIDED RIVERS
MEGAFAN
FAN
CLOSED BASIN:
PLAYA/LAKES, ALLUVIAL FANS
218 Ma
197 Ma
SUGARLOAF ARKOSE
?
TURNERS FALLS Fm.
DEERFIELD BASALT
FALL RIVER BEDS
MT, TOBY CONGLOMERATE
220 Ma
210 Ma
200 Ma
190 Ma
180 Ma
170 Ma
C
N
R
H
S
P
T
A
B
B
UPPER TRIASSIC
LOWER JURASSIC
MIDDLE JURASSIC

Amherst block is cut by a down-to-the-west normal fault on strike with the EBF north of the Mt. Toby block (Chandler, 1978); 3) the fault formed normal to N20E-S20W extension (Section 1.3.2); and 4) the Mt. Toby Conglomerate rests on Paleozoic basement of the Mt. Toby block, suggesting that the Sugarloaf Arkose was never deposited on the block (Hubert et al., 2008). The dip of the fault was controlled by the foliation of the west flank of the Pelham dome, locally 40^{o} W (Wise, 1992).

Displacement previously accommodated by smaller normal faults was transferred to the larger Deerfield BBF, leading to the 'deaths' of many of the faults (Gawthorpe and Leeder, 2000). Without the minor NNE-SSW faults to channel them, valley rivers shifted to a more southerly flow. It seems likely that several alluvial fans built off the Deerfield BBF. These fans would be earlier members of the alluvial-fan facies that identifies the next tectono-stratigraphic stage, described below. Fans from this time are not observed because they are buried by the early Jurassic alluvial fans of the Mt. Toby Conglomerate (Figure 2).

Increased displacement along the Deerfield BBF initiated eastward-flowing piedmont rivers that drained Devonian rocks in highlands west of the basin. The resulting hanging wall megafan probably forced the valley rivers eastward, another potential source of paleocurrent variation.

The valley and piedmont rivers coexisted from about half-way through deposition of the Sugarloaf Arkose to the top of the unit (Figure 44). The piedmont rivers evidently discharged into the through-flowing valley rivers (Figure 43B).

3.2.3 Propagation and Integration of the Basin-Bounding Faults

As extension continued through the late Triassic, the Deerfield BBF propagated NNE along the northwest flank of the Pelham dome (Figure 43C). The relative timing of propagation is based on the appearance of the alluvial-fan facies in the northeast corner of the Deerfield basin. The Deerfield BBF extended into the Hartford basin, where the alluvial fan in the New Haven arkose built from the scarp as seen on I-91 next to the power plant (Handy, 1977; Wise, 1992). Alluvial fans may have existed along the entire length of the normal fault, but are buried by Jurassic strata.

The presence of mud intraclasts in the upper two-thirds of the megafan indicates the preserved strata become increasingly distal with time (Hubert et al., 2008). Widening and deepening of the basin increased the drainage catchment westward, and the megafan on-lapped the flexural margin. The megafan also grew to the north, overlapping previously-deposited valley river sediment in the middle of the basin, but did not build southeast into the Hartford basin. The Belchertown igneous complex in Whately may have formed highlands that limited the southern extent of the megafan.

Valley-river redbeds are present north and south of the megafan (Figure 7). There is no evidence of closed-basin lake or playa strata below the unconformity at the base of the Fall River beds unconformity, which suggests the valley rivers flowed past the toe of the megafan into the Hartford basin. At times of high sediment flux, the piedmont rivers may have choked and obstructed the valley rivers. Discharge choking would force avulsions in the valley rivers, presumably toward the BBF (Gawthorpe and Leeder, 2000)

As the Deerfield BBF propagated SSW, the Central graben BBF of the Hartford basin grew to the NNE (Wise, 1992, 2008 pers. com.). The faults overlapped in the

vicinity of Amherst, forming a relay ramp between the Central graben BBF to the east and the Deerfield BBF to the west (Figure 43C). The relay ramp formed a 'soft linkage' zone between the Deerfield BBF footwall anticline and the hanging wall syncline of the Central graben BBF (Walsh and Watterson, 1988) (Figure 43B).

Relay ramps provide topographic lows between fault segment anticlines, which may be breached by rivers (Anders and Schlische, 1994; Gawthorpe and Leeder, 2000; Trudgill, 2002). Valley rivers flowing NNE to SSW prior to relay ramp formation may have been captured and re-directed down the ramp (Trudgill, 2002). Redirection of earlier rivers explains the presence of Sugarloaf Arkose on the otherwise topographically-high Amherst block.

Joints and faults commonly form on relay ramps as the fault tips continue to propagate past each other. If extension continues long enough, the cross-ramp faults link the fault segments, forming an integrated fault with an along-strike kink or bend (Peacock and Sanderson, 1991). The Deerfield BBF and Central graben BBF were linked by such cross-ramp faults along the west flank of the Pelham dome (Figure 5). The tightly-spaced fault package just south of the Mt. Toby block is typical of én échelon ramp faulting: overlapping, synthetic faults step basinward down the relay ramp (Moustafa, 2002).

The connection across the Amherst block formed an integrated basin-bounding fault linking the early Deerfield and Hartford 'sag' basins in a composite basin (Schlische and Anders, 1996; Schlische, 2003) (Figure 43D). The Amherst block became an anticlinal, hanging-wall structural high, which subsided along the integrated BBF. The

Deerfield and Holyoke basalts were once-continuous, indicating substantial subsidence and burial of the block by about 201 Ma (Philpotts, 1998).

The unconformity between the Sugarloaf Arkose and Fall River beds represents the change from a fluvial deposition in an open basin to lacustrine and paludal strata deposited in a closed basin. Hard linkage between the Deerfield BBF and the Central graben BBF probably coincided with this depositional change: the rate of subsidence along the integrated BBF was greater than the rate of sedimentation, capturing through-flowing rivers and forming standing water bodies (Leeder and Gawthorpe, 1987; Gawthorpe and Leeder, 2000) (Figure 44). The unconformity itself formed due to sinking, slight tilting and erosion of Sugarloaf strata prior to deposition of the Fall River beds in a closed basin (Hubert et al., 2008).

The integrated BBF controlled basin subsidence into the Lower Jurassic. The local alluvial fan in the Sugarloaf Arkose continued as the Pisgah Mountain fan of the Mt. Toby Conglomerate (Wessel, 1969). The heads of the four alluvial fans of the Mt. Toby Conglomerate lie along the integrated BBF, as do fanglomerates in the Portland Formation of the Hartford basin (Hubert and Reed, 1978).

Post-depositional tectonism led to displacement along the EBF in the Late Jurassic to Cretaceous (Roden-Tice and Wintsch, 2002; 2007; Wintsch et al., 2003; Roden-Tice et al., 2008). The strata in the integrated basin were tilted to the east, and folded by differential displacement along the EBF (Schlische and Anders, 1996). Since the EBF stopped moving, erosion modified the once-continuous integrated basins: 1) the western edge of the integrated basins was removed, leaving only the deepest keel closest

to the EBF; 2) the strata that connected the Deerfield and Northfield basins were removed; and 3) the thickness of Mesozoic strata on the Amherst block was greatly thinned, partially separating the Deerfield and Hartford basins.

CHAPTER 4

SUMMARY AND CONCLUSIONS

1) The Sugarloaf Arkose is a ~2-km-thick fluvial arkose deposited in late Triassic time in the Deerfield basin, Massachusetts. The strata are mostly pebbly sandstones with minor conglomerate and mudstone. There are three depositional facies based on paleocurrent vectors and sedimentary style. The valley-river facies has dominantly NNE to SSW paleocurrent flow, and consists of channel sandstones with interbedded overbank mudstones. The piedmont-river facies (megafan) has stacked channel-fill bodies with or without overbank mudstones and W to E paleocurrents. An alluvial fan is the third facies: boulder-bearing graded beds with antidune/standing wave-forms deposited by E to W-flowing flash floods.
2) Modal analysis was made of 51 thin sections: three from each of 17 outcrops. In each thin section 300 medium-sand grains were counted. A sub-count was made of the polycrystallinity and undulosity of quartz. The whole-rock assemblage was measured by 100 points per thin section of grains, cements, matrix, and porosity. The lithology and size of 100 pebbles from 16 locations were combined with data from Stevens (1977) to assess conglomerate composition.

   In provenance analysis, the Gazzi-Dickinson point-count method minimizes the effects of grain size on composition. This type of modal analysis is restricted

to medium-size sand grains because medium sand best reflects source rock lithology, and they are abundant.

Valley-river medium sand is dominated by unit quartz, granite, granite gneiss, and plagioclase grains. Monocrystalline framework grains are mostly quartz and plagioclase, and minor K-feldspar; polycrystalline grains contain slightly more quartzite and granite than granite gneiss. Twinned is more abundant than untwinned plagioclase, and microcline is rare compared to untwinned K-feldspar. Medium-sized quartz grains are mostly monocrystalline and undulose. Polycrystalline quartz with two or three subunits is more common than aggregates of four or more subunits.

Piedmont-river medium sand is dominantly unit quartz and granitoids. The sand is quartz-rich compared to the whole rock. The sandstones vary from arkose and lithic arkose to subarkose. Unit quartz is the dominant monocrystalline grain, with plagioclase less abundant, and K-feldspar more abundant than in the valley rivers. Granite gneiss is the major polycrystalline grain; granite is virtually absent. Plagioclase and K-feldspar are mostly untwinned. In all samples, more than 25% of the polycrystalline quartz has four or more subunits, and undulose monocrystalline quartz is more abundant than non-undulose.

Alluvial-fan medium sand is subarkose and almost 75% unit quartz and rock fragments. Plagioclase is more abundant than K-feldspar, and granite gneiss is much more abundant than granite. Most of the plagioclase is untwinned, and microcline is more abundant in alluvial-fan samples than valley-

river and piedmont-river sands. Most monocrystalline quartz is undulose, and more than 25% of polycrystalline quartz has four or more subunits.

3) The tectonic provenance signals of each of the three facies are mixed on the Dickinson plots, reflecting the regional geology with its history of multiple collisional orogenies, intrusions, and metamorphism.

Valley-river sand has a combined continental block and recycled orogen provenance. Combining polycrystalline quartz with rock fragments shifts the samples away from a continental block provenance towards a 'mixed' provenance signal including dissected magmatic arc.

Mantled gneiss domes emplaced during the Acadian orogeny are the likely source of valley-river sands. The gneiss domes are the plutonic core of the Bronson Hill arc, and are draped by metasediments of the Connecticut Valley synclinorium. Granite plutons and pegmatites northeast of the Deerfield basin evidently contributed to the bedload of the valley rivers as well.

Piedmont-river sand is a mixture of transitional continental block and recycled orogen, with no clear contribution from a magmatic arc. Sources west of the basin most likely were the metasediments of the Connecticut Valley synclinorium, Devonian intrusives, and the Belchertown igneous complex (Figures 42 and 43).

Alluvial-fan sand is a mix of recycled orogen and magmatic arc provenance. The fan is adjacent to the Pelham Dome. The mantling Devonian metasediments must have been quartzite-rich.

Conglomerates in all three facies contain abundant pink K-feldspar and granitoid pebbles, plus quartz, phyllite, schist, and amphibolite. Quartzite is common, and a major constituent of the alluvial-fan conglomerates. Comparison of medium sand and pebbles shows a major size-controlled difference.

4) The paleoclimate was continually dry-dominated monsoonal, with superimposed wetter/dryer Milankovitch cycles.

Tectonism controlled the existence of each facies. This allows the timing of the sedimentary facies to be used to date the tectonic events. The valley rivers flowed from NNE to SSW in an elongate sag basin, oriented perpendicular to the regional N70W-S70E extension. The broad basin likely had minor horst and graben topography, which was in-filled by fluvial redbeds. The basin was hydraulically-open because rate of sedimentation exceeded subsidence, and the rivers flowed probably SSW into what is now the Hartford basin. The earliest strata in the Sugarloaf Arkose are ~218 Ma, so tectonic subsidence began just before this time.

The piedmont rivers began to build a megafan into the basin about half-way up in the Sugarloaf Arkose. The accommodation space for the megafan was generated by a basin-bounding fault (BBF) to the east. The BBF was oriented NNE-SSW, and continued regional extension caused the fault to propagate at the fault tips.

As the Deerfield BBF lengthened, the basin widened westward onto the footwall and deepened as throw increased on the fault. The megafan responded by increasing in size, on-lapping valley-river strata. The major valley river was

redirected, to flow NE-SW past the toe of the megafan and downslope into the Hartford basin.

The Central graben BBF in the Hartford basin propagated NNE, passing the Deerfield BBF on the east and forming the relay ramp of the Amherst block between them. The faults became hard linked by cross-ramp faults, forming an integrated basin-bounding fault: the eastern margin of a composite basin, into which CAMP basalts flowed about at the Triassic-Jurassic boundary. The unconformity separating the Sugarloaf Arkose and Fall River beds may have formed at this time.

5) Diagenetic effects are divided into early and late mesogenetic stages. Early mesogenesis (burial to 2-3 km) included dehydration of limonite soil stains to hematite grain coats, mechanical compaction, and coeval precipitation of albite and quartz cements. Albite overgrowths were accompanied by partial to complete albite replacement of many plagioclase and K-feldspar grains. Late mesogenesis (burial to >3 km) included precipitation of carbonate and authigenic hematite cements, illite replacement of feldspar, and mosaic albite cement.

Accelerated late Jurassic-Cretaceous motion on the integrated basin-bounding fault created the Eastern Border Fault. Pronounced subsidence in the Deerfield and Hartford basins generated hanging-wall synclines. Subsequent erosion has removed most of the Mesozoic strata on the Amherst block, leaving only ~1 km of west-dipping, anticlinally folded Sugarloaf Arkose along the west flank of the block. The Deerfield basin was tilted to the east, and the western margin eroded, leaving only the keel of the original basin.

APPENDIX A

SAMPLE LOCATIONS

Appendices A1, A2, and A3 list the locations of all thin sections from the valley-river, piedmont-river, and alluvial-fan facies, respectively. Each thin section is numbered, corresponding to numbers on figures presented earlier in this work. The nearest public street, town, latitude, and longitude for sampled outcrops have been noted. Appendix A4 includes the locations of outcrops where pebble petrology (only) was observed for use in this study.

APPENDIX A1: SAMPLE LOCATIONS FOR VALLEY RIVER FACIES

ID NO.	SAMPLE	STREET	TOWN	LATITUDE	LONGITUDE
1	10.13-4	I-91 Deerfield River	Greenfield	42°32'24" N	72°37'32" W
2	10.13-5	I-91 Deerfield River	Greenfield	"	"
3	SF-I91-1A	I-91 Deerfield River	Greenfield	"	"
4	SF-D1	Lower Rd.	Deerfield	42°32'55" N	72°37'08" W
5	SF-D2B	Lower Rd.	Deerfield	"	"
6	SF-D3	Lower Rd.	Deerfield	"	"
7	SF-G11	I-91 Exit 27	Greenfield	42°36'53" N	72°35'44" W
8	SF-I91-3A	I-91 Exit 27	Greenfield	"	"
9	SF-I91-3B	I-91 Exit 27	Greenfield	"	"
10	8.23-5	Leyden Rd.	Greenfield	42°36'39" N	72°36'51" W
11	8.23-7	Leyden Rd.	Greenfield	"	"
12	RS75-192	Leyden Rd.	Greenfield	"	"
13	4.29-1	Bernardston Rd.	Greenfield	42°36'34" N	72°35'09" W
14	4.29-2	Bernardston Rd.	Greenfield	"	"
15	4.29-4	Bernardston Rd.	Greenfield	"	"
16	01-CP-H1	Cheapside St.	Greenfield	42°34'21" N	72°35'22" W
17	SF-CS4	Cheapside St.	Greenfield	"	"
18	SF-CS6	Cheapside St.	Greenfield	"	"
19	9.11-1	North Parkway St.	Greenfield	42°35'36" N	72°35'13" W
20	10.5-3	North Parkway St.	Greenfield	"	"
21	RS75-113	North Parkway St.	Greenfield	"	"

APPENDIX A2: SAMPLE LOCATIONS FOR PIEDMONT RIVER FACIES

ID NO.	SAMPLE	STREET	TOWN	LATITUDE	LONGITUDE
1	7.7-1	Mountain Rd.	Deerfield	42°28'15" N	72°35'31" W
2	7.7-5	Mountain Rd.	Deerfield	"	"
3	SF-SR2	Mountain Rd.	Deerfield	"	"
4	9.21-2	River Rd.	Deerfield	42°28'52" N	72°34'43" W
5	9.21-5	River Rd.	Deerfield	"	"
6	9.21-6	River Rd.	Deerfield	"	"
7	10.11-1	French's Ferry St.	Sunderland	42°28'40" N	72°34'29" W
8	10.11-2	French's Ferry St.	Sunderland	"	"
9	10.11-3	French's Ferry St.	Sunderland	"	"
10	10.11-9	North Silver Ln.	Sunderland	42°28'15" N	72°34'20" W
11	10.11-10	North Silver Ln.	Sunderland	"	"
12	RS75-S3	North Silver Ln.	Sunderland	"	"
13	10.13-7	Bull Hill Rd.	Sunderland	42°26'45" N	72°32'42" W
14	10.13-8	Bull Hill Rd.	Sunderland	"	"
15	SF-BH6	Bull Hill Rd.	Sunderland	"	"
16	11.13-4	Rice's Ferry Rd.	Deerfield	42°32'51" N	72°35'26" W
17	11.13-6	Rice's Ferry Rd.	Deerfield	"	"
18	SF-PR1	Rice's Ferry Rd.	Deerfield	"	"
19	10.16-1	Kellogg St.	Hatfield	42°23'38" N	72°35'24" W
20	10.16-2	Kellogg St.	Hatfield	"	"
21	10.16-3	Kellogg St.	Hatfield	"	"
22	10.16-9	Meadow St.	Hadley	42°23'47" N	72°35'21" W
23	10.16-10	Meadow St.	Hadley	"	"
24	10.16-11	Meadow St.	Hadley	"	"

APPENDIX A3: SAMPLE LOCATIONS FOR ALLUVIAL FAN FACIES

ID NO.	SAMPLE	STREET	TOWN	LATITUDE	LONGITUDE
1	SF-FR1B	Scout Rd.	Gill	42°38'03" N	72°32'50" W
2	SF-FR2B	Scout Rd.	Gill	"	"
3	SF-FR3	Scout Rd.	Gill	"	"
4	10.9-2	West Gill Rd.	Gill	42°37'42" N	72°32'27" W
5	SF-WGR1	West Gill Rd.	Gill	"	"
6	SF-WGR2	West Gill Rd.	Gill	"	"

APPENDIX A4: ADDITIONAL PEBBLE COUNT LOCATIONS

ID NO.	SAMPLE	STREET	TOWN	LATITUDE	LONGITUDE
-	RS-221	Elm and Colrain St.	Greenfield	42°35'15" N	72°36'40" W
-	RS-225	Elm and Colrain St.	Greenfield	"	"
-	RS-251	Country Club Rd.	Greenfield	42°36'47" N	72°35'57" W
-	RS-252	Country Club Rd.	Greenfield	"	"
-	MW-3	Country Club Rd.	Greenfield	"	"
-	RS-201	South Cross Rd.	Gill	42°37'23" N	72°32'13" W
-	RS-151	Main Rd.	Gill	42°37'33" N	72°31'24" W

APPENDIX B

PETROGRAPHIC OPERATIONAL DEFINITIONS

The following definitions were used during point-counting of thin sections to determine modal analyses using the Gazzi-Dickinson point-counting method. Definitions have been adapted from Basu et al., 1975, Carozzi, 1993, Folk, 1980, Hubert, 2007 pers. com., Taylor, 1991, and Tortosa et al., 1991.

QUARTZ

Unit monocrystalline: 1 unit grain with straight to slightly undulose extinction. Grains are typically subequant, and rarely contain microlites and/or vacuoles.

Vein monocrystalline: 1 unit grain with 2 or more planes of fluid inclusions. Grains are typically subequant, and rarely contain microlites and/or vacuoles.

Annealed polycrystalline: 2 or more units with smooth, non-sutured boundaries, containing up to 10% mica (undifferentiated). Extinction may be straight to slightly undulose, with different optical orientations among sub-units. Vacuoles are uncommon.

Vein polycrystalline: 2 or more units with smooth, non-sutured boundaries and 2 or more planes of fluid inclusions. Extinction is semi-composite straight to undulose, with parallel sub-units almost in optical continuity (partly due to comb structure). Abundant vacuoles may impart milky color.

FELDSPAR

Untwinned plagioclase: Unstained, differentiated from quartz microlites and cleavage. Plagioclase in the Sugarloaf Arkose is commonly altered by albitization along cleavage and albite replacement domains in optical continuity with albite overgrowths. Plagioclase grains may contain up to 25% albite or illite alteration.

Twinned plagioclase: Unstained grains differentiated from quartz by twinning (commonly albite twinning law), microlites, and cleavage. Grains are commonly altered, as above. Plagioclase grains may contain up to 25% albite or illite alteration.

Albitized plagioclase: Plagioclase grains with more than 25% albitization, or grains that cannot be differentiated between prior categories due to degree of albititzation.

Untwinned K-feldspar: Stained yellow by sodium cobaltinitrate. K-feldspar may contain up to 25% albite or illite alteration.

Microcline K-feldspar: Stained yellow, displays polysynthetic twinning (scotch plaid). K-feldspar may contain up to 25% albite or illite alteration.

Illite replacement of feldspar: Feldspar grains with more than 25% illitization (typically K-feldspar), or grains that cannot be differentiated between prior categories due to degree of illitization (mostly plagioclase?).

ROCK FRAGMENTS

Granite: Rock fragment composed of 10% or more subequant quartz units with smooth, non-sutured boundaries, 10-90% feldspar units, and with or without mica. Feldspars may be partly to completely replaced by illite.

Granite gneiss: Rock fragment composed of 10% or more equidimensional to elongate quartz units with sutured and/or crenulated boundaries, 10-90% feldspar units, and with or without mica. Extinction of quartz units is strongly undulose. Plagioclase (if any) is untwinned. Feldspars may be partly to completely replaced by illite.

Schistose quartz: Rock fragment composed 60-90% quartz and 10-40% mica.

Schist: Rock fragment composed of 10% or less quartz and 40% or more mica.

Quartzite: 2 or more elongate, sub-parallel units with crenulated, sutured, and/or smooth, non-sutured boundaries, containing up to 10% mica. Extinction of quartz units is strongly undulose. Some microlites and vacuoles may be present.

Groundmass: Fine-grained (<0.625 mm) matrix in metamorphic rock fragments. Only counted when 1.) the entire rock fragment was 0.25-0.5 mm 2.) mineral under cross-hairs could be identified; and 3.) rock fragment did not include mineral subunits greater than 0.25 mm.

ACCESSORIES, POROSITY, MATRIX

Muscovite: Colorless in plane light, no pleochroism.

Biotite: Brown, green or red-brown in plane light, commonly alters to hematite.

Chlorite: Pale green in plane light, may flash blue at extinction.

Garnet: Colorless in plane light, high relief, fracture grain, may have one or more recognizable crystal faces, but typically rounded.

Hematite-stained matrix: Particles less than 30 microns in size coated by hematite or hydrated iron oxides.

Porosity: Typically filled with blue epoxy, black under crossed nicols. Pore space not filled with blue epoxy was not counted, due to potential grain plucking as thin sections were polished.

CEMENTS

Hematite rim: "Early" hematite (Taylor, 1991), includes rims on detrital grains and stained clay coats on detrital grains.

Hematite cement: "Late" hematite (Taylor, 1991), post-dates pore-filling albite and quartz. Includes stains on prior cements and biotite alteration to hematite.

Interstitial albite: Mosaic of randomly-oriented microcrystalline albite, commonly intergrown with quartz overgrowths. Not present in illite diagenetic zones.

Albite overgrowth: Cement precipitated as overgrowth on plagioclase and K-feldspar grains. Overgrowth may be twinned if parent grain is twinned, and is commonly in optical continuity with host plagioclase grains. Not present in illite diagenetic zones.

Illite: Distinguished from detrital micas by lack of large sheet-like plates or flakes. This category does not include illite replacement of feldspar grains.

Kaolinite: Characteristic 'book' grain groups or individual grains, within illite matrix (cement or replacement).

Quartz overgrowth: Anhedral quartz lacks inclusions and is intergrown with interstitial albite.

Carbonates: Calcite is stained pink by potassium ferrycyanide and Alizarin red-S; ferroan calcite is purple; dolomite unstained; and ferroan dolomite sky blue.

BASU-TORTOSA METHOD

Non-undulose: Medium sand-sized (0.25-0.5 mm) unit quartz that undergoes complete extinction with stage rotation of 5^{o} or less.

Undulose: Medium sand-sized unit quartz that undergoes sweeping extinction with stage rotation greater than 5^{o}.

Coarsely-polycrystalline: Medium sand-sized polycrystalline quartz composed of 2 or 3 units and less than 10% of another mineral phase.

Finely-polycrystalline: Medium sand-sized polycrystalline quartz composed of 4 or more units and less than 10% of another mineral phase.

APPENDIX C

MODAL ANALYSES

Appendix C1 shows Gazzi-Dickinson method results for 21 thin sections from the valley-river facies, Appendix C2 shows results for 24 thin sections from the piedmont-river facies, and Appendix C3 shows results for six thin sections from the alluvial-fan facies. In Appendices C1-C3, WR indicates point-counts of all grains that fell under the cross-hairs, whereas MS indicates that only medium sand-sized grains were counted. Q is quartz, F is feldspar, R is rock fragment, Plag. is plagioclase feldspar, Kspar is K-feldspar, Micro. is microcline, ACC. is accessory minerals, HEM. is hematite, ALB. is albite, and CO_3^- is carbonate minerals.

Appendix C4 shows Basu-Tortosa method results for thin sections from the valley-river facies, Appendix C5 shows results from the piedmont-river facies, and Appendix C6 shows results from the alluvial-fan facies. The number of thin sections analyzed from each facies is the same as Appendices C1-C3.

All analyses were performed by the author. Sample locations are given in Appendix A. Operational definitions of petrographic constituents are in Appendix B.

APPENDIX C1: MODAL ANALYSES FOR VALLEY RIVER FACIES

		LOCATION:	I-91 Location 1			
		FIGURE ID NO.:	1	2	3	-
		SAMPLE:	10.13-4	10.13-5	I91-1A	MEAN
		COUNT TYPE:	WR	WR	WR	WR
		N:	100	100	100	-
FRAMEWORK GRAINS						
QUARTZ	Unit monocrystalline		41.0	38.0	40.0	39.7
	Vein monocrystalline		3.0	1.0	1.0	1.7
	Annealed polycrystalline		10.0	5.0	10.0	8.3
	Vein polycrystalline		1.0	0.0	4.0	1.7
FELDSPAR	Plag.	Untwinned single grain	0.0	0.0	0.0	0.0
		Twinned single grain	0.0	0.0	0.0	0.0
		Albitized single grain	0.0	0.0	0.0	0.0
	Kspar	Untwinned single grain	0.0	0.0	0.0	0.0
		Perthite single grain	0.0	0.0	0.0	0.0
		Microcline single grain	0.0	0.0	0.0	0.0
	Illite replacement of feldspar		1.0	2.0	2.0	1.7
QUARTZ IN ROCK FRAGMENT	Granite		1.0	0.0	1.0	0.7
	Granite gneiss		2.0	1.0	2.0	1.7
	Schistose quartz		0.7	0.0	0.0	0.2
	Groundmass in schistose quartz		0.3	0.0	0.0	0.1
	Schist		1.0	0.0	1.0	0.7
	Groundmass in schist		2.0	0.0	0.0	0.7
	Quartzite		5.0	1.0	1.0	2.3
	Groundmass in quartzite		1.0	1.0	2.0	1.3
FELDSPAR IN ROCK FRAGMENT	Plag.	Untwinned granite	0.0	0.0	0.0	0.0
		Twinned granite	0.0	0.0	0.0	0.0
		Untwinned granite gneiss	0.0	0.0	0.0	0.0
		Twinned granite gneiss	0.0	0.0	0.0	0.0
	Kspar	Untwinned granite	0.0	0.0	0.0	0.0
		Perthite granite	0.0	0.0	0.0	0.0
		Micro. granite	0.0	0.0	0.0	0.0
		Untwinned granite gneiss	0.0	0.0	0.0	0.0
		Perthite granite gneiss	0.0	0.0	0.0	0.0
		Micro. granite gneiss	0.0	0.0	0.0	0.0
	Illite replacement in granite		3.0	2.0	2.0	2.3
	Illite replacement in granite gneiss		3.0	5.0	1.0	3.0
MICA IN ROCK FRAGMENT	Muscovite	Granite	1.0	1.0	1.0	1.0
		Granite gneiss	1.0	0.0	0.0	0.3
		Quartzite	0.0	0.0	0.0	0.0
		Schistose quartz	0.0	0.0	0.0	0.0
		Schist	3.0	0.0	2.0	1.7
	Biotite	Granite	0.0	0.0	0.0	0.0
		Granite gneiss	0.0	0.0	0.0	0.0
		Quartzite	0.0	0.0	0.0	0.0
		Schistose quartz	0.0	0.0	0.0	0.0
		Schist	0.0	0.0	0.0	0.0
		FRAMWORK TOTAL	**79.0**	**57.0**	**70.0**	**68.7**

APPENDIX C1, CONTINUED

	LOCATION:	I-91 Location 1			
	FIGURE ID NO.:	1	2	3	-
	SAMPLE:	10.13-4	10.13-5	I91-1A	MEAN
	COUNT TYPE:	WR	WR	WR	WR
	N:	100	100	100	-
ACCESSORIES, POROSITY, MATRIX					
ACC.	Muscovite single grain	2.0	4.0	8.0	4.7
	Biotite single grain	1.0	5.0	2.0	2.7
	Chlorite replacement single grain	0.0	0.0	0.0	0.0
	Garnet	0.0	0.0	0.0	0.0
Hematite-stained matrix		5.0	2.0	1.0	2.7
Porosity		0.0	1.0	5.0	2.0
ACC., POROSITY, MATRIX TOTAL		**8.0**	**12.0**	**16.0**	**12.0**
CEMENTS					
HEM.	Rim	5.0	8.0	1.0	4.7
	Cement	1.0	5.0	1.0	2.3
ALB.	Interstitial	0.0	0.0	0.0	0.0
	Overgrowth	0.0	0.0	0.0	0.0
Illite		7.0	15.0	11.0	11.0
Kaolinite		0.0	0.0	0.0	0.0
Quartz overgrowth		0.0	3.0	1.0	1.3
CO3-	Calcite	0.0	0.0	0.0	0.0
	Fe-calcite	0.0	0.0	0.0	0.0
	Dolomite	0.0	0.0	0.0	0.0
	Fe-dolomite	0.0	0.0	0.0	0.0
CEMENT TOTAL		**13.0**	**31.0**	**14.0**	**19.3**
THIN SECTION TOTAL		**100.0**	**100.0**	**100.0**	**100.0**

APPENDIX C1, CONTINUED

LOCATION:			I-91 Location 1			
FIGURE ID NO.:			1	2	3	-
SAMPLE:			10.13-4	10.13-5	I91-1A	MEAN
COUNT TYPE:			MS	MS	MS	MS
N:			300	300	300	-
FRAMEWORK GRAINS						
QUARTZ	Unit monocrystalline		35.7	32.0	38.3	35.3
	Vein monocrystalline		5.0	4.7	6.0	5.2
	Annealed polycrystalline		10.0	11.0	9.7	10.2
	Vein polycrystalline		4.0	2.0	1.7	2.6
FELDSPAR	Plag.	Untwinned single grain	0.0	0.0	0.0	0.0
		Twinned single grain	0.0	0.0	0.0	0.0
		Albitized single grain	0.0	0.0	0.0	0.0
	Kspar	Untwinned single grain	0.0	0.0	0.0	0.0
		Perthite single grain	0.0	0.0	0.0	0.0
		Microcline single grain	0.0	0.0	0.0	0.0
	Illite replacement of feldspar		7.3	13.0	11.0	10.4
QUARTZ IN ROCK FRAGMENT	Granite		2.7	4.0	3.3	3.3
	Granite gneiss		6.7	7.0	7.0	6.9
	Schistose quartz		1.0	0.7	1.0	0.9
	Groundmass in schistose quartz		0.0	1.0	0.0	0.3
	Schist		1.0	0.3	0.0	0.4
	Groundmass in schist		0.7	0.7	1.0	0.8
	Quartzite		5.0	5.0	4.0	4.7
	Groundmass in quartzite		4.0	0.3	0.7	1.7
FELDSPAR IN ROCK FRAGMENT	Plag.	Untwinned granite	0.0	0.0	0.0	0.0
		Twinned granite	0.0	0.0	0.0	0.0
		Untwinned granite gneiss	0.0	0.0	0.0	0.0
		Twinned granite gneiss	0.0	0.0	0.0	0.0
	Kspar	Untwinned granite	0.0	0.0	0.0	0.0
		Perthite granite	0.0	0.0	0.0	0.0
		Micro. granite	0.0	0.0	0.0	0.0
		Untwinned granite gneiss	0.0	0.0	0.0	0.0
		Perthite granite gneiss	0.0	0.0	0.0	0.0
		Micro. granite gneiss	0.0	0.0	0.0	0.0
	Illite replacement in granite		2.0	3.7	4.3	3.3
	Illite replacement in granite gneiss		3.3	4.7	3.7	3.9
MICA IN ROCK FRAGMENT	Muscovite	Granite	0.0	0.3	0.3	0.2
		Granite gneiss	0.0	0.0	0.0	0.0
		Quartzite	0.0	0.0	0.3	0.1
		Schistose quartz	0.0	1.7	0.7	0.8
		Schist	1.7	0.3	1.0	1.0
	Biotite	Granite	0.0	0.0	0.0	0.0
		Granite gneiss	0.0	0.0	0.0	0.0
		Quartzite	0.0	0.0	0.0	0.0
		Schistose quartz	0.0	0.0	0.0	0.0
		Schist	0.0	0.0	0.7	0.2
	FRAMWORK TOTAL		**91.0**	**92.3**	**93.7**	**92.3**

APPENDIX C1, CONTINUED

	LOCATION:	I-91 Location 1			
	FIGURE ID NO.:	1	2	3	-
	SAMPLE:	10.13-4	10.13-5	I91-1A	MEAN
	COUNT TYPE:	MS	MS	MS	MS
	N:	300	300	300	-
ACCESSORIES, POROSITY, MATRIX					
ACC.	Muscovite single grain	7.7	6.0	5.7	6.5
	Biotite single grain	1.3	1.7	0.7	1.2
	Chlorite replacement single grain	0.0	0.0	0.0	0.0
	Garnet	-	-	-	-
Hematite-stained matrix		-	-	-	-
Porosity		-	-	-	-
	ACC., POROSITY, MATRIX TOTAL	**9.0**	**7.7**	**6.4**	**7.7**
CEMENTS					
HEM.	Rim	-	-	-	-
	Cement	-	-	-	-
ALB.	Interstitial	-	-	-	-
	Overgrowth	-	-	-	-
Illite		-	-	-	-
Kaolinite		-	-	-	-
Quartz overgrowth		-	-	-	-
CO3-	Calcite	-	-	-	-
	Fe-calcite	-	-	-	-
	Dolomite	-	-	-	-
	Fe-dolomite	-	-	-	-
	CEMENT TOTAL	**-**	**-**	**-**	**-**
	THIN SECTION TOTAL	**100.0**	**100.0**	**100.0**	**100.0**

APPENDIX C1, CONTINUED

LOCATION:	Lower Rd.					
FIGURE ID NO.:		4	5	6	-	
SAMPLE:		D-1	D-2B	D-3	MEAN	
COUNT TYPE:		WR	WR	WR	WR	
N:		100	100	100	-	
FRAMEWORK GRAINS						
QUARTZ	Unit monocrystalline		40.0	34.0	34.0	36.0
	Vein monocrystalline		4.0	0.0	2.0	2.0
	Annealed polycrystalline		9.0	12.0	12.0	11.0
	Vein polycrystalline		1.0	1.0	2.0	1.3
FELDSPAR	Plag.	Untwinned single grain	0.0	0.0	0.0	0.0
		Twinned single grain	0.0	0.0	0.0	0.0
		Albitized single grain	0.0	0.0	0.0	0.0
	Kspar	Untwinned single grain	0.0	0.0	0.0	0.0
		Perthite single grain	0.0	0.0	0.0	0.0
		Microcline single grain	0.0	0.0	0.0	0.0
	Illite replacement of feldspar		3.0	5.0	5.0	4.3
QUARTZ IN ROCK FRAGMENT	Granite		0.0	1.0	2.0	1.0
	Granite gneiss		1.0	2.0	2.0	1.7
	Schistose quartz		0.0	0.0	0.0	0.0
	Groundmass in schistose quartz		0.0	0.0	0.0	0.0
	Schist		0.0	0.0	1.0	0.3
	Groundmass in schist		0.0	0.0	0.0	0.0
	Quartzite		3.0	3.0	2.0	2.7
	Groundmass in quartzite		1.0	3.0	0.0	1.3
FELDSPAR IN ROCK FRAGMENT	Plag.	Untwinned granite	0.0	0.0	0.0	0.0
		Twinned granite	0.0	0.0	0.0	0.0
		Untwinned granite gneiss	0.0	0.0	0.0	0.0
		Twinned granite gneiss	0.0	0.0	0.0	0.0
	Kspar	Untwinned granite	0.0	0.0	0.0	0.0
		Perthite granite	0.0	0.0	0.0	0.0
		Micro. granite	0.0	0.0	0.0	0.0
		Untwinned granite gneiss	0.0	0.0	0.0	0.0
		Perthite granite gneiss	0.0	0.0	0.0	0.0
		Micro. granite gneiss	0.0	0.0	0.0	0.0
	Illite replacement in granite		1.0	2.0	1.0	1.3
	Illite replacement in granite gneiss		0.0	2.0	3.0	1.7
MICA IN ROCK FRAGMENT	Muscovite	Granite	0.0	0.0	0.0	0.0
		Granite gneiss	0.0	0.0	1.0	0.3
		Quartzite	1.0	1.0	1.0	1.0
		Schistose quartz	0.0	0.0	0.0	0.0
		Schist	1.0	0.0	2.0	1.0
	Biotite	Granite	0.0	0.0	0.0	0.0
		Granite gneiss	0.0	0.0	0.0	0.0
		Quartzite	0.0	0.0	0.0	0.0
		Schistose quartz	0.0	0.0	0.0	0.0
		Schist	0.0	0.0	0.0	0.0
	FRAMWORK TOTAL		**65.0**	**66.0**	**70.0**	**67.0**

APPENDIX C1, CONTINUED

	LOCATION:	Lower Rd.			
	FIGURE ID NO.:	4	5	6	-
	SAMPLE:	D-1	D-2B	D-3	MEAN
	COUNT TYPE:	WR	WR	WR	WR
	N:	100	100	100	-
ACCESSORIES, POROSITY, MATRIX					
ACC.	Muscovite single grain	5.0	6.0	6.0	5.7
	Biotite single grain	4.0	6.0	4.0	4.7
	Chlorite replacement single grain	0.0	0.0	0.0	0.0
	Garnet	0.0	0.0	0.0	0.0
Hematite-stained matrix		7.0	8.0	1.0	5.3
Porosity		2.0	2.0	0.0	1.3
	ACC., POROSITY, MATRIX TOTAL	**18.0**	**22.0**	**11.0**	**17.0**
CEMENTS					
HEM.	Rim	0.0	1.0	4.0	1.7
	Cement	2.0	3.0	2.0	2.3
ALB.	Interstitial	0.0	0.0	0.0	0.0
	Overgrowth	0.0	0.0	0.0	0.0
Illite		10.0	7.0	8.0	8.3
Kaolinite		2.0	0.0	3.0	1.7
Quartz overgrowth		3.0	1.0	2.0	2.0
CO3-	Calcite	0.0	0.0	0.0	0.0
	Fe-calcite	0.0	0.0	0.0	0.0
	Dolomite	0.0	0.0	0.0	0.0
	Fe-dolomite	0.0	0.0	0.0	0.0
	CEMENT TOTAL	**17.0**	**12.0**	**19.0**	**16.0**
	THIN SECTION TOTAL	**100.0**	**100.0**	**100.0**	**100.0**

APPENDIX C1, CONTINUED

		LOCATION:	Lower Rd.			
		FIGURE ID NO.:	4	5	6	-
		SAMPLE:	D-1	D-2B	D-3	MEAN
		COUNT TYPE:	MS	MS	MS	MS
		N:	300	300	300	-
FRAMEWORK GRAINS						
QUARTZ		Unit monocrystalline	26.7	40.3	34.3	33.8
		Vein monocrystalline	14.3	9.3	8.3	10.7
		Annealed polycrystalline	14.0	8.3	11.0	11.1
		Vein polycrystalline	4.0	0.7	2.3	2.3
FELDSPAR	Plag.	Untwinned single grain	0.0	0.0	0.0	0.0
		Twinned single grain	0.0	0.0	0.0	0.0
		Albitized single grain	0.0	0.0	0.0	0.0
	Kspar	Untwinned single grain	0.0	0.0	0.0	0.0
		Perthite single grain	0.0	0.0	0.0	0.0
		Microcline single grain	0.0	0.0	0.0	0.0
		Illite replacement of feldspar	6.3	6.7	6.0	6.3
QUARTZ IN ROCK FRAGMENT		Granite	7.0	6.0	4.3	5.8
		Granite gneiss	0.0	3.3	4.3	2.5
		Schistose quartz	2.0	1.7	2.0	1.9
		Groundmass in schistose quartz	0.3	1.0	0.3	0.5
		Schist	0.0	0.0	0.0	0.0
		Groundmass in schist	0.0	0.0	0.0	0.0
		Quartzite	12.0	4.0	9.3	8.4
		Groundmass in quartzite	3.3	2.3	2.0	2.5
FELDSPAR IN ROCK FRAGMENT	Plag.	Untwinned granite	0.0	0.0	0.0	0.0
		Twinned granite	0.0	0.0	0.0	0.0
		Untwinned granite gneiss	0.0	0.0	0.0	0.0
		Twinned granite gneiss	0.0	0.0	0.0	0.0
	Kspar	Untwinned granite	0.0	0.0	0.0	0.0
		Perthite granite	0.0	0.0	0.0	0.0
		Micro. granite	0.0	0.0	0.0	0.0
		Untwinned granite gneiss	0.0	0.0	0.0	0.0
		Perthite granite gneiss	0.0	0.0	0.0	0.0
		Micro. granite gneiss	0.0	0.0	0.0	0.0
		Illite replacement in granite	1.0	1.7	1.0	1.2
		Illite replacement in granite gneiss	1.0	2.0	3.7	2.2
MICA IN ROCK FRAGMENT	Muscovite	Granite	0.0	0.0	1.3	0.4
		Granite gneiss	0.0	0.7	0.0	0.2
		Quartzite	1.3	0.3	1.0	0.9
		Schistose quartz	0.3	0.0	0.0	0.1
		Schist	2.0	0.0	1.0	1.0
	Biotite	Granite	0.0	0.0	0.0	0.0
		Granite gneiss	0.0	0.0	0.0	0.0
		Quartzite	0.0	0.3	0.3	0.2
		Schistose quartz	0.0	0.0	0.0	0.0
		Schist	0.0	0.0	0.0	0.0
		FRAMWORK TOTAL	**95.7**	**88.7**	**92.1**	**92.2**

APPENDIX C1, CONTINUED

	LOCATION:	Lower Rd.			
	FIGURE ID NO.:	4	5	6	-
	SAMPLE:	D-1	D-2B	D-3	MEAN
	COUNT TYPE:	MS	MS	MS	MS
	N:	300	300	300	-
ACCESSORIES, POROSITY, MATRIX					
ACC.	Muscovite single grain	3.7	8.3	5.7	5.9
	Biotite single grain	0.7	3.0	2.3	2.0
	Chlorite replacement single grain	0.0	0.0	0.0	0.0
	Garnet	-	-	-	-
Hematite-stained matrix		-	-	-	-
Porosity		-	-	-	-
	ACC., POROSITY, MATRIX TOTAL	**4.3**	**11.3**	**8.0**	**7.9**
CEMENTS					
HEM.	Rim	-	-	-	-
	Cement	-	-	-	-
ALB.	Interstitial	-	-	-	-
	Overgrowth	-	-	-	-
Illite		-	-	-	-
Kaolinite		-	-	-	-
Quartz overgrowth		-	-	-	-
CO3-	Calcite	-	-	-	-
	Fe-calcite	-	-	-	-
	Dolomite	-	-	-	-
	Fe-dolomite	-	-	-	-
	CEMENT TOTAL	**-**	**-**	**-**	**-**
	THIN SECTION TOTAL	**100.0**	**100.0**	**100.0**	**100.0**

APPENDIX C1, CONTINUED

		LOCATION:	I-91 Location 3			
		FIGURE ID NO.:	7	8	9	-
		SAMPLE:	I91-3A	I91-3B	SF-G11	MEAN
		COUNT TYPE:	WR	WR	WR	WR
		N:	100	100	100	-
FRAMEWORK GRAINS						
QUARTZ		Unit monocrystalline	28.0	30.0	20.0	26.0
		Vein monocrystalline	0.0	4.0	0.0	1.3
		Annealed polycrystalline	5.0	3.0	7.0	5.0
		Vein polycrystalline	0.0	1.0	0.0	0.3
FELDSPAR	Plag.	Untwinned single grain	4.5	3.5	2.0	3.3
		Twinned single grain	5.5	3.5	6.0	5.0
		Albitized single grain	1.0	2.0	0.0	1.0
	Kspar	Untwinned single grain	3.0	4.0	6.0	4.3
		Perthite single grain	1.0	3.0	0.0	1.3
		Microcline single grain	1.0	0.0	1.0	0.7
		Illite replacement of feldspar	0.0	0.0	0.0	0.0
QUARTZ IN ROCK FRAGMENT		Granite	5.0	2.0	4.0	3.7
		Granite gneiss	2.0	3.0	6.0	3.7
		Schistose quartz	0.0	0.0	0.3	0.1
		Groundmass in schistose quartz	0.0	0.0	0.7	0.2
		Schist	0.0	0.0	0.7	0.2
		Groundmass in schist	0.0	0.0	0.3	0.1
		Quartzite	4.0	3.0	1.0	2.7
		Groundmass in quartzite	1.0	0.0	0.0	0.3
FELDSPAR IN ROCK FRAGMENT	Plag.	Untwinned granite	1.0	0.0	1.0	0.7
		Twinned granite	2.0	2.0	1.0	1.7
		Untwinned granite gneiss	0.0	0.0	2.0	0.7
		Twinned granite gneiss	1.0	0.0	4.0	1.7
	Kspar	Untwinned granite	1.5	1.0	1.0	1.2
		Perthite granite	0.5	0.0	0.0	0.2
		Micro. granite	2.0	0.0	1.0	1.0
		Untwinned granite gneiss	1.0	0.0	1.0	0.7
		Perthite granite gneiss	0.0	0.0	0.0	0.0
		Micro. granite gneiss	0.0	0.0	1.0	0.3
		Illite replacement in granite	0.0	0.0	0.0	0.0
		Illite replacement in granite gneiss	0.0	0.0	0.0	0.0
MICA IN ROCK FRAGMENT	Muscovite	Granite	0.0	0.0	1.0	0.3
		Granite gneiss	0.0	0.0	1.0	0.3
		Quartzite	0.0	1.0	1.0	0.7
		Schistose quartz	0.0	1.0	0.0	0.3
		Schist	2.0	1.0	1.0	1.3
	Biotite	Granite	0.0	0.0	0.0	0.0
		Granite gneiss	0.0	0.0	0.0	0.0
		Quartzite	0.0	0.0	0.0	0.0
		Schistose quartz	0.0	0.0	0.0	0.0
		Schist	0.0	1.0	1.0	0.7
		FRAMWORK TOTAL	**72.0**	**69.0**	**72.0**	**71.0**

APPENDIX C1, CONTINUED

	LOCATION:	I-91 Location 3			
	FIGURE ID NO.:	7	8	9	-
	SAMPLE:	I91-3A	I91-3B	SF-G11	MEAN
	COUNT TYPE:	WR	WR	WR	WR
	N:	100	100	100	-
ACCESSORIES, POROSITY, MATRIX					
ACC.	Muscovite single grain	2.0	6.0	2.0	3.3
	Biotite single grain	0.0	2.0	0.0	0.7
	Chlorite replacement single grain	0.0	0.0	0.0	0.0
	Garnet	0.0	0.0	0.0	0.0
Hematite-stained matrix		1.0	8.0	3.0	4.0
Porosity		1.0	1.0	2.0	1.3
ACC., POROSITY, MATRIX TOTAL		**4.0**	**17.0**	**8.0**	**9.7**
CEMENTS					
HEM.	Rim	2.0	1.0	2.0	1.7
	Cement	7.0	8.0	3.0	6.0
ALB.	Interstitial	6.0	4.0	4.0	4.7
	Overgrowth	0.0	0.0	3.0	1.0
Illite		0.0	0.0	0.0	0.0
Kaolinite		0.0	0.0	0.0	0.0
Quartz overgrowth		0.0	0.0	2.0	0.7
CO3-	Calcite	1.0	0.0	5.0	2.0
	Fe-calcite	2.0	1.0	1.0	1.3
	Dolomite	0.0	0.0	0.0	0.0
	Fe-dolomite	6.0	0.0	0.0	2.0
CEMENT TOTAL		**24.0**	**14.0**	**20.0**	**19.3**
THIN SECTION TOTAL		**100.0**	**100.0**	**100.0**	**100.0**

APPENDIX C1, CONTINUED

		LOCATION:	I-91 Location 3			
		FIGURE ID NO.:	7	8	9	-
		SAMPLE:	I91-3A	I91-3B	SF-G11	MEAN
		COUNT TYPE:	MS	MS	MS	MS
		N:	300	300	300	-
FRAMEWORK GRAINS						
QUARTZ		Unit monocrystalline	36.0	47.3	41.0	41.4
		Vein monocrystalline	1.0	0.0	0.7	0.6
		Annealed polycrystalline	11.0	7.0	8.3	8.8
		Vein polycrystalline	0.0	0.0	0.0	0.0
FELDSPAR	Plag.	Untwinned single grain	6.0	4.0	4.7	4.9
		Twinned single grain	7.0	6.7	2.0	5.2
		Albitized single grain	0.0	0.7	0.0	0.2
	Kspar	Untwinned single grain	4.9	5.0	7.5	5.8
		Perthite single grain	2.0	1.2	0.0	1.1
		Microcline single grain	2.1	2.8	2.0	2.3
		Illite replacement of feldspar	0.0	0.0	0.0	0.0
QUARTZ IN ROCK FRAGMENT		Granite	5.0	2.7	3.7	3.8
		Granite gneiss	4.0	3.7	5.3	4.3
		Schistose quartz	1.0	0.7	1.3	1.0
		Groundmass in schistose quartz	2.0	0.3	1.0	1.1
		Schist	0.3	0.0	0.0	0.1
		Groundmass in schist	0.0	0.3	0.0	0.1
		Quartzite	6.3	9.3	5.0	6.9
		Groundmass in quartzite	0.0	0.0	2.0	0.7
FELDSPAR IN ROCK FRAGMENT	Plag.	Untwinned granite	1.7	0.0	0.0	0.6
		Twinned granite	2.0	0.3	0.3	0.9
		Untwinned granite gneiss	1.0	1.0	0.7	0.9
		Twinned granite gneiss	0.0	2.3	3.0	1.8
	Kspar	Untwinned granite	1.0	1.1	1.7	1.3
		Perthite granite	0.6	0.0	0.0	0.2
		Micro. granite	1.4	0.0	0.5	0.6
		Untwinned granite gneiss	0.7	1.0	1.0	0.9
		Perthite granite gneiss	0.0	0.0	0.0	0.0
		Micro. granite gneiss	0.3	0.9	1.0	0.7
		Illite replacement in granite	0.0	0.0	0.0	0.0
		Illite replacement in granite gneiss	0.0	0.0	0.0	0.0
MICA IN ROCK FRAGMENT	Muscovite	Granite	0.0	0.3	0.0	0.1
		Granite gneiss	0.0	0.0	0.0	0.0
		Quartzite	0.0	0.0	0.0	0.0
		Schistose quartz	0.0	0.3	0.3	0.2
		Schist	1.7	0.3	0.7	0.9
	Biotite	Granite	0.0	0.0	0.0	0.0
		Granite gneiss	0.0	0.0	0.0	0.0
		Quartzite	0.0	0.0	0.0	0.0
		Schistose quartz	0.0	0.0	0.0	0.0
		Schist	0.3	0.0	0.3	0.2
		FRAMWORK TOTAL	**99.4**	**99.3**	**99.0**	**99.2**

APPENDIX C1, CONTINUED

	LOCATION:	I-91 Location 3			
	FIGURE ID NO.:	7	8	9	-
	SAMPLE:	I91-3A	I91-3B	SF-G11	MEAN
	COUNT TYPE:	MS	MS	MS	MS
	N:	300	300	300	-
ACCESSORIES, POROSITY, MATRIX					
ACC.	Muscovite single grain	0.7	0.7	1.0	0.8
	Biotite single grain	0.0	0.0	0.0	0.0
	Chlorite replacement single grain	0.0	0.0	0.0	0.0
	Garnet	-	-	-	-
Hematite-stained matrix		-	-	-	-
Porosity		-	-	-	-
	ACC., POROSITY, MATRIX TOTAL	**0.7**	**0.7**	**1.0**	**0.8**
CEMENTS					
HEM.	Rim	-	-	-	-
	Cement	-	-	-	-
ALB.	Interstitial	-	-	-	-
	Overgrowth	-	-	-	-
Illite		-	-	-	-
Kaolinite		-	-	-	-
Quartz overgrowth		-	-	-	-
CO3-	Calcite	-	-	-	-
	Fe-calcite	-	-	-	-
	Dolomite	-	-	-	-
	Fe-dolomite	-	-	-	-
	CEMENT TOTAL	**-**	**-**	**-**	**-**
	THIN SECTION TOTAL	**100.0**	**100.0**	**100.0**	**100.0**

APPENDIX C1, CONTINUED

		LOCATION:	Leyden Rd.			
		FIGURE ID NO.:	10	11	12	-
		SAMPLE:	8.23-5	8.23-7	RS75-192	MEAN
		COUNT TYPE:	WR	WR	WR	WR
		N:	100	100	100	-
FRAMEWORK GRAINS						
QUARTZ		Unit monocrystalline	14.0	11.0	18.0	14.3
		Vein monocrystalline	2.0	8.0	4.0	4.7
		Annealed polycrystalline	5.0	3.0	7.0	5.0
		Vein polycrystalline	1.0	2.0	2.0	1.7
FELDSPAR	Plag.	Untwinned single grain	4.5	3.5	3.0	3.7
		Twinned single grain	4.5	7.5	3.0	5.0
		Albitized single grain	2.0	1.0	9.0	4.0
	Kspar	Untwinned single grain	6.0	3.0	2.0	3.7
		Perthite single grain	1.0	2.0	3.0	2.0
		Microcline single grain	3.0	5.0	8.0	5.3
		Illite replacement of feldspar	0.0	0.0	0.0	0.0
QUARTZ IN ROCK FRAGMENT		Granite	1.0	4.0	2.0	2.3
		Granite gneiss	3.0	7.0	3.0	4.3
		Schistose quartz	0.0	0.0	1.0	0.3
		Groundmass in schistose quartz	0.0	0.0	0.0	0.0
		Schist	1.0	0.0	0.0	0.3
		Groundmass in schist	1.0	0.0	0.0	0.3
		Quartzite	4.0	2.0	8.0	4.7
		Groundmass in quartzite	1.0	2.0	0.0	1.0
FELDSPAR IN ROCK FRAGMENT	Plag.	Untwinned granite	1.0	1.0	1.0	1.0
		Twinned granite	2.0	2.0	1.0	1.7
		Untwinned granite gneiss	0.0	0.0	0.0	0.0
		Twinned granite gneiss	1.0	0.0	0.0	0.3
	Kspar	Untwinned granite	3.7	0.5	1.5	1.9
		Perthite granite	0.3	0.5	0.5	0.4
		Micro. granite	0.0	0.0	0.0	0.0
		Untwinned granite gneiss	2.0	0.0	0.0	0.7
		Perthite granite gneiss	0.0	0.0	1.0	0.3
		Micro. granite gneiss	0.0	0.0	0.0	0.0
		Illite replacement in granite	0.0	0.0	0.0	0.0
		Illite replacement in granite gneiss	0.0	0.0	0.0	0.0
MICA IN ROCK FRAGMENT	Muscovite	Granite	1.0	1.0	1.0	1.0
		Granite gneiss	0.0	0.0	0.0	0.0
		Quartzite	2.0	0.0	1.0	1.0
		Schistose quartz	1.0	2.0	0.0	1.0
		Schist	3.0	4.0	4.0	3.7
	Biotite	Granite	0.0	0.0	0.0	0.0
		Granite gneiss	0.0	0.0	0.0	0.0
		Quartzite	0.0	0.0	0.0	0.0
		Schistose quartz	0.0	0.0	0.0	0.0
		Schist	0.0	0.0	0.0	0.0
		FRAMWORK TOTAL	**71.0**	**72.0**	**84.0**	**75.7**

APPENDIX C1, CONTINUED

	LOCATION:	Leyden Rd.			
	FIGURE ID NO.:	10	11	12	-
	SAMPLE:	8.23-5	8.23-7	RS75-192	MEAN
	COUNT TYPE:	WR	WR	WR	WR
	N:	100	100	100	-
ACCESSORIES, POROSITY, MATRIX					
ACC.	Muscovite single grain	3.0	5.0	4.0	4.0
	Biotite single grain	2.0	2.0	1.0	1.7
	Chlorite replacement single grain	0.0	0.0	0.0	0.0
	Garnet	0.0	0.0	0.0	0.0
Hematite-stained matrix		5.0	3.0	3.0	3.7
Porosity		1.0	2.0	0.0	1.0
	ACC., POROSITY, MATRIX TOTAL	**11.0**	**12.0**	**8.0**	**10.3**
CEMENTS					
HEM.	Rim	2.0	1.0	2.0	1.7
	Cement	3.0	4.0	2.0	3.0
ALB.	Interstitial	4.0	5.0	2.0	3.7
	Overgrowth	4.0	1.0	1.0	2.0
Illite		0.0	0.0	0.0	0.0
Kaolinite		0.0	0.0	0.0	0.0
Quartz overgrowth		2.0	1.0	0.0	1.0
CO3-	Calcite	3.0	2.0	1.0	2.0
	Fe-calcite	0.0	2.0	0.0	0.7
	Dolomite	0.0	0.0	0.0	0.0
	Fe-dolomite	0.0	0.0	0.0	0.0
	CEMENT TOTAL	**18.0**	**16.0**	**8.0**	**14.0**
	THIN SECTION TOTAL	**100.0**	**100.0**	**100.0**	**100.0**

APPENDIX C1, CONTINUED

		LOCATION:	Leyden Rd.			
		FIGURE ID NO.:	10	11	12	-
		SAMPLE:	8.23-5	8.23-7	RS75-192	MEAN
		COUNT TYPE:	MS	MS	MS	MS
		N:	300	300	300	-
FRAMEWORK GRAINS						
QUARTZ		Unit monocrystalline	19.3	22.7	21.3	21.1
		Vein monocrystalline	11.7	13.3	14.3	13.1
		Annealed polycrystalline	11.7	6.7	7.3	8.5
		Vein polycrystalline	1.7	4.3	3.3	3.1
FELDSPAR	Plag.	Untwinned single grain	2.0	5.0	4.3	3.8
		Twinned single grain	8.0	4.7	4.6	5.8
		Albitized single grain	3.0	1.7	2.3	2.3
	Kspar	Untwinned single grain	4.4	1.5	2.4	2.8
		Perthite single grain	1.0	0.5	2.0	1.2
		Microcline single grain	1.6	0.6	0.7	1.0
		Illite replacement of feldspar	7.0	0.0	3.3	3.4
QUARTZ IN ROCK FRAGMENT		Granite	2.0	2.3	3.0	2.4
		Granite gneiss	2.0	2.0	1.0	1.7
		Schistose quartz	3.0	1.0	4.7	2.9
		Groundmass in schistose quartz	0.3	5.0	1.0	2.1
		Schist	1.0	0.3	0.7	0.7
		Groundmass in schist	0.0	1.7	2.0	1.2
		Quartzite	9.3	11.0	10.3	10.2
		Groundmass in quartzite	0.0	1.0	0.0	0.3
FELDSPAR IN ROCK FRAGMENT	Plag.	Untwinned granite	2.0	0.0	0.0	0.7
		Twinned granite	1.0	1.3	0.7	1.0
		Untwinned granite gneiss	0.7	0.0	1.0	0.6
		Twinned granite gneiss	0.0	1.0	1.0	0.7
	Kspar	Untwinned granite	2.0	1.0	0.9	1.3
		Perthite granite	0.0	0.0	0.0	0.0
		Micro. granite	0.0	0.0	0.0	0.0
		Untwinned granite gneiss	0.3	0.7	0.0	0.3
		Perthite granite gneiss	0.0	0.0	1.0	0.3
		Micro. granite gneiss	0.0	0.0	0.0	0.0
		Illite replacement in granite	0.0	0.0	0.0	0.0
		Illite replacement in granite gneiss	0.0	0.0	0.0	0.0
MICA IN ROCK FRAGMENT	Muscovite	Granite	2.7	0.0	0.3	1.0
		Granite gneiss	0.7	0.3	1.3	0.8
		Quartzite	1.3	0.0	0.3	0.5
		Schistose quartz	0.0	2.0	1.3	1.1
		Schist	0.0	3.0	0.7	1.2
	Biotite	Granite	0.3	1.0	0.0	0.4
		Granite gneiss	0.0	0.0	0.7	0.2
		Quartzite	0.0	0.0	0.0	0.0
		Schistose quartz	0.0	0.0	0.3	0.1
		Schist	0.0	0.0	0.0	0.0
		FRAMWORK TOTAL	**100.0**	**95.7**	**98.0**	**97.9**

APPENDIX C1, CONTINUED

	LOCATION:	Leyden Rd.			
	FIGURE ID NO.:	10	11	12	-
	SAMPLE:	8.23-5	8.23-7	RS75-192	MEAN
	COUNT TYPE:	MS	MS	MS	MS
	N:	300	300	300	-
ACCESSORIES, POROSITY, MATRIX					
ACC.	Muscovite single grain	0.0	2.7	1.7	1.5
	Biotite single grain	0.0	1.7	0.3	0.7
	Chlorite replacement single grain	0.0	0.0	0.0	0.0
	Garnet	-	-	-	-
Hematite-stained matrix		-	-	-	-
Porosity		-	-	-	-
	ACC., POROSITY, MATRIX TOTAL	**0.0**	**4.3**	**2.0**	**2.1**
CEMENTS					
HEM.	Rim	-	-	-	-
	Cement	-	-	-	-
ALB.	Interstitial	-	-	-	-
	Overgrowth	-	-	-	-
Illite		-	-	-	-
Kaolinite		-	-	-	-
Quartz overgrowth		-	-	-	-
CO3-	Calcite	-	-	-	-
	Fe-calcite	-	-	-	-
	Dolomite	-	-	-	-
	Fe-dolomite	-	-	-	-
	CEMENT TOTAL	**-**	**-**	**-**	**-**
	THIN SECTION TOTAL	**100.0**	**100.0**	**100.0**	**100.0**

APPENDIX C1, CONTINUED

		LOCATION:	Bernardston Rd.			
		FIGURE ID NO.:	13	14	15	-
		SAMPLE:	4.29-1	4.29-2	4.29-4	MEAN
		COUNT TYPE:	WR	WR	WR	WR
		N:	100	100	100	-
FRAMEWORK GRAINS						
QUARTZ		Unit monocrystalline	7.0	12.0	9.0	9.3
		Vein monocrystalline	3.0	3.0	4.0	3.3
		Annealed polycrystalline	4.0	6.0	10.0	6.7
		Vein polycrystalline	0.0	0.0	2.0	0.7
FELDSPAR	Plag.	Untwinned single grain	6.0	4.0	3.0	4.3
		Twinned single grain	7.0	6.0	12.0	8.3
		Albitized single grain	1.0	0.0	2.0	1.0
	Kspar	Untwinned single grain	0.0	1.0	0.0	0.3
		Perthite single grain	0.0	0.0	0.0	0.0
		Microcline single grain	0.0	0.0	0.0	0.0
		Illite replacement of feldspar	0.0	0.0	0.0	0.0
QUARTZ IN ROCK FRAGMENT		Granite	5.0	2.0	1.0	2.7
		Granite gneiss	1.0	2.0	2.0	1.7
		Schistose quartz	2.0	2.0	1.3	1.8
		Groundmass in schistose quartz	6.0	0.0	3.7	3.2
		Schist	3.0	4.0	1.0	2.7
		Groundmass in schist	7.0	0.0	6.0	4.3
		Quartzite	2.0	6.0	4.0	4.0
		Groundmass in quartzite	1.0	0.0	0.0	0.3
FELDSPAR IN ROCK FRAGMENT	Plag.	Untwinned granite	2.0	2.0	3.0	2.3
		Twinned granite	3.0	2.0	5.0	3.3
		Untwinned granite gneiss	0.0	1.0	2.0	1.0
		Twinned granite gneiss	1.0	3.0	3.0	2.3
	Kspar	Untwinned granite	2.0	0.0	0.0	0.7
		Perthite granite	0.0	0.0	0.0	0.0
		Micro. granite	0.0	0.0	0.0	0.0
		Untwinned granite gneiss	0.0	0.0	0.0	0.0
		Perthite granite gneiss	0.0	0.0	0.0	0.0
		Micro. granite gneiss	0.0	0.0	0.0	0.0
		Illite replacement in granite	0.0	0.0	0.0	0.0
		Illite replacement in granite gneiss	0.0	0.0	0.0	0.0
MICA IN ROCK FRAGMENT	Muscovite	Granite	3.0	0.8	1.0	1.6
		Granite gneiss	1.0	0.3	0.0	0.4
		Quartzite	2.0	1.0	0.0	1.0
		Schistose quartz	3.0	1.0	2.0	2.0
		Schist	5.0	5.0	3.0	4.3
	Biotite	Granite	0.0	0.0	0.0	0.0
		Granite gneiss	0.0	0.0	0.0	0.0
		Quartzite	0.0	0.0	0.0	0.0
		Schistose quartz	0.0	2.0	0.0	0.7
		Schist	1.0	2.0	1.0	1.3
		FRAMWORK TOTAL	**78.0**	**68.0**	**82.0**	**76.0**

APPENDIX C1, CONTINUED

	LOCATION:	Bernardston Rd.			
	FIGURE ID NO.:	13	14	15	-
	SAMPLE:	4.29-1	4.29-2	4.29-4	MEAN
	COUNT TYPE:	WR	WR	WR	WR
	N:	100	100	100	-
ACCESSORIES, POROSITY, MATRIX					
ACC.	Muscovite single grain	2.0	4.0	2.0	2.7
	Biotite single grain	10.0	14.0	8.0	10.7
	Chlorite replacement single grain	1.0	0.0	1.0	0.7
	Garnet	0.0	0.0	0.0	0.0
Hematite-stained matrix		1.0	3.0	0.0	1.0
Porosity		0.0	1.0	0.0	0.3
ACC., POROSITY, MATRIX TOTAL		**14.0**	**22.0**	**11.0**	**15.3**
CEMENTS					
HEM.	Rim	1.0	0.0	1.0	0.7
	Cement	2.0	4.0	1.0	2.3
ALB.	Interstitial	2.0	1.0	1.0	1.3
	Overgrowth	0.0	0.0	0.0	0.0
Illite		0.0	0.0	0.0	0.0
Kaolinite		0.0	0.0	0.0	0.0
Quartz overgrowth		0.0	0.0	1.0	0.3
CO3-	Calcite	0.0	1.0	1.0	0.7
	Fe-calcite	1.0	3.0	0.0	1.3
	Dolomite	2.0	0.0	0.0	0.7
	Fe-dolomite	0.0	1.0	2.0	1.0
CEMENT TOTAL		**8.0**	**10.0**	**8.0**	**8.7**
THIN SECTION TOTAL		**100.0**	**100.0**	**100.0**	**100.0**

APPENDIX C1, CONTINUED

		LOCATION:	Bernardston Rd.			
		FIGURE ID NO.:	13	14	15	-
		SAMPLE:	4.29-1	4.29-2	4.29-4	MEAN
		COUNT TYPE:	MS	MS	MS	MS
		N:	300	300	300	-
FRAMEWORK GRAINS						
QUARTZ		Unit monocrystalline	22.7	20.3	18.7	20.6
		Vein monocrystalline	7.3	8.3	6.7	7.4
		Annealed polycrystalline	8.7	13.3	5.0	9.0
		Vein polycrystalline	1.7	1.3	3.7	2.2
FELDSPAR	Plag.	Untwinned single grain	10.0	4.7	7.0	7.2
		Twinned single grain	11.3	12.0	10.0	11.1
		Albitized single grain	0.3	0.3	1.3	0.7
	Kspar	Untwinned single grain	1.0	0.0	2.0	1.0
		Perthite single grain	0.3	0.0	1.6	0.6
		Microcline single grain	0.0	0.0	1.4	0.5
		Illite replacement of feldspar	0.0	0.0	0.0	0.0
QUARTZ IN ROCK FRAGMENT		Granite	4.0	2.0	2.0	2.7
		Granite gneiss	1.0	4.0	3.0	2.7
		Schistose quartz	4.0	0.0	1.7	1.9
		Groundmass in schistose quartz	2.0	0.7	4.0	2.2
		Schist	0.0	0.7	1.0	0.6
		Groundmass in schist	0.0	2.3	0.0	0.8
		Quartzite	15.7	8.0	16.3	13.3
		Groundmass in quartzite	0.0	4.0	0.0	1.3
FELDSPAR IN ROCK FRAGMENT	Plag.	Untwinned granite	1.0	2.3	2.7	2.0
		Twinned granite	2.0	4.0	2.0	2.7
		Untwinned granite gneiss	1.0	1.0	1.0	1.0
		Twinned granite gneiss	1.3	2.0	1.0	1.4
	Kspar	Untwinned granite	0.3	0.0	0.4	0.2
		Perthite granite	0.0	0.0	0.0	0.0
		Micro. granite	0.0	0.0	0.2	0.1
		Untwinned granite gneiss	0.0	0.0	0.0	0.0
		Perthite granite gneiss	0.0	0.0	0.0	0.0
		Micro. granite gneiss	0.0	0.0	0.0	0.0
		Illite replacement in granite	0.0	0.0	0.0	0.0
		Illite replacement in granite gneiss	0.0	0.0	0.0	0.0
MICA IN ROCK FRAGMENT	Muscovite	Granite	0.0	0.0	0.0	0.0
		Granite gneiss	0.3	0.3	0.0	0.2
		Quartzite	0.7	0.3	0.0	0.3
		Schistose quartz	1.3	0.7	0.0	0.7
		Schist	2.0	2.7	2.3	2.3
	Biotite	Granite	0.0	0.0	0.0	0.0
		Granite gneiss	0.0	0.0	0.3	0.1
		Quartzite	0.0	0.0	0.0	0.0
		Schistose quartz	0.0	0.0	0.0	0.0
		Schist	0.0	0.0	0.3	0.1
		FRAMWORK TOTAL	**97.2**	**95.3**	**95.7**	**96.1**

APPENDIX C1, CONTINUED

	LOCATION:	Bernardston Rd.			
	FIGURE ID NO.:	13	14	15	-
	SAMPLE:	4.29-1	4.29-2	4.29-4	MEAN
	COUNT TYPE:	MS	MS	MS	MS
	N:	300	300	300	-
ACCESSORIES, POROSITY, MATRIX					
ACC.	Muscovite single grain	2.3	4.0	2.0	2.8
	Biotite single grain	0.3	0.0	1.0	0.4
	Chlorite replacement single grain	0.3	0.7	1.3	0.8
	Garnet	-	-	-	-
Hematite-stained matrix		-	-	-	-
Porosity		-	-	-	-
	ACC., POROSITY, MATRIX TOTAL	**2.9**	**4.7**	**4.3**	**4.0**
CEMENTS					
HEM.	Rim	-	-	-	-
	Cement	-	-	-	-
ALB.	Interstitial	-	-	-	-
	Overgrowth	-	-	-	-
Illite		-	-	-	-
Kaolinite		-	-	-	-
Quartz overgrowth		-	-	-	-
CO3-	Calcite	-	-	-	-
	Fe-calcite	-	-	-	-
	Dolomite	-	-	-	-
	Fe-dolomite	-	-	-	-
	CEMENT TOTAL	**-**	**-**	**-**	**-**
	THIN SECTION TOTAL	**100.0**	**100.0**	**100.0**	**100.0**

APPENDIX C1, CONTINUED

		LOCATION:	Cheapside St.			
		FIGURE ID NO.:	16	17	18	-
		SAMPLE:	CS-4	CS-6	01-CP-H1	MEAN
		COUNT TYPE:	WR	WR	WR	WR
		N:	100	100	100	-
FRAMEWORK GRAINS						
QUARTZ		Unit monocrystalline	22.0	28.0	24.0	24.7
		Vein monocrystalline	3.0	1.0	2.0	2.0
		Annealed polycrystalline	5.0	2.0	4.0	3.7
		Vein polycrystalline	2.0	1.0	1.0	1.3
FELDSPAR	Plag.	Untwinned single grain	4.0	1.0	6.0	3.7
		Twinned single grain	8.0	2.0	5.0	5.0
		Albitized single grain	2.0	2.0	1.0	1.7
	Kspar	Untwinned single grain	1.0	1.0	1.0	1.0
		Perthite single grain	0.0	1.0	0.0	0.3
		Microcline single grain	1.0	0.0	0.0	0.3
		Illite replacement of feldspar	0.0	0.0	0.0	0.0
QUARTZ IN ROCK FRAGMENT		Granite	3.0	0.0	3.0	2.0
		Granite gneiss	1.0	0.0	4.0	1.7
		Schistose quartz	1.0	0.0	0.0	0.3
		Groundmass in schistose quartz	0.0	0.0	1.0	0.3
		Schist	0.0	0.3	0.0	0.1
		Groundmass in schist	1.0	1.7	0.0	0.9
		Quartzite	2.0	5.0	5.0	4.0
		Groundmass in quartzite	0.0	3.0	0.0	1.0
FELDSPAR IN ROCK FRAGMENT	Plag.	Untwinned granite	2.0	1.0	1.0	1.3
		Twinned granite	3.0	3.0	1.0	2.3
		Untwinned granite gneiss	0.0	0.0	2.0	0.7
		Twinned granite gneiss	0.0	0.0	0.0	0.0
	Kspar	Untwinned granite	4.0	1.0	2.0	2.3
		Perthite granite	1.0	0.0	0.0	0.3
		Micro. granite	0.0	0.0	0.0	0.0
		Untwinned granite gneiss	0.0	0.0	0.0	0.0
		Perthite granite gneiss	0.0	0.0	0.0	0.0
		Micro. granite gneiss	0.0	0.0	0.0	0.0
		Illite replacement in granite	0.0	0.0	0.0	0.0
		Illite replacement in granite gneiss	0.0	0.0	0.0	0.0
MICA IN ROCK FRAGMENT	Muscovite	Granite	1.0	0.0	0.0	0.3
		Granite gneiss	0.0	0.0	1.0	0.3
		Quartzite	0.0	0.0	0.0	0.0
		Schistose quartz	1.0	0.0	0.0	0.3
		Schist	3.0	2.0	2.0	2.3
	Biotite	Granite	0.8	0.0	0.0	0.3
		Granite gneiss	0.3	0.0	0.0	0.1
		Quartzite	0.0	0.0	0.0	0.0
		Schistose quartz	0.0	0.0	0.0	0.0
		Schist	0.0	0.0	0.0	0.0
		FRAMWORK TOTAL	**72.0**	**56.0**	**66.0**	**64.7**

APPENDIX C1, CONTINUED

	LOCATION:	Cheapside St.			
	FIGURE ID NO.:	16	17	18	-
	SAMPLE:	CS-4	CS-6	01-CP-H1	MEAN
	COUNT TYPE:	WR	WR	WR	WR
	N:	100	100	100	-
ACCESSORIES, POROSITY, MATRIX					
ACC.	Muscovite single grain	3.0	8.0	6.0	5.7
	Biotite single grain	0.0	2.0	0.0	0.7
	Chlorite replacement single grain	0.0	0.0	0.0	0.0
	Garnet	0.0	0.0	0.0	0.0
Hematite-stained matrix		4.0	22.0	15.0	13.7
Porosity		5.0	1.0	2.0	2.7
	ACC., POROSITY, MATRIX TOTAL	**12.0**	**33.0**	**23.0**	**22.7**
CEMENTS					
HEM.	Rim	3.0	0.0	1.0	1.3
	Cement	4.0	10.0	8.0	7.3
ALB.	Interstitial	0.0	1.0	1.0	0.7
	Overgrowth	6.0	0.0	0.0	2.0
Illite		0.0	0.0	0.0	0.0
Kaolinite		0.0	0.0	0.0	0.0
Quartz overgrowth		3.0	0.0	1.0	1.3
CO3-	Calcite	0.0	0.0	0.0	0.0
	Fe-calcite	0.0	0.0	0.0	0.0
	Dolomite	0.0	0.0	0.0	0.0
	Fe-dolomite	0.0	0.0	0.0	0.0
	CEMENT TOTAL	**16.0**	**11.0**	**11.0**	**12.7**
	THIN SECTION TOTAL	**100.0**	**100.0**	**100.0**	**100.0**

APPENDIX C1, CONTINUED

		LOCATION:	Cheapside St.			
		FIGURE ID NO.:	16	17	18	-
		SAMPLE:	CS-4	CS-6	01-CP-H1	MEAN
		COUNT TYPE:	MS	MS	MS	MS
		N:	300	300	300	-
FRAMEWORK GRAINS						
QUARTZ		Unit monocrystalline	32.3	28.3	23.3	28.0
		Vein monocrystalline	3.0	3.7	4.0	3.6
		Annealed polycrystalline	5.0	4.0	7.0	5.3
		Vein polycrystalline	0.3	1.0	1.0	0.8
FELDSPAR	Plag.	Untwinned single grain	5.7	3.0	5.7	4.8
		Twinned single grain	5.0	9.0	10.0	8.0
		Albitized single grain	0.3	0.7	0.7	0.6
	Kspar	Untwinned single grain	4.0	2.7	1.3	2.7
		Perthite single grain	2.3	1.0	1.0	1.4
		Microcline single grain	0.0	0.0	0.4	0.1
		Illite replacement of feldspar	0.0	0.0	0.0	0.0
QUARTZ IN ROCK FRAGMENT		Granite	6.3	5.7	6.0	6.0
		Granite gneiss	2.0	6.0	6.3	4.8
		Schistose quartz	0.0	0.0	0.3	0.1
		Groundmass in schistose quartz	0.0	0.0	0.0	0.0
		Schist	0.0	0.0	1.0	0.3
		Groundmass in schist	3.7	1.0	1.0	1.9
		Quartzite	12.0	12.0	15.0	13.0
		Groundmass in quartzite	0.0	3.3	2.7	2.0
FELDSPAR IN ROCK FRAGMENT	Plag.	Untwinned granite	1.0	2.0	2.0	1.7
		Twinned granite	2.0	2.0	1.7	1.9
		Untwinned granite gneiss	0.0	1.0	1.0	0.7
		Twinned granite gneiss	1.7	1.7	0.0	1.1
	Kspar	Untwinned granite	3.0	2.0	0.8	1.9
		Perthite granite	0.9	0.3	0.0	0.4
		Micro. granite	0.1	1.7	0.0	0.6
		Untwinned granite gneiss	0.2	0.0	0.0	0.1
		Perthite granite gneiss	0.0	0.0	0.0	0.0
		Micro. granite gneiss	0.5	0.3	0.2	0.3
		Illite replacement in granite	0.0	0.0	0.0	0.0
		Illite replacement in granite gneiss	0.0	0.0	0.0	0.0
MICA IN ROCK FRAGMENT	Muscovite	Granite	0.0	0.0	0.7	0.2
		Granite gneiss	0.0	0.0	0.3	0.1
		Quartzite	0.0	0.3	1.0	0.4
		Schistose quartz	0.3	0.0	0.0	0.1
		Schist	3.0	3.3	3.3	3.2
	Biotite	Granite	0.0	0.0	0.0	0.0
		Granite gneiss	0.0	0.0	0.0	0.0
		Quartzite	0.0	0.0	0.0	0.0
		Schistose quartz	0.0	0.0	0.0	0.0
		Schist	0.0	0.7	0.7	0.5
		FRAMWORK TOTAL	**94.7**	**96.7**	**98.7**	**96.7**

APPENDIX C1, CONTINUED

	LOCATION:	Cheapside St.			
	FIGURE ID NO.:	16	17	18	-
	SAMPLE:	CS-4	CS-6	01-CP-H1	MEAN
	COUNT TYPE:	MS	MS	MS	MS
	N:	300	300	300	-
ACCESSORIES, POROSITY, MATRIX					
ACC.	Muscovite single grain	5.3	3.0	0.7	3.0
	Biotite single grain	0.0	0.3	0.7	0.3
	Chlorite replacement single grain	0.0	0.0	0.0	0.0
	Garnet	-	-	-	-
Hematite-stained matrix		-	-	-	-
Porosity		-	-	-	-
	ACC., POROSITY, MATRIX TOTAL	**5.3**	**3.3**	**1.3**	**3.3**
CEMENTS					
HEM.	Rim	-	-	-	-
	Cement	-	-	-	-
ALB.	Interstitial	-	-	-	-
	Overgrowth	-	-	-	-
Illite		-	-	-	-
Kaolinite		-	-	-	-
Quartz overgrowth		-	-	-	-
CO3-	Calcite	-	-	-	-
	Fe-calcite	-	-	-	-
	Dolomite	-	-	-	-
	Fe-dolomite	-	-	-	-
	CEMENT TOTAL	**-**	**-**	**-**	**-**
	THIN SECTION TOTAL	**100.0**	**100.0**	**100.0**	**100.0**

APPENDIX C1, CONTINUED

		LOCATION:	North Parkway St.			
		FIGURE ID NO.:	19	20	21	-
		SAMPLE:	9.11-1	10.5-3	RS75-113	MEAN
		COUNT TYPE:	WR	WR	WR	WR
		N:	100	100	100	-
FRAMEWORK GRAINS						
QUARTZ		Unit monocrystalline	37.0	28.0	35.0	33.3
		Vein monocrystalline	1.0	0.0	5.0	2.0
		Annealed polycrystalline	14.0	4.0	6.0	8.0
		Vein polycrystalline	1.0	2.0	0.0	1.0
FELDSPAR	Plag.	Untwinned single grain	0.0	1.5	2.0	1.2
		Twinned single grain	4.0	5.5	10.0	6.5
		Albitized single grain	5.0	8.0	2.0	5.0
	Kspar	Untwinned single grain	0.0	0.0	0.0	0.0
		Perthite single grain	0.0	0.0	0.0	0.0
		Microcline single grain	0.0	12.0	7.0	6.3
		Illite replacement of feldspar	0.0	0.0	0.0	0.0
QUARTZ IN ROCK FRAGMENT		Granite	0.0	2.0	1.0	1.0
		Granite gneiss	4.0	1.0	1.0	2.0
		Schistose quartz	0.0	0.0	0.0	0.0
		Groundmass in schistose quartz	0.0	0.0	0.0	0.0
		Schist	1.0	0.3	2.0	1.1
		Groundmass in schist	0.0	0.7	0.0	0.2
		Quartzite	4.0	1.0	1.0	2.0
		Groundmass in quartzite	1.0	1.0	0.0	0.7
FELDSPAR IN ROCK FRAGMENT	Plag.	Untwinned granite	1.0	1.0	1.0	1.0
		Twinned granite	2.0	1.0	1.0	1.3
		Untwinned granite gneiss	1.0	0.0	0.0	0.3
		Twinned granite gneiss	0.0	0.0	1.0	0.3
	Kspar	Untwinned granite	0.0	0.0	0.0	0.0
		Perthite granite	0.0	0.0	0.0	0.0
		Micro. granite	6.0	0.0	0.0	2.0
		Untwinned granite gneiss	0.0	0.0	0.0	0.0
		Perthite granite gneiss	0.0	0.0	0.0	0.0
		Micro. granite gneiss	3.0	0.0	0.0	1.0
		Illite replacement in granite	0.0	0.0	0.0	0.0
		Illite replacement in granite gneiss	0.0	0.0	0.0	0.0
MICA IN ROCK FRAGMENT	Muscovite	Granite	0.0	1.0	0.0	0.3
		Granite gneiss	1.0	0.0	0.0	0.3
		Quartzite	2.0	1.0	0.0	1.0
		Schistose quartz	1.0	0.0	1.0	0.7
		Schist	2.0	3.0	1.0	2.0
	Biotite	Granite	0.0	0.0	0.0	0.0
		Granite gneiss	0.0	0.0	0.0	0.0
		Quartzite	0.0	0.0	0.0	0.0
		Schistose quartz	0.0	0.0	0.0	0.0
		Schist	0.0	0.0	0.0	0.0
		FRAMWORK TOTAL	**92.0**	**74.0**	**77.0**	**81.0**

APPENDIX C1, CONTINUED

	LOCATION:	North Parkway St.			
	FIGURE ID NO.:	19	20	21	-
	SAMPLE:	9.11-1	10.5-3	RS75-113	MEAN
	COUNT TYPE:	WR	WR	WR	WR
	N:	100	100	100	-
ACCESSORIES, POROSITY, MATRIX					
ACC.	Muscovite single grain	1.0	2.0	5.0	2.7
	Biotite single grain	0.0	3.0	3.0	2.0
	Chlorite replacement single grain	0.0	0.0	0.0	0.0
	Garnet	0.0	0.0	0.0	0.0
Hematite-stained matrix		0.0	4.0	0.0	1.3
Porosity		0.0	1.0	1.0	0.7
	ACC., POROSITY, MATRIX TOTAL	**1.0**	**10.0**	**9.0**	**6.7**
CEMENTS					
HEM.	Rim	0.0	0.0	0.0	0.0
	Cement	0.0	8.0	1.0	3.0
ALB.	Interstitial	0.0	1.0	0.0	0.3
	Overgrowth	2.0	3.0	5.0	3.3
Illite		0.0	0.0	0.0	0.0
Kaolinite		0.0	0.0	0.0	0.0
Quartz overgrowth		5.0	4.0	5.0	4.7
CO3-	Calcite	0.0	0.0	0.0	0.0
	Fe-calcite	0.0	0.0	1.0	0.3
	Dolomite	0.0	0.0	0.0	0.0
	Fe-dolomite	0.0	0.0	2.0	0.7
	CEMENT TOTAL	**7.0**	**16.0**	**14.0**	**12.3**
	THIN SECTION TOTAL	**100.0**	**100.0**	**100.0**	**100.0**

APPENDIX C1, CONTINUED

		LOCATION:	North Parkway St.			
		FIGURE ID NO.:	19	20	21	-
		SAMPLE:	9.11-1	10.5-3	RS75-113	MEAN
		COUNT TYPE:	MS	MS	MS	MS
		N:	300	300	300	-
FRAMEWORK GRAINS						
QUARTZ		Unit monocrystalline	16.0	20.3	17.7	18.0
		Vein monocrystalline	23.7	22.3	19.3	21.8
		Annealed polycrystalline	6.7	7.7	5.7	6.7
		Vein polycrystalline	5.3	3.7	6.7	5.2
FELDSPAR	Plag.	Untwinned single grain	0.0	1.0	2.0	1.0
		Twinned single grain	6.0	8.0	5.0	6.3
		Albitized single grain	8.0	7.3	8.7	8.0
	Kspar	Untwinned single grain	5.0	3.7	5.0	4.6
		Perthite single grain	2.0	2.0	1.3	1.8
		Microcline single grain	2.3	4.0	3.3	3.2
		Illite replacement of feldspar	0.0	0.0	0.0	0.0
QUARTZ IN ROCK FRAGMENT		Granite	1.3	2.3	2.0	1.9
		Granite gneiss	2.0	0.0	2.0	1.3
		Schistose quartz	1.0	0.7	0.3	0.7
		Groundmass in schistose quartz	2.3	2.0	3.0	2.4
		Schist	0.0	0.0	0.0	0.0
		Groundmass in schist	0.0	0.0	0.0	0.0
		Quartzite	2.7	1.3	1.0	1.7
		Groundmass in quartzite	0.0	0.0	1.0	0.3
FELDSPAR IN ROCK FRAGMENT	Plag.	Untwinned granite	2.0	2.0	1.3	1.8
		Twinned granite	1.0	3.3	3.0	2.4
		Untwinned granite gneiss	2.0	1.0	1.0	1.3
		Twinned granite gneiss	2.3	1.0	2.0	1.8
	Kspar	Untwinned granite	3.8	1.0	2.7	2.5
		Perthite granite	0.2	0.0	0.0	0.1
		Micro. granite	0.0	0.6	0.0	0.2
		Untwinned granite gneiss	1.0	0.8	2.0	1.3
		Perthite granite gneiss	0.0	0.0	0.0	0.0
		Micro. granite gneiss	0.0	0.3	0.7	0.3
		Illite replacement in granite	0.0	0.0	0.0	0.0
		Illite replacement in granite gneiss	0.0	0.0	0.0	0.0
MICA IN ROCK FRAGMENT	Muscovite	Granite	0.0	0.7	0.0	0.2
		Granite gneiss	0.0	0.0	0.0	0.0
		Quartzite	0.0	0.3	0.0	0.1
		Schistose quartz	1.0	0.0	1.3	0.8
		Schist	0.7	0.7	0.7	0.7
	Biotite	Granite	0.0	0.0	0.0	0.0
		Granite gneiss	0.0	0.0	0.0	0.0
		Quartzite	0.0	0.0	0.0	0.0
		Schistose quartz	0.0	0.0	0.0	0.0
		Schist	0.0	0.0	0.0	0.0
		FRAMWORK TOTAL	**96.0**	**98.0**	**98.7**	**97.6**

APPENDIX C1, CONTINUED

	LOCATION:	North Parkway St.			
	FIGURE ID NO.:	19	20	21	-
	SAMPLE:	9.11-1	10.5-3	RS75-113	MEAN
	COUNT TYPE:	MS	MS	MS	MS
	N:	300	300	300	-
ACCESSORIES, POROSITY, MATRIX					
ACC.	Muscovite single grain	4.0	1.3	0.7	2.0
	Biotite single grain	0.0	0.7	0.7	0.5
	Chlorite replacement single grain	0.0	0.0	0.0	0.0
	Garnet	-	-	-	-
Hematite-stained matrix		-	-	-	-
Porosity		-	-	-	-
	ACC., POROSITY, MATRIX TOTAL	**4.0**	**2.0**	**1.4**	**2.5**
CEMENTS					
HEM.	Rim	-	-	-	-
	Cement	-	-	-	-
ALB.	Interstitial	-	-	-	-
	Overgrowth	-	-	-	-
Illite		-	-	-	-
Kaolinite		-	-	-	-
Quartz overgrowth		-	-	-	-
CO3-	Calcite	-	-	-	-
	Fe-calcite	-	-	-	-
	Dolomite	-	-	-	-
	Fe-dolomite	-	-	-	-
	CEMENT TOTAL	**-**	**-**	**-**	**-**
	THIN SECTION TOTAL	**100.0**	**100.0**	**100.0**	**100.0**

APPENDIX C2: MODAL ANALYSES FOR PIEDMONT RIVER FACIES

		LOCATION:	Sugarloaf Mt. Rd.			
		FIGURE ID NO.:	1	2	3	-
		SAMPLE:	7.7-1	7.7-5	SF-SR2	MEAN
		COUNT TYPE:	WR	WR	WR	WR
		N:	100	100	100	-
FRAMEWORK GRAINS						
QUARTZ		Unit monocrystalline	23.0	19.0	25.0	22.3
		Vein monocrystalline	1.0	1.0	1.0	1.0
		Annealed polycrystalline	6.0	4.0	4.0	4.7
		Vein polycrystalline	5.0	1.0	2.0	2.7
FELDSPAR	Plag.	Untwinned single grain	1.0	3.0	3.0	2.3
		Twinned single grain	1.0	2.0	2.0	1.7
		Albitized single grain	1.0	3.0	3.0	2.3
	Kspar	Untwinned single grain	1.5	1.0	2.0	1.5
		Perthite single grain	0.5	0.0	1.0	0.5
		Microcline single grain	0.0	1.0	0.0	0.3
		Illite replacement of feldspar	0.0	0.0	0.0	0.0
QUARTZ IN ROCK FRAGMENT		Granite	1.0	2.0	2.0	1.7
		Granite gneiss	3.0	5.0	3.0	3.7
		Schistose quartz	0.3	0.3	0.3	0.3
		Groundmass in schistose quartz	0.7	1.7	0.7	1.0
		Schist	0.3	0.0	0.0	0.1
		Groundmass in schist	1.7	1.0	1.0	1.2
		Quartzite	4.0	8.0	2.0	4.7
		Groundmass in quartzite	2.0	2.0	2.0	2.0
FELDSPAR IN ROCK FRAGMENT	Plag.	Untwinned granite	1.0	0.5	0.0	0.5
		Twinned granite	1.0	0.0	0.0	0.3
		Untwinned granite gneiss	2.0	3.0	3.0	2.7
		Twinned granite gneiss	2.0	0.5	1.0	1.2
	Kspar	Untwinned granite	1.0	1.0	0.0	0.7
		Perthite granite	0.0	0.0	0.0	0.0
		Micro. granite	0.0	0.0	0.0	0.0
		Untwinned granite gneiss	1.0	2.5	1.0	1.5
		Perthite granite gneiss	1.0	0.5	1.0	0.8
		Micro. granite gneiss	0.0	0.0	3.0	1.0
		Illite replacement in granite	0.0	0.0	0.0	0.0
		Illite replacement in granite gneiss	0.0	0.0	0.0	0.0
MICA IN ROCK FRAGMENT	Muscovite	Granite	0.0	0.0	0.0	0.0
		Granite gneiss	0.0	1.0	1.0	0.7
		Quartzite	0.0	0.0	0.0	0.0
		Schistose quartz	2.0	1.0	2.0	1.7
		Schist	1.0	2.0	4.0	2.3
	Biotite	Granite	0.0	0.0	0.0	0.0
		Granite gneiss	0.0	0.0	0.0	0.0
		Quartzite	0.0	0.0	0.0	0.0
		Schistose quartz	0.0	0.0	0.0	0.0
		Schist	0.0	2.0	1.0	1.0
		FRAMWORK TOTAL	**65.0**	**69.0**	**71.0**	**68.3**

APPENDIX C2, CONTINUED

	LOCATION:	Sugarloaf Mt. Rd.			
	FIGURE ID NO.:	1	2	3	-
	SAMPLE:	7.7-1	7.7-5	SF-SR2	MEAN
	COUNT TYPE:	WR	WR	WR	WR
	N:	100	100	100	-
ACCESSORIES, POROSITY, MATRIX					
ACC.	Muscovite single grain	3.0	2.0	3.0	2.7
	Biotite single grain	1.0	1.0	1.0	1.0
	Chlorite replacement single grain	0.0	0.0	0.0	0.0
	Garnet	0.0	0.0	0.0	0.0
Hematite-stained matrix		5.0	1.0	7.0	4.3
Porosity		4.0	2.0	0.0	2.0
ACC., POROSITY, MATRIX TOTAL		**13.0**	**6.0**	**11.0**	**10.0**
CEMENTS					
HEM.	Rim	4.0	5.0	3.0	4.0
	Cement	2.0	3.0	6.0	3.7
ALB.	Interstitial	10.0	12.0	7.0	9.7
	Overgrowth	1.0	2.0	1.0	1.3
Illite		0.0	0.0	0.0	0.0
Kaolinite		0.0	0.0	0.0	0.0
Quartz overgrowth		2.0	1.0	1.0	1.3
CO3-	Calcite	0.0	0.0	0.0	0.0
	Fe-calcite	1.0	0.0	0.0	0.3
	Dolomite	1.0	2.0	0.0	1.0
	Fe-dolomite	0.0	0.0	0.0	0.0
CEMENT TOTAL		**22.0**	**25.0**	**18.0**	**21.7**
THIN SECTION TOTAL		**100.0**	**100.0**	**100.0**	**100.0**

APPENDIX C2, CONTINUED

		LOCATION:	Sugarloaf Mt. Rd.			
		FIGURE ID NO.:	1	2	3	-
		SAMPLE:	7.7-1	7.7-5	SF-SR2	MEAN
		COUNT TYPE:	MS	MS	MS	MS
		N:	300	300	300	-
FRAMEWORK GRAINS						
QUARTZ		Unit monocrystalline	32.7	34.3	30.0	32.3
		Vein monocrystalline	9.7	4.3	9.0	7.7
		Annealed polycrystalline	7.3	9.3	10.0	8.9
		Vein polycrystalline	1.0	0.0	0.7	0.6
FELDSPAR	Plag.	Untwinned single grain	6.3	8.3	4.3	6.3
		Twinned single grain	2.0	4.0	3.0	3.0
		Albitized single grain	1.0	0.7	0.3	0.7
	Kspar	Untwinned single grain	2.0	3.2	2.7	2.6
		Perthite single grain	1.9	0.0	2.0	1.3
		Microcline single grain	1.1	0.5	0.3	0.6
		Illite replacement of feldspar	0.0	0.0	0.0	0.0
QUARTZ IN ROCK FRAGMENT		Granite	0.0	0.0	0.0	0.0
		Granite gneiss	6.0	5.3	5.7	5.7
		Schistose quartz	2.3	3.3	2.0	2.5
		Groundmass in schistose quartz	2.0	2.0	4.0	2.7
		Schist	0.7	0.0	0.3	0.3
		Groundmass in schist	1.0	1.7	1.7	1.5
		Quartzite	12.0	10.0	12.0	11.3
		Groundmass in quartzite	1.3	1.3	2.3	1.6
FELDSPAR IN ROCK FRAGMENT	Plag.	Untwinned granite	0.0	1.0	0.7	0.6
		Twinned granite	0.0	0.0	0.0	0.0
		Untwinned granite gneiss	0.7	3.3	2.0	2.0
		Twinned granite gneiss	0.0	2.0	1.0	1.0
	Kspar	Untwinned granite	0.0	0.0	0.0	0.0
		Perthite granite	0.0	0.0	0.0	0.0
		Micro. granite	0.0	0.0	0.0	0.0
		Untwinned granite gneiss	1.0	1.1	0.0	0.7
		Perthite granite gneiss	0.3	0.5	0.7	0.5
		Micro. granite gneiss	0.7	0.8	0.3	0.6
		Illite replacement in granite	0.0	0.0	0.0	0.0
		Illite replacement in granite gneiss	0.0	0.0	0.0	0.0
MICA IN ROCK FRAGMENT	Muscovite	Granite	0.0	0.0	0.0	0.0
		Granite gneiss	0.3	0.7	0.3	0.4
		Quartzite	0.0	0.0	0.0	0.0
		Schistose quartz	2.0	0.3	0.7	1.0
		Schist	1.7	0.0	1.3	1.0
	Biotite	Granite	0.0	0.0	0.0	0.0
		Granite gneiss	0.0	0.0	0.0	0.0
		Quartzite	0.0	0.0	0.0	0.0
		Schistose quartz	0.3	0.0	0.0	0.1
		Schist	0.0	1.0	0.3	0.4
		FRAMWORK TOTAL	**97.3**	**98.0**	**97.6**	**97.6**

APPENDIX C2, CONTINUED

	LOCATION:	Sugarloaf Mt. Rd.			
	FIGURE ID NO.:	1	2	3	-
	SAMPLE:	7.7-1	7.7-5	SF-SR2	MEAN
	COUNT TYPE:	MS	MS	MS	MS
	N:	300	300	300	-
ACCESSORIES, POROSITY, MATRIX					
ACC.	Muscovite single grain	0.7	0.7	0.3	0.5
	Biotite single grain	0.7	0.7	1.0	0.8
	Chlorite replacement single grain	1.3	0.7	1.0	1.0
	Garnet	-	-	-	-
Hematite-stained matrix		-	-	-	-
Porosity		-	-	-	-
	ACC., POROSITY, MATRIX TOTAL	**2.7**	**2.0**	**2.3**	**2.3**
CEMENTS					
HEM.	Rim	-	-	-	-
	Cement	-	-	-	-
ALB.	Interstitial	-	-	-	-
	Overgrowth	-	-	-	-
Illite		-	-	-	-
Kaolinite		-	-	-	-
Quartz overgrowth		-	-	-	-
CO3-	Calcite	-	-	-	-
	Fe-calcite	-	-	-	-
	Dolomite	-	-	-	-
	Fe-dolomite	-	-	-	-
	CEMENT TOTAL	**-**	**-**	**-**	**-**
	THIN SECTION TOTAL	**100.0**	**100.0**	**100.0**	**100.0**

APPENDIX C2, CONTINUED

		LOCATION:	River Rd.			
		FIGURE ID NO.:	4	5	6	-
		SAMPLE:	9.21-2	9.21-5	9.21-6	MEAN
		COUNT TYPE:	WR	WR	WR	WR
		N:	100	100	100	-
FRAMEWORK GRAINS						
QUARTZ		Unit monocrystalline	22.0	21.0	25.0	22.7
		Vein monocrystalline	2.0	2.0	5.0	3.0
		Annealed polycrystalline	5.0	6.0	7.0	6.0
		Vein polycrystalline	1.0	0.0	3.0	1.3
FELDSPAR	Plag.	Untwinned single grain	6.0	2.0	2.0	3.3
		Twinned single grain	2.0	2.0	1.0	1.7
		Albitized single grain	2.0	4.0	5.0	3.7
	Kspar	Untwinned single grain	2.0	0.5	2.0	1.5
		Perthite single grain	1.0	0.5	2.0	1.2
		Microcline single grain	0.0	1.0	0.0	0.3
		Illite replacement of feldspar	0.0	0.0	0.0	0.0
QUARTZ IN ROCK FRAGMENT		Granite	2.0	2.0	0.0	1.3
		Granite gneiss	4.0	8.0	2.0	4.7
		Schistose quartz	0.0	0.0	1.3	0.4
		Groundmass in schistose quartz	1.0	0.0	0.7	0.6
		Schist	0.0	0.0	1.0	0.3
		Groundmass in schist	1.0	1.0	0.0	0.7
		Quartzite	2.0	2.0	7.0	3.7
		Groundmass in quartzite	3.0	1.0	0.0	1.3
FELDSPAR IN ROCK FRAGMENT	Plag.	Untwinned granite	1.0	1.0	1.0	1.0
		Twinned granite	0.0	0.0	0.0	0.0
		Untwinned granite gneiss	1.0	3.0	4.0	2.7
		Twinned granite gneiss	2.0	1.0	3.0	2.0
	Kspar	Untwinned granite	2.0	0.0	0.0	0.7
		Perthite granite	0.0	0.0	0.0	0.0
		Micro. granite	0.0	1.0	1.0	0.7
		Untwinned granite gneiss	2.0	2.7	4.0	2.9
		Perthite granite gneiss	0.0	0.3	1.0	0.4
		Micro. granite gneiss	0.0	0.0	0.0	0.0
		Illite replacement in granite	0.0	0.0	0.0	0.0
		Illite replacement in granite gneiss	0.0	0.0	0.0	0.0
MICA IN ROCK FRAGMENT	Muscovite	Granite	0.0	1.0	0.0	0.3
		Granite gneiss	1.0	1.0	1.0	1.0
		Quartzite	0.0	1.0	0.0	0.3
		Schistose quartz	1.0	2.0	2.0	1.7
		Schist	4.0	4.0	4.0	4.0
	Biotite	Granite	0.0	0.0	0.0	0.0
		Granite gneiss	1.0	0.0	0.0	0.3
		Quartzite	0.0	0.0	0.0	0.0
		Schistose quartz	0.0	0.0	1.0	0.3
		Schist	0.0	0.0	1.0	0.3
		FRAMWORK TOTAL	**71.0**	**71.0**	**87.0**	**76.3**

APPENDIX C2, CONTINUED

	LOCATION:	River Rd.			
	FIGURE ID NO.:	4	5	6	-
	SAMPLE:	9.21-2	9.21-5	9.21-6	MEAN
	COUNT TYPE:	WR	WR	WR	WR
	N:	100	100	100	-
ACCESSORIES, POROSITY, MATRIX					
ACC.	Muscovite single grain	8.0	3.0	3.0	4.7
	Biotite single grain	2.0	5.0	2.0	3.0
	Chlorite replacement single grain	0.0	0.0	0.0	0.0
	Garnet	0.0	0.0	0.0	0.0
Hematite-stained matrix		7.0	0.0	1.0	2.7
Porosity		0.0	2.0	0.0	0.7
	ACC., POROSITY, MATRIX TOTAL	**17.0**	**10.0**	**6.0**	**11.0**
CEMENTS					
HEM.	Rim	2.0	2.0	2.0	2.0
	Cement	8.0	2.0	2.0	4.0
ALB.	Interstitial	2.0	4.0	1.0	2.3
	Overgrowth	0.0	10.0	2.0	4.0
Illite		0.0	0.0	0.0	0.0
Kaolinite		0.0	0.0	0.0	0.0
Quartz overgrowth		0.0	1.0	0.0	0.3
CO3-	Calcite	0.0	0.0	0.0	0.0
	Fe-calcite	0.0	0.0	0.0	0.0
	Dolomite	0.0	0.0	0.0	0.0
	Fe-dolomite	0.0	0.0	0.0	0.0
	CEMENT TOTAL	**12.0**	**19.0**	**7.0**	**12.7**
	THIN SECTION TOTAL	**100.0**	**100.0**	**100.0**	**100.0**

APPENDIX C2, CONTINUED

		LOCATION:	River Rd.			
		FIGURE ID NO.:	4	5	6	-
		SAMPLE:	9.21-2	9.21-5	9.21-6	MEAN
		COUNT TYPE:	MS	MS	MS	MS
		N:	300	300	300	-
FRAMEWORK GRAINS						
QUARTZ		Unit monocrystalline	28.3	29.3	32.7	30.1
		Vein monocrystalline	12.3	12.0	14.3	12.9
		Annealed polycrystalline	9.3	7.3	6.0	7.5
		Vein polycrystalline	2.7	2.3	3.0	2.7
FELDSPAR	Plag.	Untwinned single grain	4.0	2.0	2.0	2.7
		Twinned single grain	2.0	2.2	3.0	2.4
		Albitized single grain	1.3	1.0	0.0	0.8
	Kspar	Untwinned single grain	2.0	2.7	3.3	2.7
		Perthite single grain	1.7	3.0	2.0	2.2
		Microcline single grain	0.0	0.3	0.0	0.1
		Illite replacement of feldspar	0.0	0.0	0.0	0.0
QUARTZ IN ROCK FRAGMENT		Granite	0.0	0.3	0.3	0.2
		Granite gneiss	6.0	5.0	5.0	5.3
		Schistose quartz	1.7	2.0	2.7	2.1
		Groundmass in schistose quartz	2.0	2.0	1.0	1.7
		Schist	0.3	0.3	0.3	0.3
		Groundmass in schist	1.7	1.0	1.0	1.2
		Quartzite	11.7	8.7	7.3	9.2
		Groundmass in quartzite	0.0	1.0	0.0	0.3
FELDSPAR IN ROCK FRAGMENT	Plag.	Untwinned granite	0.0	1.0	0.0	0.3
		Twinned granite	0.0	0.3	0.0	0.1
		Untwinned granite gneiss	1.0	2.0	2.7	1.9
		Twinned granite gneiss	1.7	1.0	2.0	1.6
	Kspar	Untwinned granite	0.0	0.0	0.0	0.0
		Perthite granite	0.0	0.0	0.0	0.0
		Micro. granite	0.0	0.0	0.0	0.0
		Untwinned granite gneiss	2.0	2.3	2.0	2.1
		Perthite granite gneiss	0.7	1.0	0.3	0.7
		Micro. granite gneiss	0.3	0.3	0.0	0.2
		Illite replacement in granite	0.0	0.0	0.0	0.0
		Illite replacement in granite gneiss	0.0	0.0	0.0	0.0
MICA IN ROCK FRAGMENT	Muscovite	Granite	0.0	0.0	0.3	0.1
		Granite gneiss	0.7	1.0	0.3	0.7
		Quartzite	0.0	0.0	0.0	0.0
		Schistose quartz	0.3	0.7	1.7	0.9
		Schist	2.3	1.7	0.7	1.6
	Biotite	Granite	0.0	0.0	0.0	0.0
		Granite gneiss	0.0	0.0	0.0	0.0
		Quartzite	0.0	0.0	0.0	0.0
		Schistose quartz	0.3	0.3	0.0	0.2
		Schist	0.0	0.3	0.3	0.2
		FRAMWORK TOTAL	**96.3**	**95.3**	**94.3**	**95.3**

APPENDIX C2, CONTINUED

	LOCATION:	River Rd.			
	FIGURE ID NO.:	4	5	6	-
	SAMPLE:	9.21-2	9.21-5	9.21-6	MEAN
	COUNT TYPE:	MS	MS	MS	MS
	N:	300	300	300	-
ACCESSORIES, POROSITY, MATRIX					
ACC.	Muscovite single grain	1.3	2.7	2.3	2.1
	Biotite single grain	2.3	1.7	2.7	2.2
	Chlorite replacement single grain	0.0	0.3	0.7	0.3
	Garnet	-	-	-	-
Hematite-stained matrix		-	-	-	-
Porosity		-	-	-	-
	ACC., POROSITY, MATRIX TOTAL	**3.7**	**4.7**	**5.7**	**4.7**
CEMENTS					
HEM.	Rim	-	-	-	-
	Cement	-	-	-	-
ALB.	Interstitial	-	-	-	-
	Overgrowth	-	-	-	-
Illite		-	-	-	-
Kaolinite		-	-	-	-
Quartz overgrowth		-	-	-	-
CO3-	Calcite	-	-	-	-
	Fe-calcite	-	-	-	-
	Dolomite	-	-	-	-
	Fe-dolomite	-	-	-	-
	CEMENT TOTAL	**-**	**-**	**-**	**-**
	THIN SECTION TOTAL	**100.0**	**100.0**	**100.0**	**100.0**

APPENDIX C2, CONTINUED

		LOCATION:	French's Ferry St.			
		FIGURE ID NO.:	7	8	9	-
		SAMPLE:	10.11-1	10.11-2	10.11-3	MEAN
		COUNT TYPE:	WR	WR	WR	WR
		N:	100	100	100	-
FRAMEWORK GRAINS						
QUARTZ		Unit monocrystalline	14.0	10.0	20.0	14.7
		Vein monocrystalline	2.0	7.0	2.0	3.7
		Annealed polycrystalline	3.0	5.0	5.0	4.3
		Vein polycrystalline	2.0	3.0	7.0	4.0
FELDSPAR	Plag.	Untwinned single grain	2.0	4.0	3.5	3.2
		Twinned single grain	1.0	2.0	1.5	1.5
		Albitized single grain	3.0	2.0	0.0	1.7
	Kspar	Untwinned single grain	1.5	3.0	2.0	2.2
		Perthite single grain	1.5	1.0	1.0	1.2
		Microcline single grain	2.0	4.0	3.0	3.0
		Illite replacement of feldspar	0.0	0.0	0.0	0.0
QUARTZ IN ROCK FRAGMENT		Granite	2.0	2.0	0.0	1.3
		Granite gneiss	7.0	4.0	5.0	5.3
		Schistose quartz	0.0	2.0	0.3	0.8
		Groundmass in schistose quartz	1.0	0.0	0.7	0.6
		Schist	0.0	0.0	1.0	0.3
		Groundmass in schist	1.0	1.0	0.0	0.7
		Quartzite	5.0	7.0	7.0	6.3
		Groundmass in quartzite	2.0	0.0	0.0	0.7
FELDSPAR IN ROCK FRAGMENT	Plag.	Untwinned granite	2.0	2.0	1.0	1.7
		Twinned granite	1.0	0.0	0.0	0.3
		Untwinned granite gneiss	1.0	3.0	0.0	1.3
		Twinned granite gneiss	3.0	1.0	4.0	2.7
	Kspar	Untwinned granite	0.0	1.0	0.0	0.3
		Perthite granite	0.0	0.0	0.0	0.0
		Micro. granite	0.0	1.0	1.0	0.7
		Untwinned granite gneiss	2.0	2.0	3.0	2.3
		Perthite granite gneiss	0.0	0.0	0.0	0.0
		Micro. granite gneiss	2.0	4.0	1.0	2.3
		Illite replacement in granite	0.0	0.0	0.0	0.0
		Illite replacement in granite gneiss	0.0	0.0	0.0	0.0
MICA IN ROCK FRAGMENT	Muscovite	Granite	0.0	0.0	0.0	0.0
		Granite gneiss	1.0	1.0	2.0	1.3
		Quartzite	0.0	0.0	1.0	0.3
		Schistose quartz	2.0	1.0	1.0	1.3
		Schist	3.0	4.0	3.0	3.3
	Biotite	Granite	0.0	0.0	0.0	0.0
		Granite gneiss	0.0	0.0	0.0	0.0
		Quartzite	0.0	0.0	0.0	0.0
		Schistose quartz	0.0	2.0	0.0	0.7
		Schist	1.0	0.0	2.0	1.0
		FRAMWORK TOTAL	**68.0**	**79.0**	**78.0**	**75.0**

APPENDIX C2, CONTINUED

	LOCATION:	French's Ferry St.			
	FIGURE ID NO.:	7	8	9	-
	SAMPLE:	10.11-1	10.11-2	10.11-3	MEAN
	COUNT TYPE:	WR	WR	WR	WR
	N:	100	100	100	-
ACCESSORIES, POROSITY, MATRIX					
ACC.	Muscovite single grain	5.0	5.0	4.0	4.7
	Biotite single grain	3.0	4.0	3.0	3.3
	Chlorite replacement single grain	0.0	0.0	0.0	0.0
	Garnet	0.0	0.0	0.0	0.0
Hematite-stained matrix		2.0	0.0	3.0	1.7
Porosity		1.0	0.0	0.0	0.3
	ACC., POROSITY, MATRIX TOTAL	**11.0**	**9.0**	**10.0**	**10.0**
CEMENTS					
HEM.	Rim	1.0	3.0	1.0	1.7
	Cement	4.0	1.0	2.0	2.3
ALB.	Interstitial	9.0	4.0	3.0	5.3
	Overgrowth	2.0	1.0	1.0	1.3
Illite		0.0	0.0	0.0	0.0
Kaolinite		0.0	0.0	0.0	0.0
Quartz overgrowth		2.0	0.0	1.0	1.0
CO3-	Calcite	1.0	2.0	2.0	1.7
	Fe-calcite	2.0	1.0	2.0	1.7
	Dolomite	0.0	0.0	0.0	0.0
	Fe-dolomite	0.0	0.0	0.0	0.0
	CEMENT TOTAL	**21.0**	**12.0**	**12.0**	**15.0**
	THIN SECTION TOTAL	**100.0**	**100.0**	**100.0**	**100.0**

APPENDIX C2, CONTINUED

		LOCATION:	French's Ferry St.			
		FIGURE ID NO.:	7	8	9	-
		SAMPLE:	10.11-1	10.11-2	10.11-3	MEAN
		COUNT TYPE:	MS	MS	MS	MS
		N:	300	300	300	-
FRAMEWORK GRAINS						
QUARTZ		Unit monocrystalline	34.3	31.3	25.3	30.3
		Vein monocrystalline	8.7	6.3	4.7	6.5
		Annealed polycrystalline	11.0	10.7	13.3	11.7
		Vein polycrystalline	3.0	2.3	4.0	3.1
FELDSPAR	Plag.	Untwinned single grain	4.0	2.0	3.0	3.0
		Twinned single grain	1.0	2.3	0.7	1.3
		Albitized single grain	2.3	3.0	2.3	2.6
	Kspar	Untwinned single grain	2.0	4.8	7.2	4.7
		Perthite single grain	2.0	2.0	1.0	1.7
		Microcline single grain	0.0	0.7	1.1	0.6
		Illite replacement of feldspar	0.0	0.0	0.0	0.0
QUARTZ IN ROCK FRAGMENT		Granite	4.3	0.0	1.0	1.8
		Granite gneiss	4.3	5.7	6.3	5.5
		Schistose quartz	0.3	1.0	2.3	1.2
		Groundmass in schistose quartz	1.3	1.0	1.0	1.1
		Schist	0.0	0.0	0.7	0.2
		Groundmass in schist	0.3	0.3	1.0	0.5
		Quartzite	9.0	11.0	10.0	10.0
		Groundmass in quartzite	0.0	1.0	0.7	0.6
FELDSPAR IN ROCK FRAGMENT	Plag.	Untwinned granite	0.3	0.0	0.3	0.2
		Twinned granite	1.0	0.0	0.0	0.3
		Untwinned granite gneiss	1.0	4.0	2.0	2.3
		Twinned granite gneiss	1.0	0.0	3.3	1.4
	Kspar	Untwinned granite	1.2	1.0	0.2	0.8
		Perthite granite	0.0	0.0	0.0	0.0
		Micro. granite	0.2	0.0	0.1	0.1
		Untwinned granite gneiss	2.7	3.0	2.0	2.6
		Perthite granite gneiss	0.3	0.5	0.0	0.3
		Micro. granite gneiss	0.3	0.5	1.0	0.6
		Illite replacement in granite	0.0	0.0	0.0	0.0
		Illite replacement in granite gneiss	0.0	0.0	0.0	0.0
MICA IN ROCK FRAGMENT	Muscovite	Granite	0.0	0.0	0.0	0.0
		Granite gneiss	0.0	0.7	1.3	0.7
		Quartzite	0.0	0.0	0.0	0.0
		Schistose quartz	0.3	0.3	0.7	0.4
		Schist	0.7	1.3	2.0	1.3
	Biotite	Granite	0.0	0.3	0.0	0.1
		Granite gneiss	0.3	0.0	0.0	0.1
		Quartzite	0.0	0.0	0.0	0.0
		Schistose quartz	0.0	0.0	0.0	0.0
		Schist	0.0	0.0	0.0	0.0
		FRAMWORK TOTAL	**95.3**	**97.0**	**98.6**	**97.0**

APPENDIX C2, CONTINUED

	LOCATION:	French's Ferry St.			
	FIGURE ID NO.:	7	8	9	-
	SAMPLE:	10.11-1	10.11-2	10.11-3	MEAN
	COUNT TYPE:	MS	MS	MS	MS
	N:	300	300	300	-
ACCESSORIES, POROSITY, MATRIX					
ACC.	Muscovite single grain	4.0	2.7	1.3	2.7
	Biotite single grain	0.7	0.3	0.0	0.3
	Chlorite replacement single grain	0.0	0.0	0.0	0.0
	Garnet	-	-	-	-
Hematite-stained matrix		-	-	-	-
Porosity		-	-	-	-
ACC., POROSITY, MATRIX TOTAL		**4.7**	**3.0**	**1.3**	**3.0**
CEMENTS					
HEM.	Rim	-	-	-	-
	Cement	-	-	-	-
ALB.	Interstitial	-	-	-	-
	Overgrowth	-	-	-	-
Illite		-	-	-	-
Kaolinite		-	-	-	-
Quartz overgrowth		-	-	-	-
CO3-	Calcite	-	-	-	-
	Fe-calcite	-	-	-	-
	Dolomite	-	-	-	-
	Fe-dolomite	-	-	-	-
CEMENT TOTAL		**-**	**-**	**-**	**-**
THIN SECTION TOTAL		**100.0**	**100.0**	**100.0**	**100.0**

APPENDIX C2, CONTINUED

		LOCATION:	North Silver Ln.			
		FIGURE ID NO.:	10	11	12	-
		SAMPLE:	10.11-9	10.11-10	RS75-S3	MEAN
		COUNT TYPE:	WR	WR	WR	WR
		N:	100	100	100	-
FRAMEWORK GRAINS						
QUARTZ		Unit monocrystalline	26.0	21.0	23.0	23.3
		Vein monocrystalline	1.0	7.0	1.0	3.0
		Annealed polycrystalline	4.0	6.0	6.0	5.3
		Vein polycrystalline	0.0	2.0	1.0	1.0
FELDSPAR	Plag.	Untwinned single grain	2.5	3.0	2.0	2.5
		Twinned single grain	0.5	1.0	2.0	1.2
		Albitized single grain	5.0	2.0	4.0	3.7
	Kspar	Untwinned single grain	5.0	3.5	2.5	3.7
		Perthite single grain	1.0	0.5	0.5	0.7
		Microcline single grain	1.0	1.0	0.0	0.7
		Illite replacement of feldspar	0.0	0.0	0.0	0.0
QUARTZ IN ROCK FRAGMENT		Granite	1.0	1.0	2.0	1.3
		Granite gneiss	5.0	4.0	4.0	4.3
		Schistose quartz	1.0	0.0	0.3	0.4
		Groundmass in schistose quartz	0.0	0.0	0.7	0.2
		Schist	1.0	1.0	1.3	1.1
		Groundmass in schist	1.0	1.0	0.7	0.9
		Quartzite	5.0	4.0	2.0	3.7
		Groundmass in quartzite	0.0	2.0	0.0	0.7
FELDSPAR IN ROCK FRAGMENT	Plag.	Untwinned granite	0.0	0.0	1.0	0.3
		Twinned granite	0.0	0.0	0.0	0.0
		Untwinned granite gneiss	1.0	0.5	3.0	1.5
		Twinned granite gneiss	2.0	1.5	0.0	1.2
	Kspar	Untwinned granite	0.0	0.0	0.0	0.0
		Perthite granite	0.0	0.0	0.0	0.0
		Micro. granite	0.0	0.0	0.0	0.0
		Untwinned granite gneiss	2.7	1.0	4.0	2.6
		Perthite granite gneiss	0.3	0.0	1.0	0.4
		Micro. granite gneiss	0.0	0.0	0.0	0.0
		Illite replacement in granite	0.0	0.0	0.0	0.0
		Illite replacement in granite gneiss	0.0	0.0	0.0	0.0
MICA IN ROCK FRAGMENT	Muscovite	Granite	0.0	0.0	1.0	0.3
		Granite gneiss	3.0	0.0	3.0	2.0
		Quartzite	1.0	0.0	0.0	0.3
		Schistose quartz	2.0	0.0	1.0	1.0
		Schist	2.0	4.0	3.0	3.0
	Biotite	Granite	0.0	0.0	0.0	0.0
		Granite gneiss	0.0	0.0	0.0	0.0
		Quartzite	0.0	0.0	0.0	0.0
		Schistose quartz	0.0	2.0	1.0	1.0
		Schist	0.0	3.0	1.0	1.3
		FRAMWORK TOTAL	**74.0**	**72.0**	**72.0**	**72.7**

APPENDIX C2, CONTINUED

	LOCATION:	North Silver Ln.			
	FIGURE ID NO.:	10	11	12	-
	SAMPLE:	10.11-9	10.11-10	RS75-S3	MEAN
	COUNT TYPE:	WR	WR	WR	WR
	N:	100	100	100	-
ACCESSORIES, POROSITY, MATRIX					
ACC.	Muscovite single grain	4.0	5.0	3.0	4.0
	Biotite single grain	1.0	3.0	1.0	1.7
	Chlorite replacement single grain	0.0	0.0	0.0	0.0
	Garnet	0.0	0.0	0.0	0.0
Hematite-stained matrix		3.0	1.0	7.0	3.7
Porosity		0.0	1.0	0.0	0.3
	ACC., POROSITY, MATRIX TOTAL	**8.0**	**10.0**	**11.0**	**9.7**
CEMENTS					
HEM.	Rim	3.0	1.0	3.0	2.3
	Cement	3.0	2.0	4.0	3.0
ALB.	Interstitial	8.0	5.0	8.0	7.0
	Overgrowth	2.0	8.0	1.0	3.7
Illite		0.0	0.0	0.0	0.0
Kaolinite		0.0	0.0	0.0	0.0
Quartz overgrowth		2.0	2.0	1.0	1.7
CO3-	Calcite	0.0	0.0	0.0	0.0
	Fe-calcite	0.0	0.0	0.0	0.0
	Dolomite	0.0	0.0	0.0	0.0
	Fe-dolomite	0.0	0.0	0.0	0.0
	CEMENT TOTAL	**18.0**	**18.0**	**17.0**	**17.7**
	THIN SECTION TOTAL	**100.0**	**100.0**	**100.0**	**100.0**

APPENDIX C2, CONTINUED

		LOCATION:	North Silver Ln.			
		FIGURE ID NO.:	10	11	12	-
		SAMPLE:	10.11-9	10.11-10	RS75-S3	MEAN
		COUNT TYPE:	MS	MS	MS	MS
		N:	300	300	300	-
FRAMEWORK GRAINS						
QUARTZ		Unit monocrystalline	30.3	27.0	33.7	30.3
		Vein monocrystalline	6.3	11.3	8.0	8.6
		Annealed polycrystalline	9.7	9.3	10.0	9.7
		Vein polycrystalline	0.3	0.7	0.7	0.6
FELDSPAR	Plag.	Untwinned single grain	7.0	5.0	7.3	6.4
		Twinned single grain	5.0	4.7	4.0	4.6
		Albitized single grain	0.7	0.0	0.3	0.3
	Kspar	Untwinned single grain	2.1	5.0	4.0	3.7
		Perthite single grain	0.0	0.4	0.5	0.3
		Microcline single grain	1.3	1.0	0.7	1.0
		Illite replacement of feldspar	0.0	0.0	0.0	0.0
QUARTZ IN ROCK FRAGMENT		Granite	0.0	0.0	0.0	0.0
		Granite gneiss	7.0	6.3	7.0	6.8
		Schistose quartz	1.0	1.0	0.0	0.7
		Groundmass in schistose quartz	0.3	0.0	0.7	0.3
		Schist	2.0	1.0	1.3	1.4
		Groundmass in schist	1.0	0.7	0.7	0.8
		Quartzite	6.7	10.0	8.0	8.2
		Groundmass in quartzite	0.0	0.7	0.3	0.3
FELDSPAR IN ROCK FRAGMENT	Plag.	Untwinned granite	0.0	1.0	0.7	0.6
		Twinned granite	0.0	0.7	0.0	0.2
		Untwinned granite gneiss	4.0	3.0	3.0	3.3
		Twinned granite gneiss	5.0	2.3	1.0	2.8
	Kspar	Untwinned granite	0.0	0.0	0.0	0.0
		Perthite granite	0.0	0.0	0.0	0.0
		Micro. granite	0.0	0.0	0.0	0.0
		Untwinned granite gneiss	2.0	2.0	2.0	2.0
		Perthite granite gneiss	0.3	0.0	0.1	0.1
		Micro. granite gneiss	0.0	0.3	0.0	0.1
		Illite replacement in granite	0.0	0.0	0.0	0.0
		Illite replacement in granite gneiss	0.0	0.0	0.0	0.0
MICA IN ROCK FRAGMENT	Muscovite	Granite	0.0	0.0	0.0	0.0
		Granite gneiss	1.0	0.0	0.7	0.6
		Quartzite	0.0	0.0	0.0	0.0
		Schistose quartz	0.0	0.0	0.0	0.0
		Schist	2.7	2.7	1.7	2.3
	Biotite	Granite	0.0	0.0	0.0	0.0
		Granite gneiss	0.0	0.0	0.0	0.0
		Quartzite	0.0	0.0	0.0	0.0
		Schistose quartz	0.0	0.3	0.0	0.1
		Schist	0.0	0.0	0.0	0.0
		FRAMWORK TOTAL	**95.7**	**96.4**	**96.4**	**96.1**

APPENDIX C2, CONTINUED

	LOCATION:	North Silver Ln.			
	FIGURE ID NO.:	10	11	12	-
	SAMPLE:	10.11-9	10.11-10	RS75-S3	MEAN
	COUNT TYPE:	MS	MS	MS	MS
	N:	300	300	300	-
ACCESSORIES, POROSITY, MATRIX					
ACC.	Muscovite single grain	4.3	2.3	3.7	3.5
	Biotite single grain	0.0	1.3	0.0	0.4
	Chlorite replacement single grain	0.0	0.0	0.0	0.0
	Garnet	-	-	-	-
Hematite-stained matrix		-	-	-	-
Porosity		-	-	-	-
	ACC., POROSITY, MATRIX TOTAL	**4.3**	**3.7**	**3.7**	**3.9**
CEMENTS					
HEM.	Rim	-	-	-	-
	Cement	-	-	-	-
ALB.	Interstitial	-	-	-	-
	Overgrowth	-	-	-	-
Illite		-	-	-	-
Kaolinite		-	-	-	-
Quartz overgrowth		-	-	-	-
CO3-	Calcite	-	-	-	-
	Fe-calcite	-	-	-	-
	Dolomite	-	-	-	-
	Fe-dolomite	-	-	-	-
	CEMENT TOTAL	**-**	**-**	**-**	**-**
	THIN SECTION TOTAL	**100.0**	**100.0**	**100.0**	**100.0**

APPENDIX C2, CONTINUED

		LOCATION:	Bull Hill Rd.			
		FIGURE ID NO.:	13	14	15	-
		SAMPLE:	10.13-7	10.13-8	SF-BH6	MEAN
		COUNT TYPE:	WR	WR	WR	WR
		N:	100	100	100	-
FRAMEWORK GRAINS						
QUARTZ		Unit monocrystalline	30.0	25.0	31.0	28.7
		Vein monocrystalline	0.0	1.0	0.0	0.3
		Annealed polycrystalline	14.0	10.0	6.0	10.0
		Vein polycrystalline	0.0	0.0	0.0	0.0
FELDSPAR	Plag.	Untwinned single grain	6.0	6.0	8.0	6.7
		Twinned single grain	2.0	4.0	4.0	3.3
		Albitized single grain	0.0	0.0	1.0	0.3
	Kspar	Untwinned single grain	1.0	2.0	2.5	1.8
		Perthite single grain	0.0	0.0	0.5	0.2
		Microcline single grain	0.0	0.0	1.0	0.3
		Illite replacement of feldspar	0.0	0.0	0.0	0.0
QUARTZ IN ROCK FRAGMENT		Granite	1.0	2.0	1.0	1.3
		Granite gneiss	2.0	5.0	3.0	3.3
		Schistose quartz	0.0	1.0	1.0	0.7
		Groundmass in schistose quartz	0.0	0.0	0.0	0.0
		Schist	0.0	0.0	2.0	0.7
		Groundmass in schist	0.0	0.0	0.0	0.0
		Quartzite	3.0	2.0	8.0	4.3
		Groundmass in quartzite	0.0	0.0	0.0	0.0
FELDSPAR IN ROCK FRAGMENT	Plag.	Untwinned granite	1.0	0.0	1.0	0.7
		Twinned granite	0.0	0.0	0.0	0.0
		Untwinned granite gneiss	1.0	1.0	2.0	1.3
		Twinned granite gneiss	2.0	1.0	1.0	1.3
	Kspar	Untwinned granite	0.0	0.0	0.0	0.0
		Perthite granite	0.0	0.0	0.0	0.0
		Micro. granite	3.0	1.0	0.0	1.3
		Untwinned granite gneiss	0.0	0.0	2.0	0.7
		Perthite granite gneiss	0.0	0.0	1.0	0.3
		Micro. granite gneiss	1.0	0.0	2.0	1.0
		Illite replacement in granite	0.0	0.0	0.0	0.0
		Illite replacement in granite gneiss	0.0	0.0	0.0	0.0
MICA IN ROCK FRAGMENT	Muscovite	Granite	0.0	1.0	0.0	0.3
		Granite gneiss	1.0	1.0	0.0	0.7
		Quartzite	3.0	1.0	0.0	1.3
		Schistose quartz	0.0	2.0	1.0	1.0
		Schist	0.0	1.0	4.0	1.7
	Biotite	Granite	0.0	0.0	0.0	0.0
		Granite gneiss	0.0	0.0	0.0	0.0
		Quartzite	0.0	0.0	0.0	0.0
		Schistose quartz	0.0	0.0	1.0	0.3
		Schist	0.0	1.0	2.0	1.0
		FRAMWORK TOTAL	**71.0**	**68.0**	**86.0**	**75.0**

APPENDIX C2, CONTINUED

	LOCATION:	Bull Hill Rd.			
	FIGURE ID NO.:	13	14	15	-
	SAMPLE:	10.13-7	10.13-8	SF-BH6	MEAN
	COUNT TYPE:	WR	WR	WR	WR
	N:	100	100	100	-
ACCESSORIES, POROSITY, MATRIX					
ACC.	Muscovite single grain	1.0	3.0	3.0	2.3
	Biotite single grain	4.0	5.0	1.0	3.3
	Chlorite replacement single grain	0.0	0.0	0.0	0.0
	Garnet	0.0	0.0	0.0	0.0
Hematite-stained matrix		3.0	1.0	0.0	1.3
Porosity		1.0	1.0	0.0	0.7
	ACC., POROSITY, MATRIX TOTAL	**9.0**	**10.0**	**4.0**	**7.7**
CEMENTS					
HEM.	Rim	5.0	6.0	2.0	4.3
	Cement	5.0	4.0	3.0	4.0
ALB.	Interstitial	3.0	2.0	1.0	2.0
	Overgrowth	1.0	4.0	2.0	2.3
Illite		0.0	0.0	0.0	0.0
Kaolinite		0.0	0.0	0.0	0.0
Quartz overgrowth		3.0	2.0	0.0	1.7
CO3-	Calcite	0.0	0.0	0.0	0.0
	Fe-calcite	0.0	0.0	0.0	0.0
	Dolomite	3.0	2.0	2.0	2.3
	Fe-dolomite	0.0	2.0	0.0	0.7
	CEMENT TOTAL	**20.0**	**22.0**	**10.0**	**17.3**
	THIN SECTION TOTAL	**100.0**	**100.0**	**100.0**	**100.0**

APPENDIX C2, CONTINUED

LOCATION:			Bull Hill Rd.			
FIGURE ID NO.:			13	14	15	-
SAMPLE:			10.13-7	10.13.8	SF-BH6	MEAN
COUNT TYPE:			MS	MS	MS	MS
N:			300	300	300	-
FRAMEWORK GRAINS						
QUARTZ	Unit monocrystalline		38.3	42.0	45.3	41.9
	Vein monocrystalline		7.3	4.3	3.3	5.0
	Annealed polycrystalline		9.7	7.7	8.7	8.7
	Vein polycrystalline		0.0	0.0	0.0	0.0
FELDSPAR	Plag.	Untwinned single grain	6.0	5.0	5.0	5.3
		Twinned single grain	3.0	1.7	3.0	2.6
		Albitized single grain	0.0	0.3	0.0	0.1
	Kspar	Untwinned single grain	4.0	5.0	4.0	4.3
		Perthite single grain	1.0	0.3	0.7	0.7
		Microcline single grain	1.0	1.3	0.3	0.9
	Illite replacement of feldspar		0.0	0.0	0.0	0.0
QUARTZ IN ROCK FRAGMENT	Granite		0.0	0.0	0.0	0.0
	Granite gneiss		5.3	11.7	8.3	8.4
	Schistose quartz		1.7	1.0	2.3	1.7
	Groundmass in schistose quartz		1.0	2.0	0.0	1.0
	Schist		0.3	1.0	2.0	1.1
	Groundmass in schist		2.0	0.3	0.0	0.8
	Quartzite		3.0	4.3	4.0	3.8
	Groundmass in quartzite		0.7	0.0	0.0	0.2
FELDSPAR IN ROCK FRAGMENT	Plag.	Untwinned granite	0.3	0.0	0.0	0.1
		Twinned granite	0.0	0.0	0.0	0.0
		Untwinned granite gneiss	4.0	2.0	0.0	2.0
		Twinned granite gneiss	0.3	1.3	3.3	1.6
	Kspar	Untwinned granite	0.0	0.0	0.0	0.0
		Perthite granite	0.0	0.0	0.0	0.0
		Micro. granite	0.0	0.0	0.0	0.0
		Untwinned granite gneiss	1.0	3.8	2.0	2.3
		Perthite granite gneiss	0.8	1.0	0.2	0.7
		Micro. granite gneiss	1.8	1.2	1.8	1.6
	Illite replacement in granite		0.0	0.0	0.0	0.0
	Illite replacement in granite gneiss		0.0	0.0	0.0	0.0
MICA IN ROCK FRAGMENT	Muscovite	Granite	0.0	0.0	0.0	0.0
		Granite gneiss	0.0	0.0	0.0	0.0
		Quartzite	0.0	0.0	0.0	0.0
		Schistose quartz	1.0	0.3	0.7	0.7
		Schist	2.7	0.7	1.3	1.5
	Biotite	Granite	0.0	0.0	0.0	0.0
		Granite gneiss	0.0	0.0	0.0	0.0
		Quartzite	0.0	0.0	0.0	0.0
		Schistose quartz	0.0	0.0	0.0	0.0
		Schist	0.0	0.7	0.7	0.5
	FRAMWORK TOTAL		**96.3**	**99.0**	**95.9**	**97.1**

APPENDIX C2, CONTINUED

	LOCATION:	Bull Hill Rd.			
	FIGURE ID NO.:	13	14	15	-
	SAMPLE:	10.13-7	10.13.8	SF-BH6	MEAN
	COUNT TYPE:	MS	MS	MS	MS
	N:	300	300	300	-
ACCESSORIES, POROSITY, MATRIX					
ACC.	Muscovite single grain	1.7	1.0	2.0	1.6
	Biotite single grain	1.7	0.0	1.0	0.9
	Chlorite replacement single grain	0.3	0.0	1.0	0.4
	Garnet	-	-	-	-
Hematite-stained matrix		-	-	-	-
Porosity		-	-	-	-
	ACC., POROSITY, MATRIX TOTAL	**3.7**	**1.0**	**4.0**	**2.9**
CEMENTS					
HEM.	Rim	-	-	-	-
	Cement	-	-	-	-
ALB.	Interstitial	-	-	-	-
	Overgrowth	-	-	-	-
Illite		-	-	-	-
Kaolinite		-	-	-	-
Quartz overgrowth		-	-	-	-
CO3-	Calcite	-	-	-	-
	Fe-calcite	-	-	-	-
	Dolomite	-	-	-	-
	Fe-dolomite	-	-	-	-
	CEMENT TOTAL	**-**	**-**	**-**	**-**
	THIN SECTION TOTAL	**100.0**	**100.0**	**100.0**	**100.0**

APPENDIX C2, CONTINUED

LOCATION:	Rice's Ferry Rd.					
FIGURE ID NO.:			16	17	18	-
SAMPLE:			11.13-4	11.13-6	SF-PR1	MEAN
COUNT TYPE:			WR	WR	WR	WR
N:			100	100	100	-
FRAMEWORK GRAINS						
QUARTZ	Unit monocrystalline		24.0	23.0	26.0	24.3
	Vein monocrystalline		1.0	1.0	1.0	1.0
	Annealed polycrystalline		2.0	4.0	4.0	3.3
	Vein polycrystalline		1.0	0.0	2.0	1.0
FELDSPAR	Plag.	Untwinned single grain	4.5	2.0	4.0	3.5
		Twinned single grain	3.5	1.0	4.0	2.8
		Albitized single grain	3.0	3.0	2.0	2.7
	Kspar	Untwinned single grain	3.0	2.0	3.0	2.7
		Perthite single grain	1.0	1.0	0.0	0.7
		Microcline single grain	3.0	0.0	0.0	1.0
	Illite replacement of feldspar		0.0	0.0	0.0	0.0
QUARTZ IN ROCK FRAGMENT	Granite		0.0	1.0	1.0	0.7
	Granite gneiss		1.0	5.0	4.0	3.3
	Schistose quartz		1.0	2.0	1.0	1.3
	Groundmass in schistose quartz		0.0	1.0	0.0	0.3
	Schist		1.0	0.3	0.0	0.4
	Groundmass in schist		1.0	0.7	1.0	0.9
	Quartzite		1.0	6.0	4.0	3.7
	Groundmass in quartzite		1.0	1.0	2.0	1.3
FELDSPAR IN ROCK FRAGMENT	Plag.	Untwinned granite	1.0	0.0	1.0	0.7
		Twinned granite	0.0	0.0	0.0	0.0
		Untwinned granite gneiss	2.0	3.0	4.0	3.0
		Twinned granite gneiss	2.0	2.0	2.0	2.0
	Kspar	Untwinned granite	0.0	1.0	0.0	0.3
		Perthite granite	0.0	0.0	0.0	0.0
		Micro. granite	0.0	0.0	0.0	0.0
		Untwinned granite gneiss	1.5	6.0	4.0	3.8
		Perthite granite gneiss	0.5	0.0	0.0	0.2
		Micro. granite gneiss	3.0	0.0	0.0	1.0
	Illite replacement in granite		0.0	0.0	0.0	0.0
	Illite replacement in granite gneiss		0.0	0.0	0.0	0.0
MICA IN ROCK FRAGMENT	Muscovite	Granite	0.0	0.0	0.0	0.0
		Granite gneiss	0.0	1.0	1.0	0.7
		Quartzite	0.0	0.0	0.0	0.0
		Schistose quartz	1.0	1.0	2.0	1.3
		Schist	4.0	1.0	2.0	2.3
	Biotite	Granite	0.0	0.0	0.0	0.0
		Granite gneiss	0.0	0.0	0.0	0.0
		Quartzite	0.0	0.0	0.0	0.0
		Schistose quartz	0.0	0.0	0.0	0.0
		Schist	1.0	1.0	2.0	1.3
	FRAMWORK TOTAL		**68.0**	**70.0**	**77.0**	**71.7**

APPENDIX C2, CONTINUED

	LOCATION:	Rice's Ferry Rd.			
	FIGURE ID NO.:	16	17	18	-
	SAMPLE:	11.13-4	11.13-6	SF-PR1	MEAN
	COUNT TYPE:	WR	WR	WR	WR
	N:	100	100	100	-
ACCESSORIES, POROSITY, MATRIX					
ACC.	Muscovite single grain	5.0	2.0	3.0	3.3
	Biotite single grain	1.0	1.0	2.0	1.3
	Chlorite replacement single grain	0.0	0.0	0.0	0.0
	Garnet	0.0	0.0	0.0	0.0
Hematite-stained matrix		12.0	9.0	2.0	7.7
Porosity		1.0	0.0	1.0	0.7
	ACC., POROSITY, MATRIX TOTAL	**19.0**	**12.0**	**8.0**	**13.0**
CEMENTS					
HEM.	Rim	3.0	4.0	2.0	3.0
	Cement	7.0	12.0	4.0	7.7
ALB.	Interstitial	2.0	2.0	3.0	2.3
	Overgrowth	1.0	0.0	5.0	2.0
Illite		0.0	0.0	0.0	0.0
Kaolinite		0.0	0.0	0.0	0.0
Quartz overgrowth		0.0	0.0	1.0	0.3
CO3-	Calcite	0.0	0.0	0.0	0.0
	Fe-calcite	0.0	0.0	0.0	0.0
	Dolomite	0.0	0.0	0.0	0.0
	Fe-dolomite	0.0	0.0	0.0	0.0
	CEMENT TOTAL	**13.0**	**18.0**	**15.0**	**15.3**
	THIN SECTION TOTAL	**100.0**	**100.0**	**100.0**	**100.0**

APPENDIX C2, CONTINUED

		LOCATION:	Rice's Ferry Rd.			
		FIGURE ID NO.:	16	17	18	-
		SAMPLE:	11.13-4	11.13-6	SF-PR1	MEAN
		COUNT TYPE:	MS	MS	MS	MS
		N:	300	300	300	-
FRAMEWORK GRAINS						
QUARTZ		Unit monocrystalline	37.3	38.1	38.7	38.0
		Vein monocrystalline	1.3	1.3	1.7	1.4
		Annealed polycrystalline	8.0	9.5	10.3	9.3
		Vein polycrystalline	1.0	0.7	0.0	0.6
FELDSPAR	Plag.	Untwinned single grain	10.3	8.5	6.7	8.5
		Twinned single grain	5.0	6.0	5.0	5.3
		Albitized single grain	0.0	0.0	0.0	0.0
	Kspar	Untwinned single grain	1.0	2.1	1.1	1.4
		Perthite single grain	1.7	1.0	2.0	1.6
		Microcline single grain	0.7	0.7	0.9	0.8
		Illite replacement of feldspar	0.0	0.0	0.0	0.0
QUARTZ IN ROCK FRAGMENT		Granite	0.0	0.0	0.0	0.0
		Granite gneiss	9.0	5.9	6.0	7.0
		Schistose quartz	0.3	0.0	1.0	0.4
		Groundmass in schistose quartz	1.0	1.5	0.0	0.8
		Schist	0.0	0.0	0.0	0.0
		Groundmass in schist	0.3	0.0	0.3	0.2
		Quartzite	7.0	2.0	11.0	6.7
		Groundmass in quartzite	0.7	8.5	0.7	3.3
FELDSPAR IN ROCK FRAGMENT	Plag.	Untwinned granite	0.0	0.0	0.0	0.0
		Twinned granite	0.0	0.0	0.0	0.0
		Untwinned granite gneiss	6.0	4.0	5.0	5.0
		Twinned granite gneiss	1.3	4.1	1.0	2.1
	Kspar	Untwinned granite	0.0	0.0	0.0	0.0
		Perthite granite	0.0	0.0	0.0	0.0
		Micro. granite	0.0	0.0	0.0	0.0
		Untwinned granite gneiss	1.7	1.0	3.0	1.9
		Perthite granite gneiss	0.0	1.0	0.3	0.4
		Micro. granite gneiss	0.0	1.7	1.3	1.0
		Illite replacement in granite	0.0	0.0	0.0	0.0
		Illite replacement in granite gneiss	0.0	0.0	0.0	0.0
MICA IN ROCK FRAGMENT	Muscovite	Granite	0.0	0.0	0.0	0.0
		Granite gneiss	0.0	0.3	0.3	0.2
		Quartzite	0.0	0.0	0.0	0.0
		Schistose quartz	0.7	0.3	0.7	0.5
		Schist	0.7	0.0	1.0	0.6
	Biotite	Granite	0.0	0.0	0.0	0.0
		Granite gneiss	0.0	0.0	0.0	0.0
		Quartzite	0.0	0.0	0.0	0.0
		Schistose quartz	0.3	0.4	0.0	0.2
		Schist	0.0	0.0	0.3	0.1
		FRAMWORK TOTAL	**95.3**	**98.6**	**98.3**	**97.4**

APPENDIX C2, CONTINUED

	LOCATION:	Rice's Ferry Rd.			
	FIGURE ID NO.:	16	17	18	-
	SAMPLE:	11.13-4	11.13-6	SF-PR1	MEAN
	COUNT TYPE:	MS	MS	MS	MS
	N:	300	300	300	-
ACCESSORIES, POROSITY, MATRIX					
ACC.	Muscovite single grain	4.3	1.4	1.7	2.5
	Biotite single grain	0.3	0.0	0.0	0.1
	Chlorite replacement single grain	0.0	0.0	0.0	0.0
	Garnet	-	-	-	-
Hematite-stained matrix		-	-	-	-
Porosity		-	-	-	-
	ACC., POROSITY, MATRIX TOTAL	**4.7**	**1.4**	**1.7**	**2.6**
CEMENTS					
HEM.	Rim	-	-	-	-
	Cement	-	-	-	-
ALB.	Interstitial	-	-	-	-
	Overgrowth	-	-	-	-
Illite		-	-	-	-
Kaolinite		-	-	-	-
Quartz overgrowth		-	-	-	-
CO3-	Calcite	-	-	-	-
	Fe-calcite	-	-	-	-
	Dolomite	-	-	-	-
	Fe-dolomite	-	-	-	-
	CEMENT TOTAL	**-**	**-**	**-**	**-**
	THIN SECTION TOTAL	**100.0**	**100.0**	**100.0**	**100.0**

APPENDIX C2, CONTINUED

		LOCATION:	Kellogg St.			
		FIGURE ID NO.:	19	20	21	-
		SAMPLE:	10.16-1	10.16-2	10.16-3	MEAN
		COUNT TYPE:	WR	WR	WR	WR
		N:	100	100	100	-
FRAMEWORK GRAINS						
QUARTZ		Unit monocrystalline	38.0	30.0	44.0	37.3
		Vein monocrystalline	4.0	3.0	5.0	4.0
		Annealed polycrystalline	9.0	7.0	8.0	8.0
		Vein polycrystalline	4.0	2.0	2.0	2.7
FELDSPAR	Plag.	Untwinned single grain	0.0	0.0	0.0	0.0
		Twinned single grain	0.0	0.0	0.0	0.0
		Albitized single grain	0.0	0.0	0.0	0.0
	Kspar	Untwinned single grain	0.0	0.0	0.0	0.0
		Perthite single grain	0.0	0.0	0.0	0.0
		Microcline single grain	0.0	0.0	0.0	0.0
		Illite replacement of feldspar	3.0	5.0	6.0	4.7
QUARTZ IN ROCK FRAGMENT		Granite	0.0	1.0	0.0	0.3
		Granite gneiss	2.0	3.0	1.0	2.0
		Schistose quartz	0.0	0.0	2.0	0.7
		Groundmass in schistose quartz	0.0	1.0	0.0	0.3
		Schist	0.0	1.0	0.0	0.3
		Groundmass in schist	0.0	0.0	0.0	0.0
		Quartzite	5.0	4.0	7.0	5.3
		Groundmass in quartzite	0.0	0.0	1.0	0.3
FELDSPAR IN ROCK FRAGMENT	Plag.	Untwinned granite	0.0	0.0	0.0	0.0
		Twinned granite	0.0	0.0	0.0	0.0
		Untwinned granite gneiss	0.0	0.0	0.0	0.0
		Twinned granite gneiss	0.0	0.0	0.0	0.0
	Kspar	Untwinned granite	0.0	0.0	0.0	0.0
		Perthite granite	0.0	0.0	0.0	0.0
		Micro. granite	0.0	0.0	0.0	0.0
		Untwinned granite gneiss	1.0	0.0	0.0	0.3
		Perthite granite gneiss	0.0	0.0	0.0	0.0
		Micro. granite gneiss	0.0	0.0	0.0	0.0
		Illite replacement in granite	0.0	2.0	0.0	0.7
		Illite replacement in granite gneiss	3.0	4.0	1.0	2.7
MICA IN ROCK FRAGMENT	Muscovite	Granite	0.0	0.0	0.0	0.0
		Granite gneiss	0.0	1.0	0.0	0.3
		Quartzite	1.0	0.0	0.0	0.3
		Schistose quartz	0.0	0.0	0.0	0.0
		Schist	0.0	0.0	0.0	0.0
	Biotite	Granite	0.0	0.0	0.0	0.0
		Granite gneiss	0.0	0.0	0.0	0.0
		Quartzite	0.0	0.0	0.0	0.0
		Schistose quartz	0.0	0.0	0.0	0.0
		Schist	0.0	0.0	0.0	0.0
		FRAMWORK TOTAL	**70.0**	**64.0**	**77.0**	**70.3**

APPENDIX C2, CONTINUED

	LOCATION:	Kellogg St.			
	FIGURE ID NO.:	19	20	21	-
	SAMPLE:	10.16-1	10.16-2	10.16-3	MEAN
	COUNT TYPE:	WR	WR	WR	WR
	N:	100	100	100	-
ACCESSORIES, POROSITY, MATRIX					
ACC.	Muscovite single grain	3.0	4.0	3.0	3.3
	Biotite single grain	5.0	3.0	8.0	5.3
	Chlorite replacement single grain	0.0	0.0	0.0	0.0
	Garnet	0.0	0.0	0.0	0.0
Hematite-stained matrix		5.0	8.0	6.0	6.3
Porosity		0.0	1.0	0.0	0.3
	ACC., POROSITY, MATRIX TOTAL	**13.0**	**16.0**	**17.0**	**15.3**
CEMENTS					
HEM.	Rim	0.0	1.0	0.0	0.3
	Cement	1.0	2.0	1.0	1.3
ALB.	Interstitial	0.0	0.0	0.0	0.0
	Overgrowth	0.0	0.0	0.0	0.0
Illite		13.0	12.0	5.0	10.0
Kaolinite		0.0	0.0	0.0	0.0
Quartz overgrowth		3.0	5.0	0.0	2.7
CO3-	Calcite	0.0	0.0	0.0	0.0
	Fe-calcite	0.0	0.0	0.0	0.0
	Dolomite	0.0	0.0	0.0	0.0
	Fe-dolomite	0.0	0.0	0.0	0.0
	CEMENT TOTAL	**17.0**	**20.0**	**6.0**	**14.3**
	THIN SECTION TOTAL	**100.0**	**100.0**	**100.0**	**100.0**

APPENDIX C2, CONTINUED

LOCATION:			Kellogg St.			
FIGURE ID NO.:			19	20	21	-
SAMPLE:			10.16-1	10.16-2	10.16-3	MEAN
COUNT TYPE:			MS	MS	MS	MS
N:			300	300	300	-
FRAMEWORK GRAINS						
QUARTZ	Unit monocrystalline		32.0	40.7	41.3	38.0
	Vein monocrystalline		12.3	11.3	10.0	11.2
	Annealed polycrystalline		9.7	8.7	10.0	9.5
	Vein polycrystalline		3.3	2.7	0.7	2.2
FELDSPAR	Plag.	Untwinned single grain	0.0	0.0	0.0	0.0
		Twinned single grain	0.0	0.0	0.0	0.0
		Albitized single grain	0.0	0.0	0.0	0.0
	Kspar	Untwinned single grain	1.0	1.5	0.7	1.1
		Perthite single grain	0.3	0.2	0.0	0.2
		Microcline single grain	0.0	0.0	0.0	0.0
	Illite replacement of feldspar		9.7	9.3	8.7	9.2
QUARTZ IN ROCK FRAGMENT	Granite		0.0	0.0	0.0	0.0
	Granite gneiss		9.7	7.3	8.0	8.3
	Schistose quartz		0.0	0.0	1.0	0.3
	Groundmass in schistose quartz		0.7	2.0	2.0	1.6
	Schist		0.0	0.3	0.0	0.1
	Groundmass in schist		0.0	0.0	0.7	0.2
	Quartzite		8.0	6.0	4.0	6.0
	Groundmass in quartzite		0.7	0.7	0.7	0.7
FELDSPAR IN ROCK FRAGMENT	Plag.	Untwinned granite	0.0	0.0	0.0	0.0
		Twinned granite	0.0	0.0	0.0	0.0
		Untwinned granite gneiss	1.0	0.3	0.0	0.4
		Twinned granite gneiss	0.0	0.0	0.0	0.0
	Kspar	Untwinned granite	0.0	0.0	0.0	0.0
		Perthite granite	0.0	0.0	0.0	0.0
		Micro. granite	0.0	0.0	0.0	0.0
		Untwinned granite gneiss	0.7	1.3	3.3	1.8
		Perthite granite gneiss	1.0	0.0	0.0	0.3
		Micro. granite gneiss	0.3	0.0	0.0	0.1
	Illite replacement in granite		0.0	0.7	0.0	0.2
	Illite replacement in granite gneiss		3.3	3.0	4.0	3.4
MICA IN ROCK FRAGMENT	Muscovite	Granite	0.0	0.0	0.0	0.0
		Granite gneiss	0.3	0.3	0.3	0.3
		Quartzite	0.0	0.0	0.0	0.0
		Schistose quartz	0.0	0.0	0.0	0.0
		Schist	0.0	0.0	0.0	0.0
	Biotite	Granite	0.0	0.0	0.0	0.0
		Granite gneiss	0.0	0.0	0.0	0.0
		Quartzite	0.0	0.0	0.0	0.0
		Schistose quartz	1.0	0.3	0.3	0.5
		Schist	0.0	0.0	0.0	0.0
	FRAMWORK TOTAL		**95.0**	**96.6**	**95.7**	**95.8**

APPENDIX C2, CONTINUED

	LOCATION:	Kellogg St.			
	FIGURE ID NO.:	19	20	21	-
	SAMPLE:	10.16-1	10.16-2	10.16-3	MEAN
	COUNT TYPE:	MS	MS	MS	MS
	N:	300	300	300	-
ACCESSORIES, POROSITY, MATRIX					
ACC.	Muscovite single grain	1.7	0.7	1.0	1.1
	Biotite single grain	3.3	2.7	3.3	3.1
	Chlorite replacement single grain	0.0	0.0	0.0	0.0
	Garnet	-	-	-	-
Hematite-stained matrix		-	-	-	-
Porosity		-	-	-	-
ACC., POROSITY, MATRIX TOTAL		**5.0**	**3.4**	**4.3**	**4.2**
CEMENTS					
HEM.	Rim	-	-	-	-
	Cement	-	-	-	-
ALB.	Interstitial	-	-	-	-
	Overgrowth	-	-	-	-
Illite		-	-	-	-
Kaolinite		-	-	-	-
Quartz overgrowth		-	-	-	-
CO3-	Calcite	-	-	-	-
	Fe-calcite	-	-	-	-
	Dolomite	-	-	-	-
	Fe-dolomite	-	-	-	-
CEMENT TOTAL		**-**	**-**	**-**	**-**
THIN SECTION TOTAL		**100.0**	**100.0**	**100.0**	**100.0**

APPENDIX C2, CONTINUED

		LOCATION:	Meadow St.			
		FIGURE ID NO.:	22	23	24	-
		SAMPLE:	10.16-9	10.16-10	10.16-11	MEAN
		COUNT TYPE:	WR	WR	WR	WR
		N:	100	100	100	-
FRAMEWORK GRAINS						
QUARTZ		Unit monocrystalline	42.0	48.0	40.0	43.3
		Vein monocrystalline	3.0	3.0	8.0	4.7
		Annealed polycrystalline	15.0	9.0	11.0	11.7
		Vein polycrystalline	2.0	1.0	3.0	2.0
FELDSPAR	Plag.	Untwinned single grain	0.0	0.0	0.0	0.0
		Twinned single grain	0.0	0.0	0.0	0.0
		Albitized single grain	0.0	0.0	0.0	0.0
	Kspar	Untwinned single grain	0.0	0.0	0.0	0.0
		Perthite single grain	0.0	0.0	0.0	0.0
		Microcline single grain	0.0	0.0	0.0	0.0
		Illite replacement of feldspar	2.0	5.0	8.0	5.0
QUARTZ IN ROCK FRAGMENT		Granite	0.0	0.0	0.0	0.0
		Granite gneiss	2.0	4.0	2.0	2.7
		Schistose quartz	0.0	0.0	0.0	0.0
		Groundmass in schistose quartz	0.0	0.0	0.0	0.0
		Schist	0.0	1.0	1.0	0.7
		Groundmass in schist	0.0	0.0	0.0	0.0
		Quartzite	3.0	3.0	5.0	3.7
		Groundmass in quartzite	0.0	0.0	0.0	0.0
FELDSPAR IN ROCK FRAGMENT	Plag.	Untwinned granite	0.0	0.0	0.0	0.0
		Twinned granite	0.0	0.0	0.0	0.0
		Untwinned granite gneiss	0.0	0.0	0.0	0.0
		Twinned granite gneiss	0.0	0.0	0.0	0.0
	Kspar	Untwinned granite	0.0	0.0	0.0	0.0
		Perthite granite	0.0	0.0	0.0	0.0
		Micro. granite	0.0	0.0	0.0	0.0
		Untwinned granite gneiss	0.0	0.0	0.0	0.0
		Perthite granite gneiss	0.0	0.0	0.0	0.0
		Micro. granite gneiss	0.0	0.0	0.0	0.0
		Illite replacement in granite	0.0	1.0	0.0	0.3
		Illite replacement in granite gneiss	4.0	3.0	2.0	3.0
MICA IN ROCK FRAGMENT	Muscovite	Granite	0.0	0.0	0.0	0.0
		Granite gneiss	0.0	0.0	0.0	0.0
		Quartzite	0.0	0.0	0.0	0.0
		Schistose quartz	2.0	0.0	1.0	1.0
		Schist	4.0	2.0	1.0	2.3
	Biotite	Granite	0.0	0.0	0.0	0.0
		Granite gneiss	0.0	0.0	0.0	0.0
		Quartzite	0.0	0.0	0.0	0.0
		Schistose quartz	0.0	0.0	0.0	0.0
		Schist	2.0	0.0	0.0	0.7
		FRAMWORK TOTAL	**81.0**	**80.0**	**82.0**	**81.0**

APPENDIX C2, CONTINUED

	LOCATION:	Meadow St.			
	FIGURE ID NO.:	22	23	24	-
	SAMPLE:	10.16-9	10.16-10	10.16-11	MEAN
	COUNT TYPE:	WR	WR	WR	WR
	N:	100	100	100	-
ACCESSORIES, POROSITY, MATRIX					
ACC.	Muscovite single grain	2.0	1.0	4.0	2.3
	Biotite single grain	4.0	5.0	7.0	5.3
	Chlorite replacement single grain	0.0	0.0	0.0	0.0
	Garnet	0.0	0.0	0.0	0.0
Hematite-stained matrix		5.0	2.0	0.0	2.3
Porosity		0.0	0.0	1.0	0.3
	ACC., POROSITY, MATRIX TOTAL	**11.0**	**8.0**	**12.0**	**10.3**
CEMENTS					
HEM.	Rim	0.0	1.0	0.0	0.3
	Cement	1.0	1.0	2.0	1.3
ALB.	Interstitial	0.0	0.0	0.0	0.0
	Overgrowth	0.0	0.0	0.0	0.0
Illite		5.0	8.0	4.0	5.7
Kaolinite		0.0	0.0	0.0	0.0
Quartz overgrowth		2.0	2.0	0.0	1.3
CO3-	Calcite	0.0	0.0	0.0	0.0
	Fe-calcite	0.0	0.0	0.0	0.0
	Dolomite	0.0	0.0	0.0	0.0
	Fe-dolomite	0.0	0.0	0.0	0.0
	CEMENT TOTAL	**8.0**	**12.0**	**6.0**	**8.7**
	THIN SECTION TOTAL	**100.0**	**100.0**	**100.0**	**100.0**

APPENDIX C2, CONTINUED

LOCATION:			Meadow St.			
FIGURE ID NO.:			22	23	24	-
SAMPLE:			10.16-9	10.16-10	10.16-11	MEAN
COUNT TYPE:			MS	MS	MS	MS
N:			300	300	300	-
FRAMEWORK GRAINS						
QUARTZ	Unit monocrystalline		45.0	46.7	33.3	41.7
	Vein monocrystalline		7.3	5.3	6.7	6.4
	Annealed polycrystalline		4.3	4.0	9.3	5.9
	Vein polycrystalline		0.0	0.7	1.0	0.6
FELDSPAR	Plag.	Untwinned single grain	0.0	0.0	0.0	0.0
		Twinned single grain	0.0	0.0	0.0	0.0
		Albitized single grain	0.0	0.0	0.0	0.0
	Kspar	Untwinned single grain	1.6	0.3	0.0	0.6
		Perthite single grain	0.0	0.0	0.0	0.0
		Microcline single grain	0.4	0.3	0.0	0.2
	Illite replacement of feldspar		11.0	14.7	14.7	13.5
QUARTZ IN ROCK FRAGMENT	Granite		0.0	0.0	0.0	0.0
	Granite gneiss		10.3	9.3	8.0	9.2
	Schistose quartz		0.7	0.7	0.0	0.5
	Groundmass in schistose quartz		0.0	0.0	1.0	0.3
	Schist		0.0	0.3	0.0	0.1
	Groundmass in schist		0.0	0.0	1.0	0.3
	Quartzite		5.0	7.0	10.0	7.3
	Groundmass in quartzite		0.0	0.0	0.3	0.1
FELDSPAR IN ROCK FRAGMENT	Plag.	Untwinned granite	0.0	0.0	0.0	0.0
		Twinned granite	0.0	0.0	0.0	0.0
		Untwinned granite gneiss	0.7	0.3	0.7	0.6
		Twinned granite gneiss	0.0	0.0	0.0	0.0
	Kspar	Untwinned granite	0.0	0.0	0.0	0.0
		Perthite granite	0.0	0.0	0.0	0.0
		Micro. granite	0.0	0.0	0.0	0.0
		Untwinned granite gneiss	2.7	0.0	0.0	0.9
		Perthite granite gneiss	1.0	0.7	0.0	0.6
		Micro. granite gneiss	0.0	0.0	0.0	0.0
	Illite replacement in granite		0.0	0.3	0.0	0.1
	Illite replacement in granite gneiss		7.7	6.3	8.0	7.3
MICA IN ROCK FRAGMENT	Muscovite	Granite	0.0	0.0	0.0	0.0
		Granite gneiss	0.0	0.0	0.0	0.0
		Quartzite	0.0	0.0	0.0	0.0
		Schistose quartz	0.0	0.0	0.3	0.1
		Schist	0.0	0.7	1.0	0.6
	Biotite	Granite	0.0	0.0	0.0	0.0
		Granite gneiss	0.3	0.0	0.7	0.3
		Quartzite	0.0	0.0	0.0	0.0
		Schistose quartz	0.0	0.0	0.0	0.0
		Schist	0.0	0.0	0.0	0.0
	FRAMWORK TOTAL		**98.0**	**97.6**	**96.0**	**97.2**

APPENDIX C2, CONTINUED

	LOCATION:	Meadow St.			
	FIGURE ID NO.:	22	23	24	-
	SAMPLE:	10.16-9	10.16-10	10.16-11	MEAN
	COUNT TYPE:	MS	MS	MS	MS
	N:	300	300	300	-
ACCESSORIES, POROSITY, MATRIX					
ACC.	Muscovite single grain	0.7	0.3	1.0	0.7
	Biotite single grain	1.3	2.0	3.0	2.1
	Chlorite replacement single grain	0.0	0.0	0.0	0.0
	Garnet	-	-	-	-
Hematite-stained matrix		-	-	-	-
Porosity		-	-	-	-
	ACC., POROSITY, MATRIX TOTAL	**2.0**	**2.3**	**4.0**	**2.8**
CEMENTS					
HEM.	Rim	-	-	-	-
	Cement	-	-	-	-
ALB.	Interstitial	-	-	-	-
	Overgrowth	-	-	-	-
Illite		-	-	-	-
Kaolinite		-	-	-	-
Quartz overgrowth		-	-	-	-
CO3-	Calcite	-	-	-	-
	Fe-calcite	-	-	-	-
	Dolomite	-	-	-	-
	Fe-dolomite	-	-	-	-
	CEMENT TOTAL	**-**	**-**	**-**	**-**
	THIN SECTION TOTAL	**100.0**	**100.0**	**100.0**	**100.0**

APPENDIX C3: MODAL ANALYSES FOR ALLUVIAL FAN FACIES

		LOCATION:	Scout Rd.			
		FIGURE ID NO.:	1	2	3	-
		SAMPLE:	FR-1B	FR-2B	FR-3	MEAN
		COUNT TYPE:	WR	WR	WR	WR
		N:	100	100	100	-
FRAMEWORK GRAINS						
QUARTZ		Unit monocrystalline	27.0	26.0	18.0	23.7
		Vein monocrystalline	0.0	2.0	2.0	1.3
		Annealed polycrystalline	14.0	8.0	20.0	14.0
		Vein polycrystalline	0.0	0.0	1.0	0.3
FELDSPAR	Plag.	Untwinned single grain	5.0	6.0	1.0	4.0
		Twinned single grain	1.0	0.0	0.0	0.3
		Albitized single grain	0.0	2.0	1.0	1.0
	Kspar	Untwinned single grain	0.0	1.0	10.0	3.7
		Perthite single grain	0.0	0.0	4.0	1.3
		Microcline single grain	1.0	0.0	1.0	0.7
		Illite replacement of feldspar	0.0	0.0	0.0	0.0
QUARTZ IN ROCK FRAGMENT		Granite	1.0	1.0	1.0	1.0
		Granite gneiss	2.0	5.0	3.0	3.3
		Schistose quartz	0.0	0.0	2.0	0.7
		Groundmass in schistose quartz	0.0	0.0	0.0	0.0
		Schist	1.0	1.0	0.0	0.7
		Groundmass in schist	0.0	0.0	0.0	0.0
		Quartzite	4.0	9.0	4.0	5.7
		Groundmass in quartzite	0.0	0.0	0.0	0.0
FELDSPAR IN ROCK FRAGMENT	Plag.	Untwinned granite	0.0	0.0	0.0	0.0
		Twinned granite	0.0	0.0	0.0	0.0
		Untwinned granite gneiss	1.0	3.0	1.0	1.7
		Twinned granite gneiss	1.0	2.0	1.0	1.3
	Kspar	Untwinned granite	0.0	2.0	0.0	0.7
		Perthite granite	0.0	0.0	0.0	0.0
		Micro. granite	0.0	0.0	0.0	0.0
		Untwinned granite gneiss	0.0	0.0	1.0	0.3
		Perthite granite gneiss	0.0	0.0	1.0	0.3
		Micro. granite gneiss	3.0	0.0	2.0	1.7
		Illite replacement in granite	0.0	0.0	0.0	0.0
		Illite replacement in granite gneiss	0.0	0.0	0.0	0.0
MICA IN ROCK FRAGMENT	Muscovite	Granite	0.0	0.0	0.0	0.0
		Granite gneiss	1.0	1.0	1.0	1.0
		Quartzite	1.0	1.0	2.0	1.3
		Schistose quartz	1.0	0.0	1.0	0.7
		Schist	1.0	2.0	3.0	2.0
	Biotite	Granite	0.0	0.0	0.0	0.0
		Granite gneiss	0.0	0.0	0.0	0.0
		Quartzite	0.0	0.0	0.0	0.0
		Schistose quartz	1.0	0.0	1.0	0.7
		Schist	1.0	0.0	1.0	0.7
		FRAMWORK TOTAL	**67.0**	**72.0**	**83.0**	**74.0**

APPENDIX C3, CONTINUED

	LOCATION:	Scout Rd.			
	FIGURE ID NO.:	1	2	3	-
	SAMPLE:	FR-1B	FR-2B	FR-3	MEAN
	COUNT TYPE:	WR	WR	WR	WR
	N:	100	100	100	-
ACCESSORIES, POROSITY, MATRIX					
ACC.	Muscovite single grain	2.0	4.0	0.0	2.0
	Biotite single grain	3.0	2.0	1.0	2.0
	Chlorite replacement single grain	0.0	0.0	0.0	0.0
	Garnet	1.0	0.0	0.0	0.3
Hematite-stained matrix		2.0	0.0	0.0	0.7
Porosity		2.0	0.0	1.0	1.0
ACC., POROSITY, MATRIX TOTAL		**10.0**	**6.0**	**2.0**	**6.0**
CEMENTS					
HEM.	Rim	2.0	3.0	2.0	7.0
	Cement	4.0	4.0	3.0	11.0
ALB.	Interstitial	3.0	2.0	2.0	7.0
	Overgrowth	3.0	3.0	3.0	9.0
Illite		0.0	0.0	0.0	0.0
Kaolinite		0.0	0.0	0.0	0.0
Quartz overgrowth		5.0	3.0	0.0	8.0
CO3-	Calcite	4.0	2.0	2.0	8.0
	Fe-calcite	0.0	2.0	1.0	3.0
	Dolomite	2.0	3.0	2.0	7.0
	Fe-dolomite	0.0	0.0	0.0	0.0
CEMENT TOTAL		**23.0**	**22.0**	**15.0**	**20.0**
THIN SECTION TOTAL		**100.0**	**100.0**	**100.0**	**100.0**

APPENDIX C3, CONTINUED

		LOCATION:	Scout Rd.			
		FIGURE ID NO.:	1	2	3	-
		SAMPLE:	FR-1B	FR-2B	FR-3	MEAN
		COUNT TYPE:	MS	MS	MS	MS
		N:	300	300	300	-
FRAMEWORK GRAINS						
QUARTZ		Unit monocrystalline	23.7	23.7	25.3	24.2
		Vein monocrystalline	6.0	4.7	6.0	5.6
		Annealed polycrystalline	10.0	7.7	10.0	9.2
		Vein polycrystalline	1.3	0.0	0.7	0.7
FELDSPAR	Plag.	Untwinned single grain	9.3	7.7	9.7	8.9
		Twinned single grain	3.0	0.0	0.0	1.0
		Albitized single grain	0.0	0.0	0.0	0.0
	Kspar	Untwinned single grain	1.0	2.0	2.0	1.7
		Perthite single grain	0.6	0.2	0.0	0.3
		Microcline single grain	1.0	0.8	0.7	0.9
		Illite replacement of feldspar	0.0	0.0	0.0	0.0
QUARTZ IN ROCK FRAGMENT		Granite	0.3	0.0	0.0	0.1
		Granite gneiss	10.3	12.0	11.7	11.3
		Schistose quartz	1.0	4.0	2.7	2.6
		Groundmass in schistose quartz	1.0	1.3	1.0	1.1
		Schist	0.0	0.0	0.0	0.0
		Groundmass in schist	0.3	0.0	0.0	0.1
		Quartzite	14.0	14.0	14.0	14.0
		Groundmass in quartzite	1.7	0.0	0.0	0.6
FELDSPAR IN ROCK FRAGMENT	Plag.	Untwinned granite	1.0	0.3	0.7	0.7
		Twinned granite	0.3	0.0	0.0	0.1
		Untwinned granite gneiss	2.0	6.0	3.3	3.8
		Twinned granite gneiss	3.3	3.3	5.0	3.9
	Kspar	Untwinned granite	0.0	0.0	0.0	0.0
		Perthite granite	0.0	0.0	0.0	0.0
		Micro. granite	0.0	0.0	0.0	0.0
		Untwinned granite gneiss	0.5	2.0	1.0	1.2
		Perthite granite gneiss	0.3	0.3	0.0	0.2
		Micro. granite gneiss	0.6	0.7	0.7	0.6
		Illite replacement in granite	0.0	0.0	0.0	0.0
		Illite replacement in granite gneiss	0.0	0.0	0.0	0.0
MICA IN ROCK FRAGMENT	Muscovite	Granite	0.0	0.0	0.0	0.0
		Granite gneiss	0.3	0.0	0.0	0.1
		Quartzite	0.3	0.0	0.0	0.1
		Schistose quartz	0.3	0.7	0.0	0.3
		Schist	0.7	4.7	1.7	2.3
	Biotite	Granite	0.0	0.0	0.0	0.0
		Granite gneiss	0.0	0.0	0.0	0.0
		Quartzite	0.0	0.0	0.0	0.0
		Schistose quartz	0.7	0.0	0.3	0.3
		Schist	1.0	0.0	0.3	0.4
		FRAMWORK TOTAL	**96.0**	**96.0**	**96.8**	**96.2**

APPENDIX C3, CONTINUED

	LOCATION:	Scout Rd.			
	FIGURE ID NO.:	1	2	3	-
	SAMPLE:	FR-1B	FR-2B	FR-3	MEAN
	COUNT TYPE:	MS	MS	MS	MS
	N:	300	300	300	-
ACCESSORIES, POROSITY, MATRIX					
ACC.	Muscovite single grain	3.3	2.3	3.3	3.0
	Biotite single grain	0.7	1.7	0.0	0.8
	Chlorite replacement single grain	0.0	0.0	0.0	0.0
	Garnet	-	-	-	-
Hematite-stained matrix		-	-	-	-
Porosity		-	-	-	-
	ACC., POROSITY, MATRIX TOTAL	**4.0**	**4.0**	**3.3**	**3.8**
CEMENTS					
HEM.	Rim	-	-	-	-
	Cement	-	-	-	-
ALB.	Interstitial	-	-	-	-
	Overgrowth	-	-	-	-
Illite		-	-	-	-
Kaolinite		-	-	-	-
Quartz overgrowth		-	-	-	-
CO3-	Calcite	-	-	-	-
	Fe-calcite	-	-	-	-
	Dolomite	-	-	-	-
	Fe-dolomite	-	-	-	-
	CEMENT TOTAL	**-**	**-**	**-**	**-**
	THIN SECTION TOTAL	**100.0**	**100.0**	**100.0**	**100.0**

APPENDIX C3, CONTINUED

		LOCATION:	West Gill Rd.			
		FIGURE ID NO.:	4	5	6	-
		SAMPLE:	10.9-2	WGR-1	WGR-2	MEAN
		COUNT TYPE:	WR	WR	WR	WR
		N:	100	100	100	-
FRAMEWORK GRAINS						
QUARTZ		Unit monocrystalline	22.0	20.0	19.0	20.3
		Vein monocrystalline	1.0	2.0	2.0	1.7
		Annealed polycrystalline	10.0	8.0	5.0	7.7
		Vein polycrystalline	0.0	0.0	1.0	0.3
FELDSPAR	Plag.	Untwinned single grain	6.0	4.5	5.0	5.2
		Twinned single grain	1.0	0.5	1.0	0.8
		Albitized single grain	2.0	3.0	1.0	2.0
	Kspar	Untwinned single grain	0.0	1.0	0.0	0.3
		Perthite single grain	0.0	2.0	0.0	0.7
		Microcline single grain	3.0	2.0	2.0	2.3
		Illite replacement of feldspar	0.0	0.0	0.0	0.0
QUARTZ IN ROCK FRAGMENT		Granite	1.0	0.0	2.0	1.0
		Granite gneiss	4.0	5.0	5.0	4.7
		Schistose quartz	2.0	0.0	0.3	0.8
		Groundmass in schistose quartz	0.0	0.0	0.7	0.2
		Schist	3.0	1.0	1.0	1.7
		Groundmass in schist	0.0	1.0	0.0	0.3
		Quartzite	4.0	2.0	2.0	2.7
		Groundmass in quartzite	1.0	1.0	2.0	1.3
FELDSPAR IN ROCK FRAGMENT	Plag.	Untwinned granite	0.0	1.0	2.0	1.0
		Twinned granite	0.0	0.0	1.0	0.3
		Untwinned granite gneiss	2.0	2.5	3.0	2.5
		Twinned granite gneiss	0.0	1.5	2.0	1.2
	Kspar	Untwinned granite	0.0	0.0	0.0	0.0
		Perthite granite	0.0	0.0	0.0	0.0
		Micro. granite	0.0	1.0	3.0	1.3
		Untwinned granite gneiss	1.0	1.0	2.0	1.3
		Perthite granite gneiss	0.0	0.0	0.0	0.0
		Micro. granite gneiss	0.0	3.0	3.0	2.0
		Illite replacement in granite	0.0	0.0	0.0	0.0
		Illite replacement in granite gneiss	0.0	0.0	0.0	0.0
MICA IN ROCK FRAGMENT	Muscovite	Granite	0.0	1.0	1.0	0.7
		Granite gneiss	0.0	2.0	0.0	0.7
		Quartzite	0.0	0.0	1.0	0.3
		Schistose quartz	2.0	1.0	1.0	1.3
		Schist	4.0	3.0	2.0	3.0
	Biotite	Granite	0.0	0.0	0.0	0.0
		Granite gneiss	0.0	0.0	0.0	0.0
		Quartzite	0.0	0.0	0.0	0.0
		Schistose quartz	1.0	1.0	1.0	1.0
		Schist	3.0	2.0	0.0	1.7
		FRAMWORK TOTAL	**73.0**	**73.0**	**71.0**	**72.3**

APPENDIX C3, CONTINUED

	LOCATION:	West Gill Rd.			
	FIGURE ID NO.:	4	5	6	-
	SAMPLE:	10.9-2	WGR-1	WGR-2	MEAN
	COUNT TYPE:	WR	WR	WR	WR
	N:	100	100	100	-
ACCESSORIES, POROSITY, MATRIX					
ACC.	Muscovite single grain	4.0	5.0	3.0	4.0
	Biotite single grain	2.0	2.0	2.0	2.0
	Chlorite replacement single grain	0.0	0.0	1.0	0.3
	Garnet	0.0	0.0	1.0	0.3
Hematite-stained matrix		3.0	0.0	5.0	2.7
Porosity		1.0	2.0	2.0	1.7
ACC., POROSITY, MATRIX TOTAL		**10.0**	**9.0**	**14.0**	**11.0**
CEMENTS					
HEM.	Rim	4.0	0.0	3.0	2.3
	Cement	3.0	2.0	6.0	3.7
ALB.	Interstitial	2.0	7.0	4.0	4.3
	Overgrowth	3.0	2.0	1.0	2.0
Illite		0.0	0.0	0.0	0.0
Kaolinite		0.0	0.0	0.0	0.0
Quartz overgrowth		3.0	2.0	1.0	2.0
CO3-	Calcite	2.0	5.0	0.0	2.3
	Fe-calcite	0.0	0.0	0.0	0.0
	Dolomite	0.0	0.0	0.0	0.0
	Fe-dolomite	0.0	0.0	0.0	0.0
CEMENT TOTAL		**17.0**	**18.0**	**15.0**	**16.7**
THIN SECTION TOTAL		**100.0**	**100.0**	**100.0**	**100.0**

APPENDIX C3, CONTINUED

		LOCATION:	West Gill Rd.			
		FIGURE ID NO.:	4	5	6	-
		SAMPLE:	10.9-2	WGR-1	WGR-2	MEAN
		COUNT TYPE:	MS	MS	MS	MS
		N:	300	300	300	-
FRAMEWORK GRAINS						
QUARTZ	Unit monocrystalline		25.3	22.3	27.0	24.9
	Vein monocrystalline		5.0	6.3	5.7	5.7
	Annealed polycrystalline		5.7	4.0	6.0	5.2
	Vein polycrystalline		0.7	0.0	1.0	0.6
FELDSPAR	Plag.	Untwinned single grain	9.0	6.0	7.0	7.3
		Twinned single grain	0.3	1.3	1.3	1.0
		Albitized single grain	0.0	0.0	0.0	0.0
	Kspar	Untwinned single grain	1.7	2.4	3.1	2.4
		Perthite single grain	2.0	2.0	0.0	1.3
		Microcline single grain	2.3	2.0	3.6	2.6
	Illite replacement of feldspar		0.0	0.0	0.0	0.0
QUARTZ IN ROCK FRAGMENT	Granite		1.3	3.7	0.7	1.9
	Granite gneiss		7.7	7.3	8.3	7.8
	Schistose quartz		1.7	2.0	1.7	1.8
	Groundmass in schistose quartz		2.0	1.0	2.0	1.7
	Schist		0.7	1.0	1.3	1.0
	Groundmass in schist		2.0	0.3	2.0	1.4
	Quartzite		11.0	13.0	10.0	11.3
	Groundmass in quartzite		1.0	0.3	2.0	1.1
FELDSPAR IN ROCK FRAGMENT	Plag.	Untwinned granite	1.0	1.0	0.0	0.7
		Twinned granite	0.0	0.7	1.0	0.6
		Untwinned granite gneiss	4.0	4.0	2.0	3.3
		Twinned granite gneiss	2.0	2.0	0.7	1.6
	Kspar	Untwinned granite	0.7	2.5	0.0	1.1
		Perthite granite	0.0	0.5	0.0	0.2
		Micro. granite	0.0	0.0	0.0	0.0
		Untwinned granite gneiss	3.0	5.0	1.0	3.0
		Perthite granite gneiss	0.3	0.7	0.2	0.4
		Micro. granite gneiss	0.0	0.0	0.5	0.2
	Illite replacement in granite		0.0	0.0	0.0	0.0
	Illite replacement in granite gneiss		0.0	0.0	0.0	0.0
MICA IN ROCK FRAGMENT	Muscovite	Granite	0.0	0.0	0.0	0.0
		Granite gneiss	0.0	0.0	0.3	0.1
		Quartzite	0.3	0.3	0.7	0.4
		Schistose quartz	1.0	0.3	1.7	1.0
		Schist	3.3	1.7	5.0	3.3
	Biotite	Granite	0.0	0.0	0.0	0.0
		Granite gneiss	0.0	0.0	0.0	0.0
		Quartzite	0.0	0.0	0.0	0.0
		Schistose quartz	0.3	0.0	0.3	0.2
		Schist	1.0	1.7	1.0	1.2
		FRAMWORK TOTAL	**96.3**	**95.4**	**97.0**	**96.2**

APPENDIX C3, CONTINUED

	LOCATION:	West Gill Rd.			
	FIGURE ID NO.:	4	5	6	-
	SAMPLE:	10.9-2	WGR-1	WGR-2	MEAN
	COUNT TYPE:	MS	MS	MS	MS
	N:	300	300	300	-
ACCESSORIES, POROSITY, MATRIX					
ACC.	Muscovite single grain	3.0	4.0	1.7	2.9
	Biotite single grain	0.7	0.7	1.3	0.9
	Chlorite replacement single grain	0.0	0.0	0.0	0.0
	Garnet	-	-	-	-
Hematite-stained matrix		-	-	-	-
Porosity		-	-	-	-
ACC., POROSITY, MATRIX TOTAL		**3.7**	**4.7**	**3.0**	**3.8**
CEMENTS					
HEM.	Rim	-	-	-	-
	Cement	-	-	-	-
ALB.	Interstitial	-	-	-	-
	Overgrowth	-	-	-	-
Illite		-	-	-	-
Kaolinite		-	-	-	-
Quartz overgrowth		-	-	-	-
CO3-	Calcite	-	-	-	-
	Fe-calcite	-	-	-	-
	Dolomite	-	-	-	-
	Fe-dolomite	-	-	-	-
CEMENT TOTAL		**-**	**-**	**-**	**-**
THIN SECTION TOTAL		**100.0**	**100.0**	**100.0**	**100.0**

APPENDIX C4: MODAL ANALYSES FOR VALLEY RIVER FACIES

LOCATION:	I-91 Location 1			
FIGURE ID NO.:	1	2	3	-
SAMPLE:	10.13-4	10.13-5	I91-1A	MEAN
N:	100	100	100	-
QUARTZ				
Non-undulose	26.0	24.0	28.0	26.0
Undulose	53.0	56.0	51.0	53.3
Coarsely-polycrystalline	18.0	16.0	17.0	17.0
Finely-polycrystalline	3.0	4.0	4.0	3.7
TOTAL	100.0	100.0	100.0	100.0
VISUAL ESTIMATES				
Sphericity	Low	High	High	-
Roundness	S-R	S-A	S-R	-
Sorting	M-P	P-V.P.	M-P	-

LOCATION:	Lower Rd.			
FIGURE ID NO.:	4	5	6	-
SAMPLE:	D-1	D-2B	D-3	MEAN
N:	100	100	100	-
QUARTZ				
Non-undulose	19.0	21.0	22.0	20.7
Undulose	56.0	61.0	60.0	59.0
Coarsely-polycrystalline	19.0	14.0	17.0	16.7
Finely-polycrystalline	6.0	4.0	1.0	3.7
TOTAL	100.0	100.0	100.0	100.0
VISUAL ESTIMATES				
Sphericity	High	High	High	-
Roundness	A	S-A	S-A	-
Sorting	P-V.P.	P	M-P	-

APPENDIX C4, CONTINUED

LOCATION:	I-91 Location 3			
FIGURE ID NO.:	7	8	9	-
SAMPLE:	I91-3A	I91-3B	SF-G11	MEAN
N:	100	100	100	-
QUARTZ				
Non-undulose	12.0	21.0	17.0	16.7
Undulose	70.0	61.0	66.0	65.7
Coarsely-polycrystalline	18.0	16.0	16.0	16.7
Finely-polycrystalline	0.0	2.0	1.0	1.0
TOTAL	100.0	100.0	100.0	100.0
VISUAL ESTIMATES				
Sphericity	Low	High	Low	-
Roundness	S-R	S-R	S-R	-
Sorting	M	M-P	M-P	-

LOCATION:	Leyden Rd.			
FIGURE ID NO.:	10	11	12	-
SAMPLE:	8.23-5	8.23-7	RS75-192	MEAN
N:	100	100	100	-
QUARTZ				
Non-undulose	11.0	16.0	14.0	13.7
Undulose	51.0	59.0	55.0	55.0
Coarsely-polycrystalline	29.0	20.0	25.0	24.7
Finely-polycrystalline	9.0	5.0	6.0	6.7
TOTAL	100.0	100.0	100.0	100.0
VISUAL ESTIMATES				
Sphericity	High	High	Low	-
Roundness	A	S-A	S-A	-
Sorting	M-P	M-P	M	-

APPENDIX C4, CONTINUED

LOCATION:	Bernardston Rd.			
FIGURE ID NO.:	13	14	15	-
SAMPLE:	4.29-1	4.29-2	4.29-4	MEAN
N:	100	100	100	-
QUARTZ				
Non-undulose	21.0	15.0	24.0	20.0
Undulose	58.0	56.0	63.0	59.0
Coarsely-polycrystalline	16.0	24.0	10.0	16.7
Finely-polycrystalline	5.0	5.0	3.0	4.3
TOTAL	100.0	100.0	100.0	100.0
VISUAL ESTIMATES				
Sphericity	High	Low	Low	-
Roundness	A	A	S-A	-
Sorting	M-P	P	P	-

LOCATION:	Cheapside St.			
FIGURE ID NO.:	16	17	18	-
SAMPLE:	CS-4	CS-6	01-CP-H1	MEAN
N:	100	100	100	-
QUARTZ				
Non-undulose	15.0	12.0	12.0	13.0
Undulose	70.0	65.0	67.0	67.3
Coarsely-polycrystalline	14.0	20.0	19.0	17.7
Finely-polycrystalline	1.0	3.0	2.0	2.0
TOTAL	100.0	100.0	100.0	100.0
VISUAL ESTIMATES				
Sphericity	Low	Low	Low	-
Roundness	A	A	S-A	-
Sorting	M-P	P	M	-

APPENDIX C4, CONTINUED

LOCATION:	North Parkway St.			
FIGURE ID NO.:	19	20	21	-
SAMPLE:	9.11-1	10.5-3	RS75-113	MEAN
N:	100	100	100	-
QUARTZ				
Non-undulose	42.0	43.0	41.0	42.0
Undulose	32.0	34.0	35.0	33.7
Coarsely-polycrystalline	22.0	20.0	19.0	20.3
Finely-polycrystalline	4.0	3.0	5.0	4.0
TOTAL	100.0	100.0	100.0	100.0
VISUAL ESTIMATES				
Sphericity	Low	Low	High	-
Roundness	S-A	S-A	S-R	-
Sorting	V.P.	P	P	-

APPENDIX C5: MODAL ANALYSES FOR PIEDMONT RIVER FACIES

LOCATION:	Sugarloaf Mountain Rd.			
FIGURE ID NO.:	1	2	3	-
SAMPLE:	7.7-1	7.7-5	SF-SR2	MEAN
N:	100	100	100	-
QUARTZ				
Non-undulose	15.0	6.0	10.0	10.3
Undulose	69.0	71.0	70.0	70.0
Coarsely-polycrystalline	11.0	17.0	14.0	14.0
Finely-polycrystalline	5.0	6.0	6.0	5.7
TOTAL	100.0	100.0	100.0	100.0
VISUAL ESTIMATES				
Sphericity	Low	Low	Low	-
Roundness	A	S-A	A	-
Sorting	P-V.P.	M-P	M-P	-

LOCATION:	River Rd.			
FIGURE ID NO.:	4	5	6	-
SAMPLE:	9.21-2	9.21-5	9.21-6	MEAN
N:	100	100	100	-
QUARTZ				
Non-undulose	29.0	25.0	20.0	24.7
Undulose	43.0	50.0	65.0	52.7
Coarsely-polycrystalline	20.0	15.0	6.0	13.7
Finely-polycrystalline	8.0	10.0	9.0	9.0
TOTAL	100.0	100.0	100.0	100.0
VISUAL ESTIMATES				
Sphericity	Low	High	Low	-
Roundness	A	A	S-A	-
Sorting	M-P	P	P	-

APPENDIX C5, CONTINUED

LOCATION:	French's Ferry St.			
FIGURE ID NO.:	7	8	9	-
SAMPLE:	10.11-1	10.11-2	10.11-3	MEAN
N:	100	100	100	-
QUARTZ				
Non-undulose	24.0	22.0	25.0	23.7
Undulose	53.0	49.0	43.0	48.3
Coarsely-polycrystalline	14.0	17.0	15.0	15.3
Finely-polycrystalline	9.0	12.0	17.0	12.7
TOTAL	100.0	100.0	100.0	100.0
VISUAL ESTIMATES				
Sphericity	High	High	Low	-
Roundness	S-A	S-R	S-A	-
Sorting	P-V.P.	P	M	-

LOCATION:	North Silver Ln.			
FIGURE ID NO.:	10	11	12	-
SAMPLE:	10.11-9	10.11-10	RS75-S3	MEAN
N:	100	100	100	-
QUARTZ				
Non-undulose	22.0	23.0	24.0	23.0
Undulose	60.0	52.0	62.0	58.0
Coarsely-polycrystalline	9.0	17.0	8.0	11.3
Finely-polycrystalline	9.0	8.0	6.0	7.7
TOTAL	100.0	100.0	100.0	100.0
VISUAL ESTIMATES				
Sphericity	High	Low	Low	-
Roundness	S-A	A	A	-
Sorting	P-V.P.	M	M-P	-

APPENDIX C5, CONTINUED

LOCATION:	Bull Hill Rd.			
FIGURE ID NO.:	13	14	15	-
SAMPLE:	10.13-7	10.13.8	SF-BH6	MEAN
N:	100	100	100	-
QUARTZ				
Non-undulose	15.0	22.0	21.0	19.3
Undulose	67.0	56.0	59.0	60.7
Coarsely-polycrystalline	13.0	16.0	14.0	14.3
Finely-polycrystalline	5.0	6.0	6.0	5.7
TOTAL	100.0	100.0	100.0	100.0
VISUAL ESTIMATES				
Sphericity	Low	Low	Low	-
Roundness	A	S-A	A	-
Sorting	M-P	M	M-P	-

LOCATION:	Rice's Ferry Rd.			
FIGURE ID NO.:	16	17	18	-
SAMPLE:	11.13-4	11.13-6	SF-PR1	MEAN
N:	100	100	100	-
QUARTZ				
Non-undulose	6.0	8.0	10.0	8.0
Undulose	72.0	70.0	70.0	70.7
Coarsely-polycrystalline	16.0	16.0	14.0	15.3
Finely-polycrystalline	6.0	6.0	6.0	6.0
TOTAL	100.0	100.0	100.0	100.0
VISUAL ESTIMATES				
Sphericity	Low	Low	High	-
Roundness	A	S-A	A	-
Sorting	M-P	M	P-V.P.	-

APPENDIX C5, CONTINUED

LOCATION:	Kellogg St.			
FIGURE ID NO.:	19	20	21	-
SAMPLE:	10.16-1	10.16-2	10.16-3	MEAN
N:	100	100	100	-
QUARTZ				
Non-undulose	25.0	26.0	27.0	26.0
Undulose	53.0	54.0	59.0	55.3
Coarsely-polycrystalline	16.0	14.0	10.0	13.3
Finely-polycrystalline	6.0	6.0	4.0	5.3
TOTAL	100.0	100.0	100.0	100.0
VISUAL ESTIMATES				
Sphericity	Low	High	High	-
Roundness	V.A.	S-A	A	-
Sorting	M-P	P	M-P	-

LOCATION:	Meadow Rd.			
FIGURE ID NO.:	22	23	24	-
SAMPLE:	10.16-9	10.16-10	10.16-11	MEAN
N:	100	100	100	-
QUARTZ				
Non-undulose	33.0	30.0	28.0	30.3
Undulose	59.0	58.0	58.0	58.3
Coarsely-polycrystalline	5.0	8.0	10.0	7.7
Finely-polycrystalline	3.0	4.0	4.0	3.7
TOTAL	100.0	100.0	100.0	100.0
VISUAL ESTIMATES				
Sphericity	Low	Low	Low	-
Roundness	V.A.	S-A	S-A	-
Sorting	P-V.P.	P	P	-

APPENDIX C6: MODAL ANALYSES FOR ALLUVIAL FAN FACIES

LOCATION:	Scout Rd.			
FIGURE ID NO.:	1	2	3	-
SAMPLE:	FR-1B	FR-2B	FR-3	MEAN
N:	100	100	100	-
QUARTZ				
Non-undulose	12.0	8.0	10.0	10.0
Undulose	62.0	76.0	73.0	70.3
Coarsely-polycrystalline	14.0	7.0	7.0	9.3
Finely-polycrystalline	12.0	9.0	10.0	10.3
TOTAL	100.0	100.0	100.0	100.0
VISUAL ESTIMATES				
Sphericity	High	High	Low	-
Roundness	A	A	S-A	-
Sorting	M-P	M	M-P	-

LOCATION:	West Gill Rd.			
FIGURE ID NO.:	4	5	6	-
SAMPLE:	10.9-2	WGR-1	WGR-2	MEAN
N:	100	100	100	-
QUARTZ				
Non-undulose	9.0	7.0	12.0	9.3
Undulose	74.0	79.0	69.0	74.0
Coarsely-polycrystalline	11.0	8.0	13.0	10.7
Finely-polycrystalline	6.0	6.0	6.0	6.0
TOTAL	100.0	100.0	100.0	100.0
VISUAL ESTIMATES				
Sphericity	High	High	High	-
Roundness	S-A	A	S-A	-
Sorting	P	M-P	M-P	-

APPENDIX D

PEBBLE PETROLOGY

Appendix D1 shows pebble petrology based on nine counts from locations in the valley-river facies. I-91 L1 is I-91 Location 1, I-91 L3 is I-91 Location 3, LR is Leyden Rd., CCR is Country Club Rd, G is granitoid rock, Q is quartzite rock, and M is metamorphic rock. Appendix D2 shows pebble petrology based on 14 counts from locations in the piedmont-river facies. The abbreviation T2-3 is 2-3 m from the bottom of the type section (Mount Sugarloaf, road outcrop along Massachusetts Route 116), and RFR is Rice's Ferry Rd. Appendix D3 shows pebble petrology based on eight counts from locations in the alluvial-fan facies. WGR is West Gill Rd., and SCR is South Cross Rd.

Analyses performed by the author include MW in the sample designation. Other pebble counts are from Stevens (1977) and include RS in the sample designation. Sample locations are given in Appendix A.

APPENDIX D1: PEBBLE PETROLOGY FOR VALLEY-RIVER FACIES

LOCATION:	I-91 L2	I-91 L1	I-91 L1	Elm St.	Elm St.
SAMPLE:	MW-1	RS-61	MW-2	RS-221	RS-225
N:	100	100	100	97	100
GQM PEBBLES					
Granite gneiss, granite, pegmatite,	15	13	28	42	39
Kspar	0	32	24	0	0
G TOTAL	15	45	52	42	39
G RECALCULATED GQM	68.2	59.2	65.0	66.7	63.9
Quartzite	3	21	22	10	11
Q RECALCULATED GQM	13.6	27.6	27.5	15.9	18.0
Schist, phyllite, amphibolite	4	10	6	11	11
M RECALCULATED GQM	18.2	13.2	7.5	17.5	18.0
GQM TOTAL	22	76	80	63	61
OTHER PEBBLES					
Quartz, vein quartz	38	24	20	32	39
Granulite	0	0	0	0	0
Intraclast	40	0	0	2	0
OTHER TOTAL	78	24	20	34	39
PEBBLE COUNT TOTAL	100	100	100	97	100
Average roundness	S-R	-	R	-	-
Average long axis	4.0	-	4.2	-	-
Average intermediate axis	2.7	-	3.0	-	-
Average short axis	2.0	-	2.1	-	-
Average shape	equant	-	equant	-	-
Number of ventifacts	5	-	7	-	-
Number of poor ventifacts	9	-	15	-	-
Number with desert varnish	2	-	0	-	-

APPENDIX D1, CONTINUED

LOCATION:	LR	CCR	CCR	CCR	-
SAMPLE:	MW-3	RS-251	RS-252	MW-4	MEAN
N:	100	100	98	100	-
GQM PEBBLES					
Granite gneiss, granite, pegmatite,	25	35	23	29	27.7
Kspar	14	6	31	19	14.0
G TOTAL	39	41	54	48	41.7
G RECALCULATED GQM	51.3	50.0	76.1	62.3	61.7
Quartzite	20	16	2	9	12.7
Q RECALCULATED GQM	26.3	19.5	2.8	11.7	18.8
Schist, phyllite, amphibolite	17	25	15	20	13.2
M RECALCULATED GQM	22.4	30.5	21.1	26.0	19.6
GQM TOTAL	76	82	71	77	67.6
OTHER PEBBLES					
Quartz, vein quartz	18	17	25	21	26.0
Granulite	0	0	0	0	0.0
Intraclast	6	1	2	2	5.9
OTHER TOTAL	24	18	27	23	31.9
PEBBLE COUNT TOTAL	100	100	98	100	99.4
Average roundness	S-R	-	-	S-R	-
Average long axis	4.5	-	-	3.9	-
Average intermediate axis	2.1	-	-	3.3	-
Average short axis	1.9	-	-	1.5	-
Average shape	prolate	-	-	oblate	-
Number of ventifacts	5	-	-	0	-
Number of poor ventifacts	25	-	-	12	-
Number with desert varnish	1	-	-	0	-

APPENDIX D2: PEBBLE PETROLOGY FOR PIEDMONT-RIVER FACIES

LOCATION:	T2-3	T18	T157	T210	T252
SAMPLE:	RS-1	RS-2	RS-3	MW-5	RS-4
N:	100	100	100	100	101
GQM PEBBLES					
Granite, gneiss, graphic granite,	26	61	50	19	46
Kspar	30	10	0	34	2
G TOTAL	56	71	50	53	48
G RECALCULATED GQM	73.7	86.6	62.5	72.6	60.0
Quartzite	2	3	5	12	3
Q RECALCULATED GQM	2.6	3.7	6.3	16.4	3.8
Schist, phyllite, amphibolite	18	8	25	8	29
M RECALCULATED GQM	23.7	9.8	31.3	11.0	36.3
GQM TOTAL	76	82	80	73	80
OTHER PEBBLES					
Quartz, vein quartz	24	18	13	27	15
Granulite	0	0	7	0	4
Intraclast	0	0	0	0	2
OTHER TOTAL	24	18	20	27	21
PEBBLE COUNT TOTAL	100	100	100	100	101
Average roundness	-	-	-	S-R	-
Average long axis	-	-	-	5.1	-
Average intermediate axis	-	-	-	3.4	-
Average short axis	-	-	-	2.0	-
Average shape	-	-	-	oblate	-
Number of ventifacts	-	-	-	12	-
Number of poor ventifacts	-	-	-	18	-
Number with desert varnish	-	-	-	1	-

APPENDIX D2, CONTINUED

LOCATION:	T257	T352	T410	T410	T410
SAMPLE:	MW-6	RS-5	RS-6	MW-7	MW-8
N:	100	98	100	100	100
GQM PEBBLES					
Granite, gneiss, graphic granite,	16	35	38	35	68
Kspar	15	0	0	21	1
G TOTAL	31	35	38	56	69
G RECALCULATED GQM	35.6	53.0	47.5	67.5	74.2
Quartzite	25	2	12	17	15
Q RECALCULATED GQM	28.7	3.0	15.0	20.5	16.1
Schist, phyllite, amphibolite	31	29	30	10	9
M RECALCULATED GQM	35.6	43.9	37.5	12.0	9.7
GQM TOTAL	87	66	80	83	93
OTHER PEBBLES					
Quartz, vein quartz	12	15	20	17	7
Granulite	1	10	0	0	0
Intraclast	0	7	0	0	0
OTHER TOTAL	13	32	20	17	7
PEBBLE COUNT TOTAL	100	98	100	100	100
Average roundness	S-R	-	-	S-R	S-R
Average long axis	5.0	-	-	4.8	5.1
Average intermediate axis	3.2	-	-	3	3.7
Average short axis	1.9	-	-	2.5	2.3
Average shape	triaxial	-	-	prolate	oblate
Number of ventifacts	24	-	-	12	2
Number of poor ventifacts	32	-	-	30	14
Number with desert varnish	6	-	-	2	2

APPENDIX D2, CONTINUED

LOCATION:	T459	T620	RFR	RFR	-
SAMPLE:	RS-7	RS-21	MW-9	MW-10	MEAN
N:	100	100	100	100	-
GQM PEBBLES					
Granite, gneiss, graphic granite,	35	75	45	50	42.8
Kspar	1	3	3	6	9.0
G TOTAL	36	78	48	56	51.8
G RECALCULATED GQM	52.9	87.6	59.3	62.2	64.3
Quartzite	1	4	15	10	9.0
Q RECALCULATED GQM	1.5	4.5	18.5	11.1	11.2
Schist, phyllite, amphibolite	31	7	18	24	19.8
M RECALCULATED GQM	45.6	7.9	22.2	26.7	24.6
GQM TOTAL	68	89	81	90	80.6
OTHER PEBBLES					
Quartz, vein quartz	18	8	19	10	15.9
Granulite	13	3	0	0	2.7
Intraclast	1	0	0	0	0.7
OTHER TOTAL	32	11	19	10	19.4
PEBBLE COUNT TOTAL	100	100	100	100	99.9
Average roundness	-	-	S-A	S-R	-
Average long axis	-	-	4.2	4.0	-
Average intermediate axis			3.0	2.7	
Average short axis	-	-	1.6	1.3	-
Average shape	-	-	oblate	oblate	-
Number of ventifacts	-	-	2	7	-
Number of poor ventifacts	-	-	16	10	-
Number with desert varnish	-	-	3	1	-

APPENDIX D3: PEBBLE PETROLOGY FOR ALLUVIAL-FAN FACIES

LOCATION:	WGR	WGR	WGR	WGR	SCR
SAMPLE:	MW-11	MW-12	MW-13	MW-14	RS-201
N:	100	100	100	100	100
GQM PEBBLES					
Granite, gneiss, graphic granite,	6	13	18	16	23
Kspar	23	15	14	14	0
G TOTAL	29	28	32	30	23
G RECALCULATED GQM	37.7	37.3	40.0	41.1	33.8
Quartzite	42	27	30	28	20
Q RECALCULATED GQM	54.5	36.0	37.5	38.4	29.4
Schist, phyllite, amphibolite	6	20	18	15	25
M RECALCULATED GQM	7.8	26.7	22.5	20.5	36.8
GQM TOTAL	77	75	80	73	68
OTHER PEBBLES					
Quartz, vein quartz	23	25	20	27	32
Granulite	0	0	0	0	0
Intraclast	0	0	0	0	0
OTHER TOTAL	23	25	20	27	32
PEBBLE COUNT TOTAL	100	100	100	100	100
Average roundness	S-R	S-A	S-A	S-R	-
Average long axis	4.4	5.9	5.0	4.9	-
Average intermediate axis	3.2	3.9	3.2	3.0	
Average short axis	2.0	2.5	2.1	1.7	-
Average shape	oblate	triaxial	triaxial	triaxial	-
Number of ventifacts	6	12	8	8	-
Number of poor ventifacts	7	10	12	2	-
Number with desert varnish	4	1	8	1	-

APPENDIX D3, CONTINUED

LOCATION:	SCR	Main Rd.	Scout Rd.	-
SAMPLE:	MW-15	RS-151	MW-16	MEAN
N:	100	100	100	-
GQM PEBBLES				
Granite, gneiss, graphic granite,	20	37	14	18.4
Kspar	8	0	20	11.8
G TOTAL	28	37	34	30.1
G RECALCULATED GQM	32.6	43.5	41.0	38.4
Quartzite	41	32	29	31.1
Q RECALCULATED GQM	47.7	37.6	34.9	39.7
Schist, phyllite, amphibolite	17	16	20	17.1
M RECALCULATED GQM	19.8	18.8	24.1	21.9
GQM TOTAL	86	85	83	78.4
OTHER PEBBLES				
Quartz, vein quartz	14	15	17	21.6
Granulite	0	0	0	0.0
Intraclast	0	0	0	0.0
OTHER TOTAL	14	15	17	21.6
PEBBLE COUNT TOTAL	100	100	100	100.0
Average roundness	S-A	-	S-R	-
Average long axis	5.3	-	5.6	-
Average intermediate axis	3.2		3.4	
Average short axis	1.9	-	2.3	-
Average shape	triaxial	-	prolate	-
Number of ventifacts	3	-	4	-
Number of poor ventifacts	13	-	15	-
Number with desert varnish	7	-	6	-

REFERENCES CITED

ANDERS, M.H., and SCHLISCHE, R.W., 1994, Overlapping faults, intrabasin highs, and the growth of normal faults: *Journal of Geology*, v. 102, p. 165-180.

ANDO, C.J., CZUCHRA, B.L., KLEMPERER, L.D., BROWN, M.D., CHEADLE, M.J., COOK, F.A., OLIVER, J.E., KAUFFMAN, S., WALSH, T., THOMSPN, J.B., LYONS, J.B., and ROSENFELD, J.L., 1984, COCORP deep seismic profiling in New England Appalachians and implications for architecture of convergent mountain chains: *AAPG Bulletin*, v. 68, p. 819-837.

BALK, R., 1956, Bedrock geology of the Massachusetts portion of the Northfield quadrangle, Massachusetts, New Hampshire, and Vermont: *United States Geological Survey Geological Quadrangle Map GQ-92*.

BARNETT, J.A.M., MORTIMER, J., RIPPON, J.H., WALSH, J.J., and WATTERSON, J., 1987, Displacement geometry in the volume constraining a single normal fault: *AAPG Bulletin*, v. 71, p. 925-937.

BASU, A., 1985, Reading provenance from detrital quartz: *in* Zuffa, G.G., ed., Provenance of Arenites: *D. Reidel Publishing Company, Holland*, p. 231-247.

BASU, A., YOUNG, S.W., SUTTNER, L.J., JAMES, W.C., and MACK, G.H., 1975, Reevaluation of the use of undulatory extinction and polycrystallinity in detrital quartz for provenance interpretation: *Journal of Sedimentary Petrology*, v. 45, p. 873-882.

BOGGS, S., Jr., 2006, Principles of Sedimentology and Stratigraphy, fourth edition: *Pearson Prentice-Hall, NJ*, 662 p.

BOLES, J.R., 1982, Active albitization of plagioclase, Gulf Coast Tertiary: *American Journal of Science*, v. 282, p. 165-180.

BRIGHAM-GRETTE, J., and RITTENOUR, T., 2003, Late Wisconsinan glacial history of the Connecticut River Valley and a new drainage history of glacial Lake Hitchcock: varves, landforms and stratigraphy: *in* Robinson, P. and Brady, J. B. (eds.), Field Trip Guidebook of the 84th Annual New England Intercollegiate Geologic Conference. *Department of Geosciences, University of Massachusetts, Amherst, Massachusetts*, v. 2, p. B6-1 to B6-64.

CAROZZI, A.V., 1993, Sedimentary Petrography: *PTR Prentice-Hall, NJ*, 263 p.

CHANDLER, W.E., 1978, Graben mechanics at the junction of the Hartford and Deerfield basins of the Connecticut Valley, Massachusetts: M.S. thesis, *Department of Geosciences, University of Massachusetts, Amherst, Massachusetts*, 151 p.

CHANDLER, M. A., RIND, D. and RUEDY, R. 1992, Pangaean climate during the Early Jurassic: GCM simulations and the sedimentary record of paleoclimate. *Geological Society of America Bulletin*, v. 104, p. 543-559.

CLARK, R.G., and LYONS, J.B., 1986, Petrogenesis of the Kinsman intrusive suite: peraluminous granitoids of western New Hampshire: *Journal of Petrology*, v. 27, p. 1365-1393.

COHEN, A.S., and COE, A.L., 2002, New geochemical evidence for the onset of volcanism in the Central Atlantic magmatic province and environmental change at the Triassic-Jurassic boundary: *Geology*, v. 30, n. 3, p. 267-270.

CONTRERAS, J., SCHOLZ, C., and KING, G.C.P., 1997, A general model for rift basin evolution: constraints of first order stratigraphic observations: *Journal of Geophysical Research*, v. 102, p. 7673-7690.

CORNET, B., 1977, The palynostratigraphy and age of the Newark supergroup: Ph. D. dissertation, *Pennsylvanian State University, PA*, 505 p.

COURTILLOT, V., 1996, Effects of mass extinctions on biodiversity: *Nature*, v. 381, p. 146-148.

COWIE, P.A., 1998, A healing-reloading feedback control on the growth rate of seismogenic faults: *Journal of Structural Geology*, v. 20, p. 1075-1087.

CRESPI, J.M., 1988, Using balanced cross sections to understand early Mesozoic extensional faulting: *in* Froelich, A.J., and Robinson, G.R. (eds.), Studies of the Early Mesozoic Basins of the Eastern United States: *United States Geologic Survey Bulletin* 1776, p. 220-229.

DE BOER, J.Z., 1992, Stress configurations during and following emplacement of ENA basalts in the northern Appalachians: *in* Puffer, J.H., and Ragland, P.C., eds., Eastern North American Mesozoic magmatism: Geological Society of America special paper 268: *Geological Society of America*, p. 361-363.

DE BOER, J.Z., and CLIFTON, A.E., 1988, Mesozoic tectogenesis: development and deformation of 'Newark' rift zones in the Appalachians (with special emphasis on the Hartford basin, Connecticut): *in* Manzpeiser, W., ed., Triassic-Jurassic Rifting: Continental breakup and the origin of the Atlantic Ocean and the passive margins: *Developments in Geotectonics*, n. 22, p. 275-306.

DICKINSON, W.R., 1970, Interpreting detrital modes of greywacke and arkose: *Journal of Sedimentary Petrology*, v. 40, p. 695-707.

DICKINSON, W.R., 1985, Interpreting provenance relations from detrital modes of sandstones: *NATO ASI Series C*, v. 148, p. 333-361.

DICKINSON, W.R., and SUCZEK, C.A., 1979, Plate tectonics and sandstone compositions: *AAPG Bulletin*, v. 63, p. 2164-2182.

DORAIS, M.J., 2003, The petrogenesis and emplacement of the New Hampshire plutonic suite: *American Journal of Science*, v. 303, p. 447-487.

DUBIEL, R. F., PARRISH, J. T., PARRISH, J. M. and GOOD, S. C, 1991, The Pangaean megamonsoon: evidence from the Upper Triassic Chinle Formation, Colorado Plateau: *Palaios*, v. 6, p. 347-370.

DUNNING, G.R., and HODYCH, J.P., 1990, U/Pb zircon and baddeleyite ages for the Palisades and Gettysburg sills of the northeastern United States: implications for the age of the Triassic/Jurassic boundary: *Geology*, v. 18, p. 795-798.

DYAR, M.D., GUNTER, M.E., and TASA, D., 2008, Mineralogy and Optical Mineralogy: *Mineralogical Society of America, VA*, 708 p.

DRZEWIECKI, P.A., and ZUIDEMA, S., 2007, Sequence stratigraphy of playa and perennial lake deposits, Jurassic East Berlin Formation, central Connecticut: *Northeastern Geology & Environmental Sciences*, v. 29, p. 49-68.

EBERLY, P.O., 1985, Brittle fracture petrofabric along a west-east traverse from the Connecticut Valley to the Narragansett Basin*:* M.S. thesis, *Department of Geosciences, University of Massachusetts, Amherst, Massachusetts*, 137 p.

ECHARFAOUI, H., HAFID, M., SALEM, A.A., and ABDERRAHMANE, A.F., 2002, Analyse sismo-stratigraphique du basin d'Abda (Maroc occidental), exemple de structures inverses pendant le rifting atlantique: *C.R. Geoscience*, v. 334, p. 371-377.

EHRENBERG, S.N., and NADEAU, P.H., 1989, Formation of diagenetic illite in sandstones of the Garn Formation, Haltenbanken area, mid-Norwegian continental shelf: *Clay Mineralogy*, v. 24, p. 233-253.

FAILL, R.T., 2003, The early Mesozoic Birdsboro central Atlantic margin basin in the Mid-Atlantic region, eastern United States: *GSA Bulletin*, v. 115, n. 4, p. 406-421.

FOLK, R.L., 1980, Petrology of Sedimentary Rocks: *Hemphill Publishing Company, TX*, 182 p.

FRANZ, A. J., 1978, Sedimentology of the Sugarloaf Arkose (Late Triassic-Early Jurassic) of the Connecticut Valley: a succession of alluvial-fan, braided-stream and meandering-stream deposits. M. S. thesis, *Department of Geosciences*, University of Massachusetts, Amherst, Massachusetts, 174 p.

FRIEDMAN, G. M., 1971, Staining: *in* Carver, R. E. (ed.), Procedures: *in* Sedimentary Petrology: New York, *John Wiley and Sons*, p. 511-530.

FROELICH, A.J., and OLSEN, P.E., 1984, Newark supergroup: a revision of the Newark group in eastern North America: *United States Geological Survey Bulletin 1537-A*, p. 55-58.

GAWTHORPE, R. L. and LEEDER, M. R., 2000, Tectono-sedimentary evolution of active extensional basins: *Basin Research*, v. 12, p. 195-218.

GAZZI, P., 1966, Le arenarie del flysch sopracretaceo dell'Apennino modenese; correlazioni con il flysch di Monghidoro: *Mineralogica e Petrografica Acta*, v. 12, p. 69-97.

HANDY, W.A.., 1976, Depositional history and diagenesis of lacustrine and fluvial sedimentary rocks of the Turners Falls and Mount Toby transition north-central Massachusetts: M.S. thesis, *Department of Geosciences, University of Massachusetts, Amherst, Massachusetts*, 115 p.

HARRISON, T.M., SPEAR, F.S., and HEIZLER, M.T., 1989, Geochronologic studies in central New England II: post-Acadian hinged and differential uplift: *Geology*, v. 17, p. 185-189.

HELMOLD, K.P., 1985, Provenance of feldspathic sandstones – the effect of diagenesis on provenance interpretations: a review: *in* Zuffa, G.G., ed., Provenance of Arenites: *D. Reidel Publishing Company, Holland*, p. 139-163.

HIBBARD, J., VAN STAAL, C., RANKIN, D., and WILLIAMS, H., 2006, Geology, lithotectonic map of the Appalachian orogen, Canada-United States of America: *Geological Survey of Canada*, Map 02096A, scale 1:1500000.

HOUSEKNECHT, D.W., 1987, Assessing the relative importance of compaction processes and cementation relative to reduction of porosity in sandstones: *AAPG Bulletin*, v. 71, p. 633-642.

HUBERT, J. F. and DUTCHER, J. A., 1999, Sedimentation, volcanism, stratigraphy, and tectonism at the Triassic-Jurassic boundary in the early Mesozoic Deerfield rift basin Massachusetts: *Northeastern Geology and Environmental Sciences*, v. 21, p. 188-201.

HUBERT, J.F., DUTCHER, J.A., and WALSH, M.P., 2008, Sedimentology, paleoclimate, and tectonic history of the early Mesozoic Sugarloaf Arkose, Deerfield basin, Massachusetts: *submitted for review*.

HUBERT, J. F., FESHBACH-MERINEY, P. E. and SMITH, M. E., 1992, The Triassic-Jurassic Hartford rift basin, Connecticut and Massachusetts: Evolution, sandstone diagenesis and hydrocarbon history: *American Association of Petroleum Geologists Bulletin*, v. 76, p.1710-1734.

HUBERT, J.F., and REED, A.A., 1978, Guide to the Mesozoic redbeds of central Connecticut: Contribution No. 32, *Department of Geosciences, University of Massachusetts, MA*, 129 p.

HUBERT, J.F., TAYLOR, J.M., RAVENHURST, C., REYNOLDS, P., and PANISH, P.T., 2001, Burial and hydrothermal diagenesis of the sandstones in the early Mesozoic Deerfield rift basin, Massachusetts: *Northeastern Geology and Environmental Sciences*, v. 23, p. 109-126.

HUTCHINSON, D.R., and GROW, J.A., 1985, New York Bight fault: *GSA Bulletin*, v. 96, p. 975-989.

HUTCHINSON, D.R., and KLITGORD, K.D., 1988, Deep structure of rift basins from the continental margin around New England: *in* Froelich, A.J., and Robinson, G.R. (eds.), Studies of the Early Mesozoic Basins of the Eastern United States: *United States Geologic Survey Bulletin* 1776, p. 220-229.

HUTCHINSON, D.R., KLITGORD, K.D., LEE, M.W., and TREHU, A.M., 1988, U.S. Geological Survey deep seismic reflection profile across the Gulf of Maine: *GSA Bulletin*, v. 100, p. 172-184.

INGERSOLL, R.V., BULLARD, T.F., FORD, R.L., GRIMM, J.P., PICKLE, J.D., and SARES, J.D., 1984, The effect of grain size on detrital modes: a test of the Gazzi-Dickinson point-counting method: *Journal of Sedimentary Petrology*, v. 54, p. 103-116.

KENT, D. V. and MUTTONI, G., 2003, Mobility of Pangea: implications for late Paleozoic and early Mesozoic paleoclimate. *in* LeTourneau, P. M., and Olsen, P. E., eds., The Great Rift Valleys of Pangea in Eastern North America: *Columbia University Press*, 2: 11–20.

KENT, D. V. and TAUXE, L., 2005, Corrected Late Triassic latitudes for continents adjacent to the North Atlantic: *Science*, v. 31, p. 240-244.

KERR, A., 1994, Magmatic, hydrothermal and surficial processes in the development of multicoloured dimension stone granites of the Topsails plateau area (NTS 12H/02): *Current Research, Newfoundland Department of Mines and Energy, Geological Survey Branch Report 94-1*, p. 147-165.

LE ROY, P., GUILLOCHEAU, F., PIQUÉ, A, and MORABET, A.M., 1997, Subsidence of the Atlantic Moroccan margin during the Mesozoic: *Canadian Journal of Science*, v. 35, p. 476-493.

LEEDER, M.R., and GAWTHORPE, R.L., 1987, Sedimentary models for extensional tilt-block/half0graben basins: *in* Coward, M.P., Dewey, J.F., and Hancock, P.L., eds., Continental extension tectonics: *Geological Society Special Publication 28*, p. 139-152.

LEIER, A. L., DeCELLES, P. G. and PELLETIER, J. D., 2005, Mountains, monsoons, and megafans: *Geology*, v. 33, p. 289-292.

LETOURNEAU, P. M. and HUBER, P. 2006. Early Jurassic eolian dune field, Pomperaug basin, Connecticut and related synrift deposits: stratigraphic framework and paleoclimate context: *Sedimentary Geology*, v. 187, p. 63-81.

LONGIARU, S., 1987, Visual comparators for estimating the degree of sorting from plane and thin section: *Journal of Sedimentary Petrology*, v. 57, p. 791-794.

LOOPE, D.B., STEINER, M.B., ROWE, C.M., and LANCASTER, N., 2004, Tropical westerlies over Pangean sand seas: *Sedimentology*, n. 51, p. 315-322.

LOUCKS, R.G., DODGE, M.M., and GALLOWAY, W.E., 1984, Regional controls on diagenesis and reservoir quality in Lower Tertiary sandstones along the Texas gulf coast: *in* McDonald, D.A., and Surdam, R.C., eds., Clastic Diagenesis, AAPG Memoir 37: *AAPG, OK*, 434 p.

LUCAS, S.G., an TANNER, L.H., 2007, The nonmarine Triassic-Jurassic boundary in the Newark Supergroup of eastern North America: *Earth-Science Review*, v. 84, p. 1-20.

LUTTRELL, G.W., 1989, Stratigraphic nomenclature of the Newark supergroup of eastern North America, *United States Geological Survey Bulletin* 1572, 136 p.

LYONS, J.B., 1997, Bedrock geological map of New Hampshire: U. S. Geological Survey Map, scale 1:250,000.

MARPLE, R., and TALWANI, P., 2006, Possible connection between the East Coast-Stafford fault system and Norumbega fault zone in southern New England: *Northeastern Geology & Environmental Sciences*, v. 28, n. 3, p. 215-230.

MARZOLI, A., RENNE, P.R., PICCIRILLO, E.M., ERNESTO, M., BELLIENI, G., and DE MIN, A., 1999, Extensive 200-million-year-old continental flood basalts of the central Atlantic magmatic province, *Science*, v. 284, p. 616-618.

MARZOLI, A., BERTRAND, H., KNIGHT, K.B., CIRILLI, S., BURATTI, N., VÉRATI, C., NOMADE, S., RENNE, P.R., YOUBI, N., MARTINI, R., ALLENBACH, K., NEUWERTH, R., RAPAILLE, C., ZANINETTI, L., and BELLIENI, G., 2004, Synchrony of the central Atlantic magmatic province and the Triassic-Jurassic boundary climactic and biotic crisis: *Geology*, v. 32, n. 11, p. 973-976.

MCCLAY, K.R., DOOLEY, T., WHITEHOUSE, P., and MILSS, M., 2002, 4-D evolution of rift systems: insights from scaled physical models: *AAPG Bulletin*, v. 86, p. 935-959.

MCHONE, J.G., 1988, Tectonic and paleostress patterns of Mesozoic intrusions in eastern North America: *in* Manspeizer, W., ed., Triassic-Jurassic rifting: continental breakup and the origin of the Atlantic Ocean and the passive margins: *Developments in Geotectonics*, n. 22, p. 607-620.

MCHONE, J.G., 2000, Non-plume magmatism and rifting during the opening of the central Atlantic Ocean: *Tectonophysics*, v. 316, p. 287-296.

MCHONE, J.G., and PHILPOTTS, A.R., 1995, The Holyoke basalt in southern Connecticut: *in* McHone, N.W., ed., Guidebook for Field Trips in Eastern Connecticut and the Hartford Basin: *State Geological and Natural History Survey of Connecticut*, Guidebook 7, p. C1-C7.

MERINEY, P.E., 1988, Sedimentology and diagenesis of Jurassic lacustrine sandstones in the Hartford and Deerfield basins, Massachusetts and Connecticut: M.S. Thesis, *Department of Geosciences, University of Massachusetts, Amherst, MA*, 401 p.

MIALL, A. D., 1996, The Geology of Fluvial Deposits: *Springer- Verlag, NY,* 582 p.

MORAD, S., BERGAN, M., KNARUD, R., and NYSTUEN, J.P., 1990, Albitization of detrital plagioclase in Triassic reservoir sandstones from the Snorre field, Norwegian North Sea: *Journal of Sedimentary Petrology*, v. 60, p. 411-425.

MORAD, S., KETZER, J.M., and DE ROS, L.F., 2000, Spatial and temporal distribution of diagenetic alterations in siliciclastic rocks: implications for mass transfer in sedimentary basins: *Sedimentology*, v. 47, p. 95-120.

MORLEY, C.K., 2002, Evolution of large normal faults: evidence from seismic reflection data: *AAPG Bulletin*, v. 86, p. 961-978.

MOUSTAFA, A.R., 2002, Controls on the geometry of transfer zones in the Suez rift and northwest Red Sea: implications for the structural geometry of rift systems: *AAPG Bulletin*, v. 86, p. 979-1002.

O'TOOLE, M.M., 1981, Chemistry and mineralogy of the Deerfield basalt at Turners Falls, Massachusetts: Unpublished senior honors thesis, *Department of Geosciences, University of Massachusetts, Amherst, MA*, 40 p.

OLSEN, P.E., 1986, A 40-million-year lake record of early Mesozoic climatic forcing: *Science*, v. 234, p. 842-848.

OLSEN, P.E., 1997, Stratigraphic record of the early Mesozoic breakup of Pangea in the Laurasia-Gondwana rift system: *Annual Reviews of Earth and Planetary Science*, v. 25, p. 337-401.

OLSEN, P.E., FOWELL, S.J., and CORNET, B., 1990, The Triassic/Jurassic boundary in continental rocks of eastern North America: a progress report: *in* Sharpton, V.L., and Ward, P.D., eds., Global Catatrophes in Earth History: *Geological Society of America Special Paper 247*, p. 585-593.

OLSEN, P.E., and KENT, D.V., 1996, Milankovitch climate forcing in the tropics of Pangea during the late Triassic: *Paleogeography, Paleoclimatology, Paleoecology*, v. 122, p. 1-26.

OLSEN, P.E., KENT, D.V., ET-TOUHAMI, M., and PUFFER, J.H., 2003, Cyclo-, magneto-, and bio-stratigraphic constraints on the duration of CAMP event and its relationship to the Triassic-Jurassic boundary: *in* Hames, W.E., McHone, J.G., Renee, P.R., and Ruppel, C., eds., The Central Atlantic Magmatic Province: Insights from fragments of Pangea: *Geophysical Monograph Series*, v. 136, p. 7-32.

OLSEN, P.E., KENT, D.V., FOWELL, S.J., SCHLISCHE, R.W., WITHJACK, M.O., and LETOURNEAU, P.M., 2000, Implications of a comparison of the stratigraphy and depositional environments of the Argana (Morocco) and Fundy (Nova Scotia, Canada) Permian-Jurassic basins: *in* Oijdi, M., and Et-Touhami, M., eds., Le Permien et le Trias du Maroc: Actes de la Première Réunion du Groupe Morocain du Permien et du Trias: *Hilal Impression*, p. 165-183.

OLSEN, P. E., MCDONALD, N. G., HUBER, P. and CORNET, B., 1992, Stratigraphy and paleoecology of the Deerfield rift basin (Triassic-Jurassic, Newark Supergroup), Massachusetts: *in* Robinson, P., and Brady, J. B., eds., Field Trip Guidebook of the 84th Annual New England Intercollegiate Geologic Conference: *Department of Geosciences, University of Massachusetts, Amherst, Massachusetts*, v. 2, p. 488-535.

OLSEN, P.E., WHITESIDE, J.H., LETOURNEAU, P., and HUBER, P., 2005, Jurassic cyclostratigraphy and paleontology of the Hartford basin: *in* McHone, N.W., and Peterson, M.J., eds., Field Trip Guidebook of the 97th Annual New England Intercollegiate Geologic Conference: *State Geological and Natural History Survey of Connecticut Guidebook*, n. 8, p. 55-105.

PÁLFY, J., MORTENSEN, J.K., CARTER, E.S., SMITH, P.L., FRIEDMAN, R.M., and TIPPER, H.W., 2000, Timing the end-Triassic mass extinction: first on land, then in the sea?: *Geology*, v. 28, p. 39-42.

PEACOCK, D.C.P., and SANDERSON, D.J., 1991, Displacement, segment linkage and relay ramps in normal fault zones: *Journal of Structural Geology*, v. 13, p. 721-733.

PETTIJOHN, F.J., 1975, Sedimentary rocks, 3rd edition: *Harper and Row, NY*, 718 p.

PETTIJOHN, F.J., POTTER, P.E., and SIEVER, R., 1987, Sand and sandstone, 2nd edition: *Springer-Verlag, NY*, 571 p.

PHILPOTTS, A.R., 1998, Nature of a flood-basalt-magma reservoir based on the compositional variation in a single flood-basalt flow and its feeder dike in the Mesozoic Hartford basin, Connecticut: *Contribution to Mineralogy and Petrology*, v. 133, p. 69-82.

PHILPOTTS, A.R., CARROLL, M., and HILL, J.M., 1996, Crystal-mush compaction and the origin of pegmatitic segregation sheets in a thick flood-basalt flow in the Mesozoic Hartford basin, Connecticut: *Journal of Petrology*, v. 37, p. 811-836.

PRATT, L.M., SHAW, C.A., and BURRUSS, R.C., 1988, Thermal histories of the Hartford and Newark basins inferred from maturation indices of organic matter: *in* Froelich, A.J., and Robinson, G.R. (eds.), Studies of the Early Mesozoic Basins of the Eastern United States: *United States Geologic Survey Bulletin* 1776, p. 220-229.

PUTNIS, A., HINRICHS, R., PUTNIS, C.V., GOLLA-SCHINDLER, U., and COLLINS, L.G., 2007, Hematite in porous red-clouded feldspars: evidence of large-scale crustal fluid-rock interaction: *Lithos*, v. 95, p. 10-18.

RAMPINO, M.R., and STOTHERS, R.B., 1988, Flood basalt volcanism during the past 250 million years: *Science*, v. 241, p. 663-668.

RASBURY, E. T., GIERLOWSKI-KORDESCH, E. H., COLE, J. M., SOOKDEO, C., SPATARO, G. and NIENSTEDT, J., 2006, Calcite cement stratigraphy of a nonpedogenic calcrete in the Triassic New Haven Arkose (Newark Supergroup): *in* Alonso-Zarza, A. M. and Tanner, L. H., eds., Paleoenvironmental Record and Applications of Calcretes and Palustrine Carbonates: *Geological Society of America Special Paper* 416, p. 203-222.

ROBINSON, P., 2003,Tectonic-stratigraphic-metamorphic perspective of the New England Caledonides, west-central Massachusetts: *in* Robinson, P. and Brady, J. B. (eds.), Field Trip Guidebook of the 84th Annual New England Intercollegiate Geologic Conference. *Department of Geosciences, University of Massachusetts, Amherst, Massachusetts,* v. 2, p. A1-1 to A1-54.

ROBINSON, P., and HALL, L.M., 1979, Tectonic synthesis of southern New England: *in* The Caledonides in the U.S.A., *IGCP Project* 27, p. 73-82.

ROBINSON, P., THOMPSON, P.J., and ELBERT, D.C., 1991, The nappe theory in the Connecticut Valley region: Thirty-five years since Jim Thompson's first proposal: *American Mineralogist*, v. 76, p. 689-712.

ROBINSON, P., TUCKER, R.D., BRADLEY, D., BERRY, H.N. IV, and OSBERG, P.H., 1998, Paleozoic orogens in New England: *Journal of Geological Society of Sweden*, v. 120, p. 119-148.

RODEN, M.K., and MILLER, D.S., 1991, Tectono-thermal history of Hartford, Deerfield, Newark and Taylorsville basins, eastern United States, using fission-track-analysis: *Swiss Bulletin of Mineralogy and Petrology*, v. 71, p. 187-203.

RODEN-TICE, M.K., TICE, S.J., and SCHOFIELD, I.S., 2000, Evidence for differential unroofing in the Adirondack Mountains, New York State, determined by apatite fission-track thermochronology: *Journal of Geology*, v. 108, p. 155-169.

RODEN-TICE, M. K. and WINTSCH, R. P., 2002, Early Cretaceous normal faulting in southern New England: evidence from apatite and fission-track ages: *The Journal of Geology*, v. 110, p. 159-178.

RODEN-TICE, M. K. and WINTSCH, R. P., 2007, Late Jurassic to early Cretaceous exhumation in eastern Massachusetts and Connecticut based on apatite fission track age gradient and discontinuities: Abstracts Volume of the Geological Society of America Northeastern Section meeting, Durham, NH.

RODGERS, J., 1985, Bedrock Geologic Map of Connecticut: Connecticut Geological and Natural History Survey, scale 1:125,000.

RODEN-TICE, M. K., FOLEY, C.N., and WINTSCH, R. P., 2008, Confirmation of Mesozoic tectonic adjustments to Paelozoic terranes in central New England: Abstracts Volume of the Geological Society of America Northeastern Section meeting, Buffalo, NY.

ROSENDAHL, B.R., 1987, Architecture of continental rifts with special reference to east Africa: *Annual Reviews of Earth and Planetary Science*, v. 15, p. 445-503.

SCHLISCHE, R.W., 1995, Geometry and origin of fault-related folds in extensional settings: *AAPG Bulletin*, v. 79, p. 987-996.

SCHLISCHE, R.W., 2003, Progress in understanding the structural geology, basin evolution, and tectonic history of the eastern North American rift system: *In* LeTourneau, P.M. and Olsen, P.E. (eds.), The Great Rift Valleys of Pangea in Eastern North America – Volume One: Tectonics, Structure, and Volcanism. *Columbia University Press, NY*, p. 21-64.

SCHLISCHE, R.W., and ANDERS, M.H., 1996, Stratigraphic effects and tectonic implications of the growth of normal faults and extensional basins: *in* Beraton, K.K., ed., Reconstructing the history of Basin and Range extension using sedimentology and stratigraphy: *GSA Special Paper 303*, p. 183-203.

SCHLISCHE, R.W., WITHJAK, M.O., and OLSEN, P.E., 2002, Relative timing of CAMP, rifting, continental breakup, an basin inversion: tectonic significance: *in* Hames, W.E., Renne, P.R., and Ruppel, C., eds., The Central Atlantic Magmatic Province: *American Geophysical Union Monograph*.

SKEHAN, J.W., 2001, Roadside Geology of Massachusetts: *Mountain Press, MT*, 378 p.

SMOOT, J. P., 1991, Eolian sand sheet and dune strata in the Upper Triassic New Haven Arkose, Hartford Basin, Connecticut: *Abstracts Volume, Joint Meeting of the Northeastern and Southeastern Sections of the Geological Society of America, Baltimore, Maryland*, p.130.

SMOOT, J.P., and OLSEN, P.E., 1994, Climatic cycles as sedimentary controls of rift-basin lacustrine deposits in the early Mesozoic Newark basin based on continuous core: *in* Lomando, A.J., Schreiber, B.C., and Harris, P.M., eds., Lacustrine Reservoirs and Depositional Systems: *SEPM Core Workshop*, n. 19, p. 201-237.

STECKLER, M.S., OMAR, G.I., KARNER, G.D., and KOHN, B.P., 1993, Pattern of hydrothermal circulation within the Newark basin from fission-track analysis: *Geology*, v. 21, p. 735-738.

STEVENS, R. L., 1977, Sedimentology of the Sugarloaf Arkose, Deerfield basin, Massachusetts: report for the M. S. degree, *Department of Geosciences, University of Massachusetts, Amherst, Massachusetts*, 84 p.

STREICKEISEN, A.L., 1979, Classification and nomenclature of volcanic rocks, lamprophyres, carbonatites, and mililitic rocks: recommendations and suggestions of the IUGS subcommission on the systematics of igneous rocks: *Geology*, v. 7, p. 331-335.

SWANSON, M.T., 1986, Preexisting fault control for Mesozoic basin formation in eastern North America: *Geology*, v. 14, p. 419-422.

TANNER, L.H., HUBERT, J.F., COFFEY B.P., and MCINERNEY, D.P., 2001, Stability of atmospheric CO_2 levels across the Triassic/Jurassic boundary: *Nature*, v. 411, p. 675-677.

TAYLOR, J.M., 1991, Diagenesis of sandstones in the early Mesozoic Deerfield basin, Massachusetts: M.S. thesis, *Department of Geosciences, University of Massachusetts, Amherst, Massachusetts*, 225 p.

THOMPSON, P.J., 1985, Stratigraphy, structure and metamorphism in the Monadnock quadrangle, New Hampshire: Ph. D. Thesis, *Department of Geosciences, University of Massachusetts, Amherst, Massachusetts*, 127 p.

THOMPSON, J.B. Jr., ROBINSON, P., CLIFFORD, T.N., and TRASK, N.J. Jr., 1968, Nappes and gneiss domes in west-central New England: *in* Zen, E. and White, W.S., Eds., Studies of Appalachian geology: northern and maritime: *John Wiley & Sons, NY*, p. 203-218.

TORTOSA, A., PALOMARES, M., and ARRIBAS, J., 1991, Quartz grain types in Holocene deposits from the Spanish Central System: some problems in provenance analysis: *in* Morton, A.C., Todd, S.P., and Haughton, P.D.W., eds., Developments in Sedimentary Provenance Studies: *Geological Society Special Publication No. 57*, p. 47-54.

TRUDGILL, B., 2002, Structural controls on drainage development in the Canyonlands graben of southeast Utah: *AAPG Bulletin*, v. 86, p. 1095-1112.

TUCKER, M.E., 2001, Sedimentary Petrology, Third Edition: *Blackwell Publishing, MA*, 262 p.

TULLIS, J., 1983, Deformation of feldspars: *in* Ribbe, T.H., ed., Feldspar Mineralogy: *Reviews in Mineralogy*, v. 2, p. 297-322.

WALKER, T.R., 1976, Diagenetic origin of continental red beds: *in* Falk, H., ed., The continental Permian in central, west, and south Europe: *Reidel Publishing Company, Holland*, p. 240-282.

WALSH, J.J., and WATTERSON, J., 1988, Analysis of the relationship between displacements and dimensions of faults: *Journal of Structural Geology*, v. 10, p. 239-247.

WENK, W.J., 1989, A seismic model of a zone of Mesozoic crustal extension in the New England region: *Northeastern Geology*, v. 11, n. 4, p. 202-208.

WERNICKE, B. and BURCHFIEL, B.C., 1982, Modes of extensional tectonics: *Journal of Structural Geology*, v. 4, p. 105-115.

WESSEL, J. M., 1969, Sedimentary history of Upper Triassic alluvial fan complex in north-central Massachusetts: unpub. M. S. thesis, *Department of Geosciences, University of Massachusetts, Amherst, Massachusetts*, 156 p.

WEST, D.P. Jr., and RODEN-TICE, M.K., 2003, Late Cretaceous reactivation of the Norumbega fault zone, Maine: evidence from apatite fission-track ages: *Geology*, v. 31, p. 649-652.

WHITMORE, G.P., CROOK, K.A.W., JOHNSON, D.P., 2004, Grain size control of mineralogy and geochemistry in modern river sediment, New Guinea collision, Papua New Guinea: *Sedimentary Geology*, v. 171, p. 129-157.

WILLARD, M.E., 1951, Bedrock geology of the Mount Toby quadrangle, Massachusetts: *United States Geological Survey Quadrangle Map*, GQ-0008.

WILSON, M., 1989, Igneous Petrogenesis: A Global Tectonic Approach: *Springer, The Netherlands*, 466 p.

WINTER, J.D., 2001, An Introduction to Igneous and Metamorphic Petrology: *Prentice-Hall, NJ*, 697 p.

WINTSCH, R. P., RODEN-TICE, M., KUNK, M. J., and ALEINIKOFF, U. S., 2003, Ductile to brittle Mesozoic overprint of Alleghanian structures, Bronson Hill Terrane, Rockville area, Connecticut: *In* Robinson, P. and Brady, J. B. (eds.), Field Trip Guidebook of the 84th Annual New England Intercollegiate Geologic Conference. *Department of Geosciences, University of Massachusetts, Amherst, Massachusetts,* v. 2, p. A3-1 to A3-31.

WITHJACK, M.O., OLSEN, P.E., and PETERSON, E., 1990, Experimental models of extensional forced folds: *AAPG Bulletin*, v. 74, p. 1038-1054.

WISE, D. U., 1992, Dip domain method applied to the Mesozoic Connecticut valley rift basins*: Tectonics*, v. 11, p. 1357-1368.

WISE, D. U. and HUBERT J. F., 2003, Evolving fault types, stress fields, and tectonics of the early Mesozoic Deerfield basin, Massachusetts. *In* Robinson, P. and Brady, J. B. (eds.), Field Trip Guidebook of the 84th Annual New England Intercollegiate Geologic Conference. *Department of Geosciences, University of Massachusetts, Amherst, Massachusetts,* v. 2, p. C5-1 to C5-30.

WITHJACK, M.O., OLSEN, P.E., and SCHLISCHE, R.W., 1995, Tectonic evolution of the Fundy rift basin, Canada: evidence of extension and shortening during passive margin development: *Tectonics*, v. 14, p. 390-405.

WITHJACK, M.O., SCHLISCHE, R.W., and OLSEN, P.E., 1998, Diachronous rifting, drifting and inversion on the passive margin of central eastern North America: an analog for other passive margins: *AAPG Bulletin*, v. 82, p. 817-835.

YARDLEY, B.W., 1989, An Introduction to Metamorphic Petrology: *Longman Scientific & Technical, UK*, 248 p.

ZEN, E-AN., 1983, Bedrock geological map of Massachusetts: U. S. Geological Survey Map, scale 1:250,000.

ZING, T., 1935, Beitrage zur Schotteranalyse: *Swiss Journal of Mineralogy and Petrology*, v. 15, p. 39-140.